

ABSTRACT

EDWARDS, ANDREW JAMES. Early Age Thermal Cracking of Mass Concrete Footings on Bridges in Coastal Environments. (Under the direction of Dr. Christopher Bobko and Dr. Rudolf Seracino).

Large volumes of concrete have the potential to experience temperature gradients because of heat released during curing that can lead to cracking. Cracking of mass concrete in coastal structures is of special concern because of its exposure to saltwater with its corrosive effects on steel reinforcement. The North Carolina Department of Transportation (NCDOT) identified several mass concrete footings in bridges along the coastal region of North Carolina with cracking problems that needed to be assessed for cracking in light of the current North Carolina mass concrete specifications. The end goal was to assist the NCDOT in updating their mass concrete specifications with improved quality control guidelines to create more durable, crack free concrete.

A finite element model was developed to predict the temperature rise and temperature distributions arising from early age concrete hydration, as well as the stresses induced by the resulting temperature gradients. The model was validated by a laboratory experiment and used to analyze several mass concrete footings in bridges in the coastal region of North Carolina for their early age thermal cracking potential. A dimensional parametric study was also conducted to study the effect of size on mass concrete and understand what may be considered “massive” mass concrete versus typical mass concrete. Reasonably sized mass concrete structures that followed the typical NCDOT control plans did not have a high likelihood of significant cracking from thermal stresses, while large mass concrete footings have a much higher risk of significant cracking even when the typical NCDOT control plans are followed. To define large mass concrete structures, a minimum dimension of 10 feet was recommended. Based this research and other studies in the literature, additions and revisions to current NCDOT mass concrete specifications were recommended.

© Copyright 2013 by Andrew James Edwards

All Rights Reserved

Early Age Thermal Cracking of Mass Concrete Footings on Bridges in Coastal Environments

by
Andrew James Edwards

A thesis submitted to the Graduate Faculty of
North Carolina State University
in partial fulfillment of the
requirements for the Degree of
Master of Science

Civil Engineering

Raleigh, North Carolina

2013

APPROVED BY:

Dr. Christopher Bobko
Co-Chair of Advisory Committee

Dr. Rudolf Seracino
Co-Chair of Advisory Committee

Dr. Paul Zia

DEDICATION

This is dedicated to all of those who have supported me and believed in me over the past six years of college. They include my parents, my brothers, my sister, my friends, and all of those at my church that have supported me of the years. Without your help and support I would not be the person I am today. Thank you.

BIOGRAPHY

Andrew James Edwards was born and raised in Raleigh, North Carolina by Allan and Vivian Edwards. He attended Grace Christian School for high school where he graduated valedictorian of his class. Andrew was accepted to the College of Engineering at North Carolina State University and began his college career in the fall of 2007. He graduated Summa Cum Laude with a Bachelor of Science degree in Civil Engineering with a focus in Structural Engineering. After graduation, he began working towards his Master of Science degree in Civil Engineering, specializing in Structural Engineering, under the guidance of Dr. Christopher Bobko and Dr. Rudolf Seracino. While enrolled in the graduate program, he worked both as a research and teaching assistant. After receiving his graduate degree in the summer of 2013, he plans on beginning a career as a designer for structural engineering firm as well as eventually earning his PE.

ACKNOWLEDGEMENTS

I would first like to thank my advisors, Dr. Christopher Bobko and Dr. Rudolf Seracino, for their guidance and support during this project. Without continued direction from you I would not have achieved this great accomplishment. I would also like to thank Dr. Paul Zia for being a member of my committee. Thank you for the immense amount of time, effort, and advice you put into this project. Your help was invaluable during this process.

I would like to thank the North Carolina Department of Transportation steering and implementation committee who oversaw this project. The steering and implementation committee included the following members:

Greg Perfetti, P.E. (Chair)

Kevin Bowen, P.E.

Tom Drda, P.E.

Brian Hanks, P.E. (Co-Chair)

Christopher A. Peoples, P.E.

Michael Robinson, P.E.

David Stark, P.E.

Mrinmay Biswas, Ph.D., P.E.

V. Owen Cordle

Joseph Geigle, P.E.

Dan Holderman, P.E.

Mustan Kadibhai, P.E.

A special thanks goes out to Kevin Bowen and Brian Hanks for their assistance with the site visits to Oak Island, Sunset Beach, and the Wilmington Bypass. Additional thanks to V. Owen Cordle for gathering and providing the mix designs for this project.

Thanks also to CRSI for their generous donation of reinforcement materials. And lastly, sincere thanks to the technical staff at the Constructed Facilities Laboratory of North Carolina State University for their help with the mass concrete block experiment. In particular, Gregory Lucier and Jerry Atkinson are acknowledged for their invaluable expertise and assistance.

TABLE OF CONTENTS

LIST OF TABLES.....	xi
LIST OF FIGURES.....	xii
EXECUTIVE SUMMARY.....	1
CHAPTER 1 INTRODUCTION.....	5
1.1 Background.....	5
1.2 Research Needs.....	6
1.3 Research Objective and Approach.....	6
1.4 Report Outline.....	7
CHAPTER 2 LITERATURE REVIEW.....	9
2.1 Introduction.....	9
2.2 Causes of Early Age Thermal Cracking.....	9
2.2.1 Thermal Gradients.....	9
2.2.2 Thermal Stresses and Restraints.....	11
2.3 Mitigation Strategies.....	13
2.3.1 Cement Mix Proportions and Supplementary Cementitious Material.....	13
2.3.2 Construction Methods.....	14
2.4 Standards/Specifications.....	15
2.4.1 ACI Specifications.....	15
2.4.2 North Carolina Specifications.....	16
2.4.3 Other State Specifications.....	17
2.4.4 Federal Government Agency Specifications.....	20
2.5 Current Research on Thermal Cracking in Early Age Mass Concrete..	23
2.5.1 University of Florida Parametric Study.....	23
2.5.2 Temperature Prediction Methods Analysis.....	27

	2.5.3 Mass Concrete Size Definition.....	28
CHAPTER 3	SITE VISITS.....	30
	3.1 Introduction.....	30
	3.2 Oak Island Bridge.....	30
	3.2.1 Site Overview.....	30
	3.2.2 Footing Properties.....	31
	3.2.3 Site Observations.....	33
	3.3 Sunset Beach Bridge.....	38
	3.3.1 Site Overview.....	38
	3.3.2 Footing Properties.....	39
	3.3.3 Site Observations.....	40
	3.4 US 17 Wilmington Bypass Bridge.....	43
	3.4.1 Site Overview.....	43
	3.4.2 Footing Properties.....	44
	3.4.3 Site Observations.....	45
	3.5 Western Wake Site.....	48
	3.5.1 Site Overview.....	48
	3.5.2 Footing Concrete Mixture.....	51
	3.5.3 Thermal Control Measures.....	51
	3.5.4 Temperature Monitoring.....	53
	3.6 Thomasville Site.....	57
	3.6.1 Site Overview.....	57
	3.6.2 Thermal Control Plan.....	58
	3.6.3 Temperature Monitoring.....	58
CHAPTER 4	FINITE ELEMENT MODELING.....	63
	4.1 Introduction.....	63
	4.2 ConcreteWorks V2.0 Assessment.....	64
	4.3 DIANA Finite Element Modeling.....	66

4.3.1	DIANA Thermal Model.....	67
4.3.1.2	Heat of Hydration.....	68
4.3.1.3	Thermal Properties.....	73
4.3.1.4	Boundary Conditions.....	76
4.3.2	DIANA Structural Model.....	77
4.3.2.2	Equivalent Age Maturity Method.....	78
4.3.2.3	Coefficient of Thermal Expansion.....	79
4.3.2.4	Modulus of Elasticity and Poisson’s Ratio.....	80
4.3.2.5	Tensile Strength.....	81
4.3.2.6	Autogenous Shrinkage.....	81
4.3.2.7	Boundary Conditions.....	81
CHAPTER 5	MASS CONCRETE BLOCK EXPERIMENT.....	84
5.1	Introduction.....	84
5.2	Block Properties.....	84
5.3	Set-up and Construction.....	85
5.4	Temperature Data Collection System.....	88
5.5	Temperature Data Results.....	89
5.6	Material Properties Testing.....	93
5.6.1	Maturity Temperature.....	96
5.6.2	Compressive Strength.....	97
5.6.3	Splitting Tensile Strength.....	100
5.6.4	Modulus of Elasticity.....	103
5.6.5	Autogenous Shrinkage.....	105
5.6.6	Properties Summary.....	109
CHAPTER 6	FINITE ELEMENT ANALYSIS RESULTS.....	111
6.1	Introduction.....	111
6.2	Concrete Block Validation Experiment.....	112
6.2.1	Thermal Analysis Results.....	112

6.2.2 Structural Analysis Results.....	118
6.3 Oak Island Footing Case Study.....	125
6.3.1 Thermal Analysis Results.....	125
6.3.2 Structural Analysis Results.....	131
6.4 Sunset Beach Footing Case Study.....	138
6.4.1 Thermal Analysis Results.....	138
6.4.2 Structural Analysis Results.....	144
6.5 Wilmington Bypass Footing Case Study.....	151
6.5.1 Thermal Analysis Results.....	151
6.5.2 Structural Analysis Results.....	157
6.6 Wilmington Bypass Footing Case Study with Insulation.....	163
6.6.1 Thermal Analysis Results.....	163
6.6.2 Structural Analysis Results.....	167
6.7 Results Summary.....	173
CHAPTER 7 PARAMETRIC STUDY ANALYSIS RESULTS.....	175
7.1 Introduction.....	175
7.2 Dimensional Study Trial 1.....	177
7.2.1 Thermal Analysis Results.....	177
7.2.2 Structural Analysis Results.....	181
7.3 Dimensional Study Trial 2.....	185
7.3.1 Thermal Analysis Results.....	185
7.3.2 Structural Analysis Results.....	189
7.4 Dimensional Study Trial 3.....	192
7.4.1 Thermal Analysis Results.....	192
7.4.2 Structural Analysis Results.....	196
7.5 Dimensional Study Trial 4.....	199
7.5.1 Thermal Analysis Results.....	199
7.5.2 Structural Analysis Results.....	203

CHAPTER 8	DISCUSSION OF RESULTS.....	207
	8.1 Introduction.....	207
	8.2 Model Validation.....	207
	8.3 Cracking Potential.....	208
	8.4 Schmidt Method vs Finite Element Model.....	210
	8.5 Mass Concrete vs Massive Mass Concrete.....	213
CHAPTER 9	CONCLUSIONS AND RECOMMENDATIONS.....	219
	9.1 Key Findings.....	219
	9.2 Recommendations for Implementations.....	222
	9.3 Future Research.....	225
		.
	LIST OF REFERENCES.....	227
	APPENDICES.....	230
APPENDIX A	Mass Concrete State Specifications Survey and Research Result.....	231
APPENDIX B	Mass Concrete Site Visit Field Report Drawings.....	251
APPENDIX C	Sample Input Commands for DIANA Model: Sunset Beach.....	272

LIST OF TABLES

Table 2-1	Mass Concrete Specifications Part 1.....	22
Table 2-2	Mass Concrete Specifications Part 2.....	23
Table 3-1	Oak Island Concrete Mix Design.....	32
Table 3-2	Sunset Beach Concrete Mix Design.....	39
Table 3-3	Wilmington Bypass Concrete Mix Design.....	45
Table 3-4	Western Wake Concrete Mix Design.....	51
Table 4-1	Typical Chemical Admixture Dosages (Riding, 2007)	72
Table 4-2	Empirical Model Chemical Input Values.....	73
Table 4-3	Material Thermal Properties.....	76
Table 5-1	Mass Concrete Mix Design.....	85
Table 5-2	Summary of Mechanical Properties for Test 2 Cylinders.....	109
Table 5-3	Summary of Shrinkage Values for Test 2 Prisms.....	110
Table 7-1	Parametric Study Trial Dimensions.....	175

LIST OF FIGURES

Figure 2-1	Stresses due to external restraint (ACI 207.2R-07).....	12
Figure 2-2	Stresses due to internal restraint (ACI 207.2R-07).....	12
Figure 2-3	Maximum stress versus maximum temperature difference with respect to block size and type of concrete used (Tia et al, 2010).....	24
Figure 2-4	Maximum temperature difference versus insulation thickness for varying concrete dimensions (Tia et al, 2010)	26
Figure 2-5	Temperature versus time of varying concrete mixes (Tia et al, 2010).....	26
Figure 3-1	Oak Island Bridge overview of footings at bents 2 and 3.....	31
Figure 3-2	Patched cracks at bent 2 footing.....	34
Figure 3-3	Bent 2 footing patched crack up close.....	35
Figure 3-4	Bent 2 footing sample surface crack.....	35
Figure 3-5	Bent 2 footing sample crack down vertical face.....	36
Figure 3-6	Bent 2 footing metal embedment along front face.....	36
Figure 3-7	Bent 3 footing typical crack.....	37
Figure 3-8	Bent 3 footing sample crack.....	37
Figure 3-9	Sunset Beach Bent 14.....	38
Figure 3-10	Bent 14 sample crack of about 0.02 inches.....	41
Figure 3-11	Column at base of bent 14.....	42
Figure 3-12	Crack along formwork joint at bent 14.....	42
Figure 3-13	US 17 Bypass overview.....	43
Figure 3-14	Bent 41 footing sample map cracking.....	46
Figure 3-15	Bent 41 footing sample map cracking along with some more severe cracking.....	47
Figure 3-16	Footing 42 sample vertical crack.....	47
Figure 3-17	Footing 42 additional horizontal cracking vertical face.....	48
Figure 3-18	Western Wake Abutment 1 footing overview.....	49

Figure 3-19	Western Wake Abutment 1 footing.....	50
Figure 3-20	Western Wake Abutment 2 footing.....	50
Figure 3-21	Abutment 1 footing’s cooling pipe layout.....	52
Figure 3-22	Temperature data from Abutment 1 footing sensors.....	54
Figure 3-23	Max temperature difference from Abutment 2 footing sensors.....	54
Figure 3-24	Temperature data from Abutment 2 footing sensors.....	55
Figure 3-25	Max temperature difference from Abutment 2 footing sensors.....	55
Figure 3-26	Temperature data from the rectangular bent footing sensors.....	56
Figure 3-27	Max temperature difference from the rectangular bent footing sensors.....	56
Figure 3-28	Thomasville End Bent 1 mass concrete pour.....	57
Figure 3-29	Plan view Thomasville End Bent 1 mass concrete pour.....	59
Figure 3-30	Elevation view from the front of the Thomasville end bent 1 mass concrete pour.....	59
Figure 3-31	Thermocouple-maturity meter setup.....	60
Figure 3-32	Temperature data from Thomasville thermocouple sensors.....	61
Figure 3-33	Temperature differences between Thomasville thermocouple sensors.....	62
Figure 4-1	Thermal analysis modeling elements: A) HX8HT isoparametric element B) BQ4HT isoparametric element.....	68
Figure 4-2	Structural modeling CHX60 isoparametric element.....	78
Figure 4-3	Block experiment boundary conditions.....	82
Figure 4-4	Oak Island footing boundary conditions.....	83
Figure 5-1	Block experiment formwork set up.....	86
Figure 5-2	Block experiment formwork base.....	86
Figure 5-3	Concrete block pour.....	87
Figure 5-4	Finished surface of concrete block with curing compound.....	88
Figure 5-5	Steel reinforcement cage with thermocouples attached.....	89
Figure 5-6	Thermocouple sensor locations.....	90
Figure 5-7	Temperature data from edge thermocouple sensors.....	91

Figure 5-8	Vertical temperature distribution.....	92
Figure 5-9	Horizontal temperature distribution.....	92
Figure 5-10	Thermocouple temperature differences.....	93
Figure 5-11	Finished concrete cylinders and prisms.....	94
Figure 5-12	Moist curing water bath.....	94
Figure 5-13	Nylon mixing drum used for the second set of tests.....	95
Figure 5-14	Cylinder temperature set up.....	96
Figure 5-15	Average temperature results from the second set of cylinder tests.....	97
Figure 5-16	Compressive strength test setup.....	98
Figure 5-17	Average compressive strength vs time from Test 1 cylinders.....	99
Figure 5-18	Average compressive strength vs equivalent age from Test 2 cylinders.....	99
Figure 5-19	Splitting tensile strength test setup.....	100
Figure 5-20	MTS machine setup.....	101
Figure 5-21	Average splitting tensile strength vs time from Test 1 cylinders.....	102
Figure 5-22	Average splitting tensile strength vs equivalent age from Test 2 cylinders.....	102
Figure 5-23	Modulus test setup.....	103
Figure 5-24	Average modulus of elasticity vs time from Test 1 cylinders.....	104
Figure 5-25	Average modulus of elasticity vs equivalent age from Test 2 cylinders.....	105
Figure 5-26	Shrinkage test mold.....	106
Figure 5-27	Shrinkage comparator measurement setup.....	107
Figure 5-28	Average strain vs time from Test 1 prisms.....	108
Figure 5-29	Average strain vs time from Test 2 prisms.....	108
Figure 6-1	Quarter block orientation.....	112
Figure 6-2	Block experiment model: A) Overall mesh B) Temperature locations.....	113
Figure 6-3	Block vertical temperature distribution.....	115
Figure 6-4	Block horizontal temperature distribution.....	115

Figure 6-5	Block maximum temperature differentials.....	116
Figure 6-6	Block vertical temperature distribution at 26 and 42 hours.....	116
Figure 6-7	Block horizontal temperature distribution at 26 and 42 hours.....	117
Figure 6-8	Block temperature profile at max temperature difference (42 hours): A) Isoparametric B) Profile view.....	117
Figure 6-9	Block stress locations.....	118
Figure 6-10	Block vertical profile equivalent age at 26 and 42 hours.....	118
Figure 6-11	Block horizontal profile equivalent age at 26 and 42 hours.....	120
Figure 6-12	Block vertical profile stress and strength at 42 hours.....	120
Figure 6-13	Block horizontal profile stress and strength at 42 hours.....	121
Figure 6-14	Block nodes principal stresses vs time.....	122
Figure 6-15	Block vertical profile cracking index at 26 and 42 hours.....	123
Figure 6-16	Block vertical profile cracking index at 26 and 42 hours.....	123
Figure 6-17	Block nodes cracking index vs time.....	124
Figure 6-18	Block cracking index contours at 42 hours: A) Isoparametric B) Profile view.....	124
Figure 6-19	Oak Island mesh close up.....	125
Figure 6-20	Oak Island temperature locations.....	126
Figure 6-21	Oak Island vertical temperature distribution.....	128
Figure 6-22	Oak Island horizontal temperature distribution.....	128
Figure 6-23	Oak Island maximum temperature differentials.....	129
Figure 6-24	Oak Island vertical profile temperature distribution at 116 hours.....	129
Figure 6-25	Oak Island horizontal profile temperature distribution at 116 hours.....	130
Figure 6-26	Oak Island temperature profile at 116 hours.....	130
Figure 6-27	Oak Island sliced temperature profile at 116 hours.....	131
Figure 6-28	Oak Island stress locations.....	132
Figure 6-29	Oak Island vertical profile equivalent age at 116 hours.....	133
Figure 6-30	Oak Island horizontal profile equivalent age at 116 hours.....	134

Figure 6-31	Oak Island vertical profile stress and strength vs time at 116 hours.....	134
Figure 6-32	Oak Island horizontal profile stress and strength vs time at 116 hours.....	135
Figure 6-33	Oak Island nodes principal stresses vs time.....	135
Figure 6-34	Oak Island vertical profile cracking index at 116 hours.....	136
Figure 6-35	Oak Island horizontal profile cracking index at 116 hours.....	136
Figure 6-36	Oak Island nodes cracking index vs time.....	137
Figure 6-37	Oak Island cracking index contours at 116 hours isoparametric view.....	137
Figure 6-38	Oak Island cracking index contours at 116 hours profile view.....	138
Figure 6-39	Sunset Beach mesh close up.....	139
Figure 6-40	Sunset Beach temperature locations.....	140
Figure 6-41	Sunset Beach vertical temperature distribution.....	140
Figure 6-42	Sunset Beach horizontal temperature distribution.....	141
Figure 6-43	Sunset Beach maximum temperature differentials.....	141
Figure 6-44	Sunset Beach vertical temperature distribution at 86 hours.....	142
Figure 6-45	Sunset Beach horizontal temperature distribution at 86 hours.....	142
Figure 6-46	Sunset Beach temperature profile at 86 hours.....	143
Figure 6-47	Sunset Beach sliced temperature profile at 86 hours.....	143
Figure 6-48	Sunset Beach stress locations.....	144
Figure 6-49	Sunset Beach vertical profile equivalent age at 46 and 86 hours.....	145
Figure 6-50	Sunset Beach horizontal profile equivalent age at 46 and 86 hours.....	146
Figure 6-51	Sunset Beach vertical profile stress and strength vs time at 86 hours.....	146
Figure 6-52	Sunset Beach horizontal profile stress and strength vs time at 86 hours.....	147
Figure 6-53	Sunset Beach nodes principal stresses vs time.....	147
Figure 6-54	Sunset Beach vertical profile cracking index at 46 and 86 hours.....	148
Figure 6-55	Sunset Beach horizontal profile cracking index at 46 and 86 hours.....	149
Figure 6-56	Sunset Beach nodes cracking index vs time.....	149
Figure 6-57	Sunset Beach cracking index contours at 86 hours isoparametric view.....	150
Figure 6-58	Sunset Beach cracking index contours at 86 hours profile view.....	150

Figure 6-59	Wilmington mesh close up.....	151
Figure 6-60	Wilmington temperature locations.....	152
Figure 6-61	Wilmington vertical temperature distribution.....	153
Figure 6-62	Wilmington horizontal temperature distribution.....	154
Figure 6-63	Wilmington maximum temperature differentials.....	154
Figure 6-64	Wilmington vertical temperature distribution at 69 and 156 hours.....	155
Figure 6-65	Wilmington horizontal temperature distribution at 69 and 156 hours.....	155
Figure 6-66	Wilmington temperature profile at 156 hours.....	156
Figure 6-67	Wilmington sliced temperature profile at 156 hours.....	156
Figure 6-68	Wilmington stress locations.....	157
Figure 6-69	Wilmington vertical profile equivalent age at 69 and 156 hours.....	158
Figure 6-70	Wilmington horizontal profile equivalent age at 69 and 156 hours.....	159
Figure 6-71	Wilmington vertical profile stress and strength vs time at 156 hour.....	159
Figure 6-72	Wilmington horizontal profile stress and strength vs time at 156 hours.....	160
Figure 6-73	Wilmington vertical profile cracking index at 69 and 156 hours.....	160
Figure 6-74	Wilmington horizontal profile cracking index at 69 and 156 hours.....	161
Figure 6-75	Wilmington nodes cracking index vs time.....	162
Figure 6-76	Wilmington cracking index contours at 156 hours isoparametric view.....	162
Figure 6-77	Wilmington cracking index contours at 156 hours profile view.....	163
Figure 6-78	Wilmington insulated vertical temperature distribution.....	164
Figure 6-79	Wilmington insulated horizontal temperature distribution.....	165
Figure 6-80	Wilmington insulated maximum temperature differentials.....	165
Figure 6-81	Wilmington insulated vertical temperature distribution at 69 and 156 hours.....	166
Figure 6-82	Wilmington insulated horizontal temperature distribution at 69 and 156 hours.....	166
Figure 6-83	Wilmington insulated temperature profile at 156 hours.....	167

Figure 6-84	Wilmington insulated vertical profile equivalent age at 69 and 156 hours.....	168
Figure 6-85	Wilmington insulated horizontal profile equivalent age at 69 and 156 hours.....	169
Figure 6-86	Wilmington insulated vertical profile stress and strength vs time at 156 hours.....	169
Figure 6-87	Wilmington insulated horizontal profile stress and strength vs time at 156 h.....	170
Figure 6-88	Wilmington insulated vertical profile cracking index at 69 and 156 hours.....	171
Figure 6-89	Wilmington insulated horizontal profile cracking index at 69 and 156 hours.....	171
Figure 6-90	Wilmington insulated nodes cracking index vs time.....	172
Figure 6-91	Wilmington insulated cracking index contours at 156 hours isoparametric view.....	172
Figure 6-92	Wilmington insulated cracking index contours at 156 hours profile view.....	172
Figure 7-1	Dimensional study temperature locations.....	176
Figure 7-2	Dimensional study cracking index locations.....	177
Figure 7-3	Trial 1 vertical temperature distribution.....	178
Figure 7-4	Trial 1 horizontal temperature distribution.....	179
Figure 7-5	Trial 1 maximum temperature differentials.....	179
Figure 7-6	Trial 1 temperature profile at 160 hours.....	180
Figure 7-7	Trial 1 sliced temperature profile at 160 hours.....	181
Figure 7-8	Trial 1 vertical profile cracking index at 99 and 160 hours.....	182
Figure 7-9	Trial 1 horizontal profile cracking index at 99 and 160 hours.....	183
Figure 7-10	Trial 1 nodal cracking index vs time.....	183
Figure 7-11	Trial 1 cracking index contours at 160 hours isoparametric view.....	184

Figure 7-12	Trial 1 cracking index contours at 160 hours profile view.....	184
Figure 7-13	Trial 2 vertical temperature distribution.....	186
Figure 7-14	Trial 2 horizontal temperature distribution.....	187
Figure 7-15	Trial 2 maximum temperature differentials.....	187
Figure 7-16	Trial 2 temperature profile at 160 hours.....	188
Figure 7-17	Trial 2 sliced temperature profile at 160 hours.....	188
Figure 7-18	Trial 2 vertical profile cracking index at 76 and 160 hours.....	190
Figure 7-19	Trial 2 horizontal profile cracking index at 76 and 160 hours.....	190
Figure 7-20	Trial 2 nodal cracking index vs time.....	191
Figure 7-21	Trial 2 cracking index contours at 160 hours isoparametric view.....	191
Figure 7-22	Trial 2 cracking index contours at 160 hours profile view.....	192
Figure 7-23	Trial 3 vertical temperature distribution.....	193
Figure 7-24	Trial 3 horizontal temperature distribution.....	194
Figure 7-25	Trial 3 maximum temperature differentials.....	194
Figure 7-26	Trial 3 temperature profile at 158 hours.....	195
Figure 7-27	Trial 3 sliced temperature profile at 158 hours.....	195
Figure 7-28	Trial 3 vertical profile cracking index at 56 and 158 hours.....	197
Figure 7-29	Trial 3 horizontal profile cracking index at 56 and 158 hours.....	197
Figure 7-30	Trial 3 nodal cracking index vs time.....	198
Figure 7-31	Trial 3 cracking index contours at 158 hours isoparametric view.....	198
Figure 7-32	Trial 3 cracking index contours at 158 hours profile view.....	199
Figure 7-33	Trial 4 vertical temperature distribution.....	201
Figure 7-34	Trial 4 horizontal temperature distribution.....	201
Figure 7-35	Trial 4 maximum temperature differentials.....	202
Figure 7-36	Trial 4 temperature profile at 109 hours.....	202
Figure 7-37	Trial 4 sliced temperature profile at 109 hours.....	203
Figure 7-38	Trial 4 vertical profile cracking index at 42 and 109 hours.....	204
Figure 7-39	Trial 4 horizontal profile cracking index at 42 and 109 hours.....	205

Figure 7-40	Trial 4 nodal cracking index vs time.....	205
Figure 7-41	Trial 4 cracking index contours at 109 hours isoparametric view.....	206
Figure 7-42	Trial 4 cracking index contours at 109 hours profile view.....	206
Figure 8-1	Wilmington Schmidt model temperature results.....	211
Figure 8-2	Wilmington Schmidt model temperature differentials.....	212
Figure 8-3	Wilmington Schmidt model vs FE Model temperature comparison.....	212
Figure 8-4	Wilmington Schmidt model vs FE Model differential comparison.....	213
Figure 8-5	Maximum temperature comparison for parametric study.....	215
Figure 8-6	Maximum temperature comparison for parametric study.....	215
Figure 8-7	Cracking index of Trials 1-4 at time of max difference A) Trial 1 – Min dimension of 12.5 feet at 160 hours B) Trial 2 – Min dimension of 10.0 feet at 160 hours C) Trial 3 – Min dimension of 7.5 feet at 158 hours D) Trial 4 – Min dimension of 5.0 feet at 109 hours.....	216
Figure 8-8	Cracking index of Trials 1-4 at time of peak temperature A) Trial 1 – Min dimension of 12.5 feet at 99 hours B) Trial 2 – Min dimension of 10.0 feet at 76 hours C) Trial 3 – Min dimension of 7.5 feet at 56 hours D) Trial 4 – Min dimension of 5.0 feet at 42 hours.....	217
Figure 9-1	Sample model of precast stay-in-place forms.....	225
Figure B-1	Oak Island Field Report 9/12/2011.....	251
Figure B-2	Sunset Beach Field Report 9/12/2011.....	258
Figure B-3	US17 Wilmington Bypass Field Report 9/12/2011.....	263

EXECUTIVE SUMMARY

Large volumes of concrete have the potential to experience temperature gradients during curing that can lead to cracking. Concrete hydration is an exothermic reaction that can produce high amounts of heat during curing, especially in the first few days or weeks after casting. This heating leads to temperature gradients within the concrete, where temperatures are high in the center of mass of the concrete and lower near the outside of the concrete, where the heat can dissipate more easily in the ambient environment. If the temperature gradients are too great, resulting tensile thermal stresses can exceed the concrete tensile strength and cause cracking, especially at early ages where the concrete is still developing its full strength. Cracking of mass concrete in coastal structures is of special concern because of its exposure to saltwater with its corrosive effects on steel reinforcement. Currently, common mitigation strategies involve modifications to concrete mix designs, precooling of mix materials, post cooling of in-place concrete, and surface insulation.

The North Carolina Department of Transportation (NCDOT) identified several mass concrete footings in bridges along the coastal region of North Carolina with cracking problems that needed to be assessed for cracking in light of the current North Carolina mass concrete specifications. The NCDOT mass concrete specifications were also to be updated with improved quality control guidelines to create more durable, crack free concrete.

The objective of this study was to create a finite element model to analyze the North Carolina bridge footings and assess them for their early age thermal cracking probability. The NCDOT mass concrete specifications were also to be assessed. This was accomplished through the following tasks:

- Site visits were performed at various mass concrete bridge footing sites around North Carolina.
- Current state, federal, and ACI mass concrete guidelines, including North Carolina's, were reviewed.

- A finite element model was created using the TNO DIANA commercial software to predict the temperature rise and temperature distribution arising from early age concrete hydration, as well as the stresses induced by the resulting temperature gradients.
- A laboratory mass concrete block experiment was performed to validate the finite element model.
- The verified finite element model was used to model current coastal bridge footings to assess them for their thermal cracking probability.
- A dimensional parametric study was also conducted based on the Wilmington Bypass footing to observe the effect of size on mass concrete.
- North Carolina's current mass concrete specifications were evaluated based on other mass concrete specifications as well as based on the results from the finite element models and site visits.

This report presents the findings from site visits to mass concrete footings in North Carolina and the experimental block tests. It also presents the findings of the thermal and structural analysis of the experimental block and three case study mass concrete footings. Specific findings related to the finite element model and the case study analyses include the following:

- ConcreteWorks was determined to be unsuitable for this research due to its inability to perform 3D stress analysis, the lack of access to stress information, the inability to choose boundary conditions, and various errors that occurred during the use of the program.
- The finite element model developed in this research using TNO DIANA accurately modeled the temperature development and resulting stresses in early age mass concrete.
- Reasonably sized mass concrete structures that followed the typical NCDOT control plans did not have a high likelihood of thermal cracking.

- Large mass concrete footings, such as the Wilmington Bypass footing, have a much higher risk of thermal cracking even when the typical NCDOT control plans are followed.
- When temperature control plans are not followed, extreme thermal gradients will form, creating a very high cracking potential and increasing the likelihood of thermal cracking.

Based on the findings of this research and the evaluation of North Carolina's current mass concrete specifications, additions and revisions to current NCDOT mass concrete specifications were recommended. The recommendations have been split into two categories: "typical" mass concrete and special cases, referred to as "massive" mass concrete structures. This "massive" mass concrete should currently be defined as a structure with a minimum dimension of 10 feet, based on this research, until future research provides a better definition. Some of the typical mass concrete recommendations are summarized as follows:

- i. A maximum allowable temperature after placement of 158 °F should be specified.
- ii. Concrete should remain covered and monitored until the difference between the internal concrete temperature and the average daily ambient temperature is below 35 °F, but in no case should the concrete be cured and protected for less than 7 days after placement.
- iii. Early formwork removal may be allowed based on evidence from match-cured cylinders.
- iv. Consider material specifications allowing the use of granulated slag replacement of cement by 50 – 70% and/or a ternary mix of granulated slag, fly ash, and Portland cement, where there is at least 20% fly ash by weight and 40% portland cement by weight. The use of fly ash replacement of cement by 30% is also allowed.

- v. Require temperature sensors at the surface nearest to the concrete's center of mass as well as at the farthest surface from the center and at the center of mass itself.
- vi. Require the Contractor to provide an analysis of the anticipated range of peak temperatures, maximum temperature gradients, time to peak temperature, as well as the time it takes to cool to the allowable temperature differential in the mass concrete elements using his proposed mix design, casting procedures, and materials. The following methods can be used:
 - a) Schmidt method with the measured adiabatic temperature curves from a semi-adiabatic calorimetry test.
 - b) An equivalent method as approved by the EngineerIf Schmidt's method is used with ACI's generic adiabatic temperature curves, care should be taken by the Engineer in recognition of the errors produced from this method.
- vii. Require immediate and future remedial actions by the Contractor if temperature differential limits are exceeded.

The special case recommendations would require more in depth calculations, analysis, and/or monitoring to highlight the special attention these "massive" mass concrete structures require.

CHAPTER 1

INTRODUCTION

1.1 Background

Concrete hydration is an exothermic reaction that can produce high amounts of heat during curing, especially in the first few days or weeks after casting. In large volumes of concrete, known as mass concrete, this heat production can produce high temperatures at the center of the concrete's mass due to the insulating effect of the concrete. When the concrete surface temperatures are lower due to the heat dissipated into the ambient environment, temperature gradients are formed. These changes in temperature create volumetric changes, expansion from heating and contraction from cooling, in the concrete. When these volumetric changes are restrained by the supports and the more mature interior concrete, tensile stresses form on the concrete's surface. If these tensile stresses become high enough, the tensile strength of the concrete will be exceeded causing cracking to occur. The likelihood of this cracking is even further increased due to the lower tensile strengths found in early age concrete that is still developing its full strength.

The cracking in mass concrete resulting from thermal gradients generated during cement hydration reactions can lead to durability issues in bridge substructures and other mass concrete structures. This can be even more troublesome for mass concrete structures in coastal regions. Bridge substructures that are surrounded by water when cast can have increased thermal gradients due to the cool water. The corrosive nature of the salt water in coastal regions can also cause deterioration of the reinforcing steel when it penetrates into the concrete through the cracks.

Currently, common practices attempt to control concrete thermal cracking by controlling the temperatures within the concrete. This is primarily done through four methods: modification of the concrete mix design, precooling of mix materials, post cooling of in-place concrete, and surface insulation. The goal of these practices is to reduce the

maximum internal temperature achieved as well as to control the rate at which heat dissipates, thus controlling the temperature gradients.

Many states, including North Carolina, and federal government agencies have special specifications to address the issues that arise with mass concrete. These specifications, however, vary from state to state, with agreement only on the typical maximum temperature differential limit of 35 °F. The North Carolina Department of Transportation (NCDOT) specifications currently define mass concrete as a structure where the minimum dimension is 6 feet or greater, where most specifications ranged from 3 feet to 6 feet. Most specifications required cooling and insulation methods to control the temperatures as well as some sort of temperature monitoring system, but there is currently little consensus about the details of implementation between the specifications.

1.2 Research Needs

The NCDOT identified several mass concrete footings in bridges along the coastal region of North Carolina with cracking problems that needed to be assessed. These footings were located on bridges near Oak Island, Sunset Beach, and Wilmington. These recent coastal bridge footings were to be analyzed in order to assess the success or failure of current mitigation practices on projects in North Carolina based on their thermal cracking probability. The NCDOT mass concrete specifications also needed to be assessed. By updating the current specifications with improved quality control guidelines, NCDOT will have more crack-free mass concrete elements during the initial construction process. These elements will be significantly more durable than cracked concrete elements, leading to reduced maintenance costs and longer service life of new bridges in coastal environments.

1.3 Research Objective and Approach

The objective of this study was to create a finite element model of the North Carolina bridge footings and assess them for their early age thermal cracking probability. The NCDOT

mass concrete specifications were also to be assessed. This was accomplished through the following tasks:

- Site visits were performed at various mass concrete bridge footing sites around North Carolina.
- Current state, federal, and ACI mass concrete guidelines, including North Carolina's, were reviewed.
- A finite element model was created to predict the temperature rise and temperature distribution arising from early age concrete hydration, as well as the stresses induced by the resulting temperature gradients.
- A laboratory mass concrete block experiment was performed to validate the finite element model.
- The verified finite element model was used to model current coastal bridge footings to assess them for their thermal cracking probability.
- A dimensional parametric study was also conducted based on the Wilmington Bypass footing to observe the effect of size on mass concrete and understand what may be considered "massive" mass concrete versus "typical" mass concrete.
- North Carolina's current mass concrete specifications were evaluated based on other mass concrete specifications as well as based on the results from the finite element models and site visits.

1.4 Report Outline

Chapter 2 is a review of the literature discussing important topics in the area of early age mass concrete hydration. Current state and federal mass concrete specifications are also reviewed.

Chapter 3 summarizes the observations from the site visits of 3 North Carolina coastal bridges as well as the site visits of two other North Carolina bridges.

Chapter 4 discusses the finite element model created using TNO DIANA to model the temperatures during early age hydration as well as the stresses induced by the resulting thermal gradients. A review of the free modeling program ConcreteWorks is also presented.

Chapter 5 describes the test procedures used to run the experimental block test that was used to validate the finite element model. This chapter also presents the data from the tests.

Chapter 6 presents thermal and stress analysis results from the experimental concrete block as well as the results from the Oak Island, Sunset Beach, and Wilmington Bypass case studies.

Chapter 7 presents thermal and stress analysis results from the parametric study.

Chapter 8 discusses the thermal and structural results presented in Chapter 6 as well as the results from the parametric presented in Chapter 7 and relates them to the experimental and field observations.

Chapter 9 presents the key findings of this research, the recommendations for implementation for the NCDOT specifications, and the recommendations for future research.

CHAPTER 2 LITERATURE REVIEW

2.1 Introduction

Thermal cracking issues were first noticed in dams where significant rises in temperature from the heat of hydration and subsequent cracking from the shrinkage that occurred during cooling were found to occur (Mehta and Monteiro, 2006). Outside of dams, however, concrete structures are significantly smaller and early age thermal effects can often be overlooked. In bigger structural concrete elements, large internal temperatures can create large temperature differentials which cause volumetric changes within the concrete element. When these volumetric changes are restrained, stresses will develop. These stresses cause cracks in the concrete when the tensile stresses exceed the concrete's early age strength. Current construction practice tries to mitigate this problem through temperature control methods.

2.2 Causes of Early Age Thermal Cracking

2.2.1 Thermal Gradients

The difference between mass concrete and normal structural concrete is the importance that thermal behavior, both in the generation and dissipation of heat, can have on concrete durability (ACI 207.1R-05). In smaller volumes of structural concrete, heat can easily be dissipated, but in mass concrete large internal temperatures can cause drastic volumetric changes. The factors that control the volumetric change are the initial placement temperature, the heat generation phase, and the heat dissipation phase (ACI 207.2R-07).

The increase in temperature during the heat generation phase is primarily controlled by the heat produced from hydration in concrete. When cement mixes with water during hydration, an exothermic reaction takes place that gives off heat. The total amount of heat liberated and the rate at which the heat is liberated is largely dependent on the chemical composition of the concrete. The heat generated has been found to be mostly a function of

the percent contents of alite (C_3S), belite (C_2S), aluminite (C_3A), and aluminoferrite (C_3AF) in the cementitious material (Mehta and Monteiro, 2006; Kim, 2010; Townsend, 1981). The rate at which the heat is generated is also influenced by the Blaine fineness of the cement, where the finer the material the faster it will react with the water, and the addition of different admixtures, such as retarders or accelerators (Mehta and Monteiro, 2006). Faster reactions generally imply a faster production of heat. The heat of hydration is typically modeled through results from adiabatic or isothermal calorimetry tests, however more recently a model has been developed to describe this heat generation. This project used an empirical model developed by Schindler and Folliard (2005) to determine the heat of hydration. This model is further discussed in Chapter 4.

The heat dissipation phase is a function of the thermal properties of the concrete: thermal diffusivity, heat capacity, and thermal conductivity. The magnitude of the heat loss is then a function of the environment in contact with the concrete (Mehta and Monteiro, 2006). When concrete structures have large mass-to-surface ratios, the heat generated in the interior is not easily dissipated through the concrete due to its low thermal conductivity and the structure almost becomes adiabatic, resulting in high internal temperatures. The increased heat on the surface of the concrete structure, however, can dissipate much more rapidly into the environment resulting in a much lower temperature rise unless the heat loss is controlled (Lu et al., 2000). When the surface temperature is much lower than the interior temperature, large temperature differentials occur.

The temperature change for a specific path through the concrete is referred to as a thermal gradient. There are two types of gradients: mass gradients or surface gradients (ACI 207.2R-07). The mass gradients are the temperature difference between the concrete mass and any restraining foundations. The surface gradients are formed from the cooling of the concrete surface temperature relative to the internal temperature.

2.2.2 Thermal Stresses and Restraints

Volumetric change, whether expansion or contraction, in early age concrete occurs mainly from changes in temperature. During the early heat generation phase, the concrete is expanding due to the increase in temperature. In this phase the internal expansion stretches the cooler external surfaces of the concrete. The concrete during this phase, however, has a relatively low modulus of elasticity and the stresses are easily relieved due to the high rate of creep (Lu et al., 2000). During the heat dissipation, or cooling, phase though, the stiffness in the concrete increases more rapidly and the internal volume of concrete resists the contraction of the concrete surface.

If concrete is not restrained, so that any volumetric change could occur freely, then thermal stresses would not occur in the concrete. In early age concrete, however, there are two types of restraints: internal restraint and external restraint. External restraint is a resistance to volumetric change that occurs due to some external support or foundation, as seen in Figure 2-1. The degree of the external restraint depends on the relative dimensions, strength, and modulus of elasticity of the restraining material (ACI 207.2R-07). Internal restraint is caused by non-uniform volume changes within concrete. When the surface concrete contracts during cooling, the internal concrete restrains the volume from contracting. Tensile stresses then form along the surface of the concrete, as seen in Figure 2-2. The effect of cracking can also be intensified when insulation and formwork is removed too early. Early removal can cause a sudden and extreme increase in the thermal gradient behind the concrete surface due to a sudden change in temperature, which causes surface cracking due to the interior restraint (ACI 207.2R-07; Lu et al, 2000). This phenomenon is referred to as thermal shock.

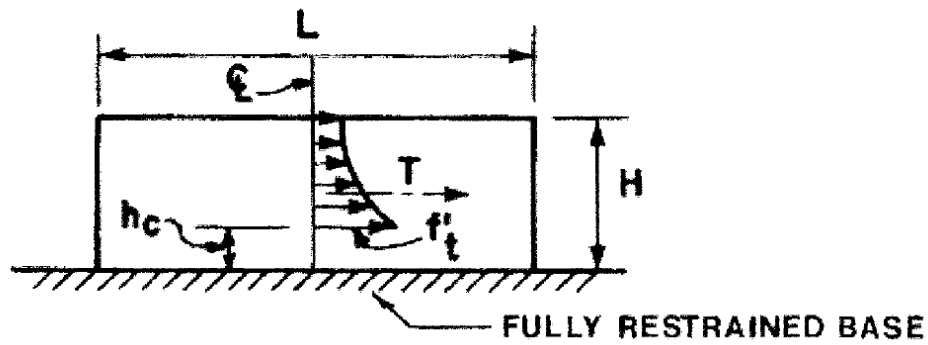


Figure 2-1. Stresses due to external restraint (ACI207.2R-07)

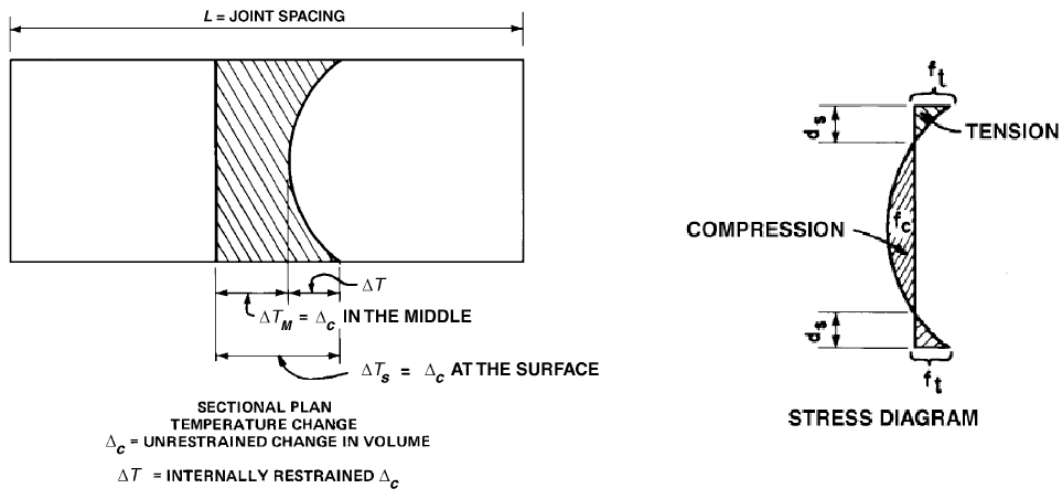


Figure 2-2. Stresses due to internal restraint (ACI207.2R-07)

When tensile stresses in the concrete exceed the tensile strength of the concrete, cracking will occur. The likelihood of cracking is also increased due to the dependence of concrete strength development on age and temperature history. At such early ages, the concrete has not developed its full strength. In addition, since the heat dissipates at a faster

rate along the surface of the concrete, the maturity and strength at the concrete surface will be less than that of the center of the concrete structure.

2.3 Mitigation Strategies

The primary way of controlling thermal stresses, and thus thermal cracking, in mass concrete is by controlling the maximum internal temperature and the rate at which it cools. One way to limit internal temperatures is to modify concrete mix proportions to reduce the rate and magnitude of heat production. In addition, the temperatures may be controlled using a combination of three other methods: precooling of materials, postcooling of in-place concrete, and surface insulation.

2.3.1 Cement Mix Proportions and Supplementary Cementitious Material

The design of mass concrete mix proportions is a balance between strength and the generation of heat within the concrete where the biggest factor is often controlling the temperature development. Typically in dam mass concrete designs, low amounts of cement are used to lower the heat produced during hydration. Structural mass concrete such as footings, however, have a need for higher strength. In these structures, the heat production is often controlled by using Portland cements, such as Type II or Type IV, or hydraulic cements, such as Type MH or Type LH, which have lower heat generation (ACI 207.1R-05). Portland cements with a percent replacement of granulated slag and/or pozzolanic material are also commonly used to provide a reduction in the concrete's maximum temperature while also increasing its workability. This is often seen as a cost effective replacement for using low heat cements like Type IV portland cement (Kim et al., 2010).

Pozzolans are siliceous materials that have no cementitious value until in the presence of moisture and calcium hydroxide (ACI 207.1R-05; Mehta and Monteiro, 2006). The most common pozzolan currently in use is fly ash where there are two types: Class F fly ash and Class C fly ash. When pozzolans are used, they reduce the overall heat of hydration as well as the rate of hydration, as seen in Figure 2-3, similar to having a cement with a higher C_2S

content which produces less heat than C_3A (Mindess et al., 2003). In addition to this, fly ash also has the added benefit of not losing its overall long term strength, despite the delayed hydration that causes lower early strength. Of the two types of fly ash, Class F fly ash is used more often due to its low CaO content which allows it to achieve lower heat production than Class C fly ash. Typically about 15 to 25% of the cement is replaced with Class F fly ash (Gajda and Vangeem, 2002).

Granulated blast-furnace slag may also be used as a replacement for cement. As with fly ash, slag decreases the heat of hydration in concrete. Higher amounts slag though are required to replace cement in these mixes, typically around 65-80%, to achieve similar properties to that of pozzolan cementitious mixes (Gajda and Vangeem, 2002). Granulated slag also has lower early strength with no long term strength loss like fly ash mixes.

2.3.2 Construction Methods

Precooling methods are one of the most effective ways of lowering thermal stresses. This is because lowering the final placement temperature of concrete lowers the final peak temperature, thus decreasing the amount of expansion that takes place during the early age heat generation period (ACI 207.4R-05; Townsend, 1981). The most influential way to reduce the concrete temperatures is through aggregate cooling because aggregates make up the bulk of concrete mixes. Aggregate stockpiles can be cooled by gathering and storing aggregate during cold seasons, by sprinkling stockpiles with cool water, by immersing coarse aggregate into cold water in holding tanks, and by processing fine aggregate in chilled water. During batching, aggregate can also be cooled by a chilled water sprayer. In more extreme cases, aggregate can be cooled using liquid nitrogen which can produce very low temperatures. It is also effective to cool concrete by cooling the batch water. This can be done using chilled water or by replacing a portion of the batch water with ice. It has been shown that it is not beneficial to cool the cementitious materials before mixing (ACI 207.4R-05; Townsend, 1981)

Postcooling is most effectively achieved by using embedded cooling pipes that circulate cool liquid through the concrete. The goal of this method is to lower the maximum temperature reached within the concrete and to reduce its cooling period (Gajda and Vangeem, 2002). The circulated liquid can be water, a water and antifreeze mixture, or a brine solution with a lower freezing point than water (ACI 207.4R-05). If used correctly, postcooling can be beneficial in allowing earlier removal of formwork and insulation by reducing the amount of time needed for cooling. If care is not taken, however, internal cracks and surface cracks could develop (Gajda and Vangeem, 2002).

Insulation is a very effective way of controlling the temperature within concrete by protecting the structure from excessive heat loss. In this method, insulation blanket or polystyrene panels are placed on the outside surface of the concrete and formwork. This method does not help in lowering the maximum concrete temperature, but it instead lowers the rate of cooling which in turn prevents large temperature gradients from developing. If the insulation is removed too early however, the surface will cool quickly resulting in cracking from thermal shock.

2.4 Standards/Specifications

The websites of various state DOT's and other agencies were searched and a brief questionnaire to several state DOTs were conducted in order to review their specifications for mass concrete construction. The specifications from three past NCDOT coastal bridge projects were also reviewed. The results of these inquiries were compiled into a single document that can be found in Appendix A, and a summary is provided in Table 2-1 and Table 2-2.

2.4.1 ACI Specifications

The American Concrete Institute (ACI) gives some guidelines for mass concrete construction specifications in *ACI 301-10: Specifications for Structural Concrete* in Section 8. In their specifications, ACI does not give minimum dimensions for mass concrete; instead

it defines it as any volume of structural concrete that needs a thermal control due to elevated temperatures from hydrating concrete. ACI does state, however, thermal limits including a maximum temperature after placement of 158 F, and a maximum temperature differential of 35 F. In addition, ACI 301 specifies that hydraulic cement with a low heat of hydration, but not a Type III or HE cement, or portland cement with Class F fly ash or slag should be used for mass concrete construction. The concrete is then specified to be cured and protected for a minimum of 7 days unless otherwise specified.

ACI 301-10 also gives some specifications for a temperature control plan. The temperature is required to be controlled and measured hourly from the time the concrete is placed until the difference between internal concrete temperatures and the average daily ambient temperatures is below the maximum temperature differential, after the peak temperature has been reached. At a minimum, two temperature sensors should be placed at the center of the mass concrete and two temperature sensors on the closest exterior face, 2 inches from the surface. If the temperature difference is exceeded immediate action should be taken to remedy the issue.

2.4.2 North Carolina Specifications

The NCDOT, unlike some States, does not have a uniform set of standard specifications. Instead, special mass concrete provisions are created on a job by job basis. A common set of special provisions has developed however where many of the jobs have similar mass concrete specifications as can be seen between the different North Carolina sites in Table 2-1 and Table 2-2, but designated mass concrete members can still vary from job to job.

These North Carolina job specifications almost all specified mass concrete as a bent or footing with a minimum dimension of 6 feet (1.5 m). A recent concrete highway bridge poured in Thomasville, NC, as discussed in Section 3.6, considered a concrete structure with a minimum dimension of 2'-10" as a mass concrete structure. A limiting temperature differential of 35 F between the interior and the exterior of the concrete is given in each of

the mass concrete provisions; however none of them have a maximum concrete temperature limit. The North Carolina provisions do have a limiting temperature range of 40 °F to 75 °F for the temperature of the concrete at placement. The concrete used in these mass concrete pours are required to be Type II portland cement with a 30% replacement of the total weight of the cementitious material by fly ash and a 5% replacement by microsilica, with the exception of the Wilmington Bypass provisions which contains no microsilica. The total cementitious material is also restricted to 690 lbs/yd³ (410 kg/m³). In addition a maximum 3 inch slump, a maximum 0.37 or 0.41 water-cement ratio (dependent on the aggregate shape), and a minimum 28 day cylinder strength of 5000 psi (34.5 MPa) is required.

The temperatures are required to be controlled using any combination of methods approved by the NCDOT as part of the thermal control plan. In addition the temperature must be monitored at one hour intervals from casting until the maximum temperature is reached and the temperature differential between the interior and exterior concrete is decreasing. No mention is made of a minimum protection period or of comparing the interior temperatures with the average ambient temperature. A minimum of six temperature sensors are required for each mass concrete pour, with one sensor at the center of mass and a second sensor 2 in. from the face of the surface furthest from the center of mass. If the temperature differential exceeds the limit, necessary revisions are required from the contractor to keep it from happening again, however no other remedial action is required by the NCDOT.

2.4.3 Other State Specifications

Although many states in the United States have identified the need for special provisions and specifications for mass concrete construction, the requirements in these specifications often differ from state to state. As a part of this project's preliminary research, a brief questionnaire was sent to the Department of Transportation in ten different states along the east coast and the Gulf of Mexico. These states included Delaware, Maryland, Virginia, South Carolina, Georgia, Florida, Alabama, Mississippi, Louisiana, and Texas. The survey covered what the states' mass concrete specifications are, what their experience with

mass concrete has been, and the idea of using precast concrete stay in place forms. Five state DOT's responded to the survey, and their responses can be seen in Appendix A.

Mass concrete specifications were obtained for Florida, Texas, South Carolina, Louisiana, Maryland, and Virginia. The minimum mass concrete dimension in these specifications ranged from 4 feet to 6 feet, with the most common limit being 5 ft. South Carolina also considers circular cross section pours with a 6 feet diameter and a length of 5 feet as mass concrete, and Florida considers 12 feet diameter drill shafts as mass concrete. A maximum temperature differential of 35 °F was observed to be unanimous throughout all of the state specifications. Many states though, like North Carolina, did not have a maximum temperature limit, but when stated it was either 160 °F or 180 °F as seen in Table 2-1 and Table 2-2. The placement temperature is limited by Texas to be between 50-75 °F, limited by South Carolina to be less than 80 °F, and limited by Virginia to be less than 95 °F. The Florida, Virginia, and Louisiana specifications also have limitations on the cement mix that is allowed to be used. Type II cement, or no high early strength cement, is allowed to be used with a combination of fly ash or granulated slag. Florida allows 18% to 20% replacement by weight of the total cementitious material when using fly ash or 50%-70% replacement when using slag. Virginia allows 25%-40% replacement by weight when using fly ash or 50%-75% replacement when using slag, but Louisiana only specifies a limit on the heat of hydration with a limit of 70 calories/gram (290 kJ/kg) at 7 days. Florida also allows a fly ash-granulated slag mix where 20% replacement of fly ash and 40% replacement of slag is allowed. No other concrete limitations were found.

In addition, the Florida, South Carolina, Texas, and Virginia specifications also require a thermal control plan to control the temperatures in the concrete. The temperatures are required to be controlled using a combination of precooling, insulation blankets, and post-cooling as with the North Carolina plans. All of these specifications also require temperature sensors to monitor the temperatures of the interior center core and the exterior surface to ensure that the temperature differentials are within the limits approved by the

engineer. Florida requires the temperatures to be monitored at a maximum of 6 hour intervals until the maximum temperature is achieved, the temperature differential is decreasing, and the center temperature is within 50 °F of the ambient temperature. South Carolina specifies that the exterior sensor needs to be 2 inches inside the concrete face nearest to the sensor at the center of the concrete and that temperatures should be recorded until the temperature in the center is within 35 °F of the lowest ambient temperature, or a maximum of 2 weeks. Virginia specifies that, for footings, sensors be placed at the center of the concrete and at the bottom and top reinforcement mats vertically in line with the center sensor, and that the temperature be monitored every hour for at least 3 days. If the temperature differential is exceeded during the curing process, Florida, South Carolina, and Virginia require the contractor to take immediate remedial action and to repair or replace the concrete that exceeded these temperature limits.

Two states specify minimum times for formwork removal. Texas requires the formwork to remain on the concrete for 4 days for curing and Virginia requires a curing period of 7 days where the formwork can only be removed with approval from the engineer.

Overall, Virginia has the most complete and detailed mass concrete specifications of any state. In addition to what has already been stated, Virginia's control plan requirements are more extensive. They require that contractors provide not only the proposed method of controlling temperatures, but also provide all calculations for the expected time to reach the peak temperature and the time needed to cool, calculations for the peak temperature based on different air and concrete temperature, a curve of maximum temperature differential allowed versus concrete strength, as well as the heat of hydration of all cementitious materials and the coefficient of thermal expansion of the concrete. It is also required that a maturity curve or match-cured cylinders be used to determine when form removal is allowed. Insulating blankets then remain on the concrete for 48 hours after form removal. Finally, Virginia also requires any cracks exceeding 0.006" to be epoxy injected.

2.4.4 Federal Government Agency Specifications

The Unified Facilities Guide Specifications (UFGS) is a set of joint specifications used in construction for government military services. It is currently used by the United States Army Corp of Engineers (USACE), the Naval Facilities Engineering Command, the Air Force Civil Engineer Support Agency, the Air Force Center for Engineering and the Environment, and the National Aeronautics and Space Administration (NASA). *UFGS-03 70 00 Mass Concrete*, which covers concrete mix designs, and *USGS-03 70 00 Marine Concrete*, which covers marine mass concrete construction specifications, were reviewed for the government agencies' guidelines on mass concrete.

In the Marine Concrete section of the specifications, mass concrete is defined as any concrete system that approaches 158 °F (70 °C) or any concrete structure with a minimum dimension of 3 feet (1 m) or more. In these specifications, the maximum temperature differential is not permitted to exceed 35 °F (20 °C) and the maximum temperature is not permitted to exceed 158 °F. The maximum concrete placement temperature is determined through thermal modeling based on expected ambient conditions. The Marine Concrete section of the specifications did not directly speak on the mass concrete mix design; it instead gave an overarching set of guidelines for marine concrete design. The Mass Concrete section of the UFGS also does not directly give any limitations for designing mass concrete mix designs, but it instead gives a general set of guidelines for making mix designs for projects containing mass concrete or mass and structural concrete.

The Marine Concrete portion of the specifications also requires a mass concrete thermal control plan at least 30 days prior to cast that contains the cooling and insulation methods, the thermocouple locations and monitoring plan, anticipated form removal schedule, and the maximum concrete placement temperature based on thermal modeling. Temperature sensors are required at a minimum to be placed at the geometric center, 3 inches inside the side face at mid height, 3 inches inside the top surface directly above the center sensor, 3 inches from the top corner where the formwork intersects, and in a shaded location

to record the ambient temperatures. The temperature controls are then required to stay in place until the difference between the ambient low temperature and mean of all functioning center sensors is below the maximum temperature differential. Remedial actions are only required to be submitted if the temperature limits are exceeded in the concrete.

The most unique aspect of these specifications however is the mock-up that is required to go alongside the thermal control plan. In this mock up, 31 cylinders are to be cast using the mass concrete design in order to test the compressive strength, the tensile strength, and the elastic modulus at 3, 7, 28, and 90 days. Predictive equations are then required for each mechanical property measured. Three 3 by 3 by 11.25 inch concrete prisms also need to be cast to measure the coefficient of thermal expansion. A 3 foot cube is also required to record the semi-adiabatic temperatures hourly for 1 week. The results of these tests can then be used by the contractor to establish the temperature control period and time for form removal

Table 2-1. Mass Concrete Specifications Part 1

	Placement Size (ft)	Max Temp Difference (°F)*	Max Temp of Concrete (°F)	Concrete Placement Temp Range (°F)
Oak Island, NC	≥ 6	≤ 35	----	40 - 75
Sunset Beach, NC	≥ 6	≤ 35	----	40 - 75
US17 Bypass, NC	≥ 1.8 (m) or 6 ft.	≤ 20 (°C) or 36 °F	----	4 - 24 (°C) or 52 - 75 °F
Florida	----	≤ 35	180	----
Texas	≥ 5	≤ 35	160	50 - 75
South Carolina	≥ 5	≤ 35	----	≤ 80
Louisiana	≥ 4	----	----	----
Maryland	≥ 6	----	----	----
Virginia	> 5	≤ 35	160	≤ 95
UFGS	> 3 or 1 m	≤ 20 (°C) or 35 °F	158	Based on thermal model

Table 2-2. Mass Concrete Specifications Part 2

	Concrete Type	Fly Ash Content (%)*	NOTES
Oak Island, NC	Class AA	30	5% microsilica in addition to fly ash
Sunset Beach, NC	Class AA	30	5% microsilica in addition to fly ash
US17 Bypass, NC	Class AA	25 - 30	-----
Florida	Type II (MH)	18 - 50	-----
Texas	----	----	Keep form in place for at least 4 days.
South Carolina	----	----	-----
Louisiana	Type II Type IP Type IS	----	Concrete mix shall generate a heat of hydration no more than 70 calories/gram (290 kJ/kg) at 7 days.
Maryland	----	----	-----
Virginia	----	25 - 40	Or use 50 - 75 % of slag as cement replacement
UFGS	----	----	Class C fly ash not permitted

Notes:

-Max temperature difference is between the interior and exterior of the mass concrete during curing.

-Fly ash percent by weight of total cementitious material.

2.5 Current Research on Thermal Cracking in Early Age Mass Concrete

2.5.1 University of Florida Parametric Study

A parametric study on mass concrete was done at the University of Florida under the direction of Dr. Mang Tia and Dr. Christopher Ferraro (2010). They studied the effect that the heat generation rate, the size of the structure, the amount of insulation, and the time of formwork and insulation removal has on mass concrete. Specifically they evaluated the peak

temperature, temperature distribution, and induced stresses in mass concrete structures (Tia et al, 2010).

Four different sized blocks were modeled using the finite element analysis model developed in their work, ranging from a 0.5 m cube to a 4 m cube. It was found that the peak temperature, maximum temperature difference, and maximum induced stress all increased with an increase in concrete dimension. It was also found that maximum stress is a function of maximum temperature difference regardless of block size, but not a function of the maximum temperature gradient alone. It was then determined that temperature difference was the better indicator of maximum stress. The maximum temperature difference, and thus the maximum stress, increases with block dimension, as seen in Figure 2-3.

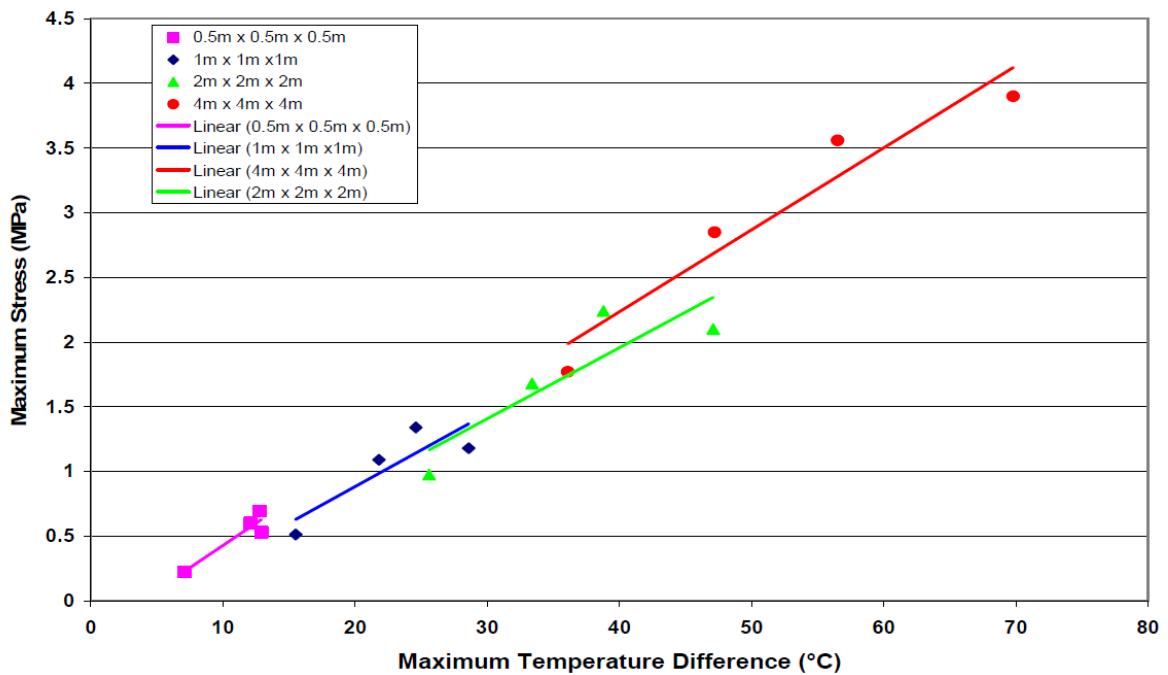


Figure 2-3. Maximum stress versus maximum temperature difference with respect to block size and type of concrete used (Tia et al, 2010)

Varying insulation thicknesses, with the same insulation value, were modeled to study its effect on the concrete temperature of varying concrete blocks with varying sizes and 100% portland cement. It was found that increasing the insulation thickness reduces the maximum temperature differences, and thus the maximum stresses, but the effectiveness of the increased thickness was dependent on concrete size. The increased insulation had a greater effect on decreasing the temperature difference in larger concrete sizes than in small concrete sizes, as seen in Figure 2-4.

The effect of varying form removal times on induced stresses was also studied. A 1 m cube of concrete was modeled using form removal times of 12 hours, 1 day, 3 days, 4 days and 6 days. A sharp increase in stress was observed to occur at the time of formwork and insulation removal. The tensile stresses were found to not exceed the tensile strengths of the concrete at any form removal time; however the tensile stresses were found to be high enough that micro-cracking could occur within the concrete until 4 days. The authors therefore suggested a minimum insulation period of 4 days to reduce the risk of micro-cracking.

Lastly, the effect of different mixes on the distribution of temperatures due to their varying rates of heat generation was studied. It was found that concretes with faster heat generation generally have higher peak temperatures. As can be seen in Figure 2-5, a 100% portland cement mix was found to have the sharpest temperature rise and the highest peak temperature, whereas the ternary blend of 50% portland cement, 30% slag, and 20% fly ash had the slowest temperature rise, and the lowest peak temperature.

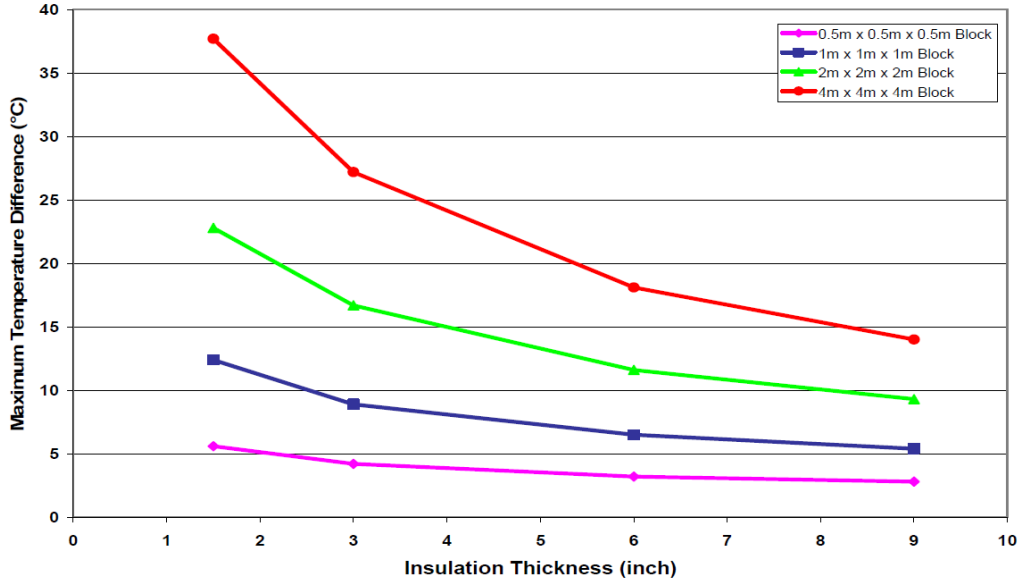


Figure 2-4. Maximum temperature difference versus insulation thickness for varying concrete dimensions (Tia et al, 2010)

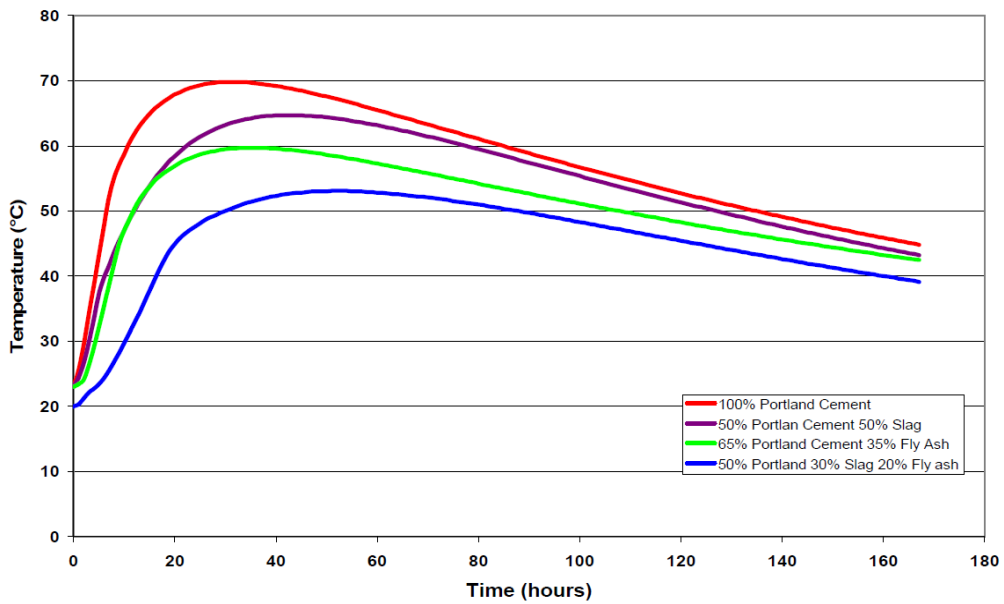


Figure 2-5. Temperature versus time of varying concrete mixes (Tia et al, 2010)

2.5.2 Temperature Prediction Methods Analysis

A study was done by Riding et al. (2006) on the effectiveness of three commonly used temperature prediction methods on calculating the maximum temperature and the time of the maximum temperature in mass concrete structures. These three common methods were: the Portland Cement Association's temperature estimation method (PCA Method), the ACI graphical method from ACI207.2R, and the Schmidt Method.

As described by Riding et al. (2006), the PCA method is a quick method for estimating the maximum temperature reached in a concrete, but it does not consider anything about the type of cement used and it does not give information about the time that the maximum temperature is reached. This method assumes that the temperature rises 12 °C for every 100 kg of cement. It is also only appropriate for concretes with cement content between 300 – 600 kg/m³ and a minimum dimension of at least 1.8 m (6 ft). The graphical method in ACI 207.2R-07 uses several empirical equations and charts to predict temperature rise for a variety of conditions. The Schmidt method, one of the more widely used methods, is based on a numerical solution for the heat transfer equation where the temperature is calculated for discrete nodes at discrete time steps, as described in ACI 207.2R-07. Typically the temperature rise for this method is calculated using the charts in ACI 207.2R, however Riding et al. also used the Schmidt method to calculate the temperatures using the adiabatic temperature from semi-adiabatic calorimetry tests. All three methods used the recommendation from ACI 207.2R that supplementary cementitious materials (SCM's) should be assumed to have half the heat of hydration of cement.

Riding et al. (2006) used these 3 methods and Schmidt's method with the adiabatic temperature results to model the temperatures of 8 mass concrete bridge members with varying size, shape, formwork, environmental exposure conditions, and mixture proportions. They found that all 3 methods underestimated the maximum temperature of the concrete structures. The graphical method in ACI and the Schmidt method both also gave poor predictions of the time at which the peak temperature took place. The Schmidt method results

were found to be greatly improved; however, when the adiabatic temperature results from semi-adiabatic calorimetry tests for each concrete mix was used in place of the ACI charts. Riding et al. (2006) attributed the errors in these results to be largely caused by the differences in modern concretes versus that which was used when the PCA and ACI guidelines were developed. Modern concrete tend to use much finer cements and consist of more chemical admixtures and more SCMs, such as fly ash, than past concrete mixes.

2.5.3 Mass Concrete Size Definition

A study was done by Ulm and Coussy (2001) to attempt to characterize a size definition of mass concrete. This study attempted to define mass concrete through the hydration heat diffusion length, the gauge length that relates thermal diffusivity and a characteristic hydration time that varies with the degree of hydration and temperature (Ulm and Coussy, 2001). Structural concrete is then defined as mass concrete when the maximum distance of any point in the concrete to its nearest free surface is greater than the heat diffusion length.

Ulm and Coussy (2001) used a series of dimensional arguments along with experimental data from normal strength concrete (NSC) and high performance concrete (HPC). They found the heat diffusion length to be 0.3 m for NSC and 0.2 for HPC. HPC has a smaller heat diffusion length because it is more susceptible to cracking due to the higher hydration rates, which results in higher temperatures.

Ulm and Coussy (2001) also discussed how the structural heat transport capacity is primarily governed by three parameters: the surface-to-volume ratio, the heat exchange length, and the heat diffusion length. The heat exchange length is associated with the formwork and the surface-to-volume ratio is a structural design parameter (Ulm and Coussy 2001). They found that the risk of early age concrete cracking could be reduced by increasing the concrete's surface-to-volume ratio and reducing the heat exchange length.

The dimensional results from this study define mass concrete by dimensions that are significantly less than typical standards. This study defined the minimal length as 0.3 m for NSC whereas most standards define the minimum dimension as 4 – 6 ft (1.2 - 1.5 m). This study, however, was based solely on temperature distribution and the maximum temperature of the concrete. The difference between their results and typical standards suggests that more than just temperature results based on thermal properties are needed to analyze and define mass concrete.

CHAPTER 3 SITE VISITS

3.1 Introduction

In order to better understand the conditions of the footings that were analyzed as part of this project, a field research trip was taken on September 12-13, 2011 to three coastal bridge sites identified by the NCDOT: Oak Island Bridge, Sunset Beach Bridge, and the US 17 Wilmington Bypass Bridge. Two additional sites where mass concrete was being placed were also visited: a highway bridge in Thomasville, NC and a railroad bridge over part of the Western Wake Freeway in Raleigh-Durham, NC. These latter two sites were visited to observe additional mass concrete examples and to gather additional information.

3.2 Oak Island Bridge

3.2.1 Site Overview

The Oak Island Bridge that was visited was part of a roadway project built as a new access to Oak Island Beach from NC 211 and is located in southeastern North Carolina. This is especially important as the bridge crosses the Intracoastal Waterway. The parts of the bridge that were identified as mass concrete were the footings at the base of the bridge bents and can be seen in Figure 3-1. Areas of observed cracking in the footing and its proximity to corrosive salt water prompted the NCDOT to recommend this bridge location for the research project.

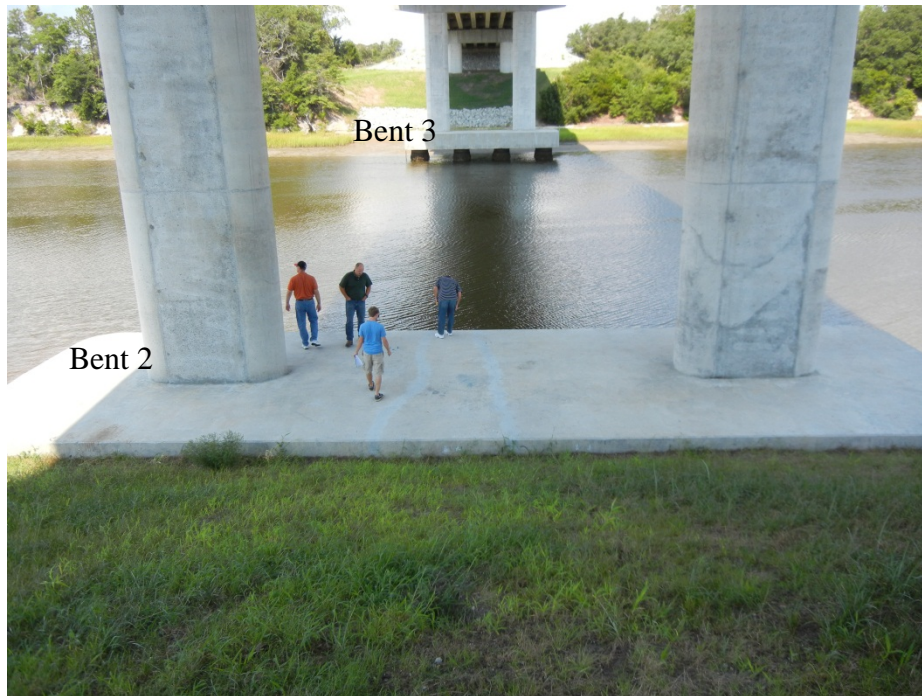


Figure 3-1. Oak Island Bridge overview of footings at bents 2 and 3

3.2.2 Footing Properties

There were two footings on this bridge that were considered mass concrete since their dimensions were 60'-6" x 20'-0" x 6'-0", the least dimension being equal to the limit of 6'-0" from the project's mass concrete specifications. The concrete mix used in these mass footings was based on the typical NCDOT design using 690 lb/yd³ of cementitious material with a 30% replacement of the cement with Class F fly ash and a 5% replacement with silica fume, as seen in Table 3-1. It should also be noted that the concrete mix had a mortar content of 16.87 cubic feet, an air content of 6.0%, and a target slump of 6.00 inches with superplasticizer. In addition, the actual concrete used in these footings had an average cylinder compressive strength of 6467 psi for bent 2 and 5820 psi for bent 3, which is above the specified minimum cylinder strength of 5000 psi.

The mass concrete footings of bent 2 and 3 were poured during early and late spring of 2008, respectively. Footing 2 was poured in six hours on March 5, 2008 from approximately 9:25am until 3:30pm with an initial concrete temperature of around 65 °F to 72 °F during the pour. Footing 3, on the other hand, was poured in eight hours on May 28, 2008 from approximately 12:10am until 8:25am with an initial concrete temperature of around 69 °F to 71 °F. As per the project’s mass concrete specification, the concrete block was cured using thermal blankets in an effort to control the temperature gradient within the concrete.

Table 3-1. Oak Island Concrete Mix Design

	Sp. Gr. (SSD)	Quantity per yd³
Cement – Type I/II		448 lb
Class F Fly ash		207 lb
Silica Fume		35 lb
Water	1.0	31.3 gal
Sand	2.64	1107 lb
#57 Stone	2.53	1600 lb
Air Entraining Agent		As Recommended
Retarder		As Recommended
Superplasticizer		As Recommended
Corrosion Inhibitor		3 gal

Temperature data from the footings at bent 2 and 3 were provided to the research team, however the thermocouple sensor locations were not given. The temperatures in footing 3 reached a maximum temperature of 160 °F around 40 hours after the pour was finished and a maximum temperature differential of 29.5 °F at around 28 hours. Both the maximum temperature and the maximum differential were under normal limits given in the standards section of the NCDOT report. The temperatures in footing 2 reached a maximum temperature of 158.7 °F around 36-48 hours after the finish of the concrete pour and maximum temperature differential of 41.0 °F at around 84 hours. This temperature differential exceeds the maximum limit of 35 °F stated in the project's mass concrete specifications, and it exceeded the limit from 51-117 hours after the concrete pour was finished. Since the thermocouple locations were not given it is not possible to identify exactly where these maximum differences occurred, but it is believed that they took place between the center of the footings and its furthest surface.

3.2.3 Site Observations

During the site visit, cracking was observed around the footings. Patch work on a couple of larger cracks was also clearly evident down the middle section of the footing at bent 2. Figures 3-2 to 3-6 show a representation of some of the cracking that was observed on site. As one can see from Figure 3-2, there were two long cracks extending across the whole top face of the footing where there is evidence of crack repair. No information could be found on when this repair was performed, but it seemed that the repaired cracks have begun to re-open to about 0.005 inches in width. In addition to this, there were vertical cracks all along the front face of the footing as seen in Figure 3-5. These cracks tended to form around the location of the imbedded sheet piling along the front face as seen in Figure 3-6. Similar cracking was also observed along the footing of bent 3 as seen in Figures 3-7 and 3-8. There were also multiple instances of smaller cracking along the footing surface that is hard to see in the photographs. The typical crack widths were 0.005-0.01 inches with some hairline cracks, and the lengths ranged from 24 inches to the full width of the footing (6 feet).

Very limited pictures and crack observations are available for the footing at bent 3 because of lack of access due to the water. Specific details of crack lengths, widths, and locations of both footings may be found on the field observation drawings that are attached in Appendix B.



Figure 3-2. Patched cracks at bent 2 footing



Figure 3-3. Bent 2 footing patched crack up close.

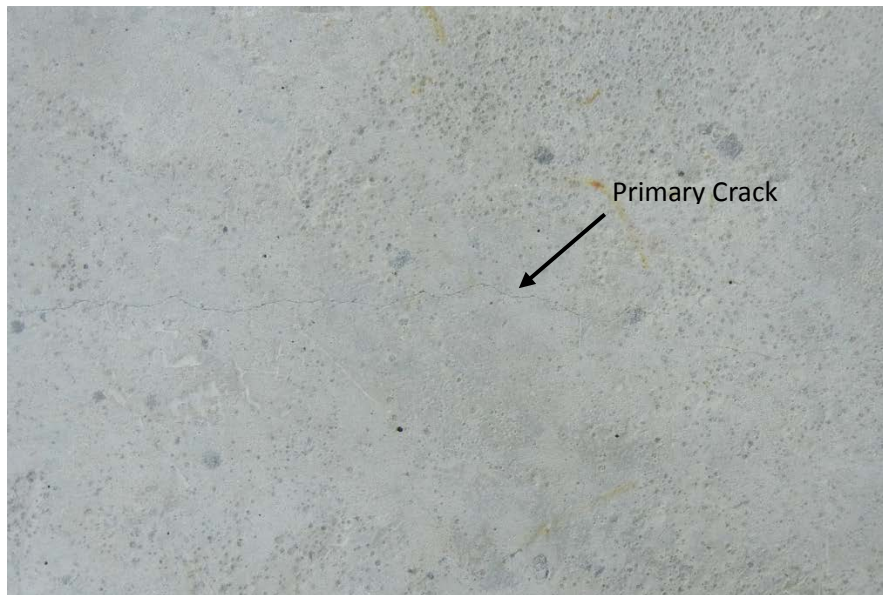


Figure 3-4. Bent 2 footing sample surface crack.

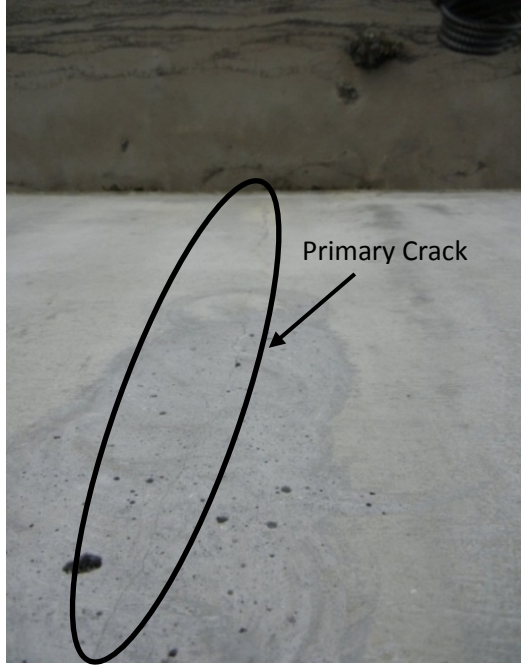


Figure 3-5. Bent 2 footing sample crack down vertical face.

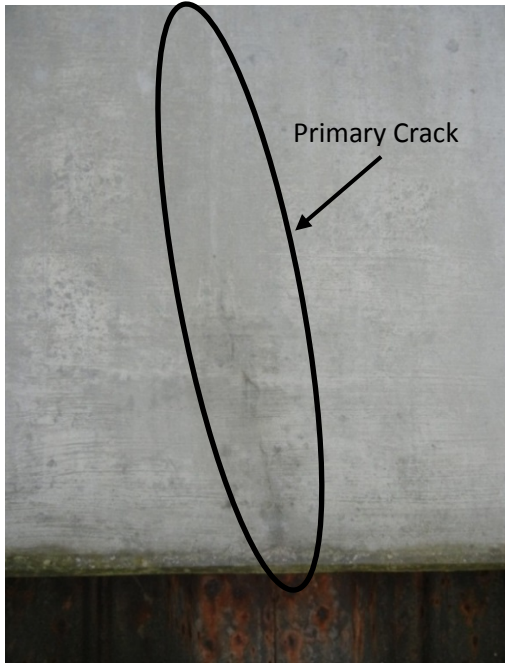


Figure 3-6. Bent 2 footing metal embedment along front face.

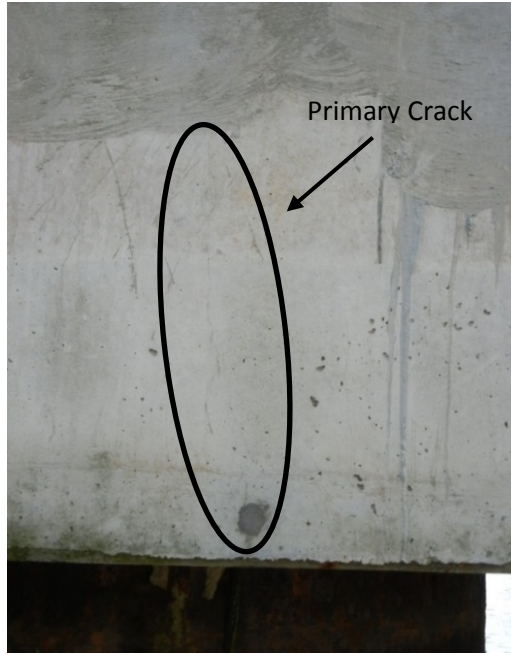


Figure 3-7. Bent 3 footing typical crack.

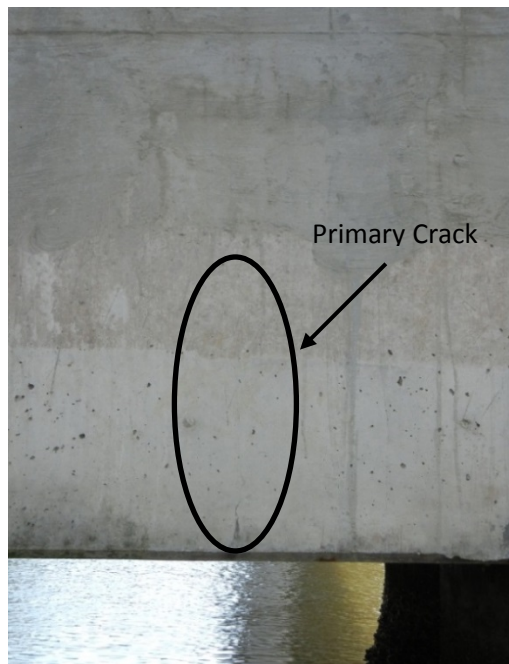


Figure 3-8. Bent 3 footing sample crack

3.3 Sunset Beach Bridge

3.3.1 Site Overview

The Sunset Beach Bridge that was visited was built over the Intracoastal Waterway by Sunset Beach near the North Carolina/South Carolina border. As with the Oak Island project, the parts of the bridge that were identified as mass concrete were the footings at the base of the bridge bents. There were multiple footings along the bridge span that met the mass concrete criteria; however only one footing was viewed because of ease of access. The other mass concrete footings were surrounded by water as seen in Figure 3-9 and a boat would have been necessary to access them.



Figure 3-9. Sunset Beach Bent 14.

3.3.2 Footing Properties

There were four footings on this bridge that were considered mass concrete since their dimensions were 42' - 0" x 27' - 0" x 6' - 0", the least dimension being equal to the limit of 6' - 0" based on the project's mass concrete specifications. As with the Oak Island Bridge, the concrete mix used in these mass footings was based on the typical NCDOT design using 690 lb/yd³ of cementitious material with a 30% replacement of the cement with Class F Fly ash and a 5% replacement with silica fume, as seen in Table 3-2. It should also be noted that the concrete mix had a mortar content of 16.28 cubic feet, an air content of 6.0%, maximum water content of 31.3 gal/ft³, and a target slump of 3.00 in. A slump of 6.00 inches was allowed with superplasticizer however. In addition, the actual concrete used in these footings had an average 28 day cylinder compressive strength of 5112 psi for the sample footing, bent 14, which is above the specified minimum cylinder strength of 5000 psi. The other three bents all had an average 28 day cylinder strength of around 6000 psi or higher.

The mass footings for this bridge project were poured during the summer of 2008 and the winter of 2008-2009. Bent footings 11 and 12 were poured in June 2008, whereas footing 14 was poured in late December 2008 and footing 13 was poured in early February 2009. The sample footing, footing 14, was poured over a six hour period on December 30, 2008 from approximately 8:25am until 2:45pm with an initial concrete temperature of approximately 60°F to 66°F during the pour. As per the project's mass concrete specification, the footing was also cured using thermal blankets in an effort to control the temperature gradient within the concrete. In addition, steel formwork was used in this pour and left in place for approximately two weeks. There was no temperature data available for any of the mass concrete footings from this site.

Table 3-2. Sunset Beach Concrete Mix Design

	Sp. Gr. (SSD)	Quantity per yd³
Cement – Type I/II		448 lb
Class F Fly ash		207 lb
Silica Fume		35 lb
Water	1.0	29.4 gal
Sand	2.64	1072 lb
#57 Stone	2.69	1800 lb
Air Entraining Agent		As Recommended
Retarder		As Recommended
Superplasticizer		As Recommended
Corrosion Inhibitor		3 gal

3.3.3 Site Observations

During this site visit, cracking was clearly visible along the top surface of the footing. A couple of cracks were also observed to continue along the whole front face of the footing. Figures 3-10 to 3-12 show a representation of some of the cracking that was observed on site. Similar to the footings at Oak Island, this footing had cracks along the top face of the footing. Unlike Oak Island, however, these cracks were wider and more visible as can be seen in Figure 3-10. The typical widths of these cracks were between 0.01-0.025 inches. These cracks also tended to start at the base of the column and move outwards toward the edge of the footing as seen in Figure 3-11. There were a few additional sets of crack lines that did not directly stem from the column base however. Also unlike the Oak Island Bridge, there were really only two main crack lines going down the front face of the footing. These vertical cracks followed what seemed to be the formwork joints down the front of the footing as can be seen in Figure 3-12. It should also be noted that the back half of the footing was covered

by soil, so no crack investigation was able to be done as the concrete was not visible. Specific details of crack lengths, widths, and locations of both footings may be found on the field observation drawings that are attached in Appendix B.

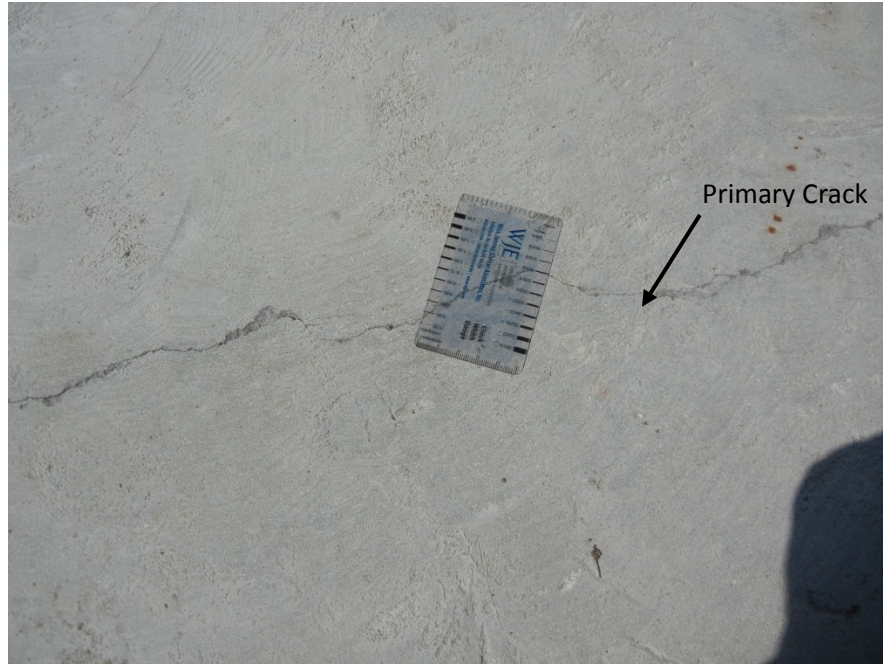


Figure 3-10. Bent 14 sample crack of about 0.02 inches.

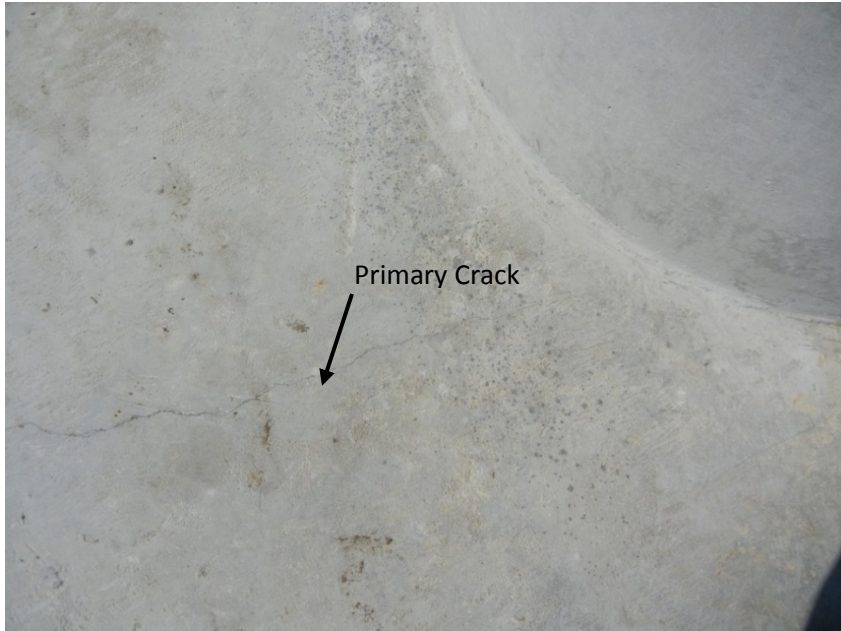


Figure 3-11. Column at base of bent 14.

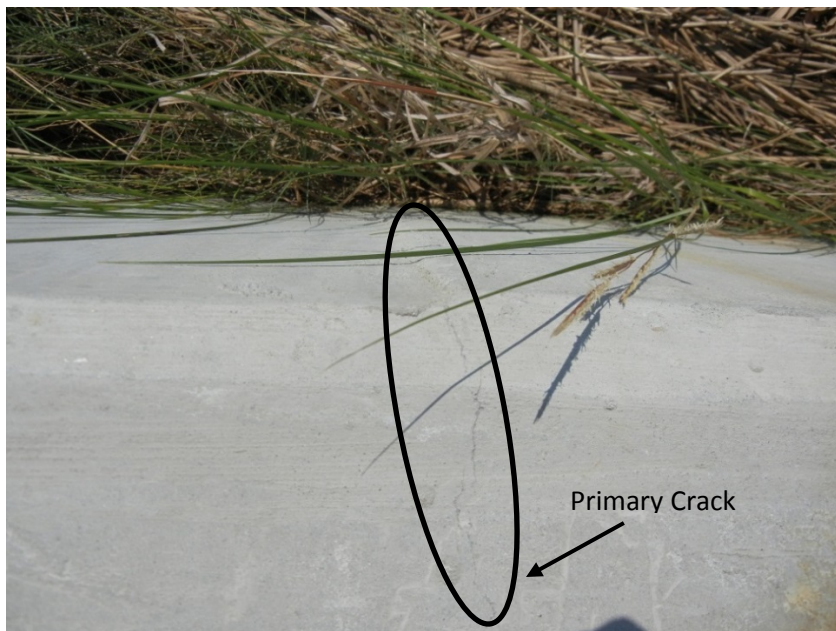


Figure 3-12. Crack along formwork joint at bent 14.

3.4 US 17 Wilmington Bypass Bridge

3.4.1 Site Overview

The US 17 Wilmington Bypass bridge, the last of the three investigation sites, is located near Wilmington, NC and connects Interstate 40 to US 17 highway. In addition, the bridge crosses over the Cape Fear River, meaning many of the mass footings were exposed to water. The footings at this site were much larger in scale than the footings at the previous two sites. This is largely due to the large span between bent 41 and bent 42, roughly 479 feet from center line to center line as seen in Figure 3-13. It should also be noted that this bridge was built in 2003, five years before Oak Island and Sunset Beach bridges.



Figure 3-13. US 17 Bypass overview.

3.4.2 Footing Properties

There were three different types or sizes of footings that fell under the project's specifications of mass concrete based on their minimum dimension. The footings of bent 41 and bent 42, the largest of the footings, had dimensions of 28.4 m x 18.6 m x 4.5 m (93' – 2" x 61' – 0" x 14' – 9"). The other footings had dimensions of 21.48 m x 7.77 m x 2.75 m (70' – 6" x 25' – 6" x 9' – 0") for the footings at bents 40 and 43, and dimensions of 6 m x 7 m x 2.5 m (19' 8" x 23' – 0" x 8' – 2") for the footing at bent 39.

Of these three different types of footings, the mix design properties and construction methods were only provided for the largest two footings. Unlike the previous two cases, the concrete mix used in these mass concrete footings was based on an older NCDOT design using 410 kg/m³ (691 lb/yd³) of cementitious material with a 25% replacement of the cement with Class F Fly ash and no silica fume, as seen in Table 3-3. It should also be noted that the concrete mix had a mortar content of 16.71 ft³, an air content of 6.0%, a maximum water content of 31.6 gal/ft³, and a target slump of 3.00 in. A slump of 8.00 in was allowed with superplasticizer. In addition, the actual concrete used in these footings had an average 28 day cylinder compressive strength of 40.5 MPa (5874 psi) for footing 41 and 37.7 MPa (5468 psi) for footing 42, both of which are above the required minimum cylinder strength of 34.5 MPa (5000 psi) as specified in the project's mass concrete specifications.

The mass concrete footings for this bridge project were poured in 2002 and 2003. Footing 41 was poured over a three day period from May 9, 2003 to May 11, 2003 with an initial concrete temperature of approximately 19°C to 22°C (66°F to 72°F). Footing 42 was also poured over a three day period from October 11, 2002 to October 13, 2002 with an initial concrete temperature of 20°C to 22°C (68°F to 72°F). Thermal blankets with an R-value of 5.2 hr-ft²-°F/Btu per inch or 2 inch Styrofoam with an R-value of 5.0 hr-ft²-°F/Btu per inch were used in an effort to control the temperature gradient within the concrete. Steel formwork was used for this pour which was stripped prior to seven days.

Table 3-3. Wilmington Bypass Concrete Mix Design

	Sp. Gr. (SSD)	Quantity per yd³
Cement – Type I/II		521 lb
Class F Fly ash		207 lb
Silica Fume		0 lb
Water	1.0	31.2 gal
Sand	2.65	1144 lb
#57 Stone	2.43	1560 lb
Air Entraining Agent		As Recommended
Retarder		As Recommended
Superplasticizer		As Recommended
Corrosion Inhibitor		3 gal

3.4.3 Site Observations

During this site visit, three different footing types were observed that clearly met and exceeded the mass concrete size limit of 1.8 m, or 6 ft. Although all three types of footings were inspected, pictures are only available for the largest set of footings due to a camera failure. However, inspection drawings were still recorded for all three footing sizes.

Figures 3-14 to 3-17 show some of the cracking that was observed on site on the footings at bents 41 and 42. As one can see from Figure 3-14 and Figure 3-15, there was extensive map cracking on the top face of the footings. The cracks were previously outlined in red spray paint during a bridge inspection done in April 2011. The cracking was much more extensive than the cracking on the two previous bridges; however this could be caused by the age difference and crack propagation over this time period. There were also a few spots of more extensive cracking where it looks like some patch work was done, as seen in Figure 3-15. In addition, there were a significant number of vertical cracks that extended

along the vertical faces of the footings, as seen in Figure 3-16. There were also a few horizontal cracks mixed in on the vertical faces as seen in Figure 3-17. The smaller footing types that were inspected had some similar cracking patterns; however they were on a smaller scale. All footing cracking patterns along with some of their spacing can be referenced from the field observation drawings that are attached in Appendix B.



Figure 3-14. Bent 41 footing sample map cracking.



Figure 3-15. Bent 41 footing sample map cracking along with some more severe cracking.

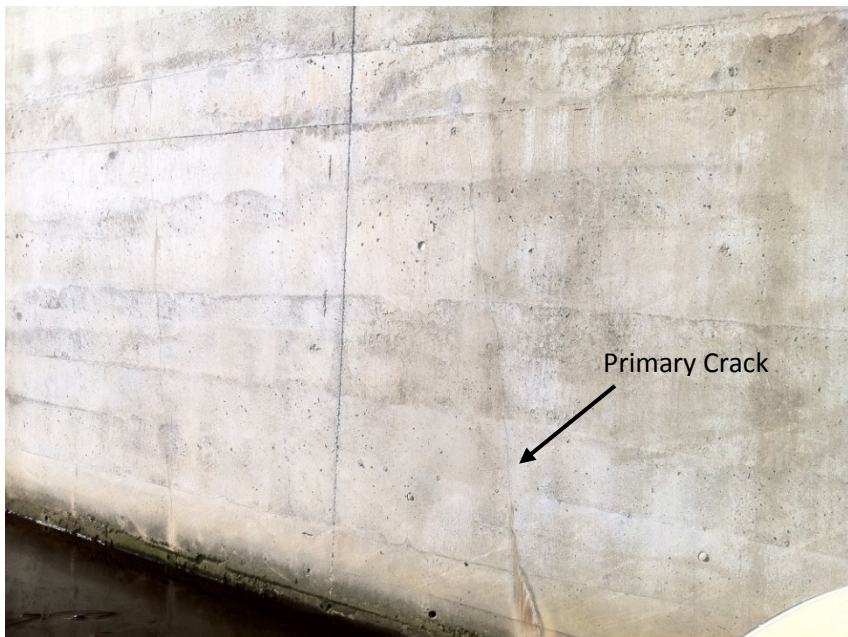


Figure 3-16. Footing 42 sample vertical crack.

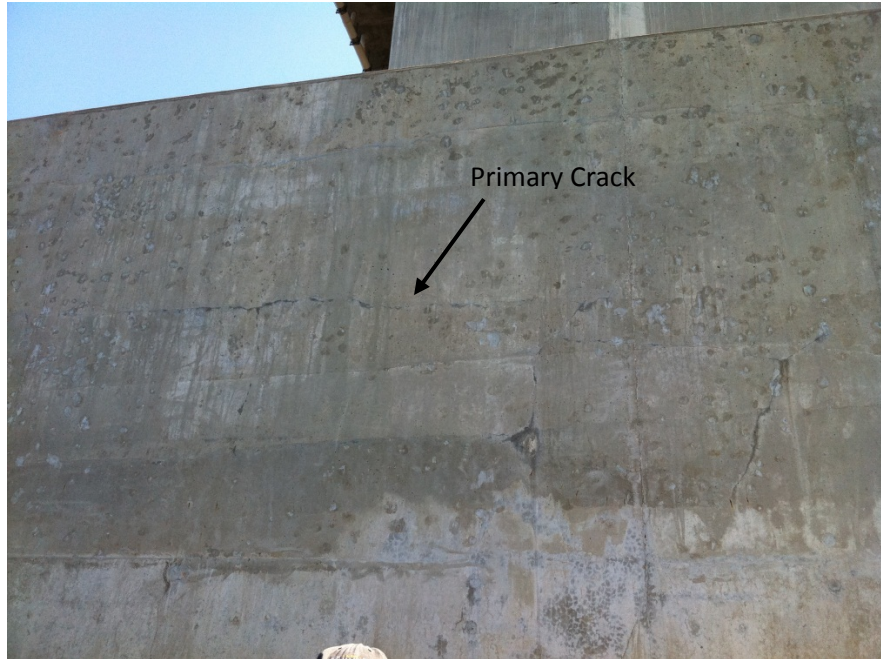


Figure 3-17. Footing 42 additional horizontal cracking on vertical face.

3.5 Western Wake Site

3.5.1 Site Overview

The Western Wake site that was visited was part of an extension of Interstate 540 in western Wake County. The part of this highway expansion project that was identified as mass concrete was the footings of a railroad bridge that spans across the multi-lane highway. There were two U-shaped footings that had outside width dimensions ranging from 13 – 24 ft, outside length dimensions ranging from approximately 49 – 99.5 ft, and a height of 5 ft, which is less than the typical NC limit of 6 ft., as seen in Figure 3-18. There was also a rectangular footing with dimensions of 16 ft wide, 94.5 ft long, and 5 ft in height in between the two U-shaped abutment footings.

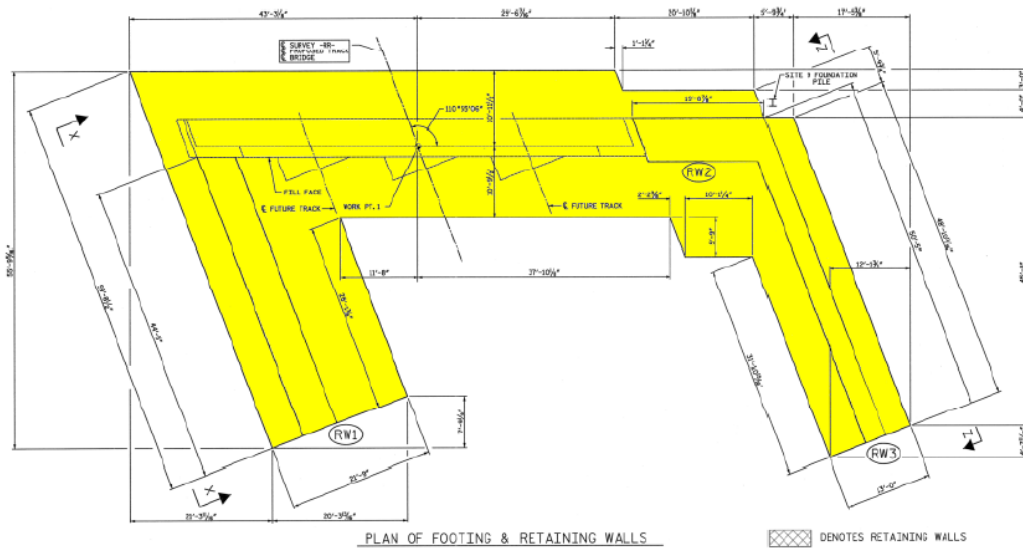


Figure 3-18. Western Wake abutment 1 footing overview

This site was visited on September 13, 2011 because it was an ongoing mass concrete pour for the NCDOT. Prior to the visit, the footing at abutment 1 had already been poured as seen in Figure 3-19, and the footing on abutment 2 was about to be poured as seen in Figure 3-20. The reason that this site was observed was because of the project’s unique mass concrete mix design, as discussed in Section 3.5.2, and its unique cooling plan, as discussed in Section 3.5.3. Temperature results were gathered by the Raleigh-Durham Roadbuilders and reviewed by the research team. The results are discussed in Section 3.5.4.



Figure 3-19. Western Wake Abutment 1 footing



Figure 3-20. Western Wake Abutment 2 footing

3.5.2 Footing Concrete Mixture

As stated in the previous section, these footings were of particular interest because of limitations put on the mix design specified for the railroad mass concrete footings. In this mix design, no pozzolan was allowed to be used as a partial replacement for the cement as seen in Table 3-4; therefore other methods of temperature control were required. It should also be noted that the concrete mix had a mortar content of 16.20 ft³, an air content of 5.0%, a w/c ratio of 0.494, and a target slump of 4.00 in.

Table 3-4. Western Wake Concrete Mix Design

	Sp. Gr.	Quantity per yd³
Cement – Type I/II		590 lb
Class F Fly ash		0 lb
Silica Fume		0 lb
Water	1.0	35 gal
Fine Aggregate (2S)	2.63	1177 lb
Course Aggregate (#67)	2.67	1800 lb
Air Entraining Agent		As Recommended
Retarder		As Recommended
Water Reducer		As Recommended

3.5.3 Thermal Control Measures

In order to control the high heat developed from a mix with no fly ash replacement, a cooling pipe system was specified, as seen in Figure 3-20, to control the maximum temperature and the maximum temperature difference. The maximum temperature allowed

was 158 °F and the maximum temperature difference between the center and the exposed concrete surface was 35 °F. It should also be noted in the cooling pipe layout that there were two rows of cooling pipes with a typical horizontal spacing of 2.5 ft, and a typical vertical spacing of 3 ft with a typical concrete cover of 1.25 ft on the top and bottom. These ¾ in diameter cooling pipes provided a flow rate of about 4-5 gallons per minute. The layout plan for this cooling pipe system can be seen in Figure 3-21.

Additionally, two thermal blankets with a thickness of 0.316 inches and an effective R-value of 1¼ hr-ft²-°F/Btu per blanket were used to help control the thermal gradient within the concrete. These blankets were used to completely cover all formed and exposed concrete as well as the protruding reinforcing steel up to 3 ft from the concrete. A concrete placement temperature of 65 °F was also used to control the maximum temperature reached.

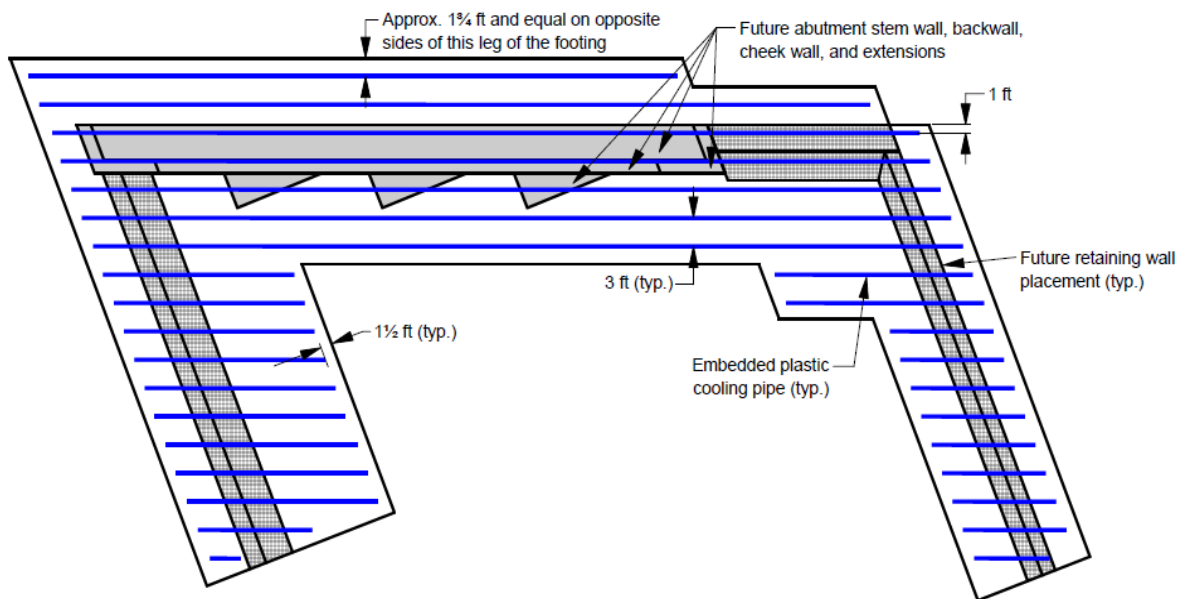


Figure 3-21. Abutment 1 footing's cooling pipe layout

3.5.4 Temperature Monitoring

In order to ensure that the temperature controls worked properly, temperature sensors were placed within each footing by the Raleigh-Durham Roadbuilders for monitoring purposes at the locations of anticipated highest temperature. Two temperature sensors were placed in the center of the concrete (mid height) at approximately the mid width and mid length of the longest leg of the footing. These sensors were also kept away from any protruding steel and equidistant from the cooling pipes. A second set of temperature sensors were placed directly above the first set of sensors approximately 2-3 inches below the concrete surface.

These temperatures were then monitored until the following prescribed thermal criteria was met: the concrete reached an age of at least 3 calendar days, the hottest portion of the concrete began cooling, and the difference between the hottest part of the concrete and the ambient temperature was below 35 °F. At that point all temperature monitoring and thermal controls were stopped.

The temperature data recorded by the Raleigh-Durham Roadbuilders of the footings at abutments 1 and 2 is shown in Figure 3-22 through Figure 3-25. The temperature data for the rectangular bent footing is also shown in Figure 3-26 and Figure 3-27. As one can see in these figures, the maximum temperature of 158 °F and the maximum difference of 35 °F were never reached due to the thermal control measures used in this pour.

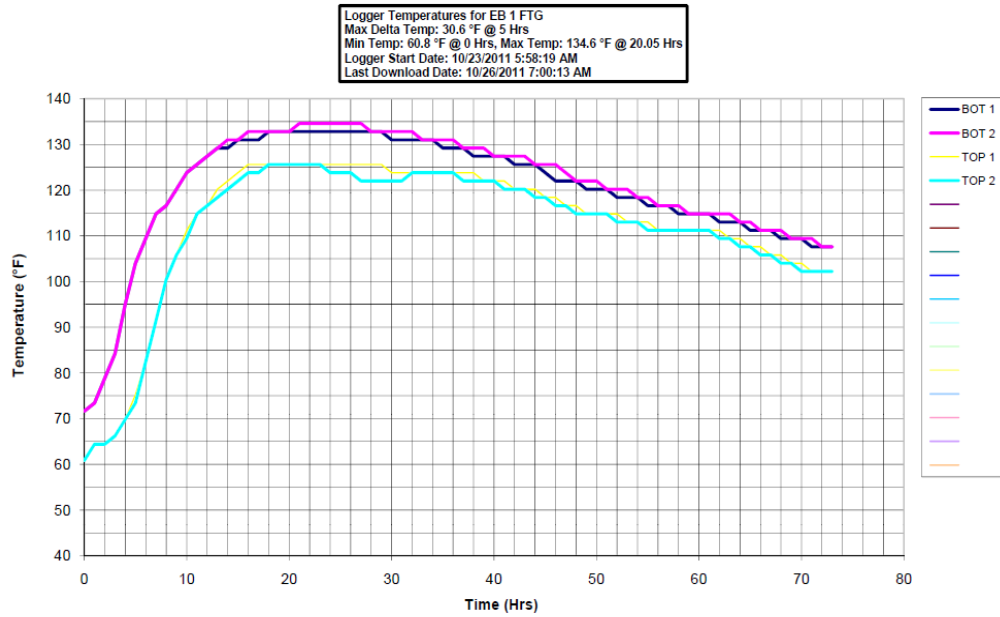


Figure 3-22. Temperature data from Abutment 1 footing sensors

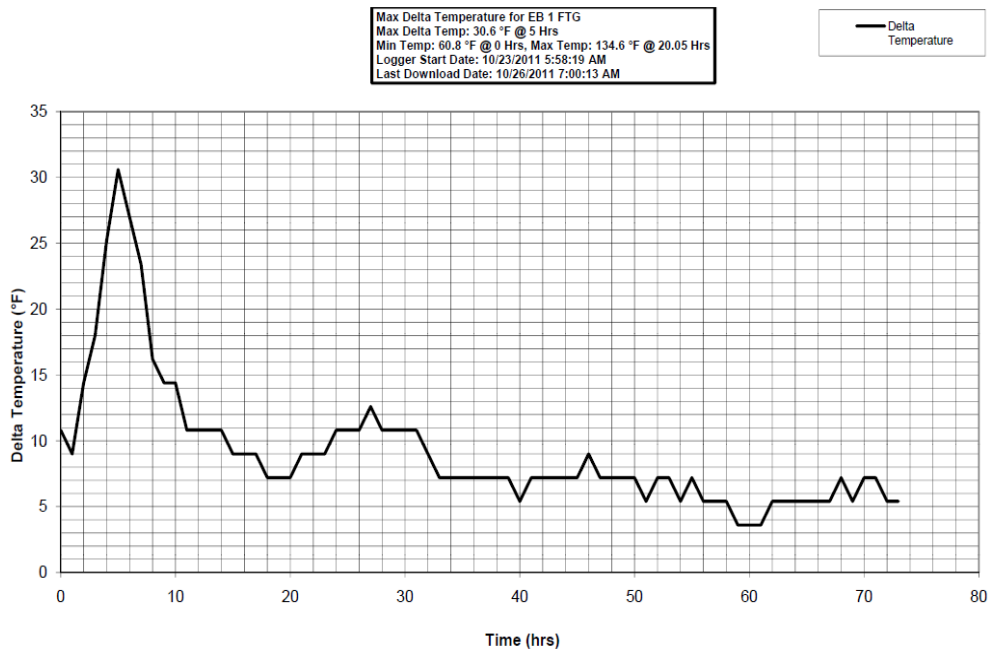


Figure 3-23. Max temperature difference from Abutment 2 footing sensors

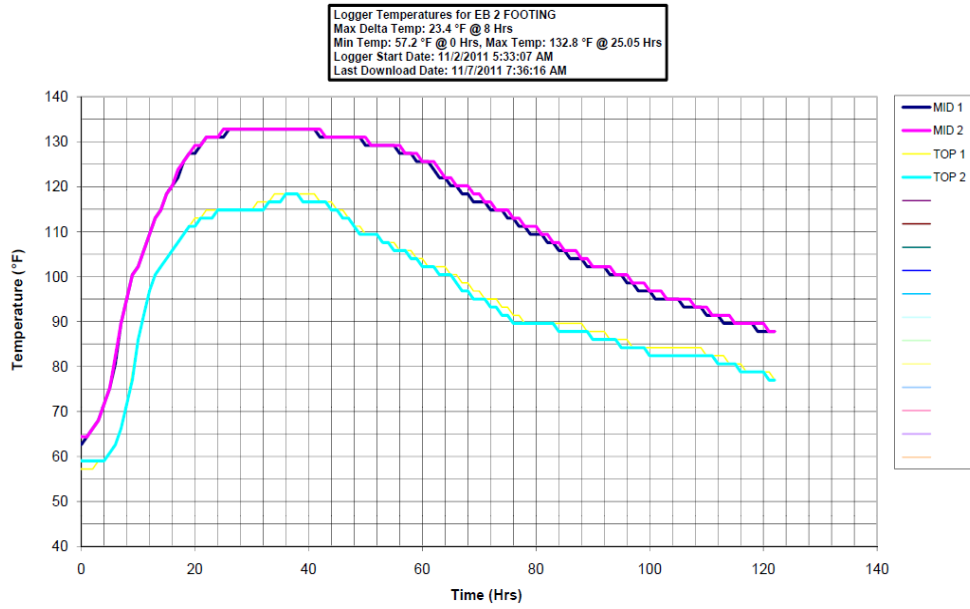


Figure 3-24. Temperature data from Abutment 2 footing sensors

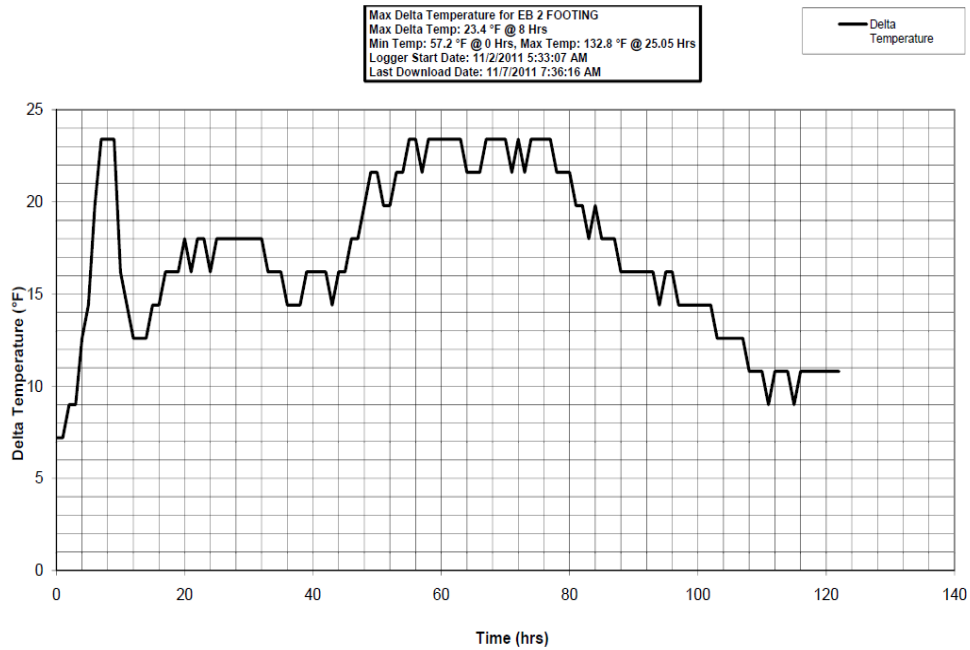


Figure 3-25. Max temperature difference from Abutment 2 footing sensors

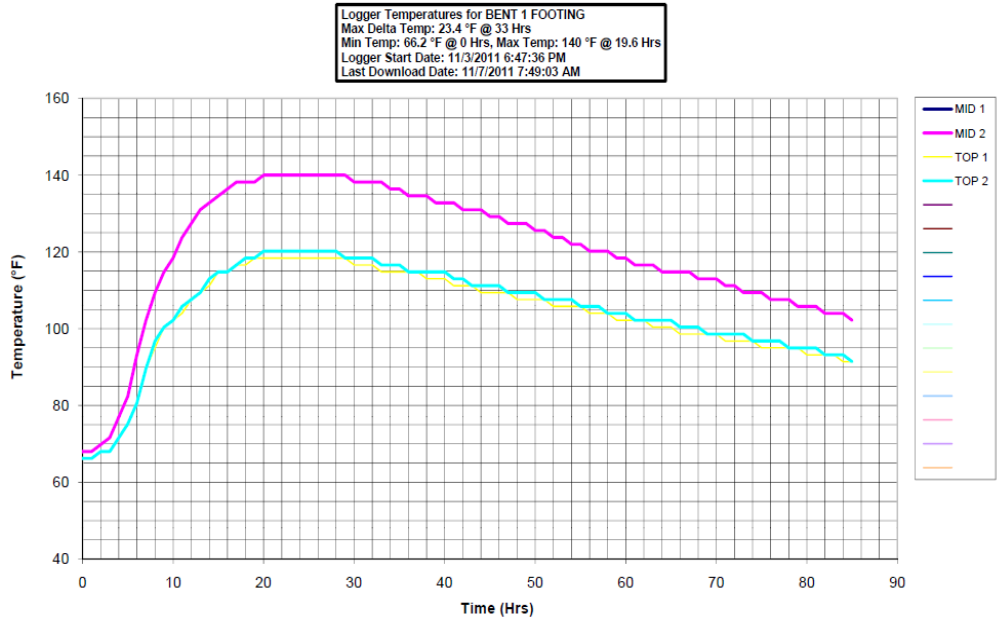


Figure 3-26. Temperature data from the rectangular bent footing sensors

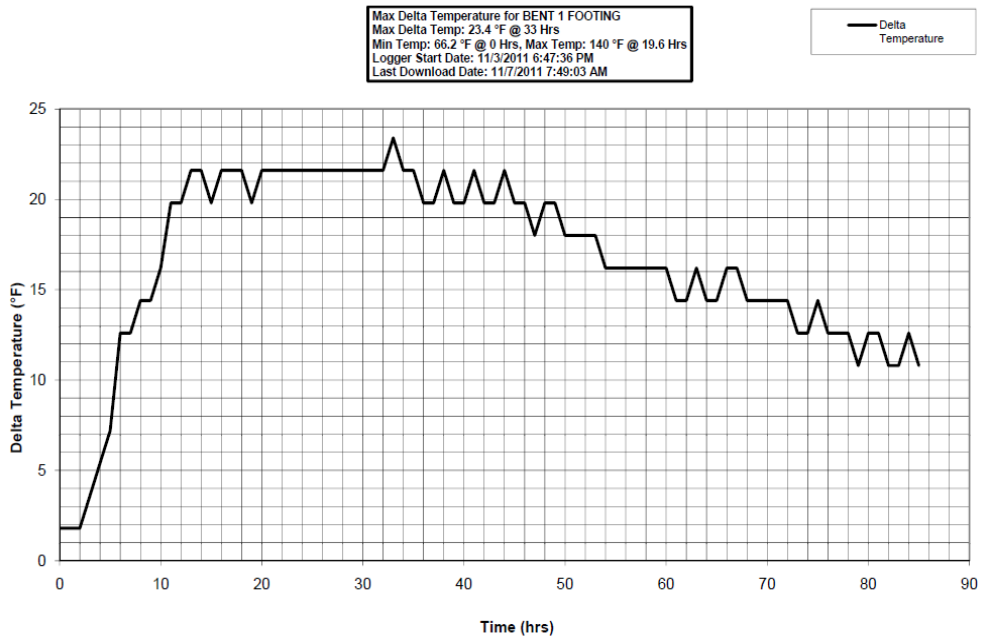


Figure 3-27. Max temperature difference from the rectangular bent footing sensors

3.6 Thomasville Site

3.6.1 Site Overview

The Thomasville site located in Davidson County, NC, was a bridge overpass that crosses over US 29/70 BUS I-85. The bridge connects Old Greensboro Road to Lexington Avenue, next to Pineywood Drive. Similar to the Western Wake site, this was another somewhat unique mass concrete pour. Unlike what most projects considered mass concrete pours, the minimum dimension of this end bent pour was 2'-10", much less than the 5-6 ft typically specified. Despite this, the NCDOT specified these end bent sections as mass concrete in the project's mass concrete specifications section.

The bridge site was visited on February 20, 2012. At the time of this visit, the abutment for End Bent 2 had already been poured on February 9, 2012 and the abutment for End Bent 2 was being prepped to be poured, as can be seen in Figure 3-28.



Figure 3-28. Thomasville End Bent 1 mass concrete pour

3.6.2 Thermal Control Plan

The thermal control plan for this pour was similar to that of the other pours at Oak Island and Sunset Beach. Unlike those plans however, there is no silica fume in the concrete mix and the minimum 28 day cylinder strength allowed is 3500 psi. No mix design was available to the research team for this mass concrete pour, but it is very likely that it too was similar to the mix designs of the Oak Island and Sunset Beach sites. In addition to this, it should be noted that wood formwork and insulation blankets were used for this mass concrete pour.

3.6.3 Temperature Monitoring

The thermal control plan for this project did not specify any type of temperature monitoring plan, therefore the members of this research team set up a system of thermocouple temperature sensors to monitor the temperature development within the concrete. The thermocouple layout can be found in Figure 3-29 and Figure 3-30. It should be noted that all thermocouples, except for sensor 1 at the very center, are located about 3-5 in from its closest surface. An ambient temperature sensor was also set up near end bent 2. Thermocouple Type-T wire was used for the sensors and a Humbolt Multi-Channel Maturity Meter was used to record the concrete temperatures through its curing period. The data acquisition setup can be seen in Figure 3-31.

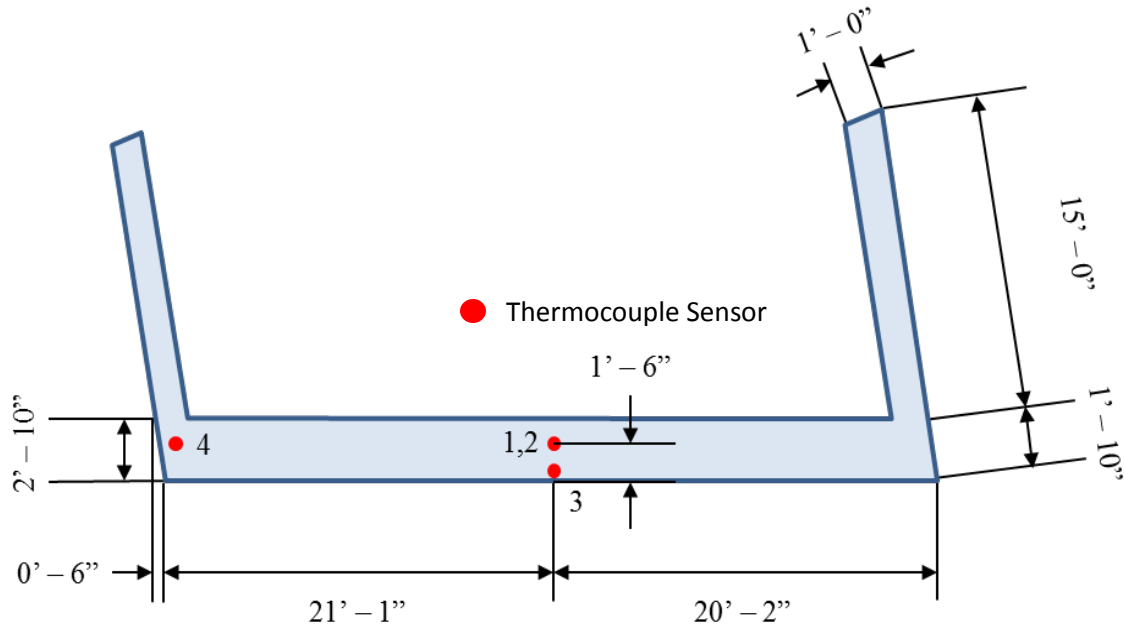


Figure 3-29. Plan view Thomasville End Bent 1 mass concrete pour

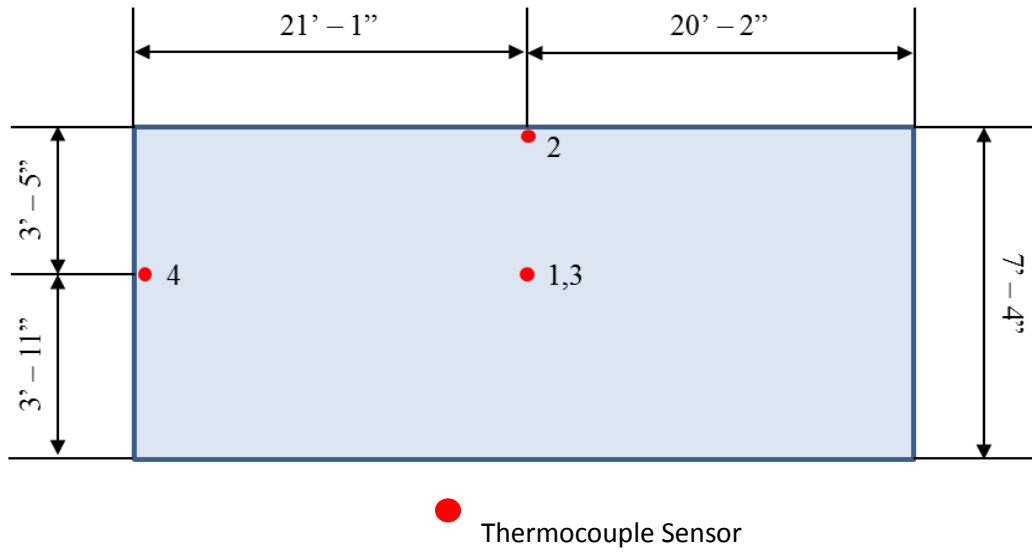


Figure 3-30. Elevation view from the front of the Thomasville End Bent 1 mass concrete pour



Figure 3-31. Thermocouple-maturity meter setup.

The results from the temperature monitoring can be found in Figure 3-32 and Figure 3-33. Figure 3-32 shows all of the temperature data from the four thermocouple sensors within the concrete as well as the thermocouple sensor taking the ambient temperature readings. Figure 3-33 is of the temperature differences between the center thermocouple, sensor 1, and the other thermocouples. In reference to Figure 3-33, “top” refers to sensor 2, “center outside” refers to sensor 3, and “center-center outside” refers to sensor 4.

This mass concrete pour was started between 9:00-10:00 am on February 23, 2012 and was finished around noon. There was a slight spike in the thermocouple data in the first 8 – 12 hours as one can see in Figure 3-32, but the cause is unknown. At approximately the 120 hours (5 days) there is another spike for sensor 3. This was likely caused by insulation removal from the top surface. The fluctuations in temperature after this point can be

attributed to insulation removal since the variation correlates with the ambient temperature. Finally, as one can see in Figure 3-33, the maximum differential of 35 °F was never reached during the curing period. There was no maximum temperature limit in the project's mass concrete specifications, but it should be noted that the typical limit of 158 °F was not reached. No cracking was ever reported from this pour to the research team.

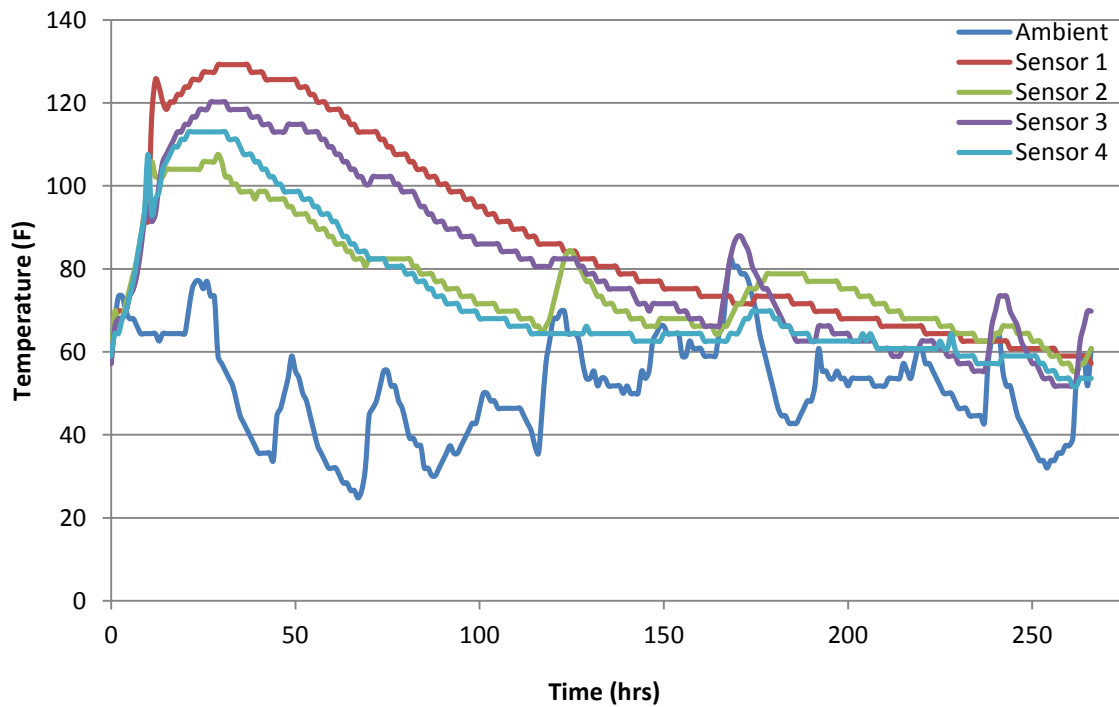


Figure 3-32. Temperature data from Thomasville thermocouple sensors

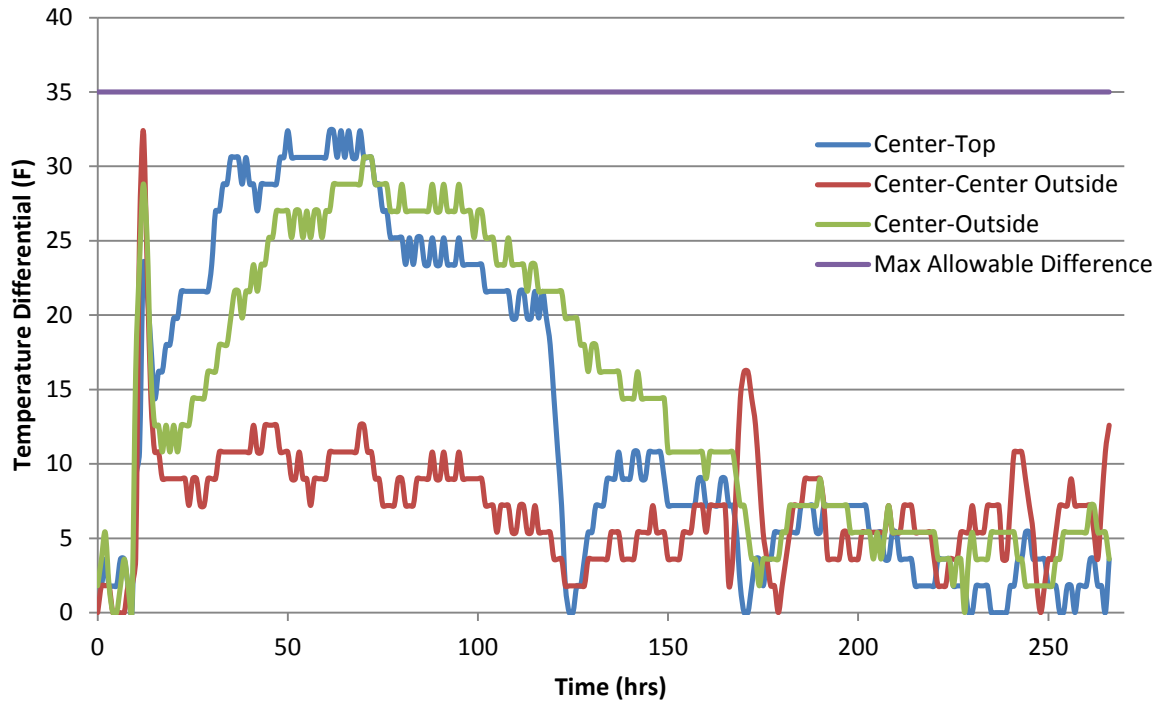


Figure 3-33. Temperature differences between Thomasville thermocouple sensors

CHAPTER 4

FINITE ELEMENT MODELING

4.1 Introduction

One of the goals of this project was to use a numerical modeling program to model mass concrete footings by predicting the spatial distributions of temperature throughout the concrete and its induced stresses. Using one such program, the temperature rise due to the internal early age hydration of the concrete and the correlating thermal gradients within the mass concrete can be computed. These thermal gradients then lead to induced thermal strains within the concrete due to internal and external restraints. Additionally, the evolution of the viscoelastic concrete mechanical properties, including elastic modulus, tensile strength, and shrinkage, can be modeled alongside the hydration induced temperatures as a function of time. The thermal strains combined with these concrete mechanical properties can then be translated into thermal stresses. When the resulting tensile thermal stresses are greater than the tensile strength of the concrete, cracking will occur.

Multiple numerical modeling computer programs were explored for use in this research. Initially ConcreteWorks V2.0, created by Riding et. al (2005) for the Texas DOT, was assessed by the research team as an option for analyzing the mass concrete footings. After detailed investigation into the program, however, it was determined that the program was unsuitable for this project for a number of reasons as described in Section 4.2. In light of this, other options were explored. The finite element software programs FEMMASSE (2013), CESAR LCPC V.5 (2011), and TNO DIANA (2005) were assessed as possible software options, as all three had early age concrete modeling components to them. FEMMASSE had a wide range of possible inputs that gave it the ability to model early age concrete temperature and stress distributions, but it lacked the ability to perform the 3D modeling that this project desired. CESAR LCPC on the other hand had the ability to create 3D models, but its input ability was more limited than the other two programs. In the end TNO DIANA was

chosen due to its wide range of input possibilities and its 3D modeling capabilities. TNO DIANA's ability to model the necessary thermal and mechanical properties, as well as its ability to model external supports, reinforcement and cooling mechanisms such as cooling pipes and thermal blankets, made it an ideal program to use for the thermal analysis of early age mass concrete footings.

4.2 ConcreteWorks V2.0 Assessment

ConcreteWorks is a free software modeling program that was created by Riding (2007), as a part of his doctoral work under the supervision of Dr. Folliard, at the University of Texas in Austin, Texas; it can be found online for free at www.texasconcreteworks.com. The concrete modeling program was developed as a modeling tool to be used by the Texas Department of Transportation to estimate the temperature development over time in mass concrete, bridge decks, precast concrete beams, and pavements based on their concrete mix design and construction methods. In addition, the program can also predict the chloride service life of mass concrete and bridge deck as well as predict the early age thermal cracking risk of mass concrete members. For this project, only the mass concrete module was assessed for its applicability.

After a period of assessing ConcreteWorks, it was concluded that the program is unsuitable for this project. ConcreteWorks was designed to be a very user friendly, easy to use program, and it does achieve this goal. The model inputs are for the most part straight forward and not difficult to interpret, and many of these inputs are information that contractors would likely have access to. This simplification, however, creates a problem when the user has a more unique problem to model because of the limited input ability of the program. This is most notable in the inability of the user to create his or her own boundary conditions. Since the stresses induced in the mass concrete footing largely depend on the restraint of the concrete, in addition to the thermal gradients, different boundary conditions can have different effects on the stress distribution. For example, the popular method of

supporting footings with concrete piles can create different stress conditions. ConcreteWorks, however, limits the boundary conditions to allow a fixed base only.

The issue of model simplification was also found in the construction input choices. The insulation blanket R-value was found to have a limit of $5.67 \text{ hr-ft}^2\text{-}^\circ\text{F}/\text{BTU}$ ($1.0 \text{ m}^2\text{-}^\circ\text{C}/\text{W}$) and the thickness was preset to be 0.02 m (0.79 in) thick. It was also found that there were limitations with the construction methods when it came to modeling the curing. The program does not allow the user to have both formwork and the insulation blankets on the concrete model at the same time. Instead, the blankets are not allowed to be modeled on the surface of the concrete until after the formwork is removed and curing methods are “stopped”.

In addition, limitations were also found with the ConcreteWorks stress output. Most notable of these was that there was no access to the stress data from the mechanical model. Despite the fact that the user inputs values to calculate the elastic modulus and strength of the concrete and the program calculates the stresses in each control volume, only the overall cracking probability of the whole model is available as output. There is no provision to determine where in the model the tensile stresses exceed the tensile strength, which leads to a very limited sense of confidence in the stresses by the user. The stress calculation was only available for a 2D plane stress model and was not available for 3D models. This could cause potential problems with the stress output if the stresses in the third direction are actually relatively large compared to the other two directions (Riding, 2007).

Lastly, there were also some limitations in the temperature calculations and results from the ConcreteWorks model. As a result of different trials, some issues were found to occur in the temperature calculations when using curing methods and/or the equivalent age maturity method in the 3D models. When curing methods were used in combination with a 3D model it resulted in inconsistent temperature graphs where the temperature would repeatedly fluctuate between the predicted temperature and 32°F (0°C). When the equivalent age function was used to calculate the maturity in a 3D analysis, an error was

found to occur resulting in unfinished temperature calculations in some cases. Once the user successfully receives a temperature output, ConcreteWorks produces the maximum temperature and the maximum temperature difference as its output for the analysis. This maximum temperature difference, however, is for the entire concrete member whereas the standard practice is to measure the maximum temperature difference between the center of the concrete member and its closest outside face. In order to compare the results with the infield data from common practice, the user must go through the temperature data and manually locate the data for the desired locations.

After this assessment, it was decided that ConcreteWorks is unsuitable for this research project. Although the program does do thermal analysis for early age concrete, the output could not be used confidently to make any conclusions for the necessary analyses. In light of these shortcomings, other programs were assessed for possible use in this research project and finally TNO DIANA was selected.

4.3 DIANA Finite Element Modeling

The commercial finite element software TNO DIANA was ultimately chosen to analyze the coastal bridge footings due to its ability to model the temperature evolution of early age concrete during hydration as well as its nonlinear mechanical properties. This is accomplished through the program's wide range of thermal and mechanical input possibilities that tailor to the user's needs as well as through its 3D modeling capabilities. TNO DIANA also provides the user with easy access to temperature and stress outputs through an easy to use graphical interface called FX+. Sample model input can be found in Appendix C.

In order to model the early age hardening coastal bridge footings, TNO DIANA combines two analyses in a coupled thermo-mechanical analysis. A thermal flow analysis is used to model the temperature evolution in concrete due to early age hydration. A structural analysis then uses the thermal gradients created within the thermal model as an external load and calculates the stresses induced from the load over time. In this staggered flow-stress

analysis, the concrete, formwork, and insulation are explicitly modeled. The concrete was modeled in both the thermal and structural analysis, whereas the formwork and insulation was only modeled in the thermal flow analysis. This was because the main area of concern was with the stresses induced within the concrete. The formwork and insulation was seen to have a negligible effect on this.

4.3.1 DIANA Thermal Model

A linear flow analysis was used to model the temperature distribution over time within hydrating concrete. These temperatures were modeled through a combination of heat of hydration, thermal heat capacity, thermal conductivity, and external environmental inputs. The concrete's coefficient of thermal expansion was also modeled; however this directly affects the thermal stresses so this is discussed in the structural model section. The temperature, the degree of hydration, and the equivalent age within the concrete versus time were then able to be extracted as output from the model.

The concrete, formwork, and insulation were modeled using linear eight-noded isoparametric brick elements, known as HX8HT elements as seen in Figure 4-1A, for the temperature flow analysis. Linearly interpolated elements were used because temperature flow changes linearly in x, y, and z directions. A 2 x 2 x 2 Gauss integration scheme was used in the integration of these elements. The external environment was then modeled using four-noded isoparametric quadrilateral boundary elements, known as BQ4HT elements in TNO DIANA, as seen in Figure 4-1B. These elements were modeled on the surface of the outside concrete, formwork, or insulation HX8HT element where they shared the corner nodes. A 2 x 2 Gauss integration scheme was used with these elements.

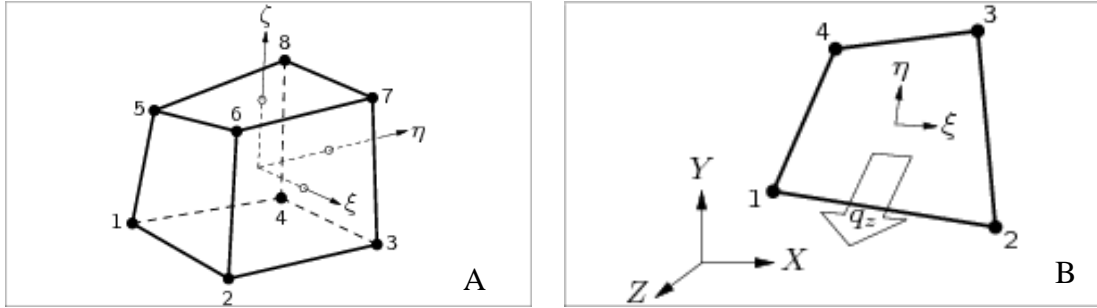


Figure 4-1: Thermal analysis modeling elements

A) HX8HT isoparametric element

B) BQ4HT isoparametric element

4.3.1.2 Heat of Hydration

The temperature change within early age concrete is largely due to the heat produced during the chemical reaction in cement hydration. TNO DIANA has three options for modeling the heat of hydration in the concrete: a pre-processing method, a direct input method, and a user-supplied subroutine method. The preprocessing method uses the adiabatic temperature rise from hydration vs. time from a semi-adiabatic or an isothermal calorimetry test as the input. The direct input method on the other hand uses the direct relationship between the rate of heat of hydration and the degree of hydration as the input. The last method, the user input method, allows the user to model the heat production rate as a function of the temperature, the degree of reaction, the equivalent age, and/or the current time. The user-supplied subroutine method was implemented in this research due to insufficient access to a calorimetry machine and for its flexibility in modeling various concrete mix proportions.

An empirical model originally developed by Schindler and Folliard (2005), later improved by Poole (2007) under the supervision of Schindler and Folliard, and most recently improved by Riding et al (2012), was used to model the early age heat of hydration

development. The empirical model, found in Equations 4-1 through 4-7, models the rate of heat generation per unit volume:

$$Q_h(t) = H_u \cdot C_c \cdot \left(\frac{\tau}{t_e}\right)^\beta \cdot \left(\frac{\beta}{t_e}\right) \cdot \alpha_u \cdot e^{-\left[\frac{\tau}{t_e}\right]^\beta} \cdot e^{\frac{E_a}{R}\left[\frac{1}{T_r} + \frac{1}{T_c}\right]} \quad (4-1)$$

where: Q_h = the rate of heat generation per unit volume (J/m³-hr)

E_a = apparent activation energy (J/mol)

R = the universal gas constant = 8.314 J/mol/K (10.732 ft³ psi/°R/lb-mol)

t_e = equivalent age (hours)

H_u = the total heat available for reaction at 100% hydration (J/gram)

C_c = the total amount of cementitious material (kg/m³)

α_u = the ultimate degree of hydration at $t = \infty$

τ = the hydration time parameter (hours)

β = the hydration slope parameter

T_r = the equivalent age reference temperature (K)

T_c = temperature of the concrete (K)

The empirical model is based on the cement constituent material properties as well as the concrete mixture proportions (Riding, 2007). The apparent activation energy, E_a , was developed by Poole (2007) using a series of 117 isothermal calorimetry tests. The equations for the total heat available for reaction, H_u , and the parameters τ , β , and α_u were updated by Riding et al. (2012) using 300 semi-adiabatic calorimetry tests. These equations were validated by Riding et al. using a collective database set of tests from Schindler and Folliard (2005), from Ge (2005), from their own tests, and from in situ construction site samples (Riding et al, 2012).

Two sets of equations were developed: one using the Rietveld method of determining cement chemical composition and one using the Bogue method based on ASTM C 150. This project used the equations based on the Bogue method of determining cement chemical

composition because that is currently the most common way that concrete plants measure their cement:

$$E_a = 41,230 + 1,416,000 * [(p_{C_3A} + p_{C_4AF}) * p_{cem} * p_{SO_3} * p_{cem}] - 347,000 * p_{Na_2O_{eq}} - 19.8 * Blaine + 29,600 * p_{FA} * p_{FA-CaO} + 16,200 * p_{slag} - 51,600 * p_{SF} - 3,090,000 * WRRET - 345,000 * ACCL \quad (4-2)$$

$$H_u = H_{cem} * p_{cem} + 461 * p_{slag} + 1800 * p_{FA-CaO} * p_{FA} + 330 * p_{SF} \quad (4-3)$$

$$H_{cem} = 500 * p_{C_3S} + 260 * p_{C_3A} + 420 * p_{C_4AF} + 624 * p_{SO_3} + 1186 * p_{FreeCa} + 850 * p_{MgO} \quad (4-4)$$

$$\alpha_u = \frac{1.031 * \frac{w}{cm}}{0.194 + \frac{w}{cm}} + \exp \left(\begin{array}{c} -0.0885 - 13.7 * p_{C_4AF} * p_{cem} \\ -283 * p_{Na_2O_{eq}} * p_{cem} \\ -9.90 * p_{FA} * p_{FA-CaO} \\ -339 * WRRET - 95.4 * PCHRWR \end{array} \right) \quad (4-5)$$

$$\tau = \exp \left(\begin{array}{c} 2.92 - 0.757 * p_{C_3S} * p_{cem} + 98.8 * p_{Na_2O} * p_{cem} + 1.44 * p_{slag} \\ + 4.12 * p_{FA} * p_{FA-CaO} - 11.4 * ACCL + 98.1 * WRRET \end{array} \right) \quad (4-6)$$

$$\beta = \exp \left(\begin{array}{c} -0.464 + 3.41 * p_{C_3S} * p_{cem} - 0.846 * p_{slag} + 107 * WRRET + 33.8 * LRWR \\ + 15.7 * MRWR + 38.3 * PCHRWR + 8.97 * NHRWR \end{array} \right) \quad (4-7)$$

where: H_{cem} = the total heat of hydration of the cement (J/kg)

p_{cem} = the cement mass to total cementitious content ratio

p_{FA} = the wt.% fly ash of the total cementitious material

p_{FA-CaO} = the wt.% of CaO in fly ash

p_{slag} = the wt.% granulated slag of the total cementitious material

p_{SF} = the wt.% silica fume of total cementitious material

Blaine = the Blaine fineness of cement (m^2/kg)

p_{C_3A} = the percent aluminatate content in the Portland cement

p_{C_4AF} = the percent ferrite content in the Portland cement

p_{C_3S} = the percent alite content in the Portland cement

p_{SO_3} = the percent SO_3 content in the Portland cement

p_{Na_2O} = the percent Na_2O content in the Portland cement

$p_{Na_2O_{eq}}$ = the percent sodium equivalent alkalis content in the Portland cement
(0.658 x %K₂O + %Na₂O)

p_{MgO} = the percent MgO content in the Portland cement

p_{FreeCa} = the percent CaO content in the Portland cement

WRRET = the wt.% solids of ASTM Type B and D water reducer/retarder per gram of cementitious material

ACCL = the wt.% solids of ASTM Type C calcium-nitrate-based accelerator per gram of cementitious material

LRWR = the ASTM Type A low range water reducer dosage

MRWR is the mid-range water reducer dosage

PCHRWR = the ASTM Type F polycarboxylate-based high range water reduce dosage

NHRWR = the ASTM Type F naphthalene or melamine-based high-range water reducer dosage.

If the chemical admixtures dosages are unknown, typical averaged values presented by Riding (2007) can be used as seen in Table 4.1.

For this research, the cementitious properties were based on the properties received for the mix design used in the verification experiment that is discussed in Chapter 5. These values were used because a typical NCDOT mass concrete mix design that resembled the footings being analyzed was used. The mixture proportions for this design can be found in Table 5.1. The mixture proportions and mixture properties were slightly altered for the Wilmington Bypass footing to more closely resemble its concrete mix design. A sample of the FORTRAN subroutine developed for the thermal analysis in TNO DIANA can be found in Appendix C.

Table 4-1. Typical Chemical Admixture Dosages (Riding, 2007)

Chemical Admixture	Dose by Mass of Cementitious Material (%)
LRWR	0.0029
WRRET	0.0035
MRWR	0.0032
NHRWR	0.0078
PCHRWR	0.0068
ACCL	0.013

Table 4-2. Empirical Model Chemical Input Values

Chemical Admixture	Value
P _{C3S}	0.61
P _{C2S}	0.12
P _{C3A}	0.07
P _{C4AF}	0.11
P _{SO3}	0.028
P _{FreeCa}	0.009
P _{MgO}	0.013
P _{Na2Oeq}	0.0047
P _{Na2O}	0.001
Blaine	400.6 m ³ /kg
P _{FA-CaO}	0.01
PCHRWR	0.00345
MRWR	0.0065

4.3.1.3 Thermal Properties

The flow of temperature throughout a 3D object is governed by two fundamental equations: the 3D extension of Fourier's law of conduction, as seen in Equation 4-8 assuming thermal conductivity is isotropic and homogeneous, and the increase of internal energy, as seen in Equation 4-9 (Mehta and Monteiro, 2006). The law of energy conservation then states that the rate of heat transfer plus the rate of internal heat generation must equal the rate of increase of internal energy, which results in the Equation 4-10.

$$w = -k \left(i \frac{\partial T}{\partial x} + j \frac{\partial T}{\partial y} + k \frac{\partial T}{\partial z} \right) \quad (4-8)$$

$$s = \rho c_h \frac{\partial T}{\partial t} dx dy dz \quad (4-9)$$

$$k \left(i \frac{\partial^2 T}{\partial x^2} + j \frac{\partial^2 T}{\partial x^2} + k \frac{\partial^2 T}{\partial x^2} \right) + q = \rho c_h \frac{\partial T}{\partial t} \quad (4-10)$$

where: w = the rate of heat transfer (J/hr)

s = increase of internal energy (J/hr)

q = rate of heat generation (J/hr)

k = thermal conductivity (J/m-hr-K)

ρ = density (kg/m³)

c_h = specific heat (J/gram/K)

$T(x,y,z)$ = the scalar temperature field

As one can see from Equation 4-10, the two important thermal properties that govern the heat flow within the concrete, aside from the internal heat generation caused by cement hydration, are its thermal conductivity and its specific heat. Thermal conductivity is the rate of heat flow through a unit area under a unit temperature gradient, or the ability of the material to conduct heat (ACI 207.2R-07). Specific heat on the other hand is the amount of heat required to raise the temperature of a unity mass one degree. When specific heat is multiplied by the concrete density it becomes the thermal heat capacity per unit volume. These terms are related in Equation 4-11 through thermal diffusivity h^2 . Diffusivity is the ability of the material to transmit heat, or the ease at which a material can undergo temperature change, and is most significantly affected by the thermal conductivity of aggregates in normal weight concretes.

$$h^2 = \frac{k}{\rho * c_h} \quad (4-11)$$

where: h^2 = diffusivity (m²/hr)

In this research, the thermal conductivity of concrete was calculated using the thermal conductivity values of the concrete constituents from *Concrete* (Mindess et al., 2003) and their volumetric fraction. This resulted in a thermal conductivity of 2.76 W/m-K, which very closely matches the ACI 207 values of 2.6-2.7 W/m-K for concrete with granite aggregate. These values, however, are for mixes with Portland cement only, and do not take into

account the effect that fly ash replacement has on the concrete's thermal conductivity. When fly ash is used to replace cement, the concrete's conductivity is reduced due to the influence of fly ash's lower density values (Bentz et al., 2010). This combined with conductivity results from a test done by Tia et al. (2010) led the researchers to use a value of 2.21 W/m-K for this model.

The concrete diffusivity was then taken to be 0.004 m²/hr from the ACI 207 value for granite aggregate. The volumetric heat capacity could then be calculated using Equation 4-11, and was found to be 2486.4 kJ/m³-K. This was found using the normal concrete conductivity value of 2.76 W/m-K. This was done due to the fact that the thermal heat capacity was found to have little change when cement was replaced with fly ash (Bentz et al., 2010).

The conductivity and heat capacity values for the insulation blankets were found based on a typical R-value requirement of 4 (h·ft²·°F/Btu) for a 1 inch blanket. This was then adjusted for the fact that most insulation blankets used are less than 1 inch thick. The conductivity and heat capacity values for the plywood and steel forms were chosen based on typical values.

TNO DIANA can model conductivity and heat capacity values as a function of time or temperature, but was taken as constant for this research. A summary of the thermal properties input into TNO DIANA's thermal model can be found in Table 4.3.

Table 4-3. Material Thermal Properties

Material	Conductivity (J/m-hr-K)	Heat Capacity (J/m³-K)
Concrete	7956	2486400
Plywood	540	85440
Steel	187200	3815100
Insulation Blankets	261	20824

4.3.1.4 Boundary Conditions

The external environmental conditions were modeled by way of boundary elements on the outside surface of the model. The wind effects were first modeled through a forced convection term associated with the boundary elements to model the heat lost to the environment by an exposed surface. TNO DIANA uses Equation 4-12 to model the heat flow due to convection based on a convection coefficient h_c . This coefficient equation can be modeled as a function of time, a function of temperature, or remain constant. This research modeled the convection coefficient as a function of time.

$$q_c = -h_c(\phi_b - \phi_e) \quad (4-12)$$

where: q_c = convective heat flow (W/m²)

h_c = convection coefficient (W/m²-K)

ϕ_b = surface boundary temperature (K)

ϕ_e = environmental temperature (K)

The convection coefficient was modeled based on the actual average wind speeds collected from historical data. This was done using Equation 4-13 (Tia, 2010), based on work from Palyvos (2008), by way of using the wind speed v (m/s) to calculate the resulting convection coefficient h_c (W/m²-K).

$$h_c = \begin{cases} 5.6 + 3.95 * v & , \quad v \leq 5 \text{ m/s} \\ 7.6 * v^{0.78} & , \quad v > 5 \text{ m/s} \end{cases} \quad (4-13)$$

In addition, the ambient temperature was also collected for each footing from local historical weather data. The weather was then modeled as a thermal potential load applied to the external boundary elements. Also, the initial temperatures of the concrete, formwork, and insulation were applied to the models. The concrete's initial temperature was assigned based on the values given by the contractor's notes. The formwork and insulation initial temperatures on the other hand were based on the average ambient temperature recorded prior to casting the concrete.

4.3.2 DIANA Structural Model

A nonlinear structural analysis was used to model the development of the stresses within the concrete over time. A nonlinear analysis was used due to the changing early age mechanical properties of the concrete. The temperatures from the thermal model are input into the structural model as a thermal load imposed on the concrete that changes with time. When temperature differences occur between the surface and interior of the concrete, temperature gradients occur. These gradients are then converted into strains through the coefficient of thermal expansion, combined with shrinkage strains, and then turned into tensile stresses through the concrete modulus of elasticity. When these principal tensile stresses exceed the tensile strength of the concrete, cracking is likely to have occurred. This is expressed as one of the outputs in TNO DIANA through the cracking index, seen in equation 4-14.

$$I_{cr}(t) = \frac{f_t(t)}{\sigma_1(t)} \quad (4-14)$$

where: I_{cr} = cracking index

f_t = tensile strength ksi (MPa)

σ_1 = principal stress ksi (MPa)

The concrete was the only part of the thermal model that was modeled in the structural model as well. The concrete was modeled using quadratic twenty-noded isoparametric solid brick elements, known as CHX60 elements as seen in Figure 4-2. Quadratically interpolated elements were used because although σ_{xx} and ϵ_{xx} vary linearly in the x-direction, they vary quadratically in the y and z-directions. A 3 x 3 x 3 Gauss integration scheme was used in the integration of these elements.

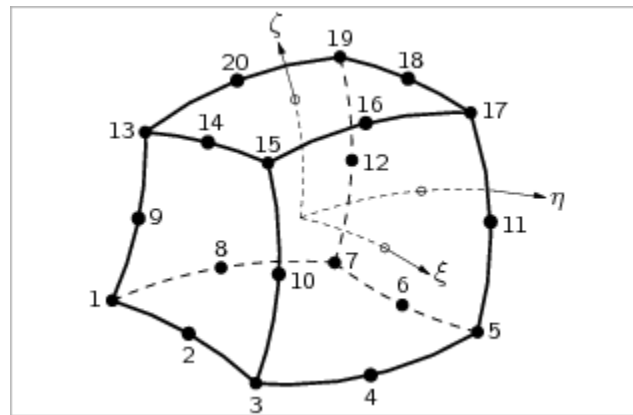


Figure 4-2: Structural modeling CHX60 isoparametric element

4.3.2.2 Equivalent Age Maturity Method

The mechanical properties of modulus of elasticity and tensile strength were modeled using the equivalent age maturity method, which is represented by Equation 4-15 (Carino and Lew, 2001). This method of analysis is useful for early age concrete because the strength throughout the hydrating concrete is not necessarily uniform. Instead, the mechanical properties, by way of the rate of hydration, are dependent on the temperature history of the concrete as well as on the time since mixing. The equivalent age itself is actually calculated in TNO DIANA's thermal analysis, but it is used in the structural analysis to relate the age of

a specific point within the concrete to its material properties based on its temperature history. This is done through the reference temperature T_r , which is traditionally considered 20 °C. The equivalent age is then the age that the concrete needs to be when cured at temperature T_r to achieve the strength of a sample concrete (from a test) curing at a different temperature (Riding, 2007). The equivalent age is calculated by:

$$t_e = \sum_0^t e^{\frac{-E_a}{R} \left[\frac{1}{T_c} - \frac{1}{T_r} \right]} \cdot \Delta t \quad (4-15)$$

where: t_e = equivalent age (hrs)

E_a = activation energy (J/mol)

R = universal gas constant = 8.314 J/mol/K (10.732 ft³ psi/°R/lb-mol)

T_c = average concrete temperature during time interval (K)

T_r = equivalent age reference temperature (K)

Δt = time interval (hrs)

4.3.2.3 Coefficient of Thermal Expansion

The coefficient of thermal expansion (CTE) is the change in unit length per degree of temperature change (Mehta and Monteiro, 2006). This directly affects how the concrete will deform due to the temperature gradients present within the concrete, thus the coefficient of thermal expansion is very important in calculating thermal stresses. It is largely dependent on the coefficient of thermal expansion of the aggregate due to the fact that the aggregate makes up the largest portion of the concrete mix. For this project, the coefficient of thermal expansion was calculated using the CTE values from Mindess (2007) and Riding (2007), and the constituent's density. This was done using Emanuel and Hulsey's (1977) method, seen in Equation 4-16 (Riding, 2007). The constituent's densities were calculated based on their associated specific gravity, and the paste density was calculated using specific gravity and volumetric fraction values. This research project used a constant coefficient of thermal expansion $\alpha_{con} = 9.6587 \mu\epsilon/^\circ\text{C}$.

$$\alpha_{con} = \frac{\alpha_{ca}d_{ca} + \alpha_{fa}d_{fa} + \alpha_p d_p}{d_{con} + d_{con} + d_{con}} \quad (4-16)$$

where: α_{con} = concrete coefficient of thermal expansion ($\mu\epsilon/^\circ\text{C}$)

α_{ca} = the coarse aggregate coefficient of thermal expansion ($\mu\epsilon/^\circ\text{C}$)

d_{ca} = the coarse aggregate density (kg/m^3)

α_{fa} = the fine aggregate coefficient of thermal expansion ($\mu\epsilon/^\circ\text{C}$)

d_{fa} = the fine aggregate density (kg/m^3)

α_p = the paste coefficient of thermal expansion ($\mu\epsilon/^\circ\text{C}$)

d_p is the paste density (kg/m^3)

4.3.2.4 Modulus of Elasticity and Poisson's Ratio

Stress modeled in three dimensional analyses requires the knowledge of both the modulus of elasticity and Poisson's ratio. The elastic modulus is the tendency of an object to deform elastically when a load is applied to it, and Poisson's ratio is the ratio of lateral strain to axial strain within the elastic region. These two terms, combined with the three dimensional Hooke's Law, help define the relationship between the applied strains and the resulting stresses.

The modulus of elasticity is found to not only be a function of time, or the age of the concrete, but also the maturity of the concrete based on its temperature history. The elastic modulus increases in the concrete as the concrete's age and maturity increases. This is important because as the concrete matures, the stresses induced by the thermal gradients increase due to the increased modulus. The modulus of elasticity was modeled in DIANA as a direct input of the modulus versus equivalent age. The values for the modulus of elasticity were measured in the lab, as described in Section 5.6.4. The compressive modulus was used as it is more conservative than the tensile modulus due to its higher values (Tia et al. 2010). In addition, the viscoelastic behavior of the concrete was modeled using the Maxwell Chain model. This was directly implemented in the DIANA material specifications.

Poisson's ratio is sometimes considered constant and other times considered to be a function of concrete age or degree of hydration (Riding, 2007). Due to this uncertainty, a constant value of 0.2 was used as this is generally assumed for concrete (Mehta and Monteiro, 2006).

4.3.2.5 Tensile Strength

Unlike normal concrete design, tensile strength is actually one of most important properties of mass concrete. The tensile strength is the concrete's ability to resist pulling stresses and is considered to represent the maximum tensile stress that the concrete can withstand. Concrete failure is usually considered to occur when the tensile stress exceeds the tensile strength. For these analyses, the split tensile strength was used as input in DIANA versus equivalent age. The values for the tensile strength were measured in the lab, as described in section 5.6.3.

4.3.2.6 Autogenous Shrinkage

Autogenous shrinkage is the "macroscopic volume reduction of cementitious materials when cement hydrates after initial set" (Mehta and Monteiro, 2006). This shrinkage is even more significant in concretes with low w/c ratios due to the lack of water for complete hydration, and is further increased with the addition of silica fume into the concrete mix (Mehta and Monteiro, 2006). Autogenous shrinkage was considered in this study and not drying shrinkage because the concrete is usually moist cured, which results in minimal moisture loss in these early ages. The shrinkage was directly modeled in DIANA as shrinkage versus time, where the shrinkage values were measured in the lab according to the test described in Section 5.6.5.

4.3.2.7 Boundary Conditions

The final part to completing the structural model is inputting appropriate boundary constraints. Each model, both the footings and as well as the experimental block, were able to be modeled as a quarter block due to their geometric planes of symmetry. Each line of

symmetry was restrained from translation displacements in the direction normal to that face of the model. In addition to this, the support boundary conditions were modeled for each case. For the block lab experiment model, the vertical displacements in the nodes along the base of the concrete were restrained. The corner nodes of the block were also pinned to give the structure more stability. The footing models had slightly different support conditions, however, as they were supported by piles. In these instances, the pile supports were modeled by fixing the nodes at the base of the concrete associated with the actual locations of each pile. Samples of how the boundary conditions were modeled can be seen in Figures 4-3 and 4-4.

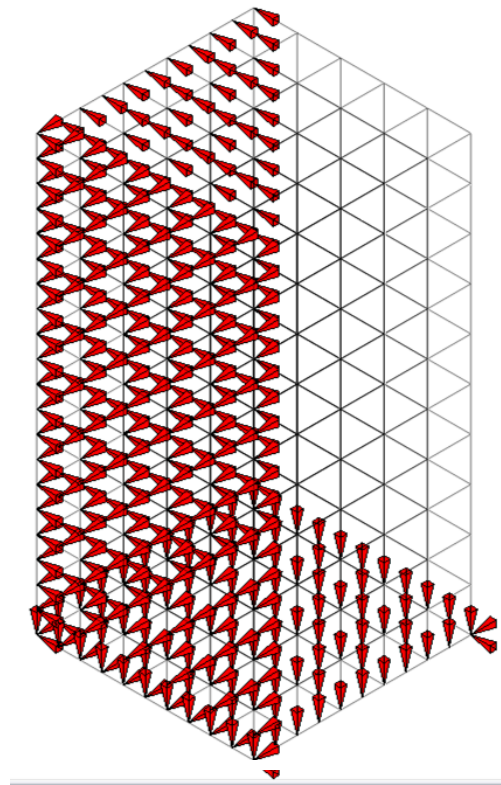


Figure 4-3: Block experiment boundary conditions

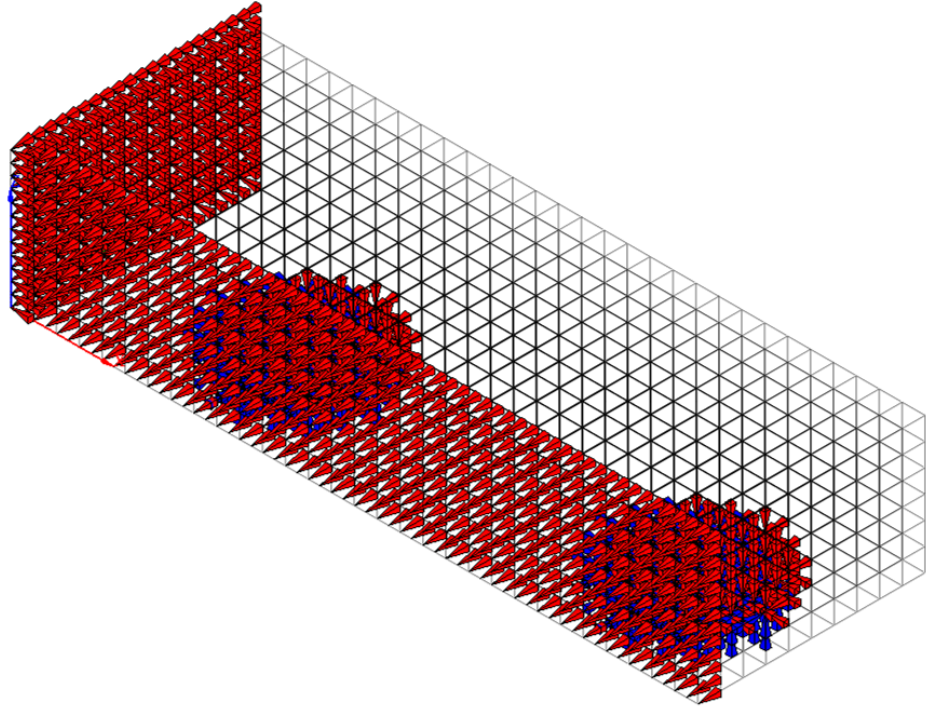


Figure 4-4: Oak Island footing boundary conditions

CHAPTER 5

MASS CONCRETE BLOCK EXPERIMENT

5.1 Introduction

Once the preliminary information gathering phase was complete, it was discovered that there was no complete set of temperature data to compare to a computer model. In light of this, the research team decided that a control mass concrete block experiment would be necessary. A typical mass concrete dimension and NCDOT mix design was used to cast the concrete block and temperature measurements were recorded at specific locations to validate the finite element analysis results.

5.2 Block Properties

It was decided that it would be best for the mix design used for the mass concrete block experiment to resemble the mix design used in the footings that were to be analyzed from Oak Island, Sunset Beach, and the US 17 Wilmington Bypass. As can be seen in Table 5.1, the same 690 lb/yd³ of cementitious material was used with a 30% replacement of Type F fly ash and a 5% replacement of silica fume. An effort was also made to keep the water cement ratio, slump, and unit weight the same. The design w/c ratio was 0.37, the design slump was 4.5 in (± 1.5 in) without SuperP and 6.0 in (± 1.5 in) with SuperP, and the unit weight was 146 lb/yd³. It should be noted that the air content in the experiment's mix design was slightly different due to the supplier's recommendation. Instead of 6.0% it was 1.5% ($\pm 1.5\%$).

The dimensions of the mass concrete block were chosen to be a 5 ft x 5 ft x 5 ft (1.52 m x 1.52 m x 1.52 m) cube. These dimensions were chosen because a minimum dimension of 5 feet was the most common size limit found among the different state mass concrete specifications, as seen in Section 2.7.4.

Table 5-1. Mass Concrete Mix Design

	Quantity (lb/yd ³)	Sp. Gr. (SSD)	Volume (ft ³)
Cement- Type I/II	448	3.15	2.28
Fly ash- Type F	207	2.20	1.51
Silica Fume	35	2.20	0.25
Water	258	1.00	4.13
Stone	1800	2.65	10.88
Sand	1194	2.63	7.28
Midrange Water Reducer- Mira 85	---	1.00	---
Super Plasticizer- EXP 950	---	1.00	---
Total	3942		27.01

5.3 Set-up and Construction

The mass concrete block experiment was set up in the yard outside of the Constructed Facilities Lab of North Carolina State University. This was done so that the concrete's reaction to the external weather could be observed. As seen in Figure 5-1, ¾" plywood forms was used to cast the concrete and the base was built out of ¾" plywood and 4 x 4 inch lumber as seen in Figure 5-2. A decision was made not to use any kind of insulation to enable the greatest temperature differential to occur within the block and lead to the best chance of thermal cracking.



Figure 5-1. Block experiment formwork set up under construction.



Figure 5-2. Block experiment formwork base.

The concrete was cast on April 9, 2012 at 1:45 pm and was finished at approximately 2:10 pm. It was also vibrated approximately every 1.5 – 2 feet, as can be seen in Figure 5-3. The concrete had an initial temperature of approximately 71.6 °F (22 °C) and an ambient temperature of 71.6 °F at the time of the pour. About an hour after casting, a curing compound (QUIKRETE Acrylic Concrete Sealer) was spread over the top surface of the concrete block as seen in Figure 5-4.



Figure 5-3. Concrete block pour.



Figure 5-4. Finished surface of concrete block with curing compound.

5.4 Temperature Data Collection System

A temperature collection system was set up to record the temperature changes during concrete hydration at predetermined locations within the concrete. Thermocouple Type-T wire with FEP (a type of Teflon) insulation and jacket was used for the temperature sensors and a Humbolt Multi-Channel Maturity Meter (the same used at the Thomasville site in Section 3.6.3) was used to record the concrete temperatures for a period of 14 days. The temperatures were recorded every 0.5 hours for the first 48 hours, and every hour for the remainder of the test. A minimal reinforcement cage was also constructed to make the thermocouple placement easier. As seen in Figure 5-5, the thermocouple sensors were tied directly to the reinforcement cage with about an inch of wire sticking out so that the wire was not in direct contact with the steel.

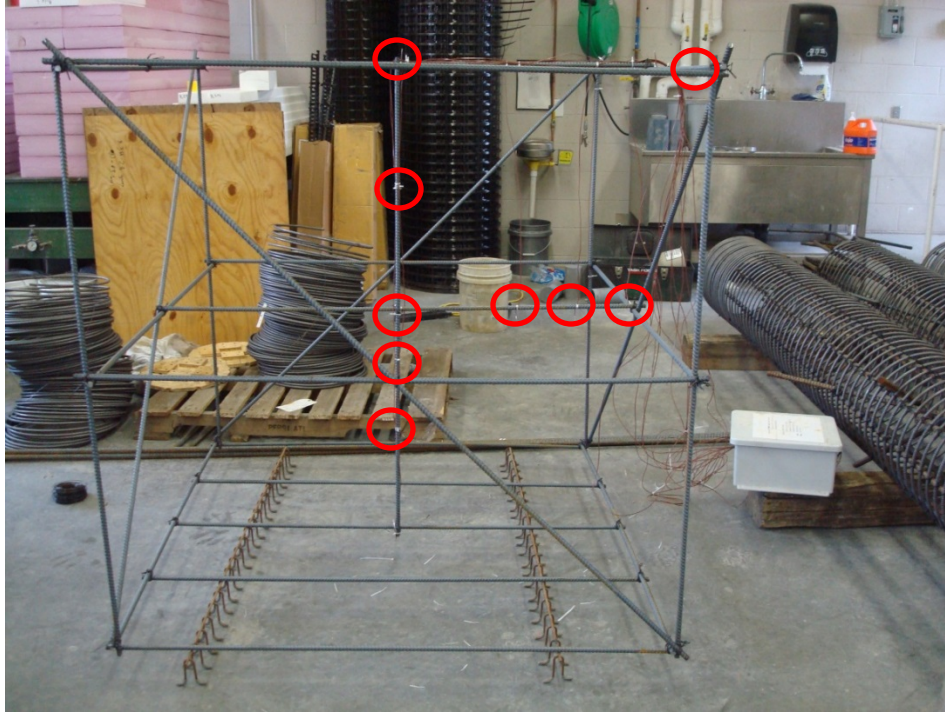


Figure 5-5. Steel reinforcement cage with thermocouples attached. (The red circles highlight locations of the exposed thermocouples.)

5.5 Temperature Data Results

The thermocouple sensor locations were strategically chosen in order to produce the most complete picture possible of the temperature profile throughout the block. As seen in Figure 5-6, due to the symmetry of the 5 foot cube only one side of the block needed to be wired, which was done through sensors 8, 11, and 3. It was decided to put sensors on the top and bottom of the concrete block because of the different boundary conditions. The vertical profile was then created by sensors 1, 2, 4, 9, and 10. Sensors 5, 6, and 7 were also put in the corners in order to get the full temperature distribution throughout the concrete block. All outside sensors were located 2-3 inches from each contributing side, based on the dimensions of the reinforcement cage. Thermocouple sensors 9, 10, and 11 were then put at the

midpoints between the center of block at node 1 and the top, bottom, and side faces; that is, they were approximately 1.25 feet from the edge of the concrete.

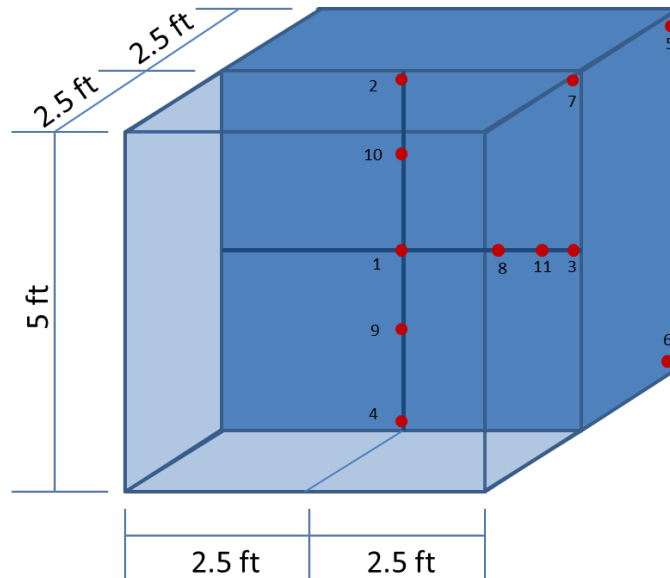


Figure 5-6. Thermocouple sensor locations

The temperatures were recorded over a 14 day period, however only 8 days (192 hours) are shown in Figures 5-7 through 5-9 since the temperatures reached a steady state by then and were primarily affected by ambient weather conditions. Sensor 9 failed a few hours after the pour and no data is available from this sensor.

Figure 5-7 shows a general overview of the temperature distribution throughout the concrete block. Figure 5-8 shows the vertical temperature distribution from the top to the bottom of the center of the concrete block, and Figure 5-9 shows the horizontal distribution from the center of the concrete to the outside edge 2.5 feet from the base. As one can see

from these figures, a maximum temperature of 152.6 °F (67°C) was reached 21.5 hours after the pour and started to decrease 28 hours after the concrete was poured. In Figure 5-10 it can be seen that the temperature differences between the center and the top of the concrete surpass the typical 35 °F limit on a few occasions, the first time being after 17.5 hours. This temperature difference reaches a maximum of 46.8 °F at 42.5 hours, as well as a peak of 41.4 °F at 20 hours and a peak of 43.2 °F at 67 hours. This temperature difference fluctuates due to the top surface's exposure to the ambient temperatures. The temperature differences between the center and the bottom and side surfaces do not fluctuate as much due to the insulating effect of the plywood formwork and the earth. It can also be noted that the temperature differences for these two profiles never reached the maximum limit of 35 °F.

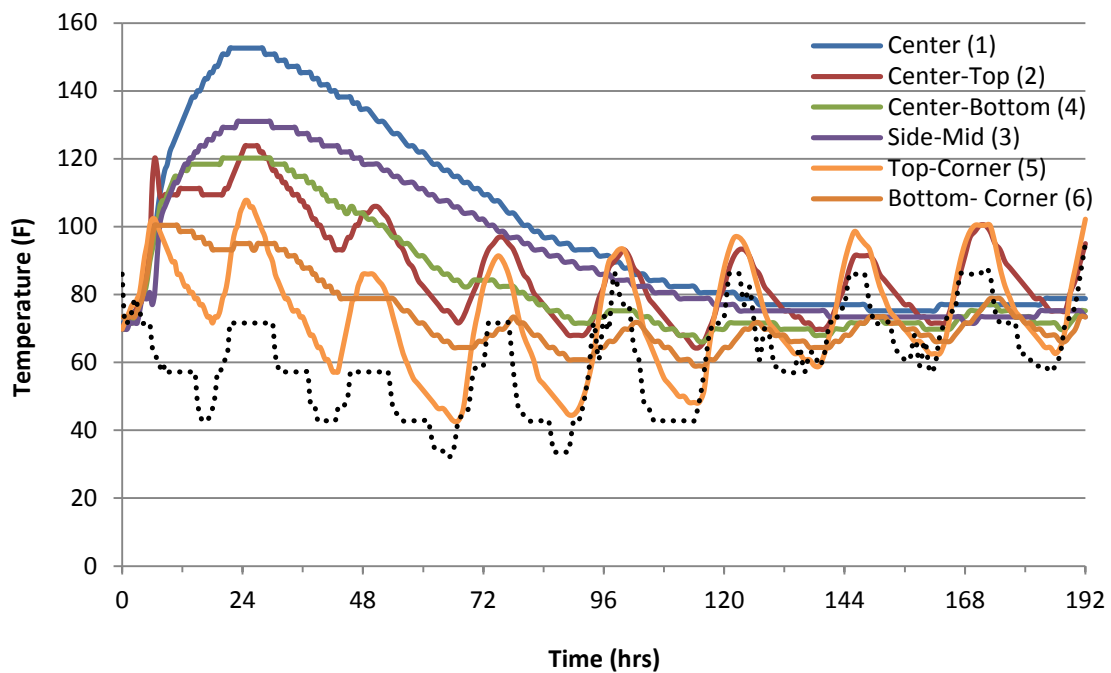


Figure 5-7. Temperature data from edge thermocouple sensors

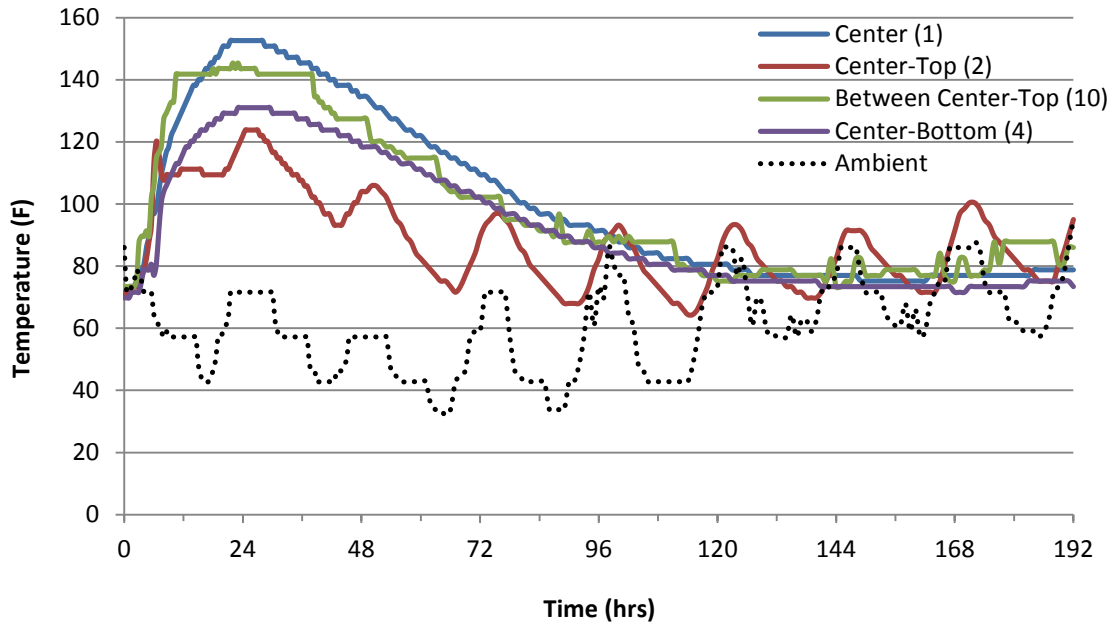


Figure 5-8. Vertical temperature distribution

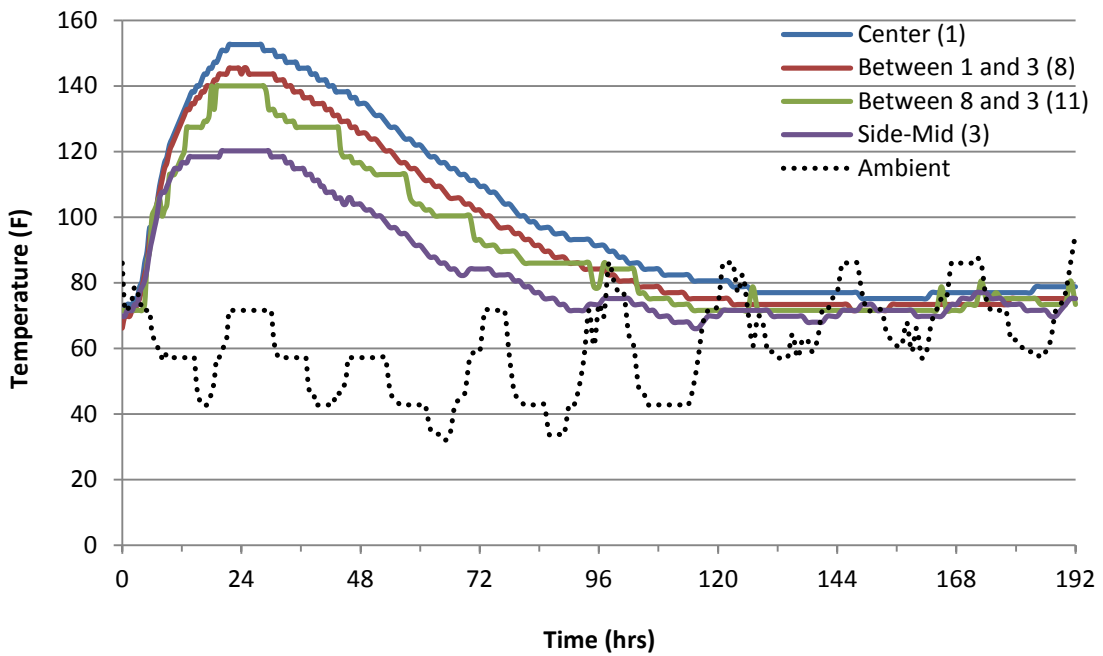


Figure 5-9. Horizontal temperature distribution

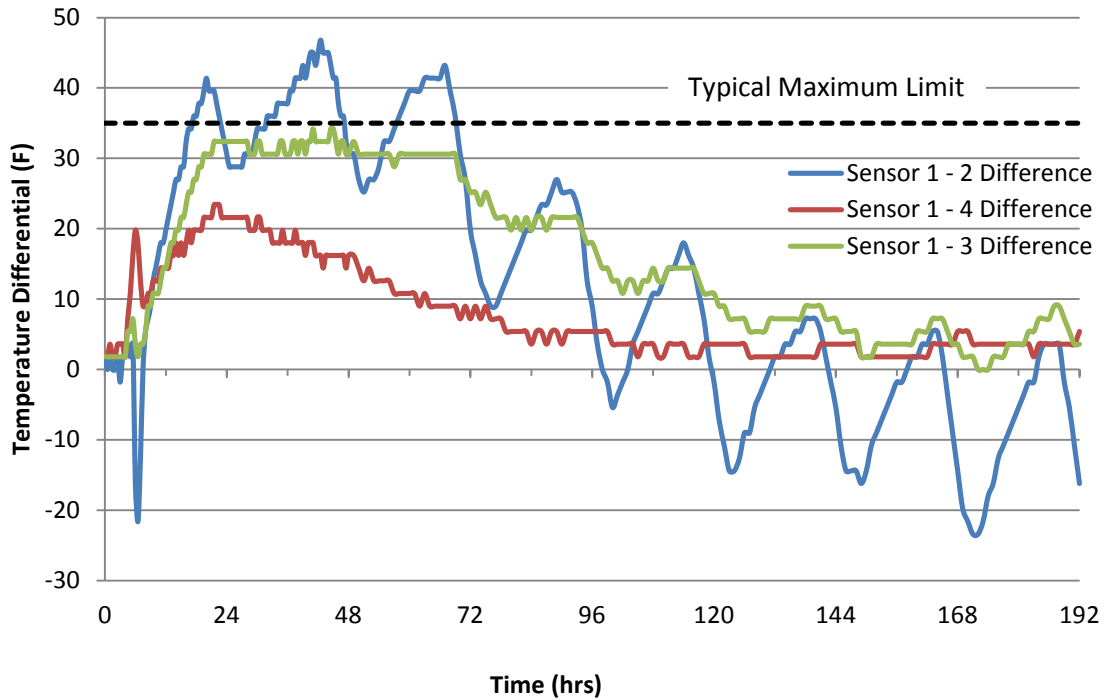


Figure 5-10. Thermocouple temperature differences

5.6 Material Properties Testing

In addition to the monitoring of the concrete temperatures, laboratory tests were done to measure the mechanical properties of the concrete used in the experiment. These tests were completed based on the maturity method in ASTM C 1074-11 and carried out at 1, 3, 7, 14, and 28 days after casting. Thirty-five 4 x 8 inch cylinders, in accordance with ASTM C 192-07, and six 1 x 1 x 11¼ inch prisms, in accordance with ASTM C 490-11, were cast for testing as seen in Figure 5-11. In addition to this, 2 cylinders were embedded with thermocouple sensors and their temperatures were recorded for 48 hours, or until the temperatures leveled out. After the cast, cylinders were allowed to cure in their molds for 24 hours, at which time they were de-molded and moist cured in a water bath in accordance with ASTM C 511-09, as seen in Figure 5-12.



Figure 5-11. Finished concrete cylinders and prisms



Figure 5-12. Moist curing water bath

Two separate sets of tests were done because in the first set of tests there was a malfunction with the temperature recording device and the temperatures were not recorded. The first set of cylinders and prisms were cast with the concrete block pour on April 9, 2012 and the second set was cast on June 5, 2012. The same material that was used in the first pour was used in the second pour, only it was proportioned for a smaller batch. One slight difference between the two batches, however, is that the second batch was mixed in the lab with a 5 cubic foot nylon drum mixer, as seen in Figure 5-13, instead of in a concrete truck.



Figure 5-13. Nylon mixing drum used for the second set of tests.

5.6.1 Maturity Temperature

The temperatures of two cylinders were measured according to the Maturity Method standard in ASTM C 1074-11. A thermocouple type-T wire was embedded in the center of each of the cylinders and the temperatures were measured for 48 hours at half hour time intervals, as seen in Figure 5-14. The average temperature results from the two cylinders from the second set of tests can be seen in Figure 5-15. The temperature was measured so that the equivalent age of the cylinders could be calculated using Equation 4-15. The equivalent age was then plotted against the correlating compressive strengths, splitting tensile strengths, and modulus of elasticity.

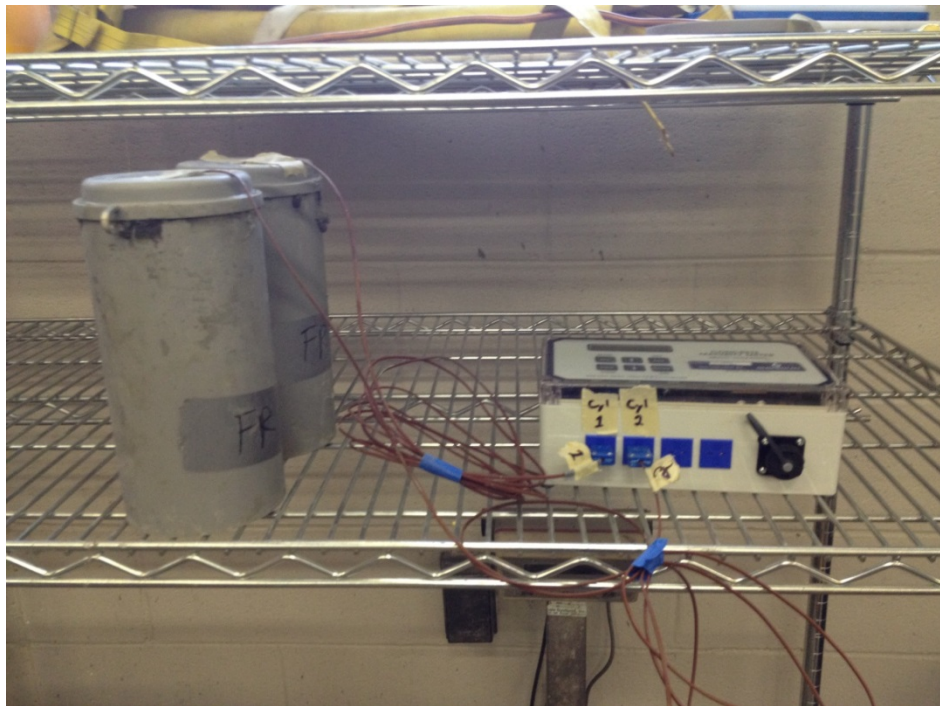


Figure 5-14. Cylinder temperature set up

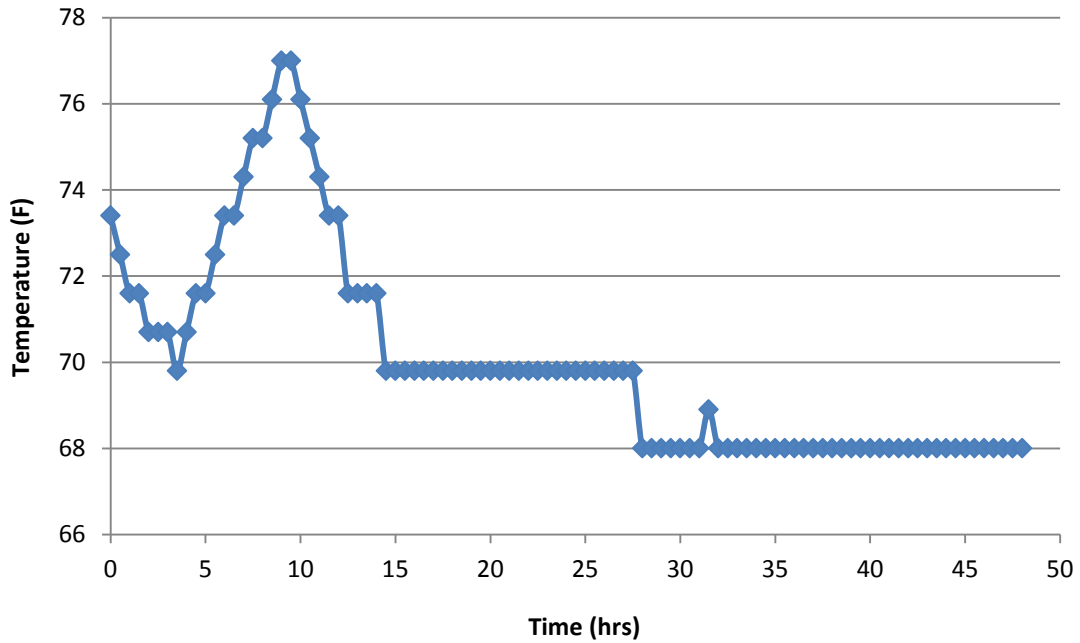


Figure 5-15. Average temperature results from the second set of cylinder tests

5.6.2 Compressive Strength

The compressive strength of the concrete was tested on 4 by 8 inch cylinders in accordance with ASTM C 39-11a. Each test cylinder was placed into the hydraulic Forney Compression Testing Machine and tested at a rate of 35 psi/s (± 7 psi/s) until failure. Neoprene pads were used at both ends of each cylinder to create a more uniform distribution of the load on the concrete. The setup can be seen in Figure 5-16.



Figure 5-16. Compressive strength test setup

As mentioned previously, there were two sets of tests done. The results from the first test can be found in Figure 5-17 and the results from the second set of tests can be seen in Figure 5-18. Figure 5-18 shows the compressive strength versus the appropriate equivalent age, whereas Figure 5-17 just shows the compressive strength versus time in days. This is because, as explained before, the temperature recorder failed during the first set of tests so the equivalent age cannot be calculated.

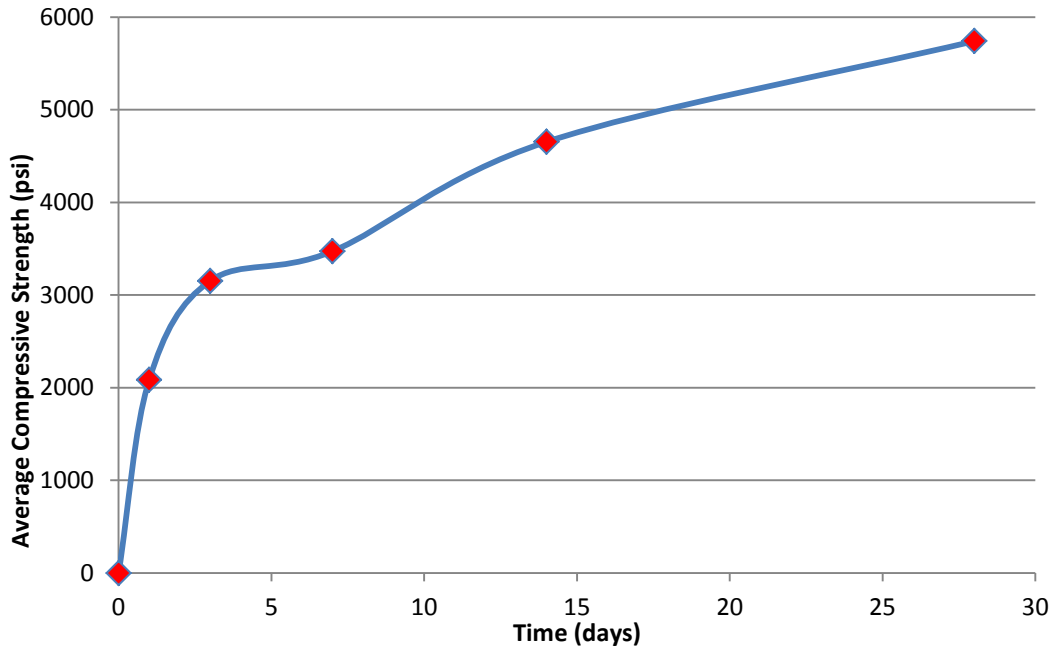


Figure 5-17. Average compressive strength vs time from Test 1 cylinders

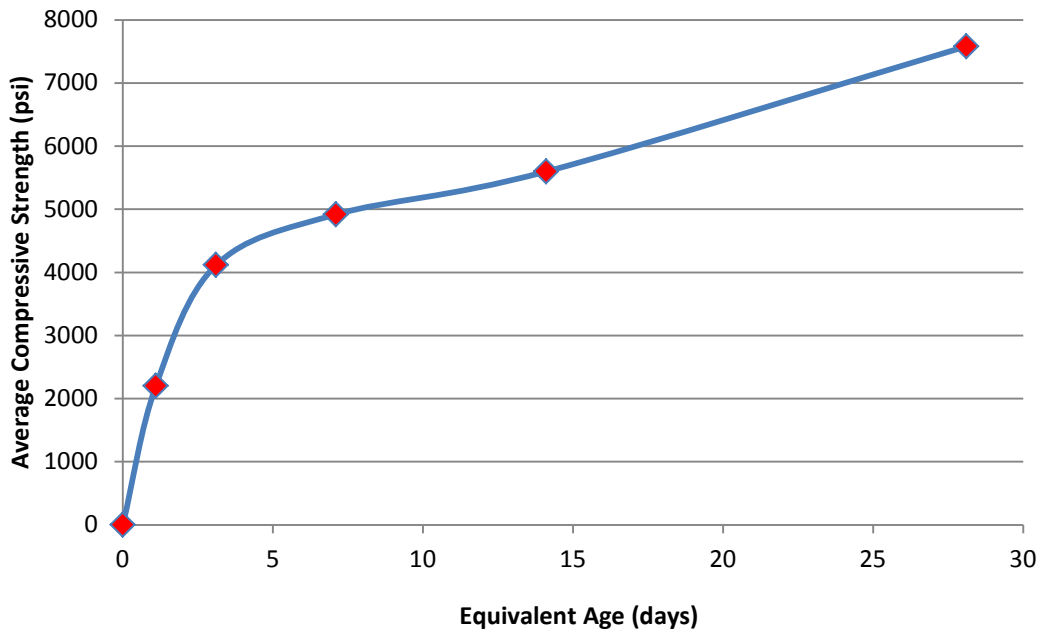


Figure 5-18. Average compressive strength vs equivalent age from Test 2 cylinders

5.6.3 Splitting Tensile Strength

The splitting tensile strength of the concrete was tested on 4 by 8 inch cylinders following ASTM C 496-11. The splitting tensile strength test was chosen over the flexural strength test because it tends to have lower values, and is thus more conservative (Mang et al, 2010). An 8 inch long piece of wood was put on the top and bottom of each cylinder diametrically opposite of each other, as seen in Figure 5-19. These were used as bearing strips between the cylinder and the upper and lower bearing blocks. Each test cylinder was then placed into the MTS actuator, as seen in Figure 5-20, and tested at a rate of 7,500 lb/min until failure. The splitting tensile strength was calculated using Equation 5-1:

$$T = \frac{2P}{\pi * l * d} \quad (5-1)$$

where: T = splitting tensile strength
P = maximum applied load
l = length
d = diameter



Figure 5-19. Splitting tensile strength test setup



Figure 5-20. MTS machine setup

The results from the first set of tests can be seen in Figure 5-21 and the results from the second test can be seen in Figure 5-22. As with the compressive strength tests, Figure 5-22 shows the splitting tensile strength versus the appropriate equivalent age, whereas Figure 5-21 just shows the splitting tensile strength versus time in days.

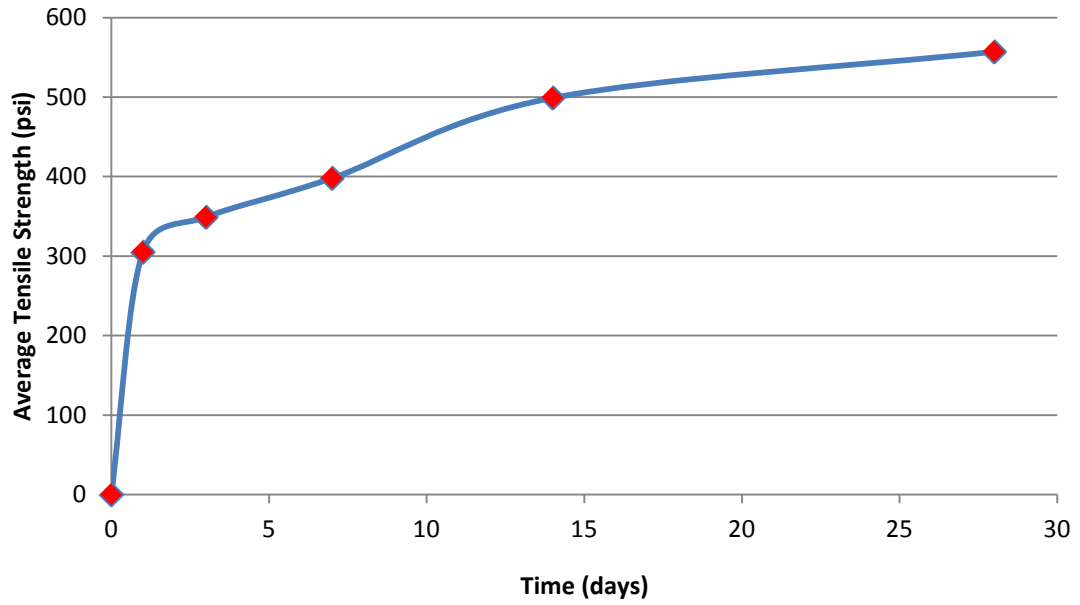


Figure 5-21. Average splitting tensile strength vs time from Test 1 cylinders

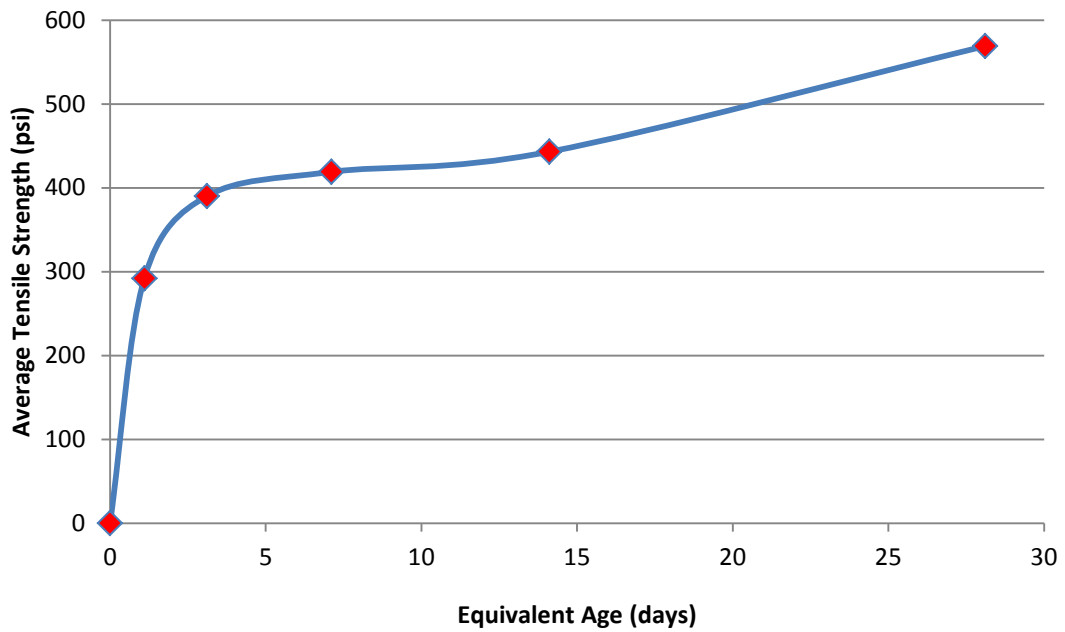


Figure 5-22. Average splitting tensile strength vs equivalent age from Test 2 cylinders

5.6.4 Modulus of Elasticity

The modulus of elasticity was determined using the compressive tests found in ASTM C 469-10 on the 4 x 8 inch cylinders. Each cylinder was setup with a strain measuring extensometer as seen in Figure 5-23. The cylinders in the second set of tests were also attached with a TML polyester wire strain gauge (PL-60-11-3LT) to confirm the accuracy of the extensometer readings. The test cylinders were placed into the hydraulic Forney Compression Testing Machine and tested at a rate of 35 psi/s (± 7 psi/s), where the load and strains were recorded by a computer.



Figure 5-23. Modulus test setup

The modulus was found by recording the load (S_1) at 0.00005 strain and the strain (ϵ_2) at 40% of the ultimate load (S_2). Equation 5-2 was used to calculate the modulus of elasticity:

$$E = \frac{(S_2 - S_1)}{(\epsilon_2 - 0.00005)} \quad (5-2)$$

The results from the first set of tests can be seen in Figure 5-24 as a function time, and the results from the second set of tests can be seen in Figure 5-25 as a function of equivalent age.

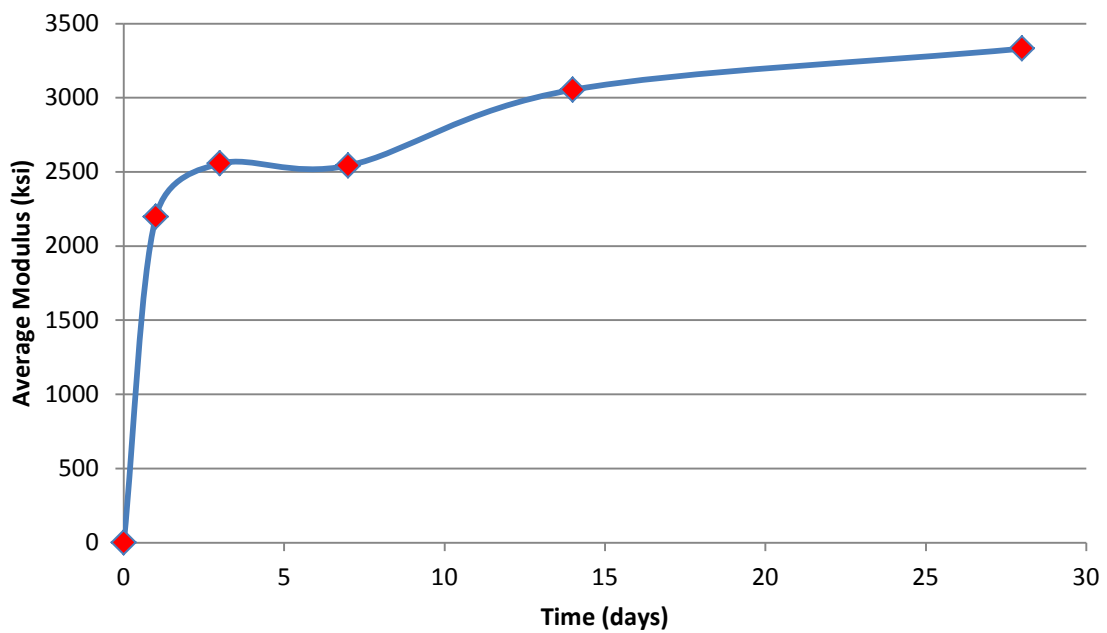


Figure 5-24. Average modulus of elasticity vs time from Test 1 cylinders

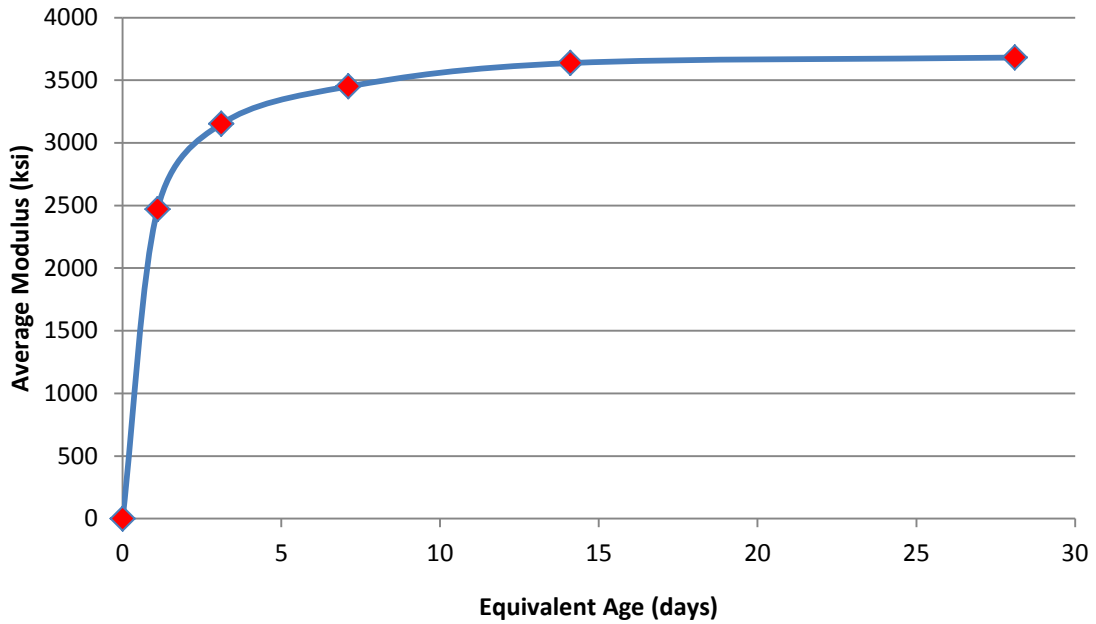


Figure 5-25. Average modulus of elasticity vs equivalent age from Test 2 cylinders

5.6.5 Autogenous Shrinkage

The autogenous shrinkage was also tested for input into the finite analysis model. This property was tested on 1 x 1 x 1 1/4 inch prisms, as seen in Figure 5-26, in accordance with ASTM C 490-11. To prevent the measurement of drying shrinkage, which is not expected to be relevant for early age mass concrete, the samples were sealed, as seen in Figure 5-27, to prevent moisture from escaping the concrete prisms. The weight of each sample was measured at each test time period to ensure that there was no significant weight loss from moisture transfer. During both sets of tests, an initial length was measured with the comparator seen in Figure 5-27 24 hours after the prisms were cast. The prisms' lengths were then measured at appropriate time periods and compared to the initial measurement to obtain the length change using Equation 5-3:

$$L = \frac{(L_x - L_i)}{G} \quad (5-3)$$

where: L = change in length at age 'x'

L_x = comparator reading of specimen minus reading of reference bar at age 'x'

L_i = comparator reading of specimen minus reading of reference bar at initial reading

G = nominal gauge length



Figure 5-26. Shrinkage test mold

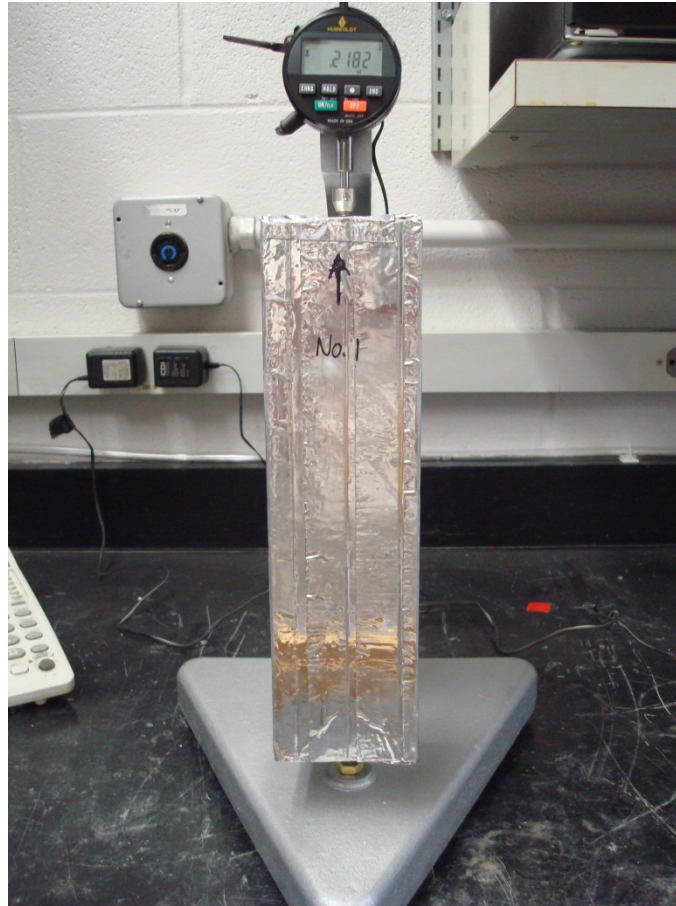


Figure 5-27. Shrinkage comparator measurement setup

The results from the first set of tests can be seen in Figure 5-28 and the results from the second set of tests can be seen in Figure 5-29. The shrinkage values were plotted against time instead of equivalent age in test 2 because there was not a direct correlation between the temperatures observed in the cylinders and the temperatures that were present in the prisms.

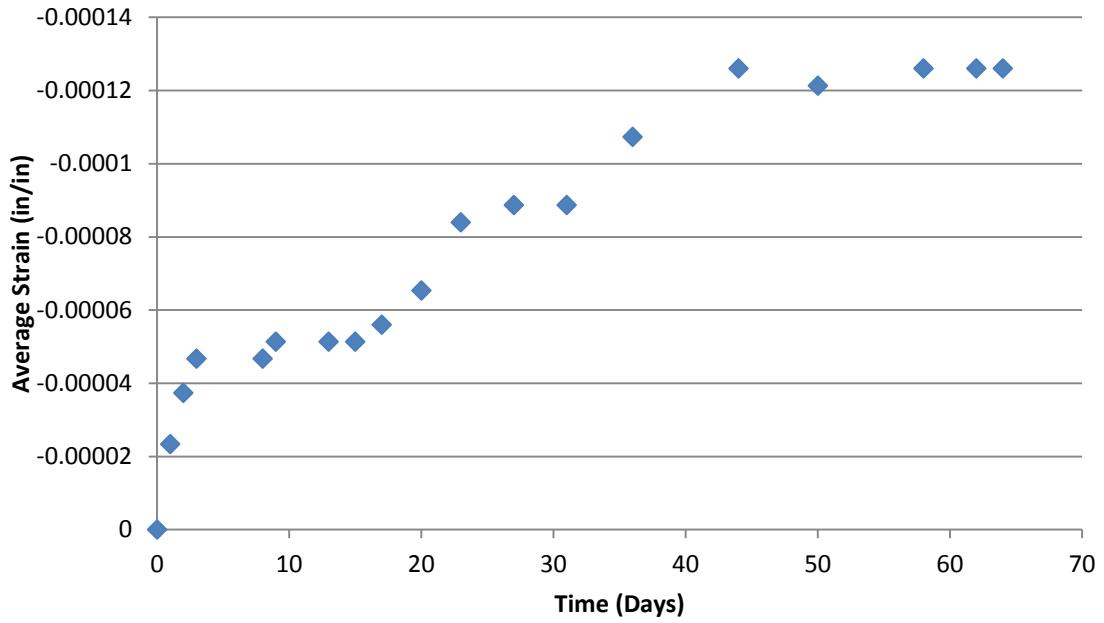


Figure 5-28. Average strain vs time from Test 1 prisms

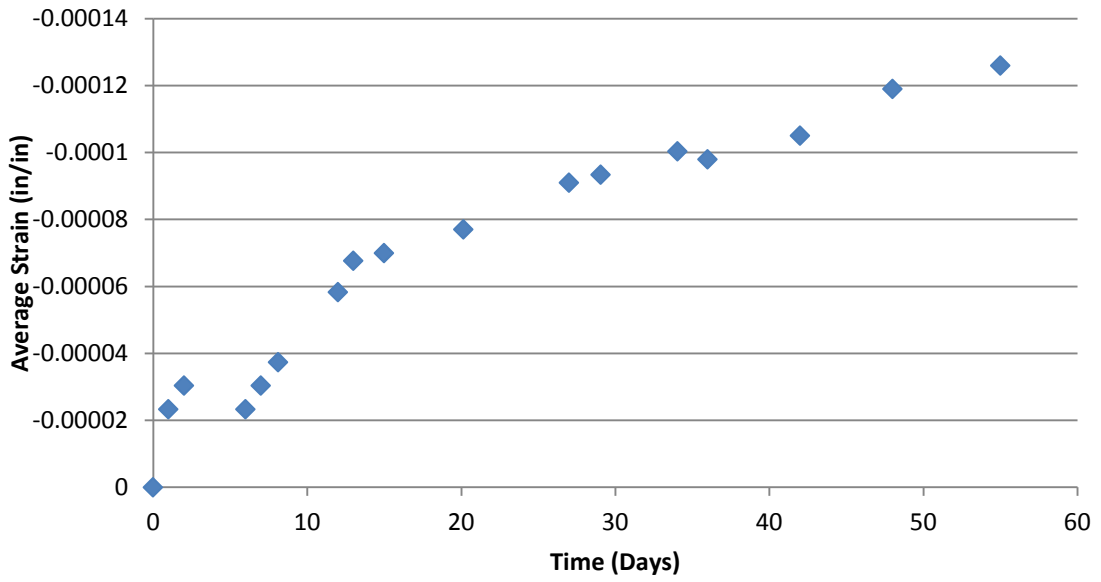


Figure 5-29. Average strain vs time from Test 2 prisms

5.6.6 Properties Summary

A summary of the mechanical properties from test 2 can be seen in Table 5-2. The results from test 2 were used due to the availability of the cylinder temperature data needed to calculate the concrete maturity. The data from test 1 validated the results from test 2 since the properties of cylinders were similar to the concrete used in the mass concrete block. The compressive strength and the modulus of elasticity of the second test are slightly higher than that of the first test. The tensile strength values, however, were much closer between the two tests. This difference in values was most likely caused by a slight difference between the two mixes. The same material was used for both batches; however it is possible that the air content and the w/c ratio may have differed slightly. The shrinkage values from test 2 can be seen in Table 5-3. The values in this table are negative because the specimens were shrinking from their original lengths during these tests.

Table 5-2. Summary of Mechanical Properties for Test 2 Cylinders

Time (hours)	Equivalent Age (hours)	Compressive Strength (ksi/MPa)	Tensile Strength (ksi/MPa)	Modulus of Elasticity (ksi/MPa)
24	26.4	2.20/15.2	0.292/2.0	2470/17031
72	74.6	4.12/28.4	0.390/2.7	3150/21724
168	170.6	4.92/33.9	0.419/2.9	3450/23790
336	338.6	5.60/38.6	0.443/3.1	3640/25080
672	674.6	7.58/52.3	0.569/3.9	3680/25380

Table 5-3. Summary of Shrinkage Values for Test 2 Prisms

Time (hours)	Average Shrinkage (in/in)
0	0
24	-2.335E-05
48	-3.035E-05
144	-2.335E-05
168	-3.035E-05
195	-3.735E-05
288	-5.833E-05
312	-6.766E-05
360	-7.000E-05
483.5	-7.700E-05
648	-9.100E-05
697.5	-9.334E-05
817	-1.003E-04

CHAPTER 6

FINITE ELEMENT ANALYSIS RESULTS

6.1 Introduction

In this chapter, the thermal and structural analysis results from the experimental concrete block as well as the results from the Oak Island, Sunset Island, and Wilmington Bypass case studies are presented. A quarter of the mass concrete structure was modeled in each case; the orientation of these models can be seen in Figure 6-1. The thermal results display the temperature distribution in the concrete block over time as well as the temperature differentials throughout the concrete over time. The structural analysis results display the equivalent age, principal stress, and tensile strength at key locations. The cracking index of these key locations is also displayed to calculate cracking probability:

$$I_{cr}(t) = \frac{f_t(t)}{\sigma_1(t)} \quad (6-1)$$

where: I_{cr} = cracking index

f_t = tensile strength ksi (MPa)

σ_1 = principal tensile stress ksi (MPa)

If the cracking index is above 1.0, the tensile strength is higher than the first principal stress and cracking should not occur. If the cracking index is less than 1.0, the first principal stress is higher than the tensile strength and cracking may occur. When the stresses are low compared to the tensile strength of the concrete, the cracking index number gets increasingly higher. TNO DIANA limits the cracking index to a maximum of 1.0 when the stress is very low or negative. Therefore, when the cracking index is 100, the stress is either a very small tensile stress or it is in compression.

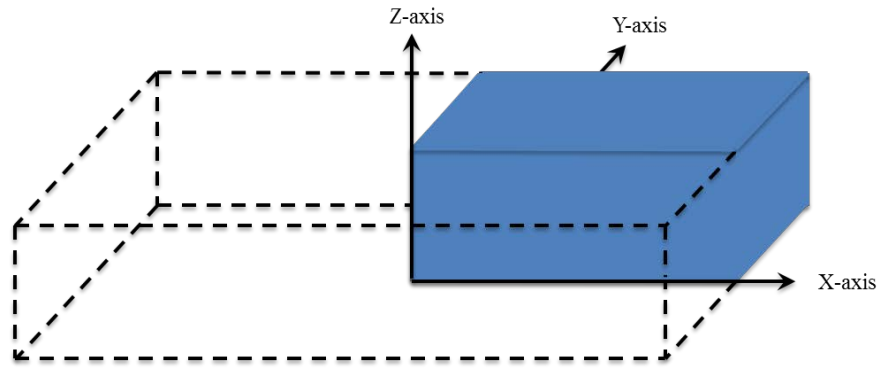


Figure 6-1: Quarter block orientation

6.2 Concrete Block Validation Experiment

6.2.1 Thermal Analysis Results

As discussed in Chapter 5, an experimental block was used to validate the finite element model used in this study. As seen in Figure 6-2, a quarter of the 5 foot concrete cube was modeled with the $\frac{3}{4}$ " plywood formwork explicitly modeled. The thermal results from the analysis run were compared to the measured results from the experiment in Chapter 5. The vertical and horizontal profiles in Figures 6-3 and 6-4 correlate to the locations shown in Figure 6-2. These locations were chosen because it is where standards and specifications typically measure temperature and temperature differentials. Some slight variation in locations between the experiment and the model exist because in the experiment the thermocouples were embedded 2-3 inches from the surface, while the nodal temperatures reported from the finite element model are at the surface

Figures 6-3 and 6-4 show the comparison of temperatures modeled in TNO DIANA, identified as a node, and the measured results of the block lab experiment. The experimental temperatures are represented by dashed lines and the predicted temperatures from the model are represented by solid lines. As these figures indicate, the finite element model was able to accurately capture and model the temperature distribution measured in the concrete block.

The model predicted a maximum temperature of 150.6 °F to occur at 26 hours and start decreasing at 29 hours, whereas the actual measured maximum temperature was found to be 152.6 °F at 21.5 hours after the pour and was found to decrease after 28 hours. The one area that the finite element model had a problem accurately predicting the measured temperature data was on the top surface of the concrete block. It was discovered that the model could not accurately predict the temperature rises found to occur in the measurements due to the direct sunlight during the daylight hours. The model is conservative in this respect, however, due to the fact that these lower temperatures actually give bigger temperature differentials. This was therefore not seen as a hindrance in the model.

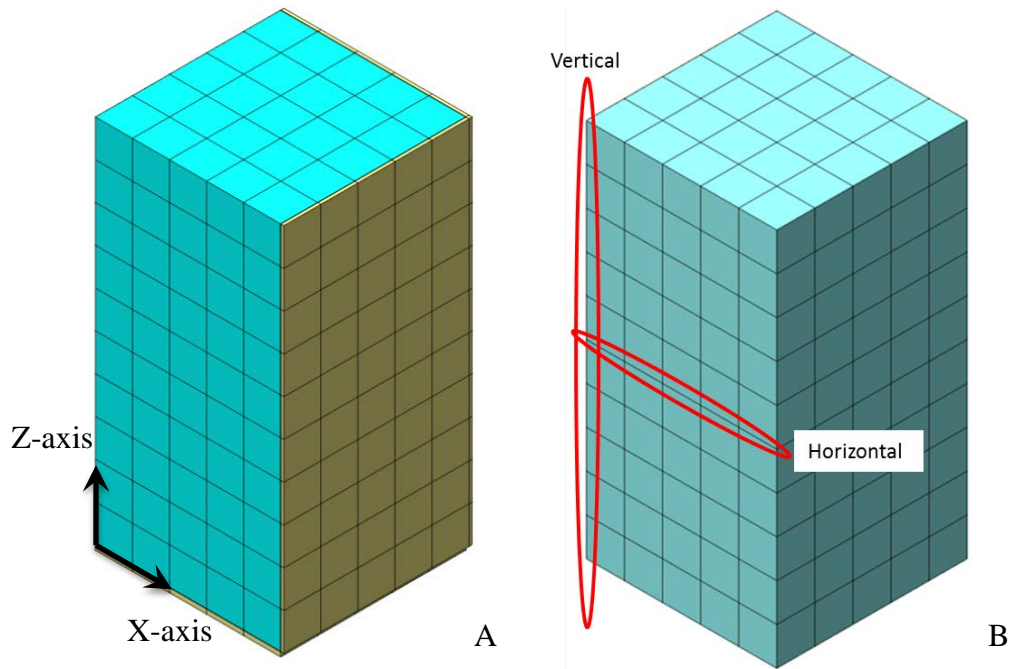


Figure 6-2: Block Experiment Model
A) Overall Mesh B) Temperature Locations

Figure 6-5 shows the comparison of temperature differentials modeled in DIANA and the differentials measured from the block lab experiment. The experimental temperatures are represented by dashed lines and the predicted temperatures from the model are represented by solid lines. Again the finite element model was able to fairly accurately predict temperature differentials measured in the concrete block due to its accurate prediction of the temperature distribution. The model predicted a maximum temperature differential of 49 °F to occur at 42 hours, where the actual measured maximum differential was 46.8 °F at 42.5 hours. The maximum temperature differential was found to exceed the typical maximum limit of 35 °F between the center and the top of the concrete block after 17 hours and to go below the limit after 72 hours, very similarly to the measured data. The model was not able to capture the fluctuation found in the measured results, however, which is again due to the model's inability to capture the temperature increase due to direct sunlight. The model was found to slightly over predict the temperature difference between the center and the bottom face of the concrete due to a slight under prediction of the bottom node's temperature. It also slightly over predicted the temperature difference between the center and the side face of the concrete, where the model had a temperature that actually surpassed the typical maximum differential limit.

Figures 6-6 and 6-7 show the vertical and horizontal temperature profiles at the time of the peak temperature at 26 hours and the time of the maximum temperature differential at 42 hours. These figures show that the temperatures within the concrete are highest near the center and reduce towards the concrete surfaces. The temperatures are slightly lower on the top surface because it is not insulated by plywood forms like the bottom and side faces are. Figure 6-8 shows a pictorial representation of the temperature distribution throughout the concrete block at 42 hours, the time of the maximum temperature differential.

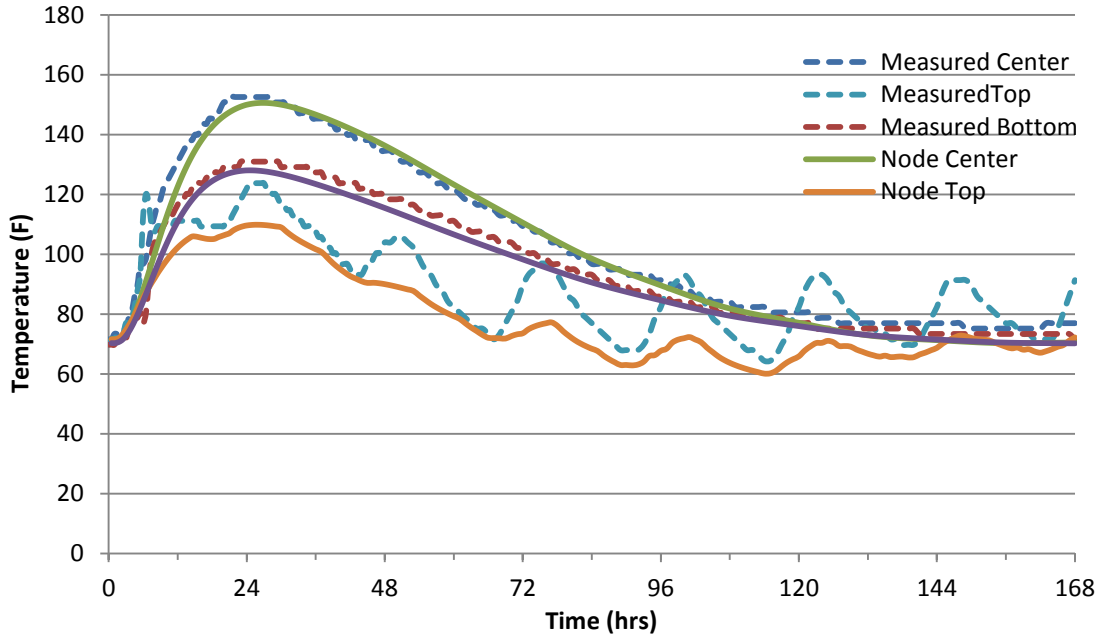


Figure 6-3: Block vertical temperature distribution

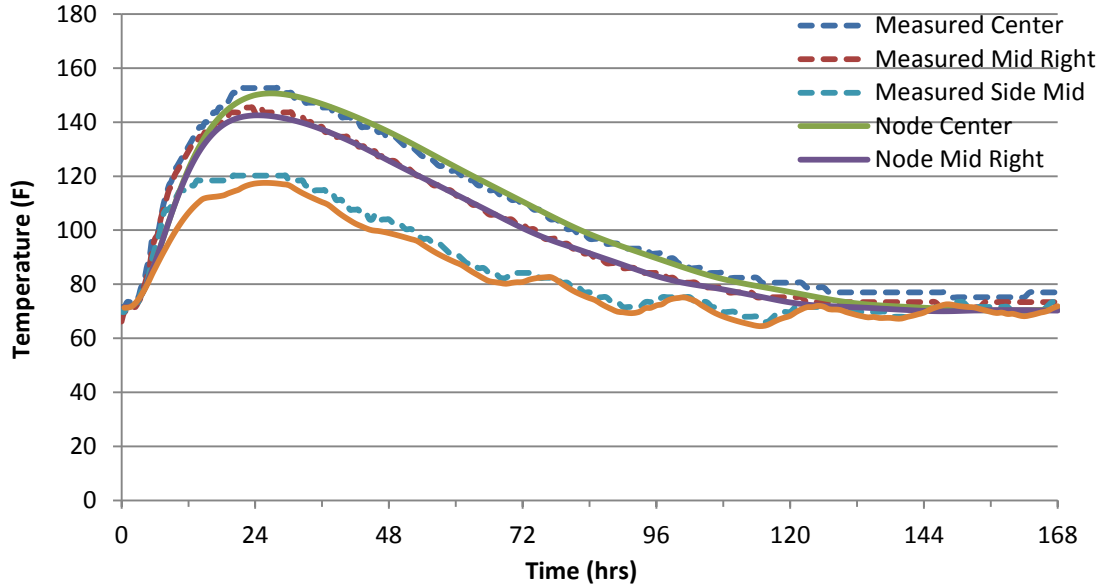


Figure 6-4: Block horizontal temperature distribution

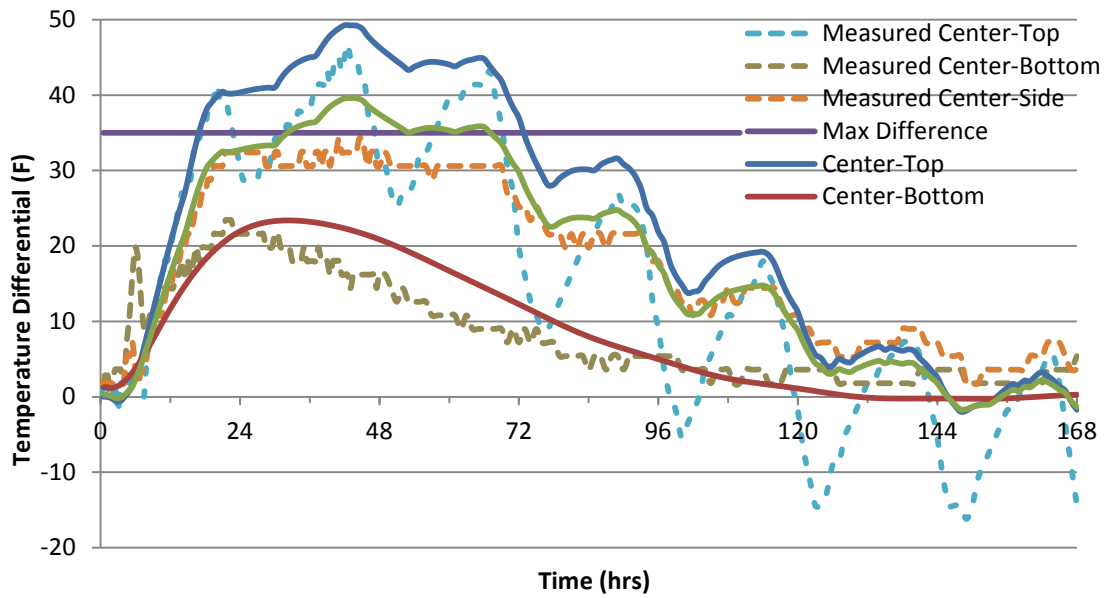


Figure 6-5: Block maximum temperature differentials

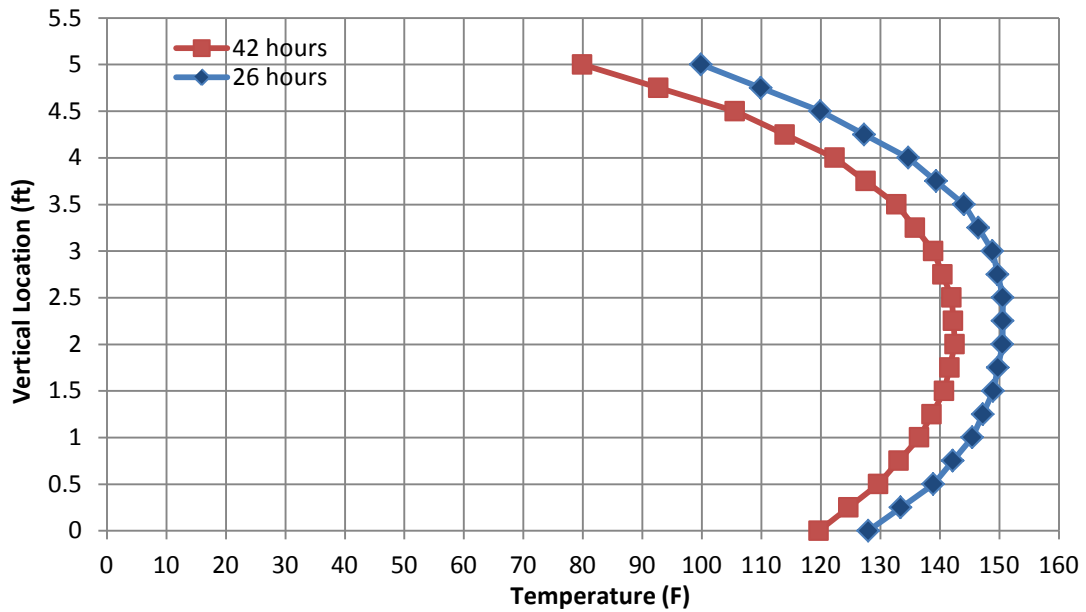


Figure 6-6: Block vertical temperature distribution at 26 and 42 hours

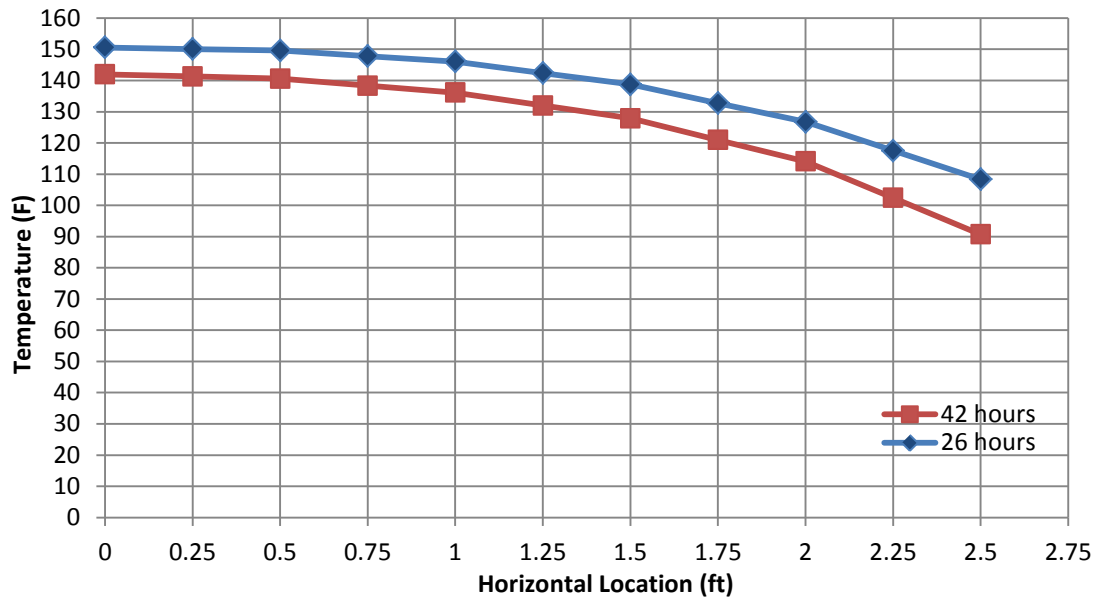


Figure 6-7: Block horizontal temperature distribution at 26 and 42 hours

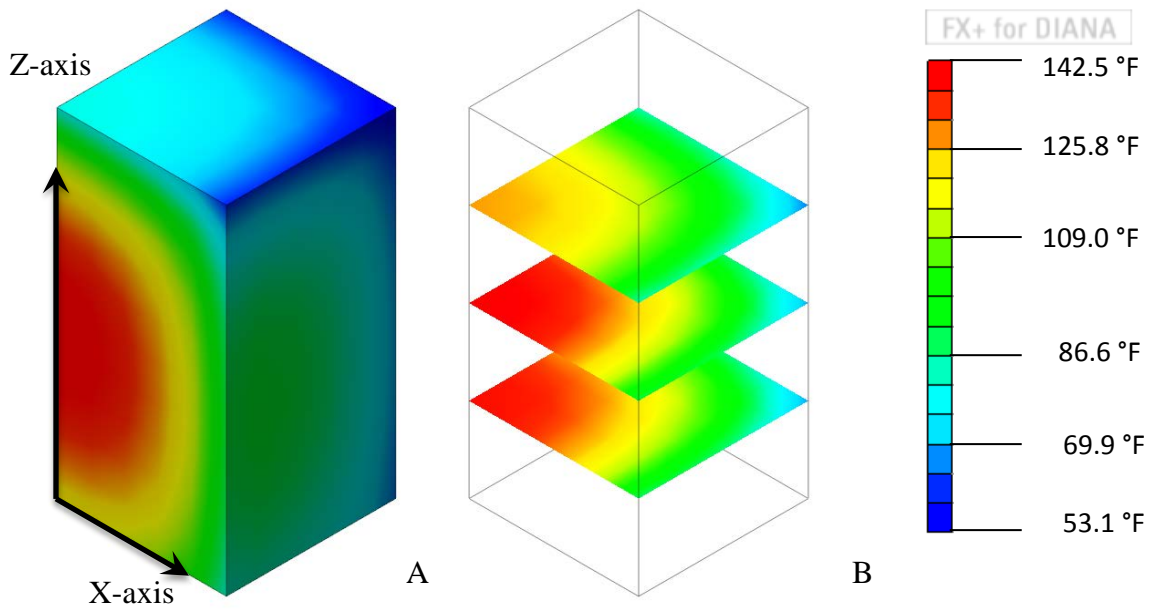


Figure 6-8: Block temperature profile at max temperature difference (42 hours)
 A) Isoparametric view B) Slice view

6.2.2 Structural Analysis Results

The structural results are calculated using the predicted temperatures from the thermal analysis and the mechanical properties measured in the lab. Figure 6-9 shows the locations at which the equivalent age, stresses, and tensile strengths were examined. These locations were chosen because they are where the biggest compressive and tensile stresses occur due to the block's boundary conditions. The biggest compression stresses occurs near the center of the block while the biggest tensile stresses due to thermal gradients occur on the surface of the concrete.

Figure 6-10 and Figure 6-11 show the vertical and horizontal equivalent age profiles, respectively, at the time of the maximum temperature, 26 hours, and the time of the maximum temperature differential, 42 hours. The equivalent age of the concrete is higher in the center of the concrete due to the higher concrete temperatures and gets lower towards the surface where the concrete temperatures are lower. This results in more mature concrete in the center and less mature concrete on the surface, as is expected. These equivalent ages are used to calculate the tensile strength throughout the concrete which has been plotted against the principal stress in Figures 6-12 and 6-13 at 42 hours in the vertical and horizontal directions, respectively. In Figure 6-12 principal stresses only exceed the tensile strength of the concrete at the top node. Through linear interpolation the stress exceeds the tensile strength 0.2 ft below the concrete surface. In Figure 6-13 the stress only exceeded the tensile strength at the node closest to the side

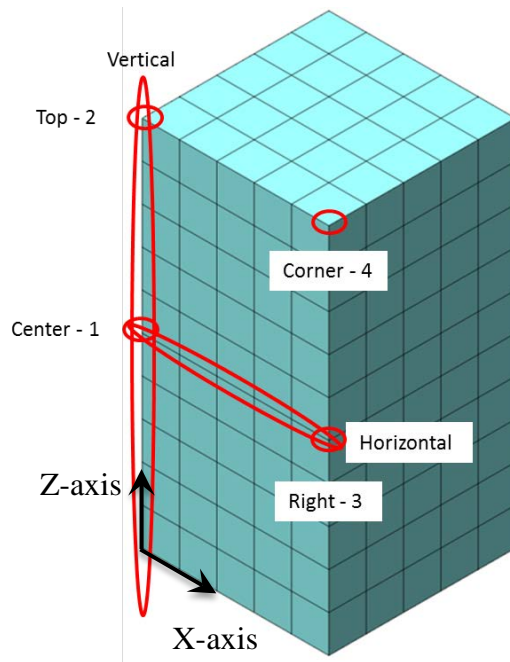


Figure 6-9: Block stress locations

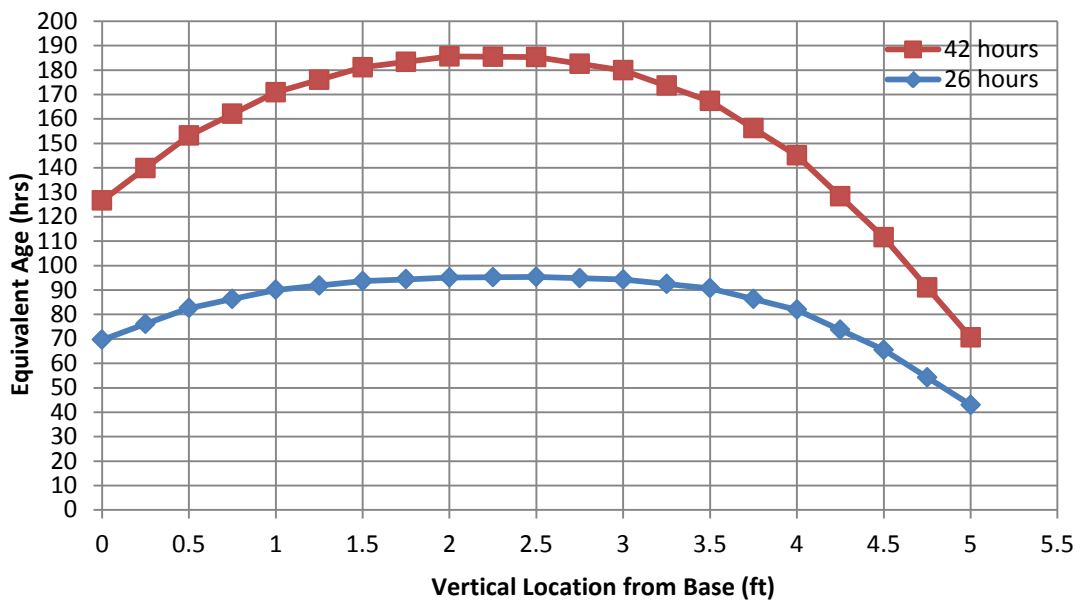


Figure 6-10: Block vertical profile equivalent age at 26 and 42 hours

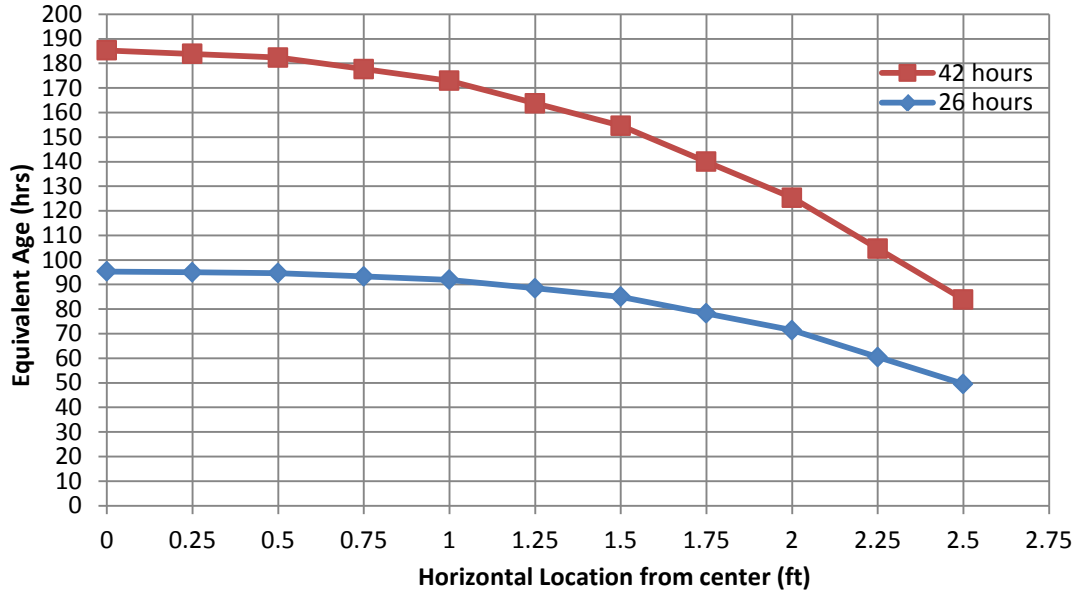


Figure 6-11: Block horizontal profile equivalent age at 26 and 42 hours

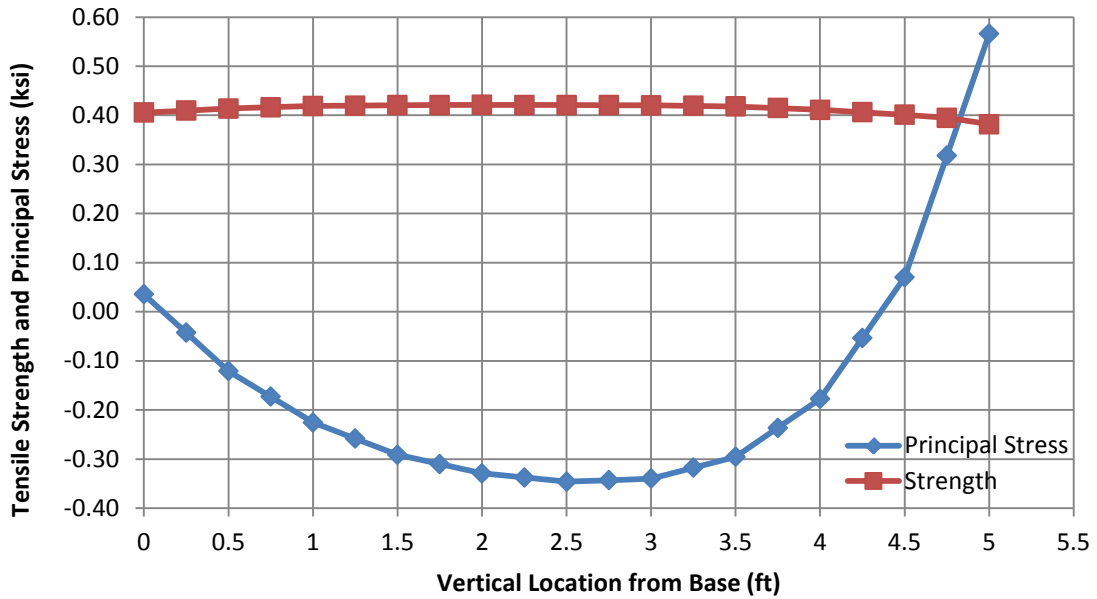


Figure 6-12: Block vertical profile stress and strength at 42 hours

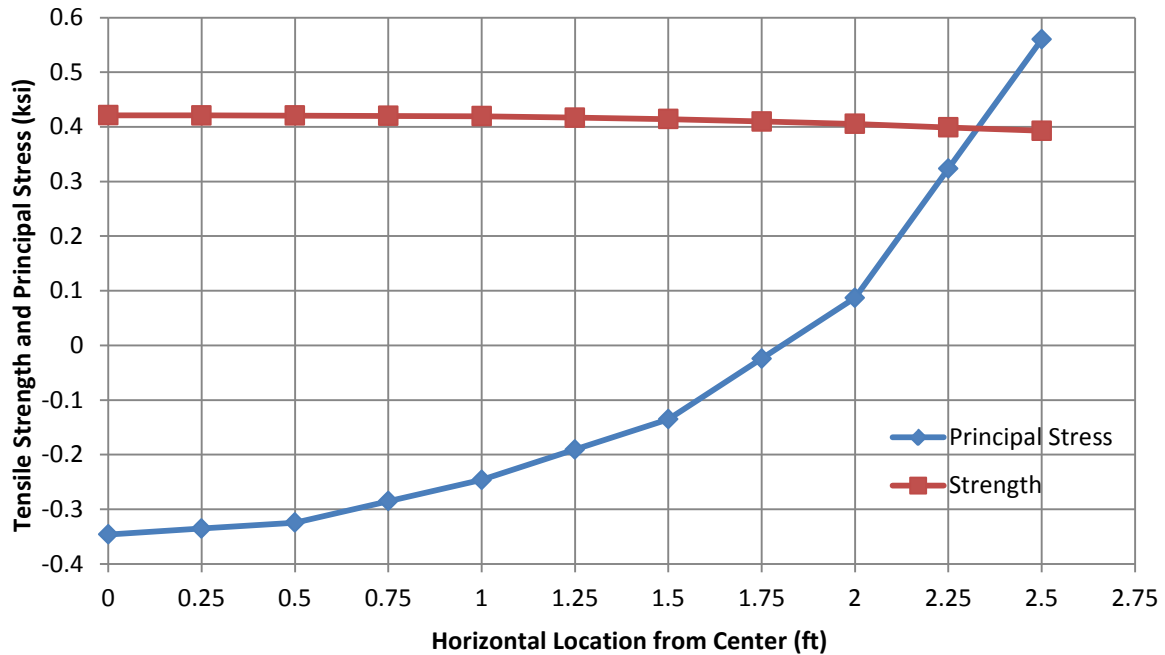


Figure 6-13: Block horizontal profile stress and strength at 42 hours

surface. Through linear interpolation the stress is found to exceed the tensile strength 0.18 ft from the surface. Figure 6-14 shows the principal stress of the previously chosen key locations over time. The center node is in compression and the surface nodes are in tension up until 120 hours where the center node actually goes into tension. The surface nodes reach high tensile stresses between 14 hours and 48 hours, where the maximum stress reached in each node is approximately 0.5 to 0.6 ksi.

Figure 6-15 and 6-16 shows the cracking index for the vertical and horizontal profiles, respectively, at 26 hours and 42 hours. As is shown in these graphs, the cracking index at the time of the peak temperature and the time of the maximum differential are virtually the same. As with the stress graphs in Figures 6-12 and 6-13, Figures 6-14 and 6-15 show the cracking index exceeding the limit of 1 only at the most outer node of each graph. Through linear interpolation the cracking index crosses 1 at a distance 0.1 ft below the

surface in the vertical profile and at a distance 0.05 ft below the surface in the horizontal profile, which is even lower than what was found from Figures 6-12 and 6-13. This is likely due to the limited fineness of the mesh. Recall that the cracking index is limited arbitrarily at a maximum value of 100 (see Section 6.1).

Figure 6-18 shows the 3-D isoparametric view and the plan view of the cracking index contours below 1 on the concrete block at 42 hours. Therefore, these renderings show the volumes in the model where cracking may occur. Only this time stamp is shown because

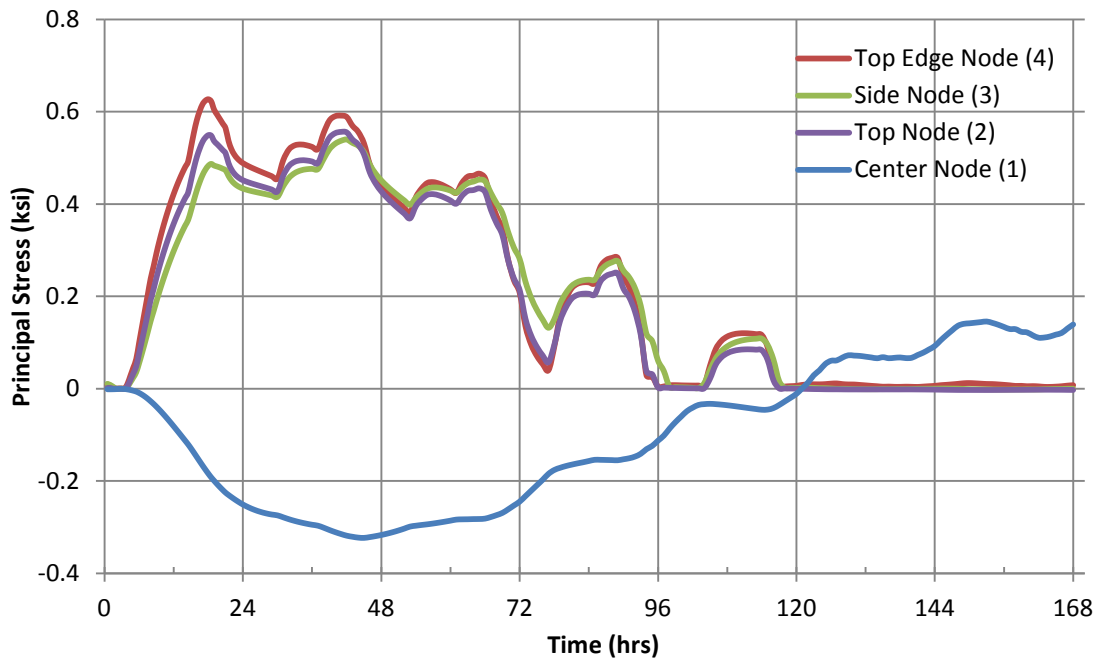


Figure 6-14: Block nodes principal stresses vs time

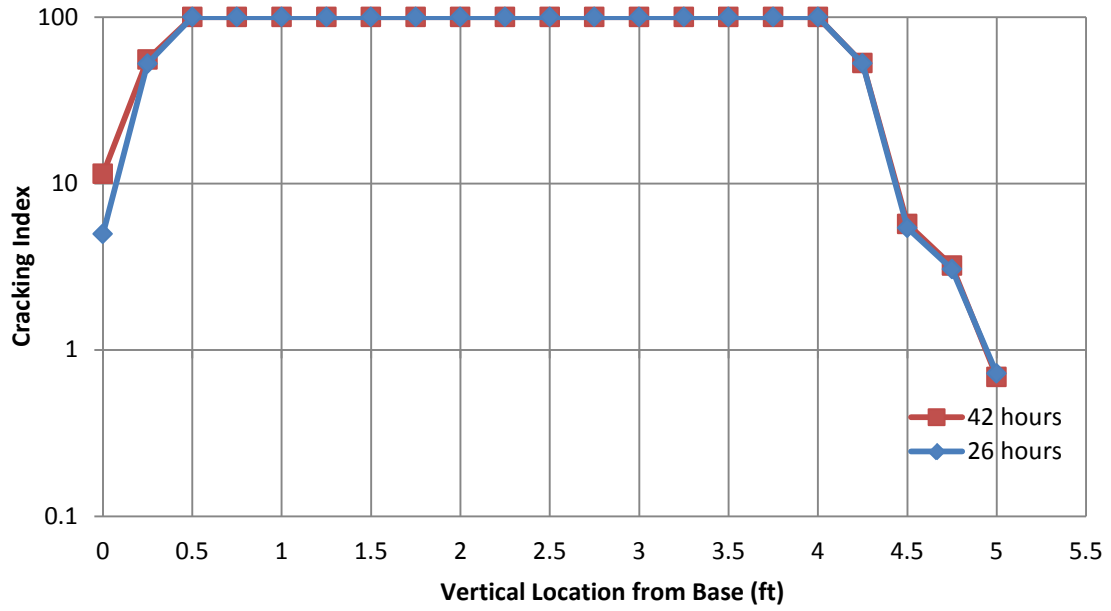


Figure 6-15: Block vertical profile cracking index at 26 and 42 hours

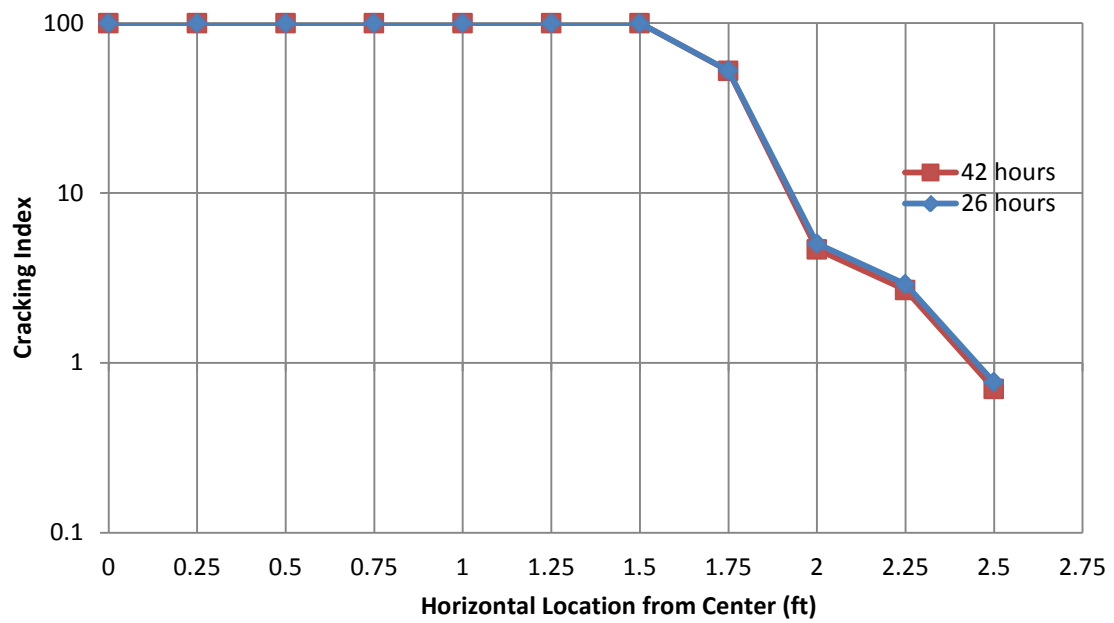


Figure 6-16: Block horizontal profile cracking index at 26 and 42 hours

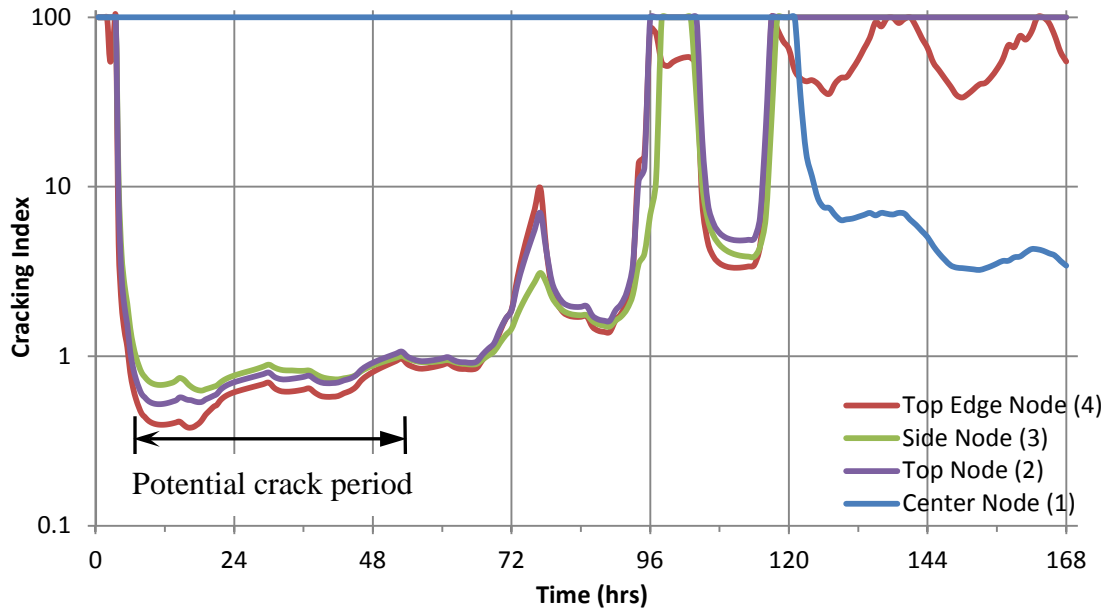


Figure 6-17: Block nodes cracking index vs time

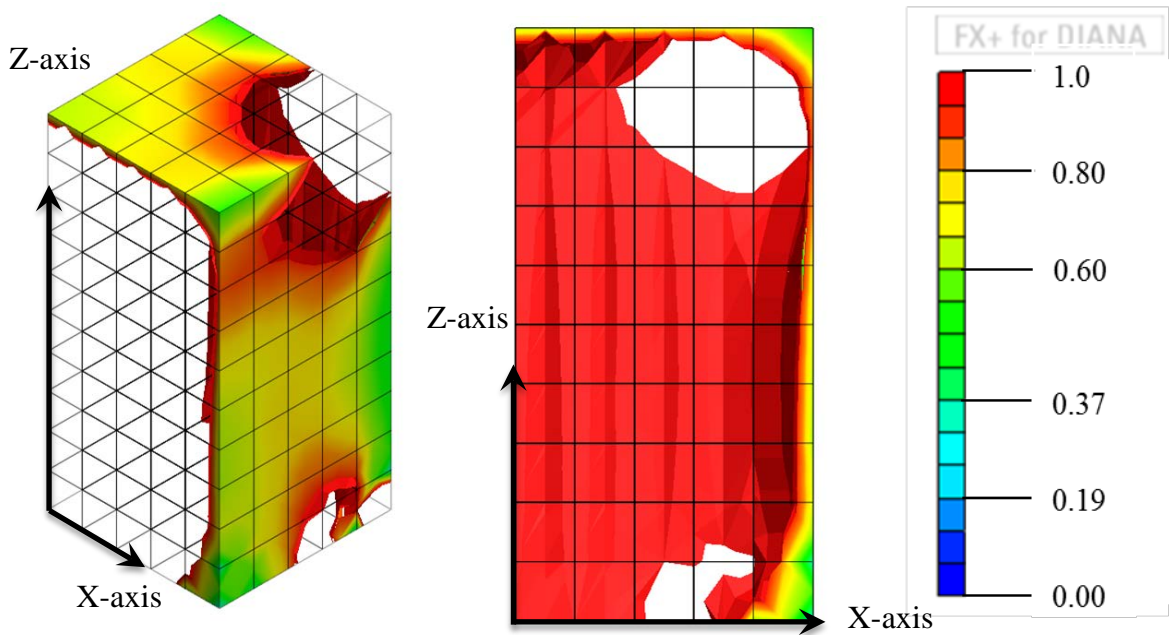


Figure 6-18: Block cracking index contours at 42 hours
 A) Isoparametric view B) Profile view

the cracking index contours at the time of the peak temperature were very similar to that of the time of the maximum temperature differential (42 hours). As was seen in the principal stress graphs and the cracking index graphs, Figure 6-18 shows that the cracking index goes below the index limit of 1, but that it does not extend past the first, most outer nodes.

6.3 Oak Island Footing Case Study

6.3.1 Thermal Analysis Results

The first case study was the Oak Island Bridge footing. As seen in Figures 6-19 and 6-20, a quarter of the footing was modeled with the steel formwork and insulation blankets explicitly modeled. The thermal results from the model were compared to field measurements given by the NCDOT. There were no locations with these measurements, however, so these field measurements were only used as a secondary check to see if the DIANA model produced reasonable results. Figure 6-20 shows the temperature locations used in Figures 6-21 through 6-25. These locations were again chosen because it is where standards and specifications typically measure temperatures and temperature differentials.

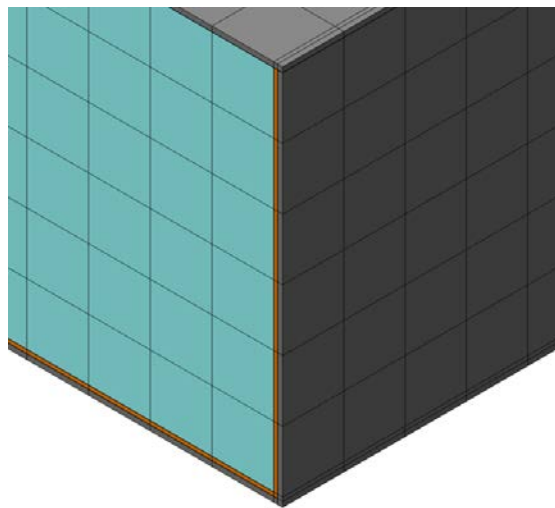


Figure 6-19: Oak Island mesh close up

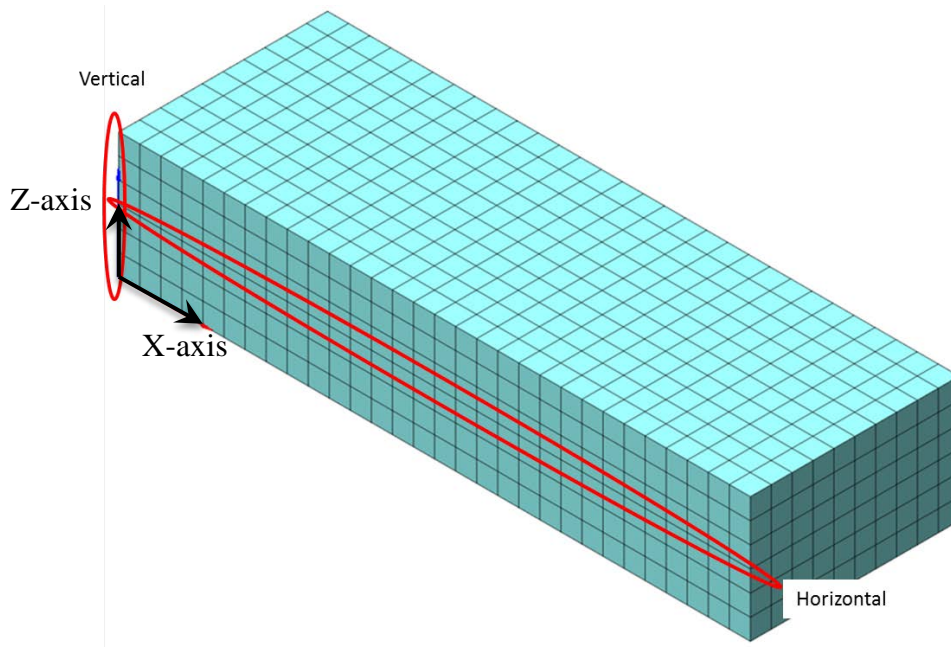


Figure 6-20: Oak Island temperature locations

Figures 6-21 and 6-22 show the comparison of temperatures modeled in DIANA, identified as nodes, and the field measurements. As these figures indicate, the finite element model closely matched the actual measurements. There is a slight offset between thermo 2 and the top node temperature rise, however. This is likely due to the fact that the model assumed one start time for the whole footing whereas the concrete pour actually took 6 hours. The model predicted a maximum temperature of 157.7 °F to occur at 51 hours and start decreasing at 54 hours, whereas the field measurement maximum was found in thermo 2 to be 158.6 °F at 56 hours where it decreased after 61 hours. It is also noted that the center and mid-right nodes have nearly identical temperatures because of the large distances between the center and side of the footing and the nearly adiabatic nature of the mid-height of the footing.

Figure 6-23 shows the comparison of temperature differentials modeled in DIANA and the differentials developed from the field measurements. The difference between the

smallest temperature measurement, thermo 2, and the two measurements with the higher temperatures, thermo 1 and thermo 3, was taken as differentials to compare to the modeled differentials. The model predicted a maximum temperature differential of 45.6 °F to occur at 116 hours between the center and the side, but only a maximum temperature differential of 33.5 °F between the center and the top, which occurs between 95 hours and 118 hours. The maximum differential in the field measurements was 43.7 °F at 83 hours to 99 hours. The modeled temperature differentials do not exactly match the differentials from the field measurements due to slight differences in surface temperatures, but they are considered to be sufficiently similar.

Figures 6-24 and 6-25 show the vertical and horizontal temperature profiles at the time of the maximum temperature differential which occurs at 116 hours. Figure 6-26 and Figure 6-27 show pictorial representations of the temperature distribution throughout the concrete block at the time of the maximum temperature differential.

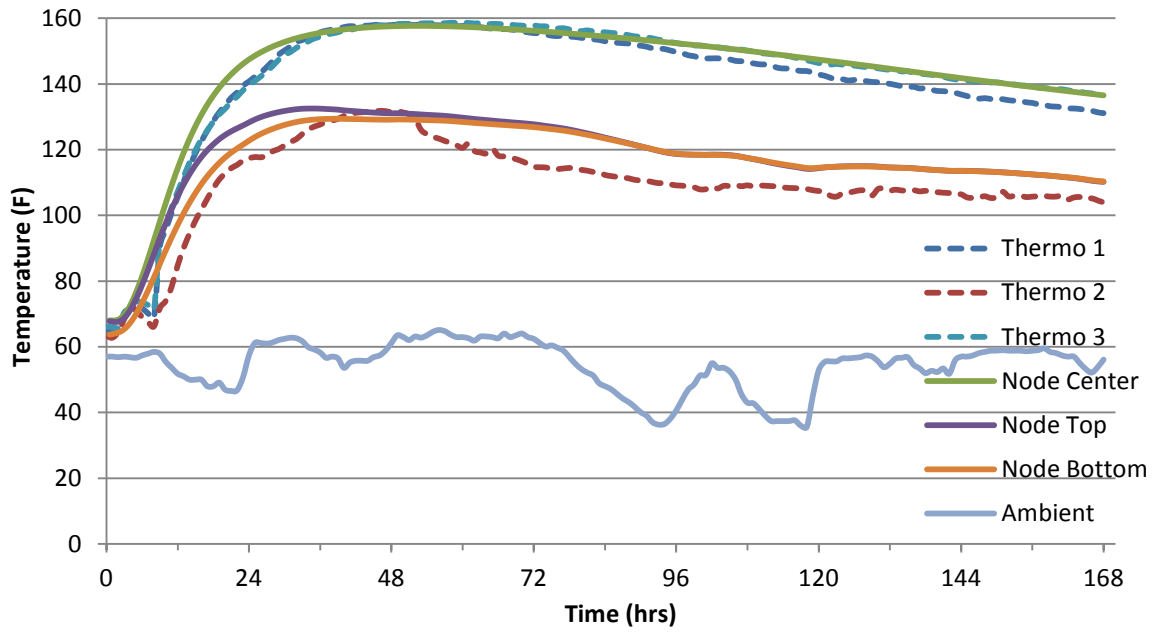


Figure 6-21: Oak Island vertical temperature distribution

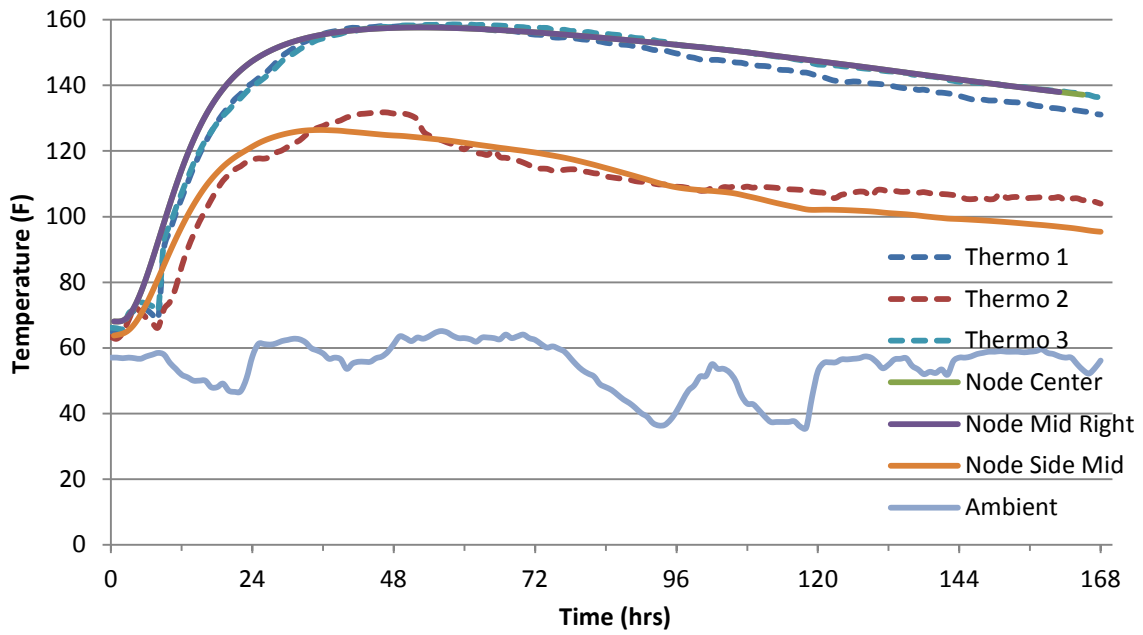


Figure 6-22: Oak Island horizontal temperature distribution

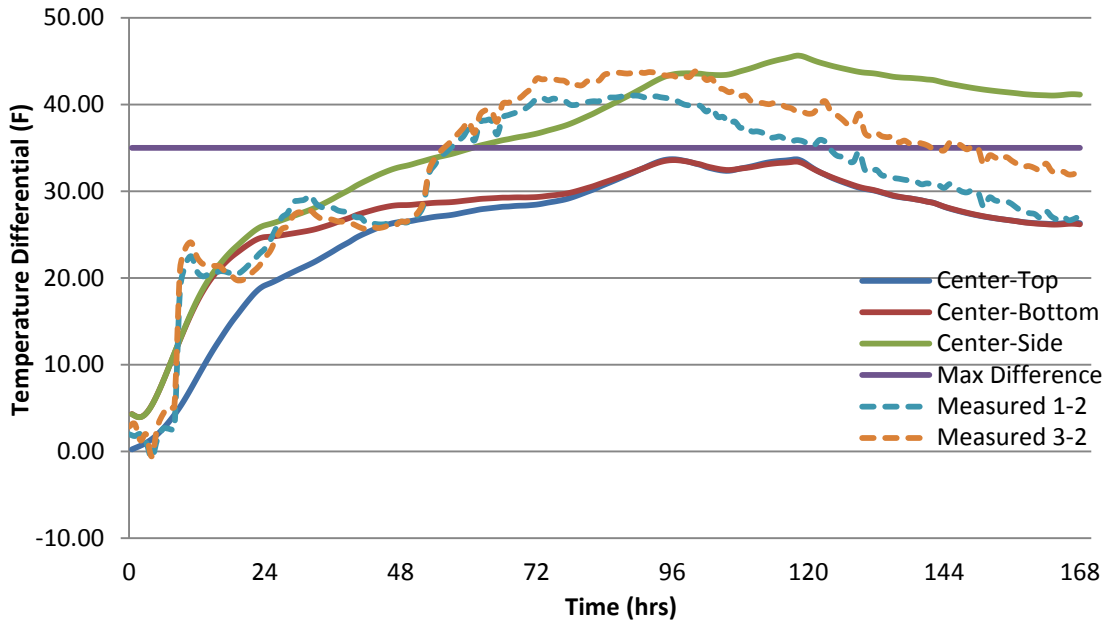


Figure 6-23: Oak Island maximum temperature differentials

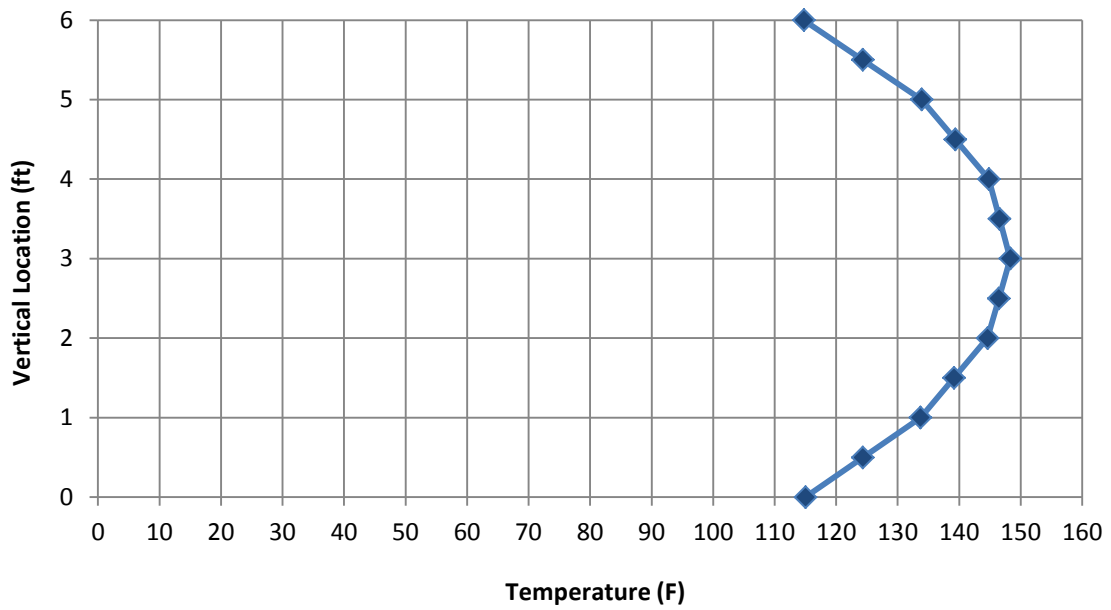


Figure 6-24: Oak Island vertical profile temperature distribution at 116 hours

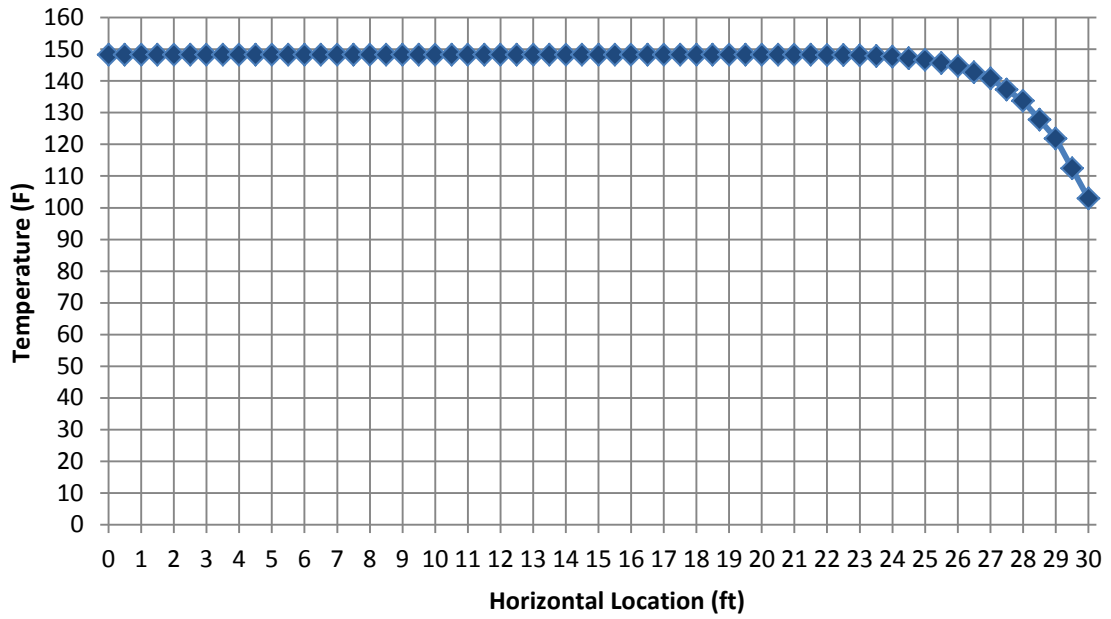


Figure 6-25: Oak Island horizontal profile temperature distribution at 116 hours

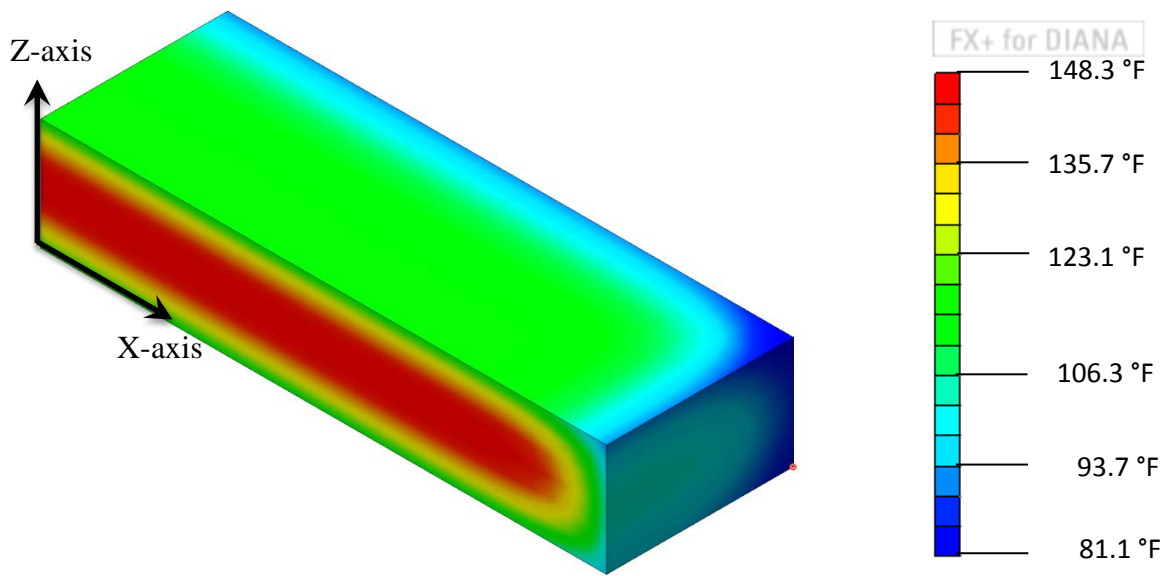


Figure 6-26: Oak Island temperature profile at 116 hours

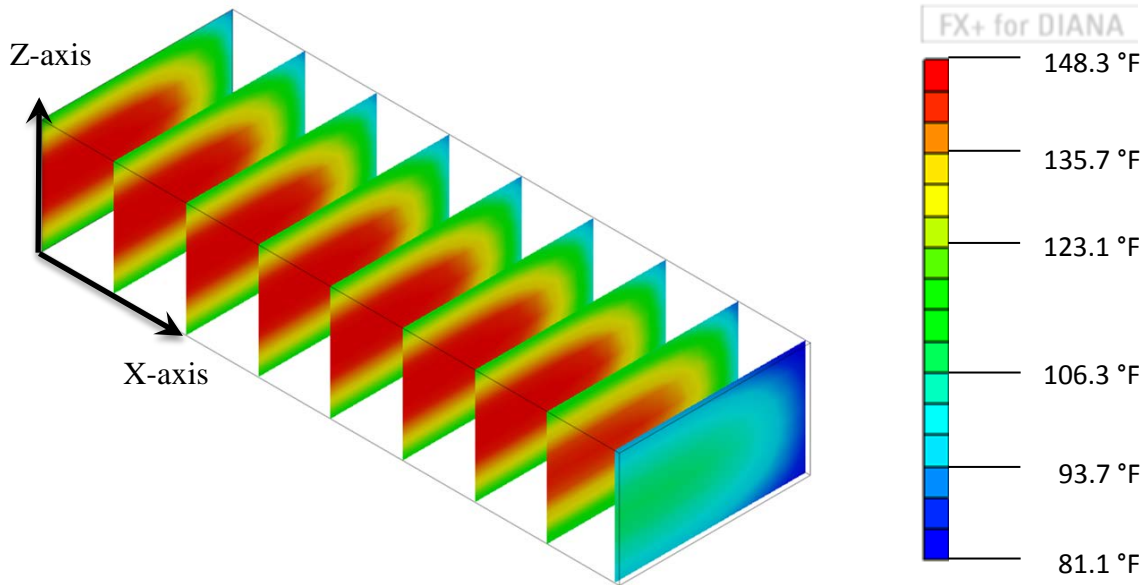


Figure 6-27: Oak Island sliced temperature profile at 116 hours

6.3.2 Structural Analysis Results

Figure 6-28 shows the locations at which the equivalent age, stresses, and tensile strengths were examined. These locations were chosen because they are where some of the biggest stresses occur due to the footing's boundary conditions. These are not the same locations as the block experiment due to the footing's different boundary conditions.

Figure 6-29 and Figure 6-30 show the vertical and horizontal equivalent age profiles, respectively, at the time of the maximum temperature differential, 116 hours. As with the block, the equivalent age of the concrete is higher in the center of the concrete due to the higher concrete temperatures and gets lower towards the surface where the concrete temperatures are lower. These equivalent ages are used to calculate the tensile strength throughout the concrete which has been plotted against the principal stress in Figures 6-31 and 6-32 at 116 hours. In Figure 6-31, the principal stress only exceeds the tensile strength of the concrete at the top node, but exceeds the strength up to 0.4 ft below the concrete surface,

found through linear interpolation. In Figure 6-32 the stress just barely reaches the tensile strength limit at the surface node of the side face and does not extend any further into the concrete. Figure 6-33 shows the principal stress of the previously chosen key locations over time. The center node is in compression and the surface nodes are in tension throughout the whole analysis. The outer nodes reach fairly high tensile stresses as well, reaching stresses up to 0.5 ksi and 0.7 ksi.

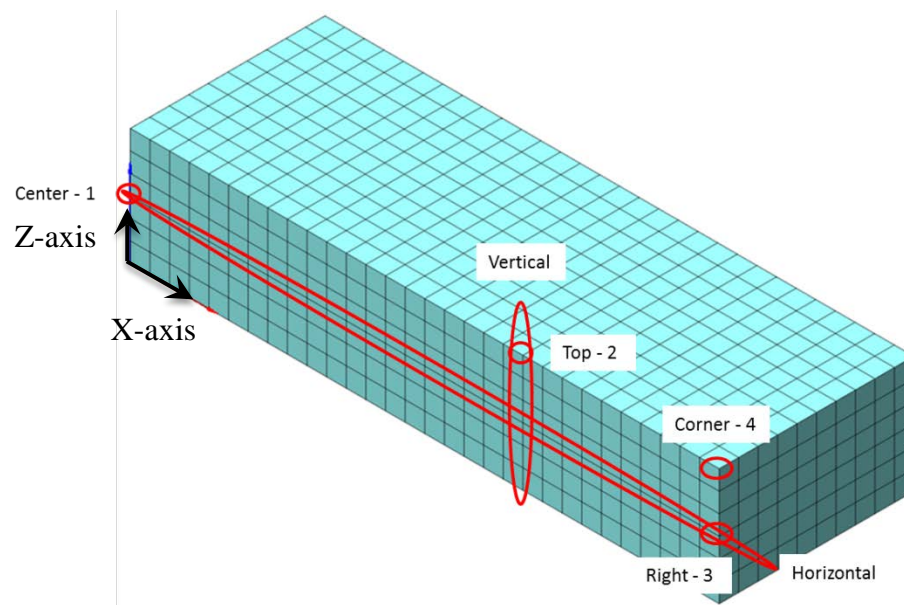


Figure 6-28: Oak Island stress locations

Figures 6-34 and 6-35 show the cracking index for the vertical and horizontal profiles, respectively, at 116 hours. As with the stress graphs in Figures 6-31 and 6-32, Figure 6-34 shows the cracking index exceeding the limit of 1.0 only at the most outer node. Through linear interpolation the cracking index is found to cross 1.0 at a distance of 0.13 feet, which is a somewhat lower than what was found using the stress figure. In Figure 6-35,

the cracking index never reaches 1.0 in the horizontal profile, which is representative of what was seen in the stress figure. Figure 6-36 shows cracking index of the previously chosen key locations over time. The center node has a high index of the entire model duration, whereas the outer nodes towards the concrete surface never quite get above the cracking index limit of 1.0, with the exception of the side node.

Figure 6-37 shows the 3-D isoparametric view and Figure 6-38 shows the plan view of the cracking index contours below 1.0 on the concrete block at 116 hours. As was seen in the principal stress graphs and the cracking index graphs, Figures 6-37 and 6-38 show that the cracking index goes below the index limit of 1.0, but that it does not extend past the first, most outer nodes. The only locations that this does occur are at the locations above the pile supports where the nodes were fixed.

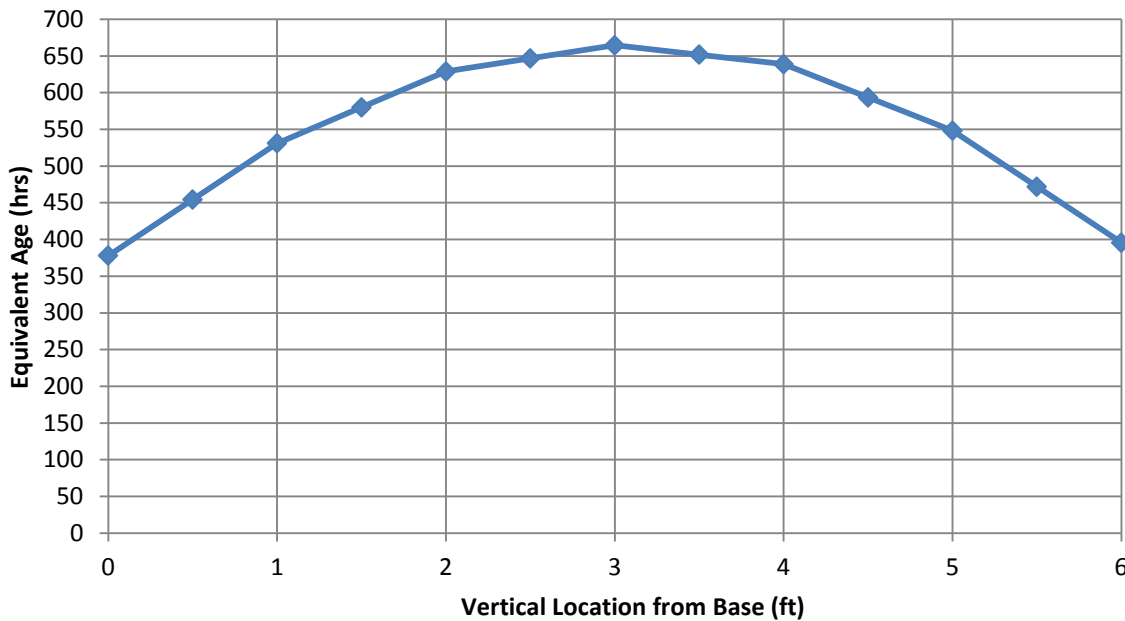


Figure 6-29: Oak Island vertical profile equivalent age at 116 hours

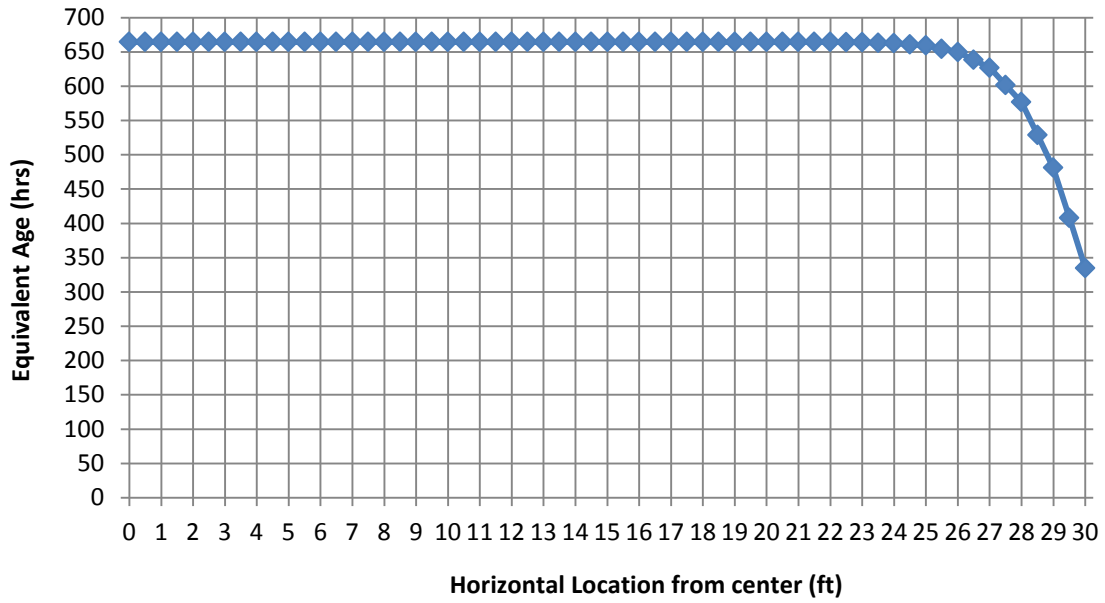


Figure 6-30: Oak Island horizontal profile equivalent age at 116 hours

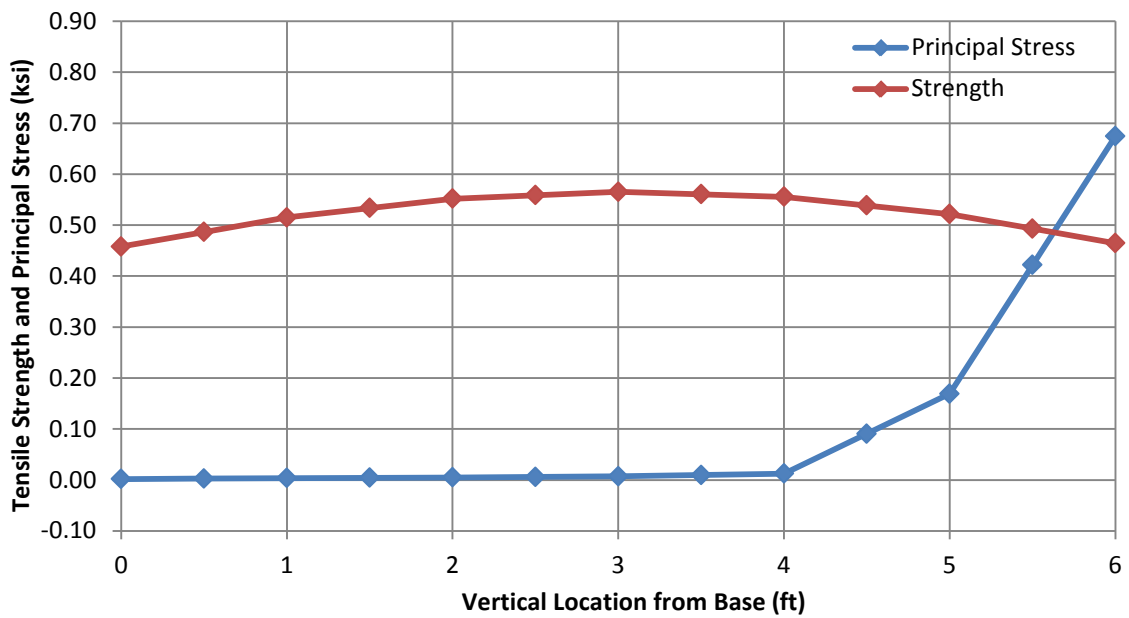


Figure 6-31: Oak Island vertical profile stress and strength vs time at 116 hours

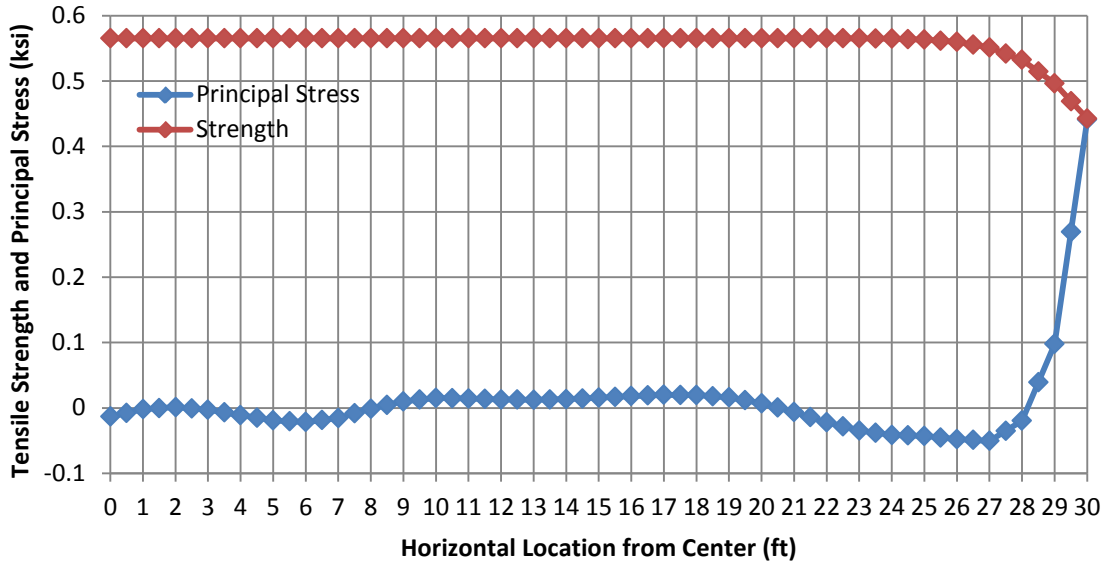


Figure 6-32: Oak Island horizontal profile stress and strength vs time at 116 hours

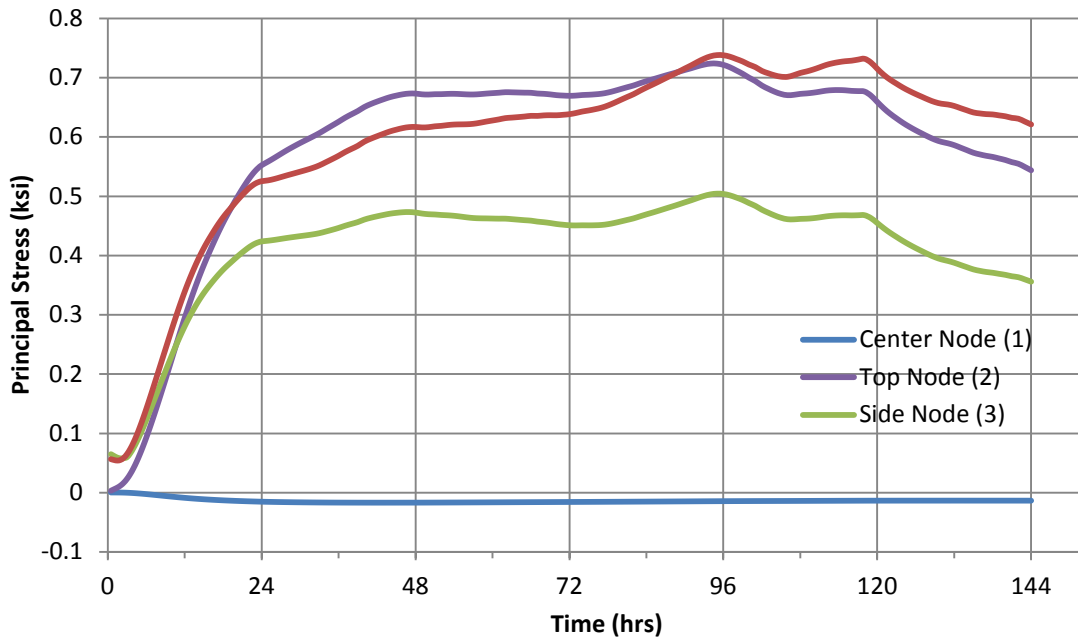


Figure 6-33: Oak Island nodes principal stresses vs time

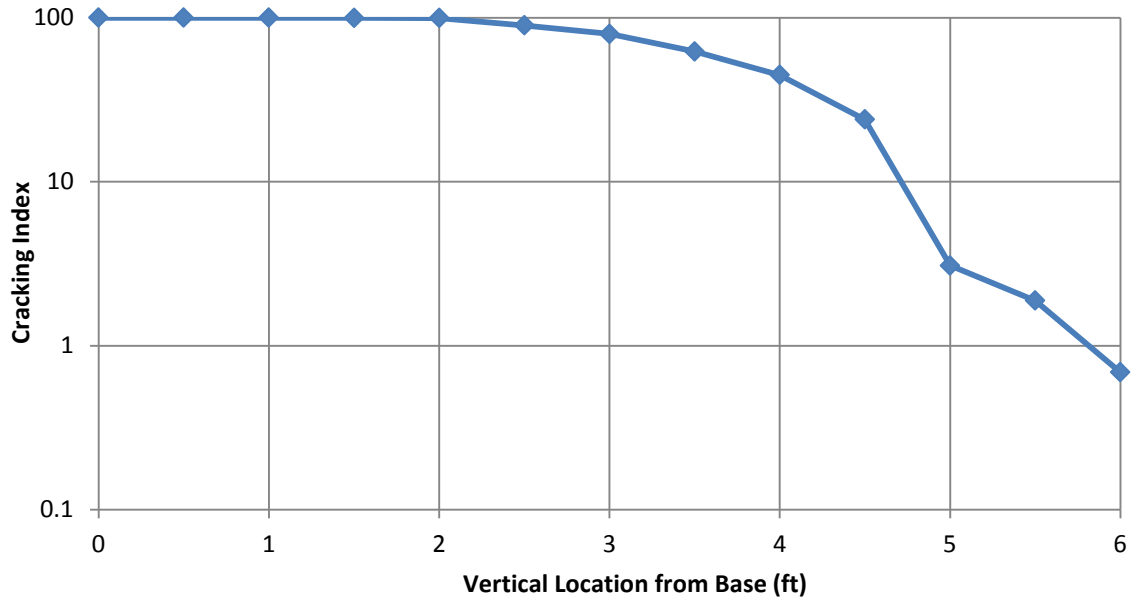


Figure 6-34: Oak Island vertical profile cracking index at 116 hours

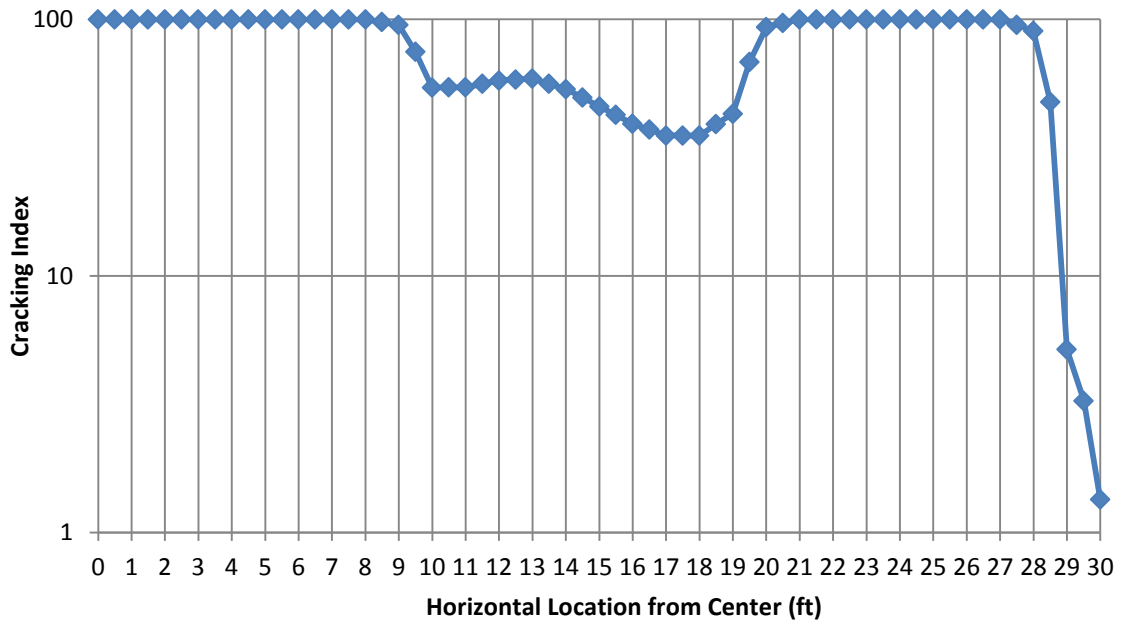


Figure 6-35: Oak Island horizontal profile cracking index at 116 hours

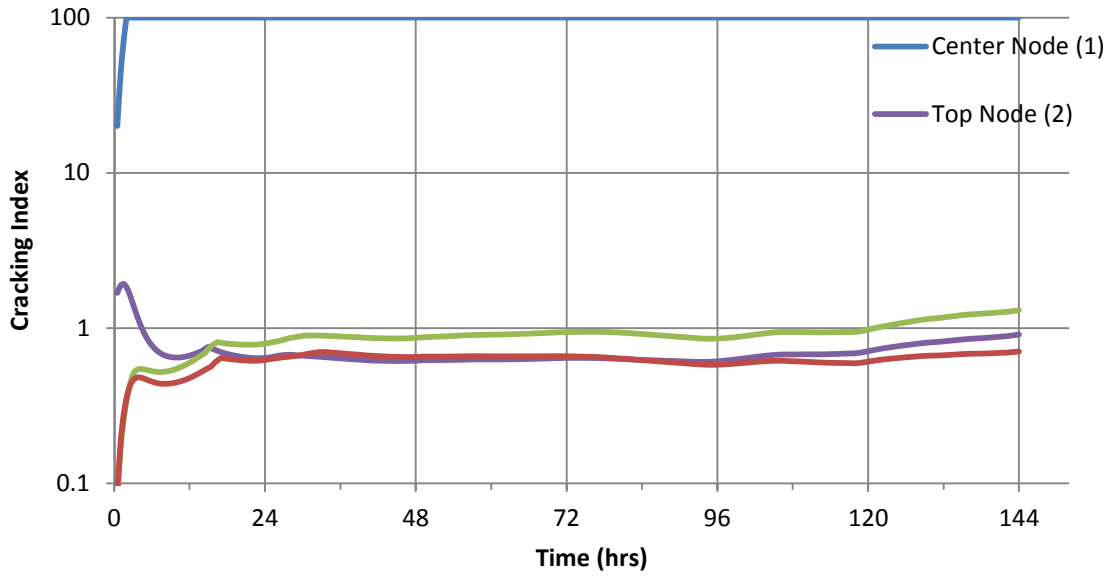


Figure 6-36: Oak Island nodes cracking index vs time

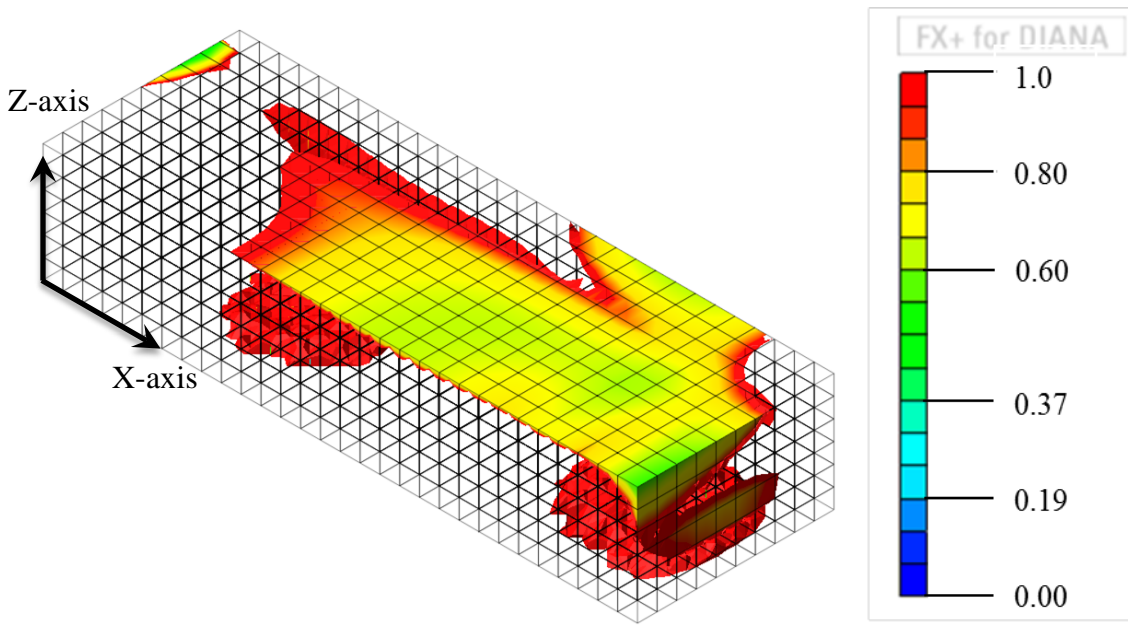


Figure 6-37: Oak Island cracking index contours at 116 hours isoparametric view

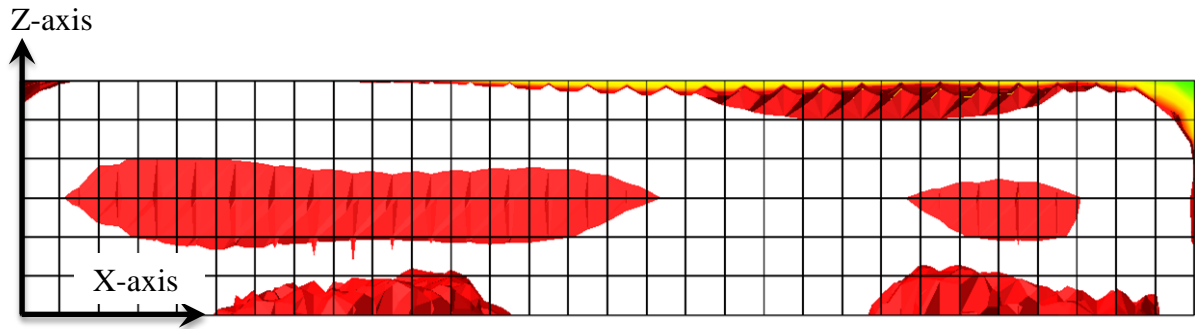


Figure 6-38: Oak Island cracking index contours at 116 hours profile view

6.4 Sunset Beach Footing Case Study

6.4.1 Thermal Analysis Results

The Sunset Beach Bridge footing was very similar to that of the Oak Island case study, only with slightly different dimensions. As seen in Figure 6-39 and 6-40, a quarter of the footing was modeled with the steel formwork and insulation blankets explicitly modeled. No results for temperature field measurements or thermocouple locations were available for this case study. Reasonable confidence in the thermal results was established, however, due to the footing's similarity to the Oak Island study. Figure 6-40 shows the temperature locations used in Figures 6-41 through 6-45.

Figures 6-41 and 6-42 show the vertical and horizontal profile temperature distributions, respectively, over time. The model predicted a maximum temperature of 152.2 °F to occur at 51 hours and start decreasing at 56 hours. There is an unusual slight temperature rise in the more outer nodes that occurs at 95 hours. The cause of this was unable to be determined. It is also noted that the center and mid-right nodes have nearly identical temperatures because of the large distances between the center and side of the footing and the nearly adiabatic nature of the mid-height of the footing.

Figure 6-43 shows the maximum temperature differentials developed in the DIANA model. The model predicted a maximum temperature differential of 37.4 °F to occur at 86 hours between the center and the side, but only a maximum temperature differential of

30.0 °F between the center and the top, which occurs approximately 46 hours after the concrete pour. A dip also occurs in the temperature differentials due to the unusual rise found in the predicted temperature data.

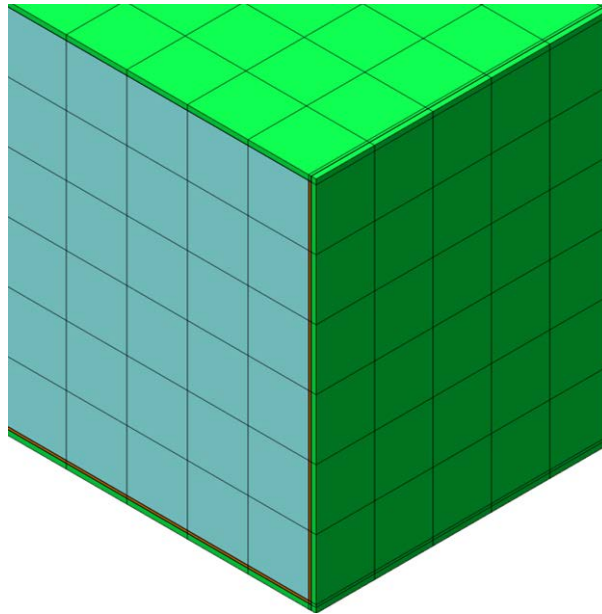


Figure 6-39: Sunset Beach mesh close up

Figures 6-44 and 6-45 show the vertical and horizontal temperature profiles at the time of the maximum temperature differential which occurs at 86 hours. Figure 6-46 and Figure 6-47 show pictorial representations of the temperature distribution throughout the concrete block at the time of the maximum temperature differential. These figures show that the temperatures within the concrete are highest in the center and get lower towards the concrete surface, as is expected.

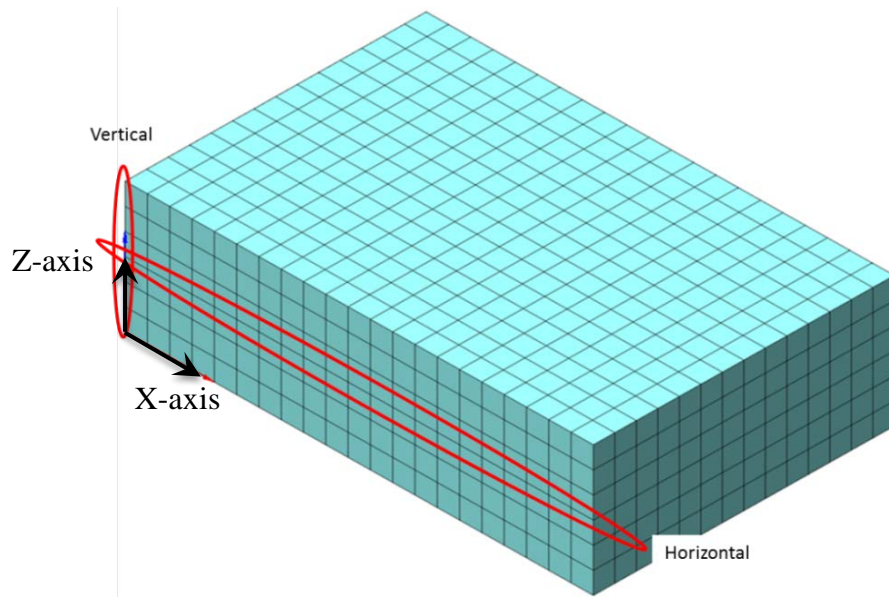


Figure 6-40: Sunset Beach temperature locations

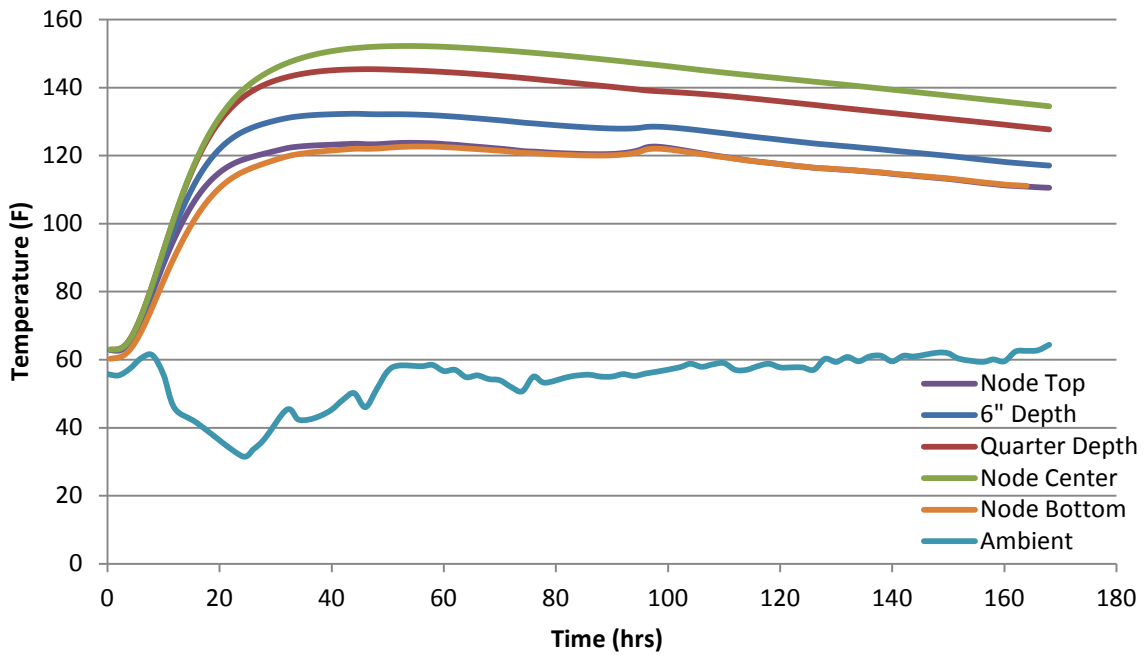


Figure 6-41: Sunset Beach vertical temperature distribution

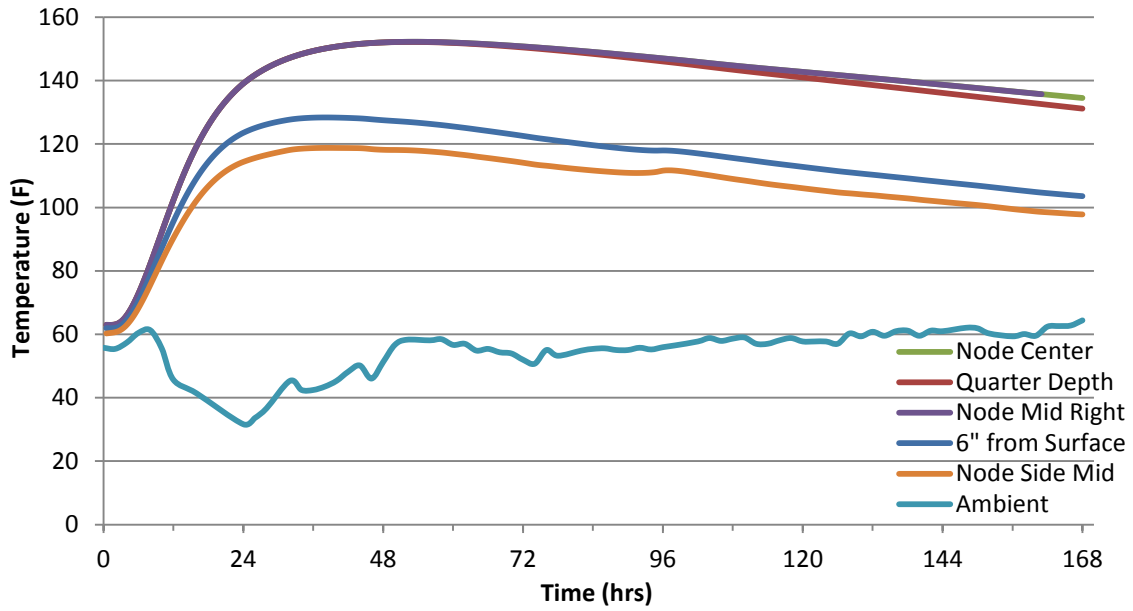


Figure 6-42: Sunset Beach horizontal temperature distribution

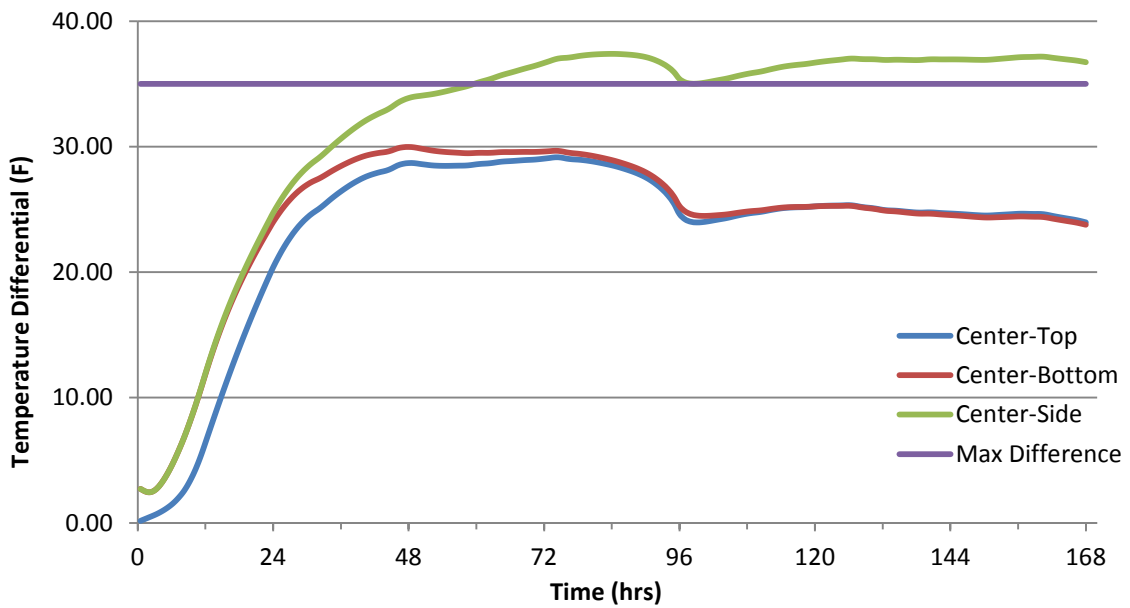


Figure 6-43: Sunset Beach maximum temperature differentials

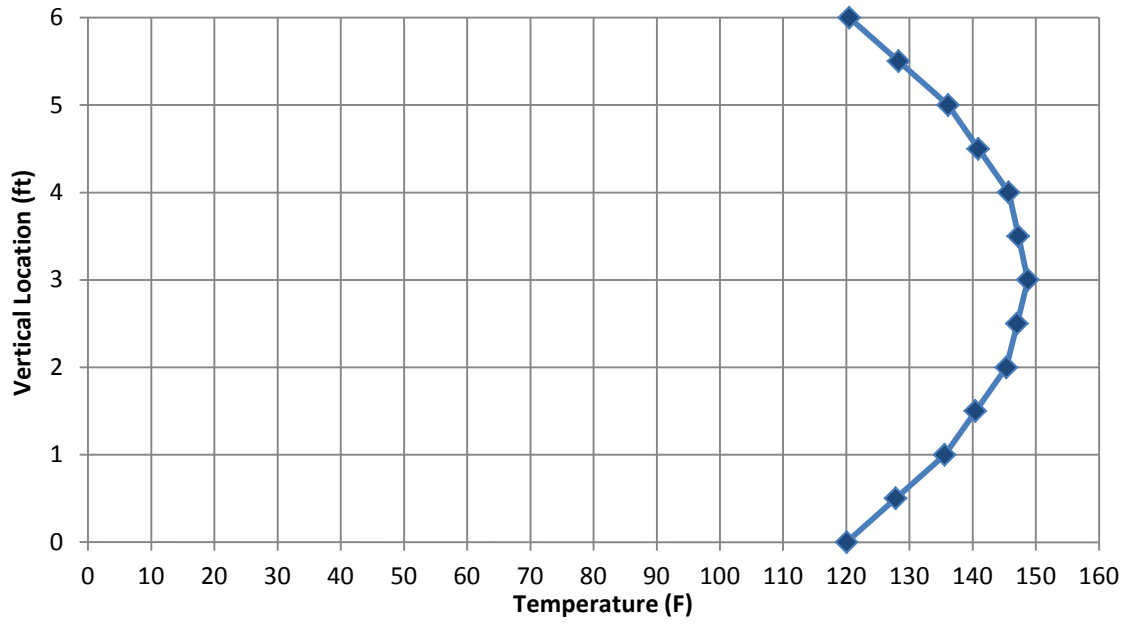


Figure 6-44: Sunset Beach vertical temperature distribution at 86 hours

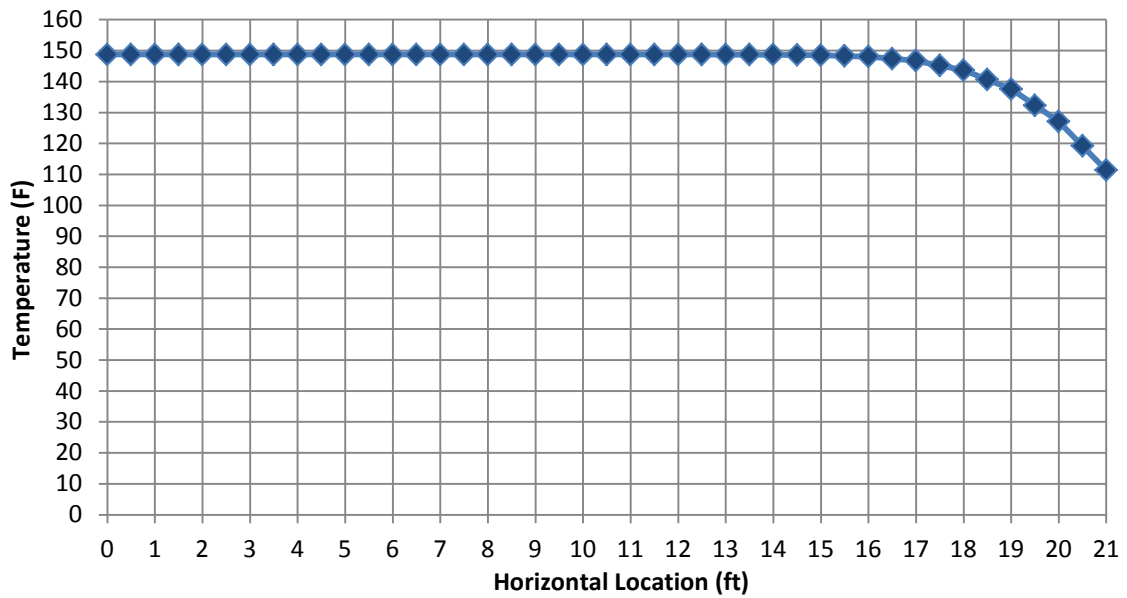


Figure 6-45: Sunset Beach horizontal temperature distribution at 86 hours

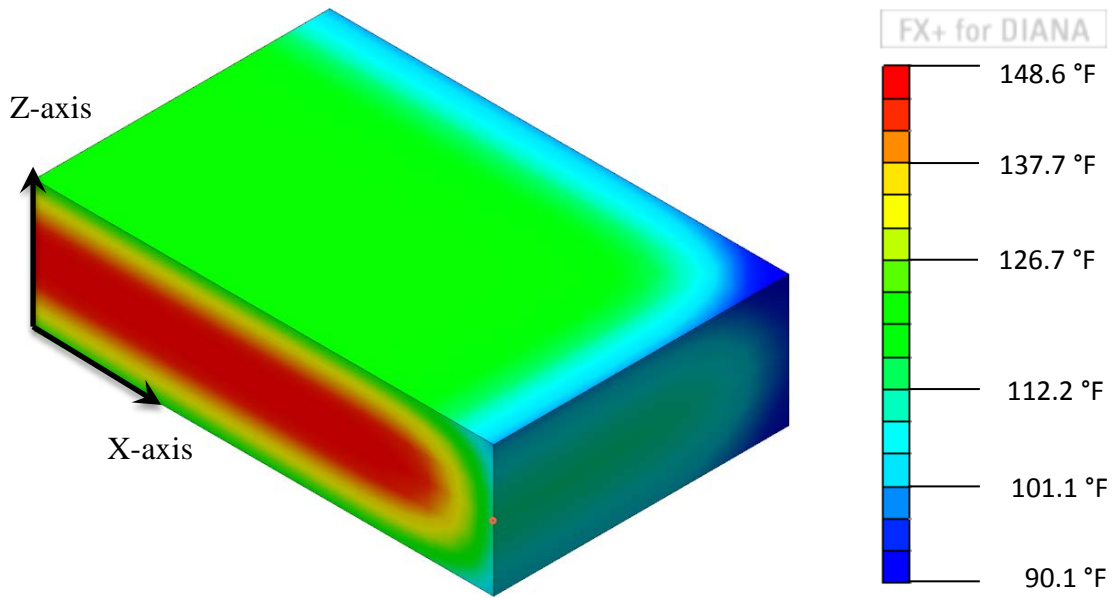


Figure 6-46: Sunset Beach temperature profile at 86 hours

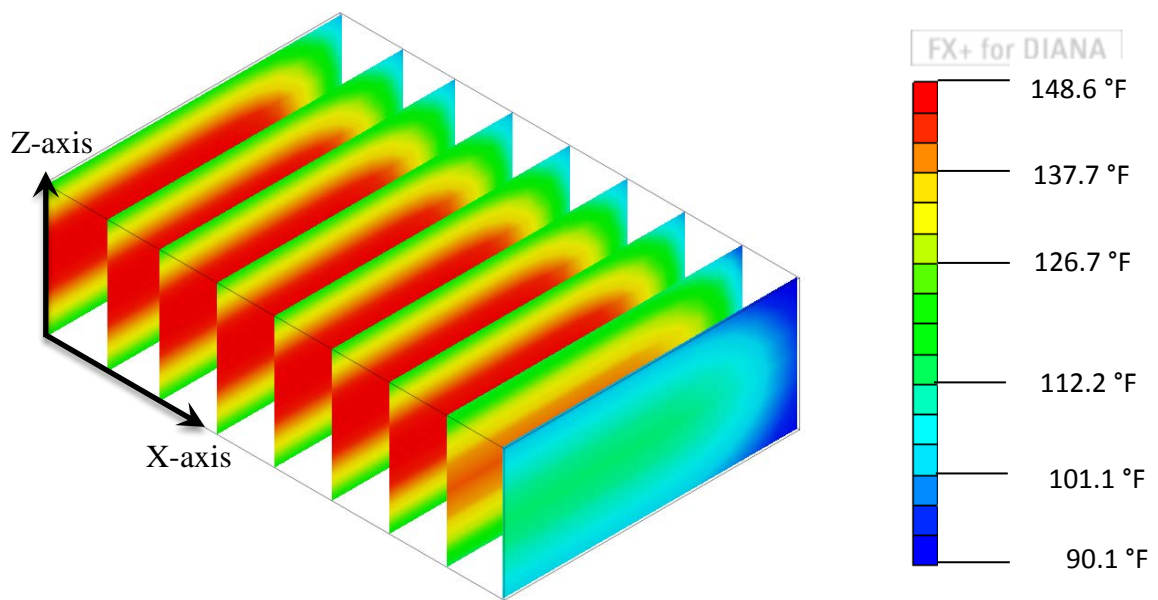


Figure 6-47: Sunset Beach sliced temperature profile at 86 hours

6.4.2 Structural Analysis Results

Figure 6-48 shows the locations at which the equivalent age, stresses, and tensile strengths were looked at. These locations were chosen because they are where some of the biggest compressive and tensile stresses occur due to the footing's boundary conditions.

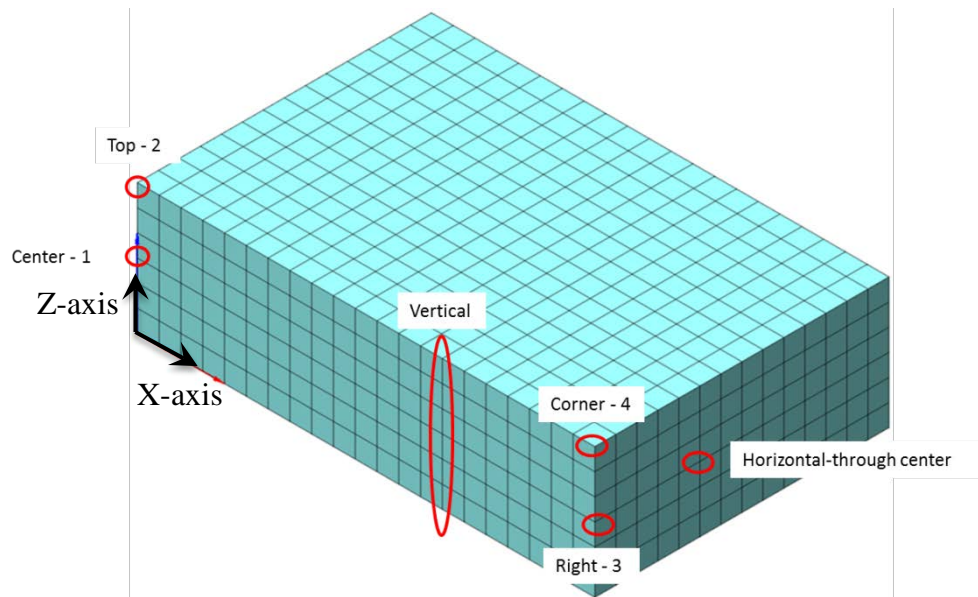


Figure 6-48: Sunset Beach stress locations

Figure 6-49 and Figure 6-50 show the vertical and horizontal equivalent age profiles, respectively, at the time of the maximum temperature differential for the side node, 86 hours, as well as at the time of the maximum differential for the top node, 46 hours. As seen in these two figures, the equivalent age increases as the concrete temperature increases. These equivalent ages are used to calculate the tensile strength throughout the concrete which has been plotted against the principal stress in Figures 6-51 and 6-52 at 86 hours. In Figure 6-51, the principal stress only exceeds the tensile strength of the concrete at the top node, but exceeds the strength up to 0.28 ft below the concrete surface, found through linear

interpolation. In Figure 6-52 the stress just barely reaches the tensile strength limit at the surface node of the side face, but it exceeds the strength up to 0.10 ft below the concrete surface, found through linear interpolation.

Figure 6-53 shows the principal stress of the previously chosen key locations over time. The center node is in compression and the surface nodes are in tension throughout the whole analysis. Most of the surface nodes, except for the far edge node, go below the tensile strength of the concrete after around 96 hours.

Figures 6-54 and 6-55 show the cracking index for the vertical and horizontal profiles, respectively, at 46 and 86 hours. Despite the differences in the strength and induced stresses at these different time periods, the cracking index remains almost identical for the most part. As with the stress graphs in Figures 6-51 and 6-52, Figures 6-54 and 6-55 show the cracking index exceeding the limit of 1 only at the most outer nodes. Through linear

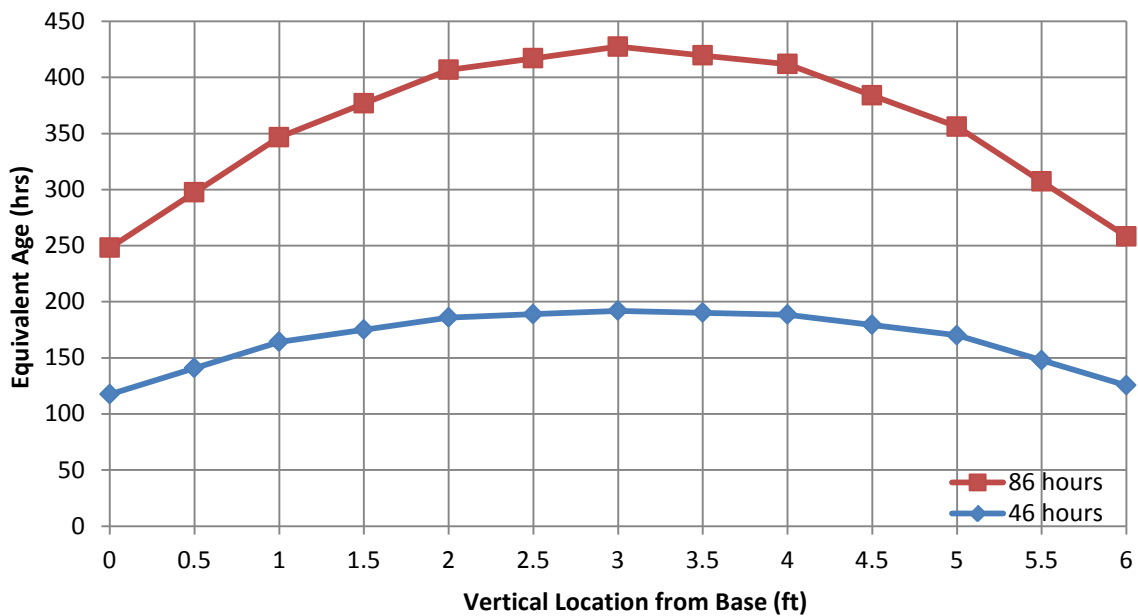


Figure 6-49: Sunset Beach vertical profile equivalent age at 46 and 86 hours

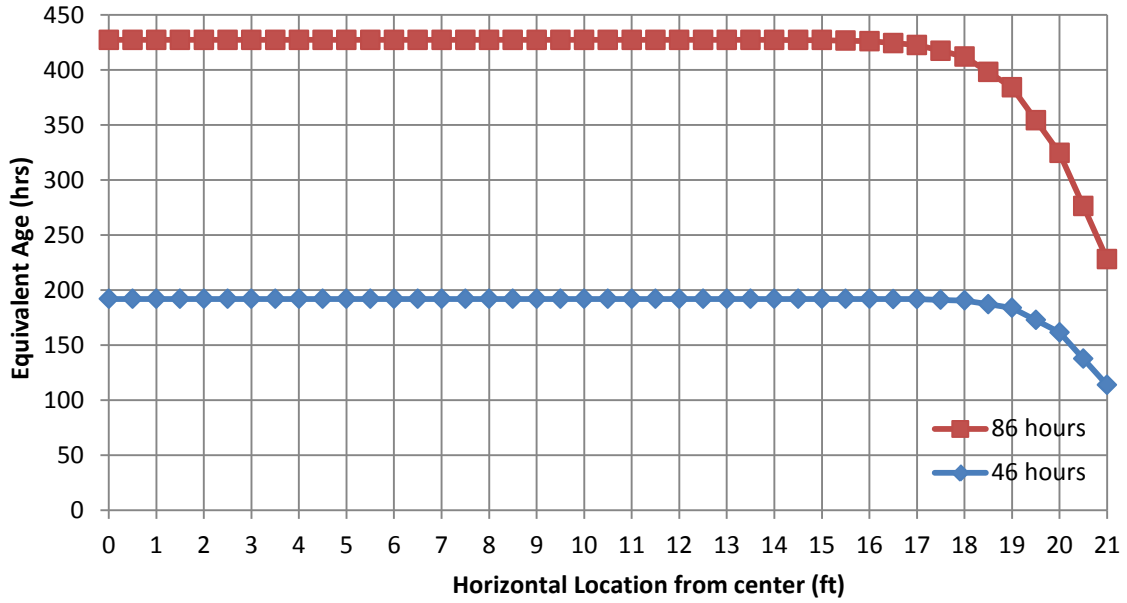


Figure 6-50: Sunset Beach horizontal profile equivalent age at 46 and 86 hours

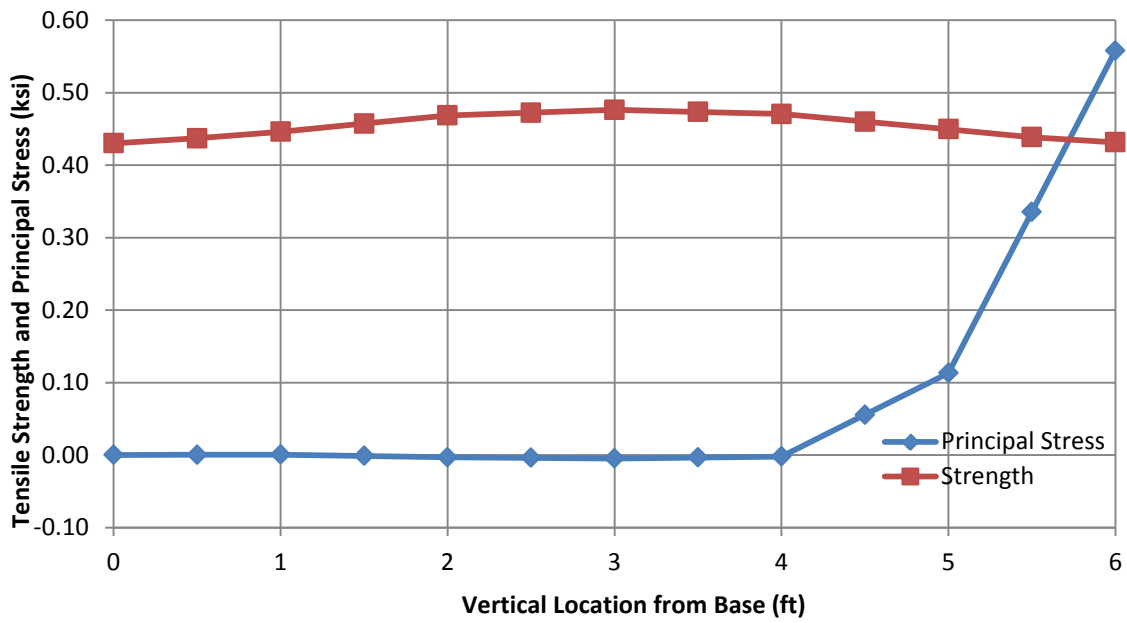


Figure 6-51: Sunset Beach vertical profile stress and strength vs time at 86 hours

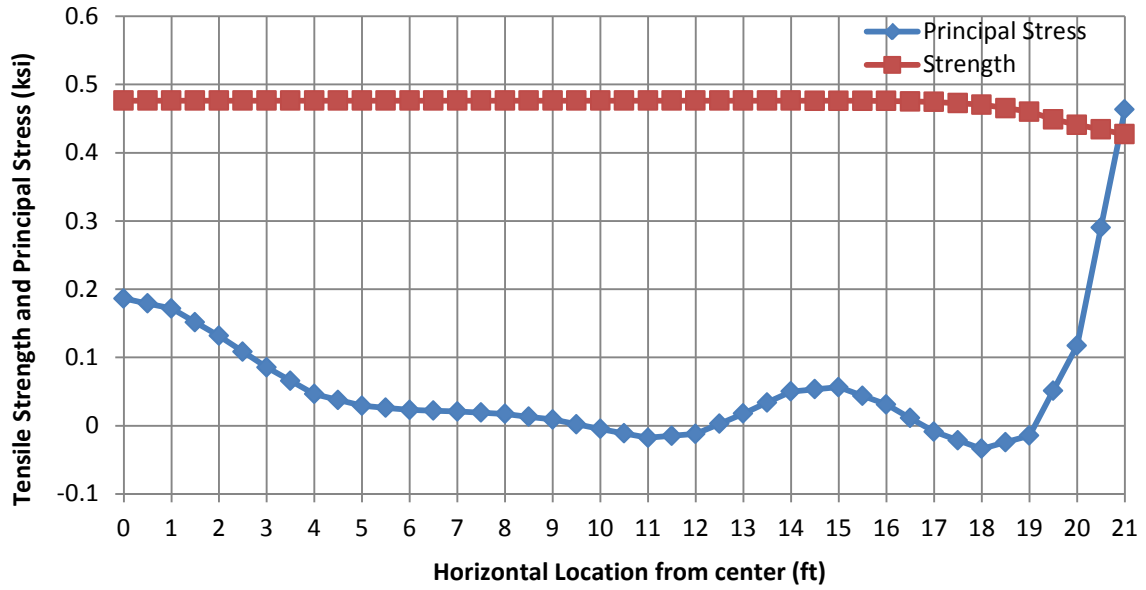


Figure 6-52: Sunset Beach horizontal profile stress and strength vs time at 86 hours

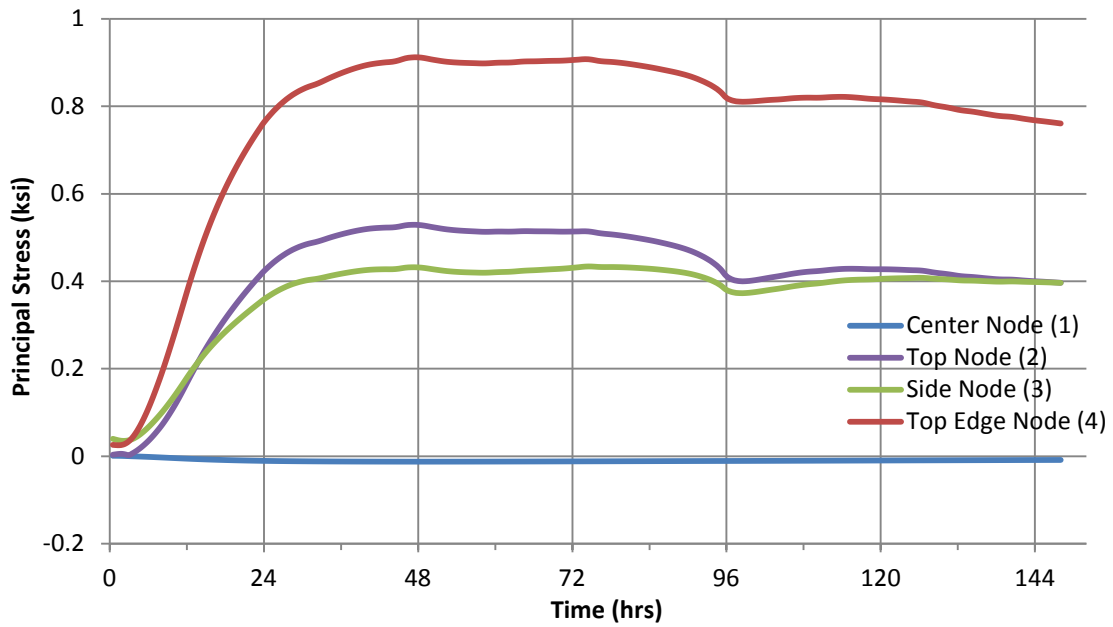


Figure 6-53: Sunset Beach nodes principal stresses vs time

interpolation the cracking index crosses 1 at a distance 0.10 ft below the surface in the vertical profile and at a distance 0.06 ft below the surface in the horizontal profile. Figure 6-56 shows the cracking index of the previously chosen key locations over time. The surface nodes except the top edge remain below 1 until about 96 hours, as seen in Figure 6-56. The top and side nodes remain close to 1 throughout the entire analysis.

Figure 6-57 shows the 3-D isoparametric view and Figure 6-58 shows the plan view of the cracking index contours below 1 on the concrete block at 86 hours. As was seen in the principal stress graphs and the cracking index graphs, Figures 6-57 and 6-58 show that the cracking index goes below the index limit of 1, but that it does not extend past the first, most outer nodes. The only locations that this does occur are at the locations above the pile supports, where the nodes were fixed, and around the top edge where there are higher stress concentrations.

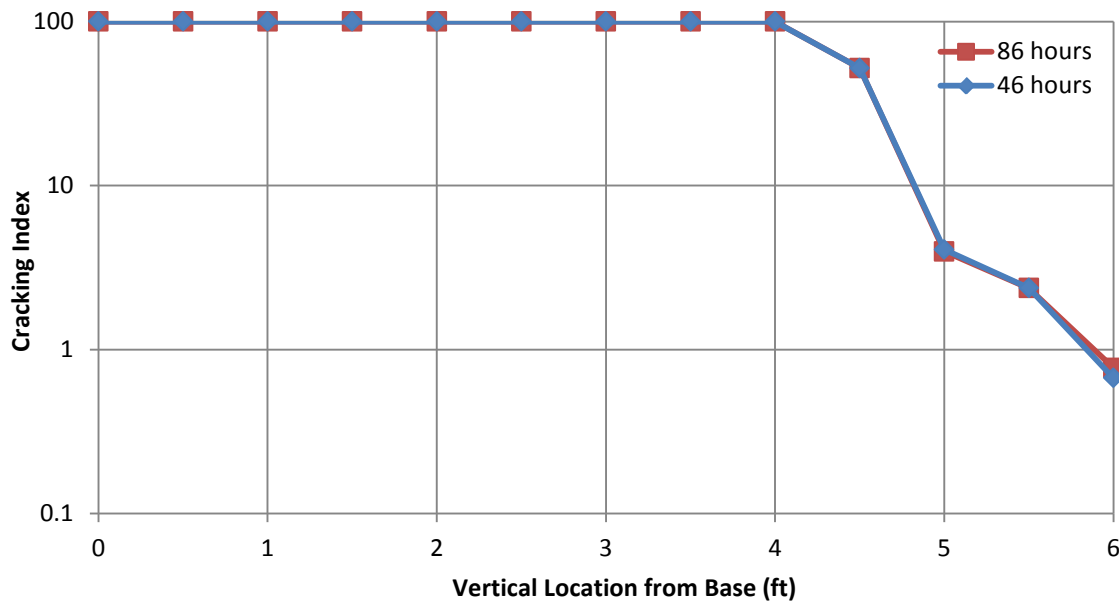


Figure 6-54: Sunset Beach vertical profile cracking index at 46 and 86 hours

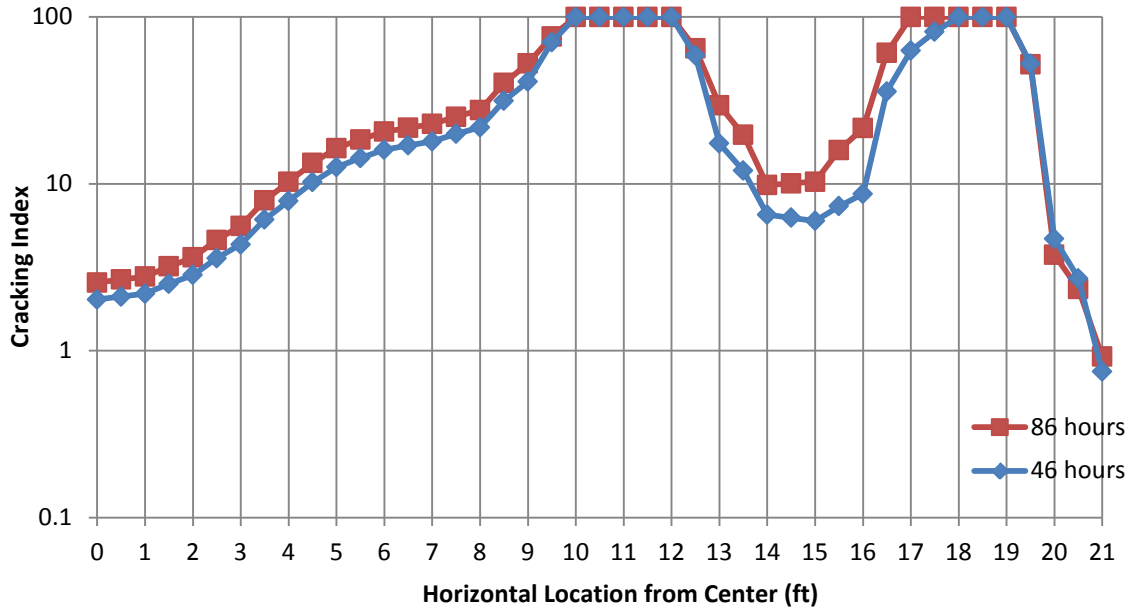


Figure 6-55: Sunset Beach horizontal profile cracking index at 46 and 86 hours

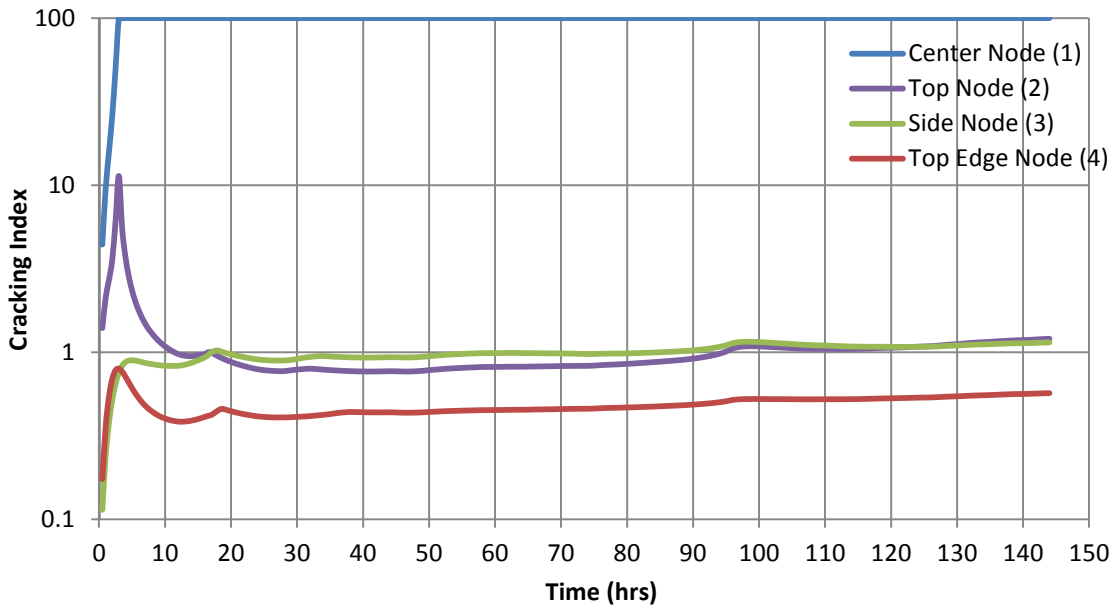


Figure 6-56: Sunset Beach nodes cracking index vs time

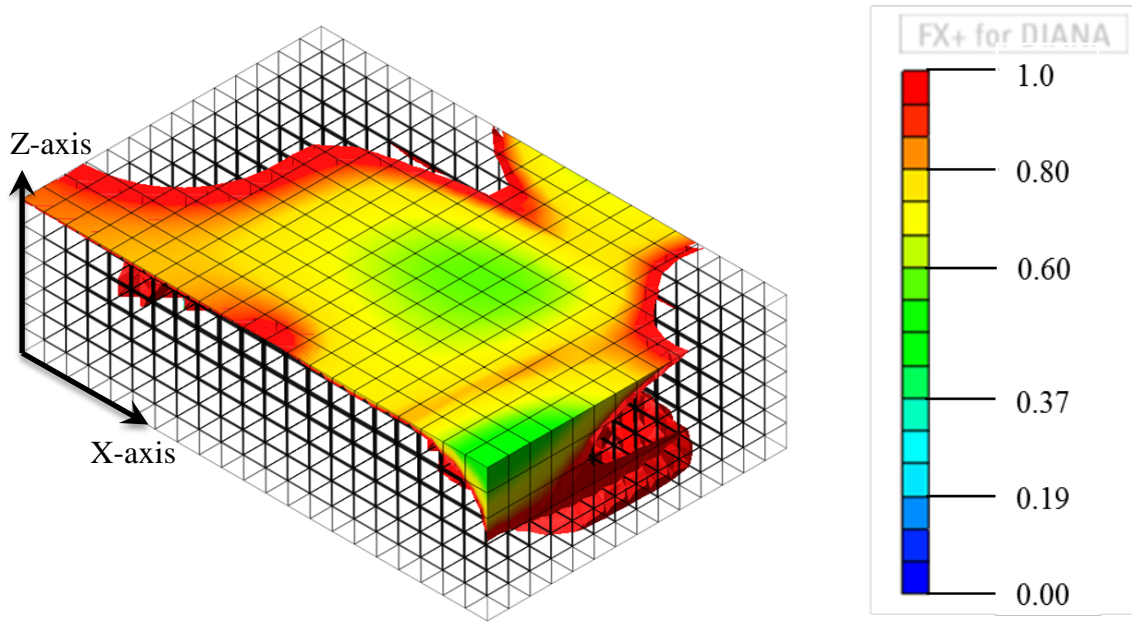


Figure 6-57: Sunset Beach cracking index contours at 86 hours isoparametric view

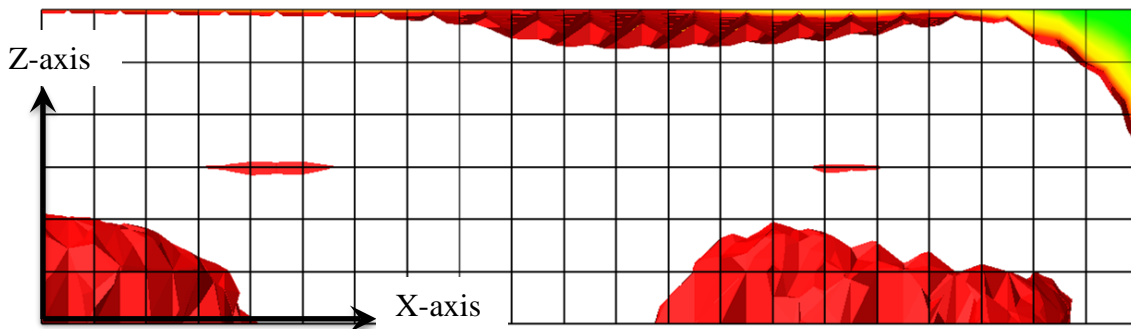


Figure 6-58: Sunset Beach cracking index contours at 86 hours profile view

6.5 Wilmington Bypass Footing Case Study

6.5.1 Thermal Analysis Results

The Wilmington Bypass Bridge footing was very different from the previous two case studies in that it is significantly larger and it had the formwork removed early, after only 70 hours. As seen in Figure 6-59 and 6-60, a quarter of the footing was modeled with the steel formwork and insulation blankets explicitly modeled. The thermocouple locations were supplied by the NCDOT; however no temperature field measurements were available for this case study. Figure 6-60 shows the temperature locations used in Figures 6-61 through 6-65.

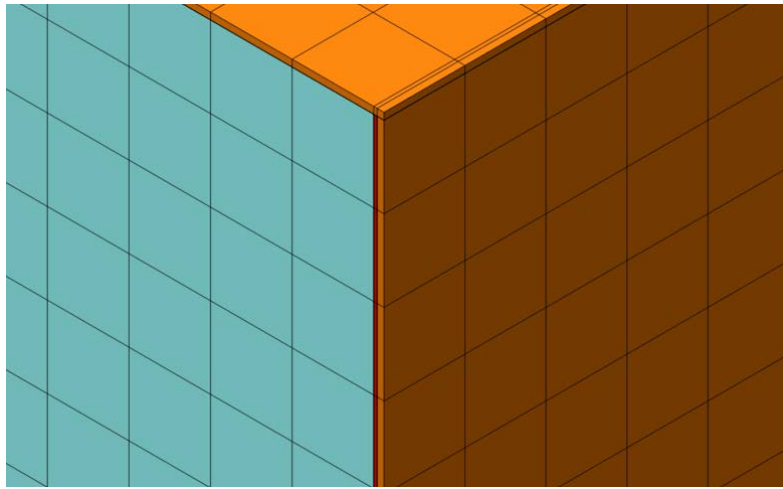


Figure 6-59: Wilmington mesh close up

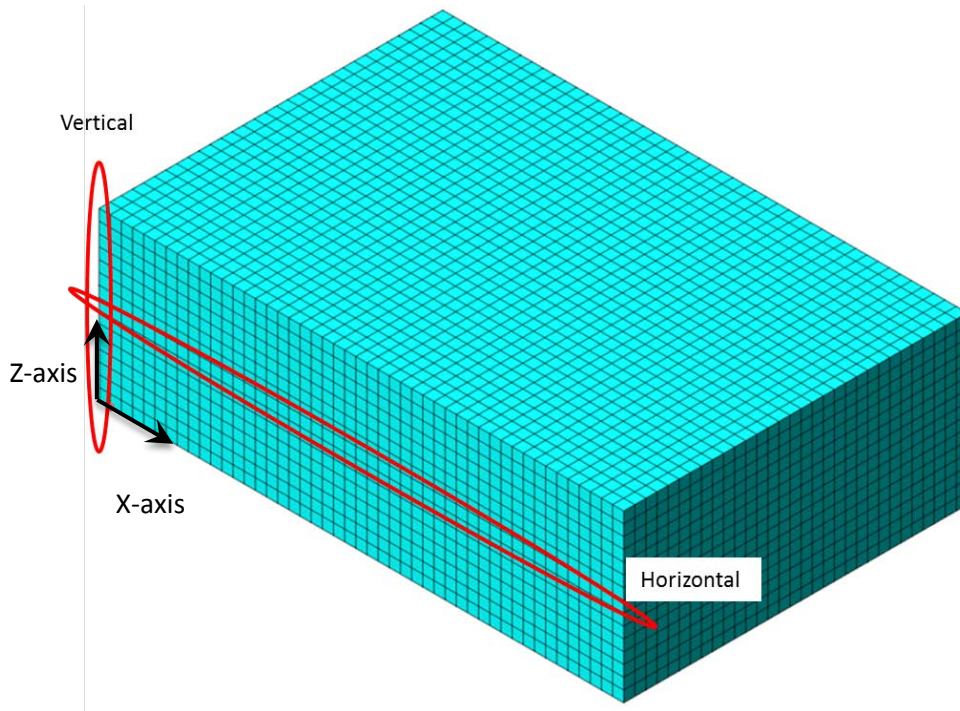


Figure 6-60: Wilmington temperature locations

Figures 6-61 and 6-62 show the vertical and horizontal profile temperature distributions, respectively, over time. The model predicted a maximum temperature of 171.8 °F to occur at 120 hours and start decreasing at 127 hours. Significant decrease in the internal temperature, however, does not occur until after 168 hours. Figures 6-61 and 6-62 also show that significant temperature drops occur on the nodes closer to the concrete surface when the formwork is removed. . It is also noted that the center and mid-right nodes have nearly identical temperatures because of the large distances between the center and side of the footing.

Figure 6-63 shows the maximum temperature differentials developed in the DIANA model. The model predicted a maximum temperature differential of 98.4 °F to occur at 156 hours between the center and all surface nodes. This is significantly higher than the other

models and is due to the extreme drop in temperature along the surface of the concrete caused by the formwork removal. The temperature differentials were more reasonable at 37.5 °F prior to form removal.

Figures 6-64 and 6-65 show the vertical and horizontal temperature profiles at the time of form removal and at the time of the maximum temperature differential, which occurs at 69 hours and 156 hours respectively. Figure 6-66 and Figure 6-67 show pictorial representations of the temperature distribution throughout the concrete block at the time of the maximum temperature differential, 156 hours. These figures show that the temperatures along the surface are low while the temperatures in the center are still high due to the internal concretes almost adiabatic behavior.

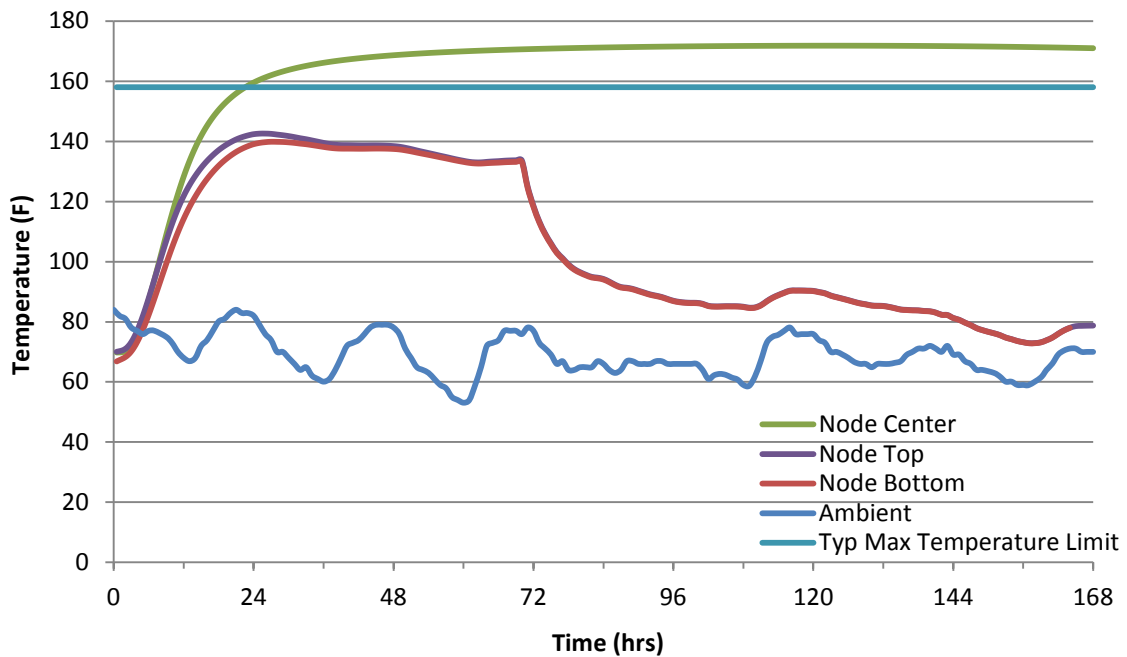


Figure 6-61: Wilmington vertical temperature distribution

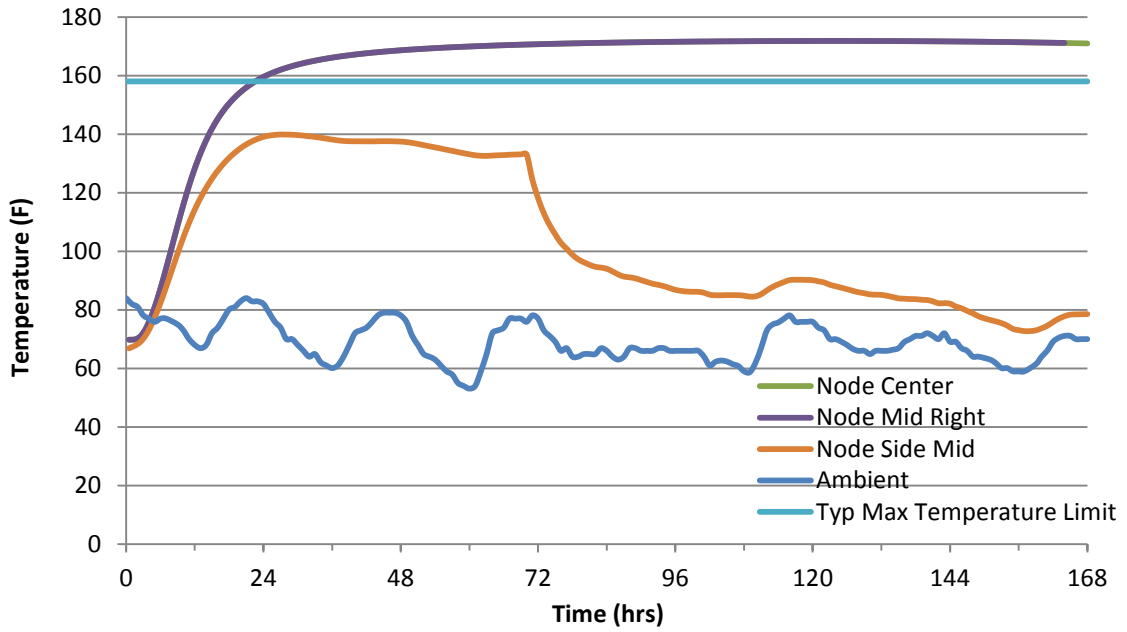


Figure 6-62: Wilmington horizontal temperature distribution

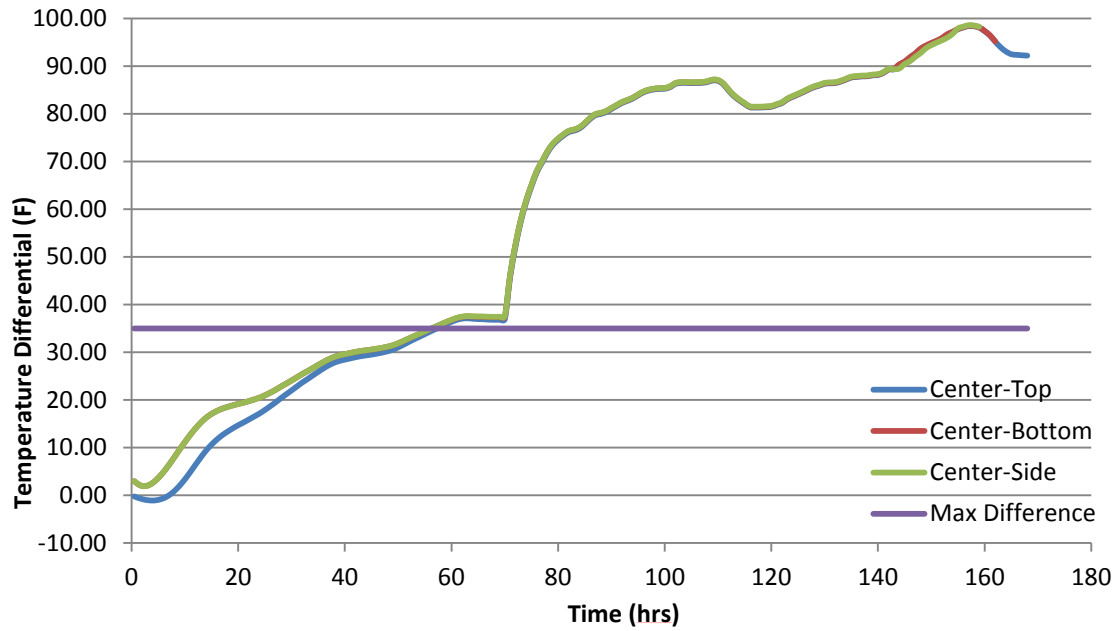


Figure 6-63: Wilmington maximum temperature differentials

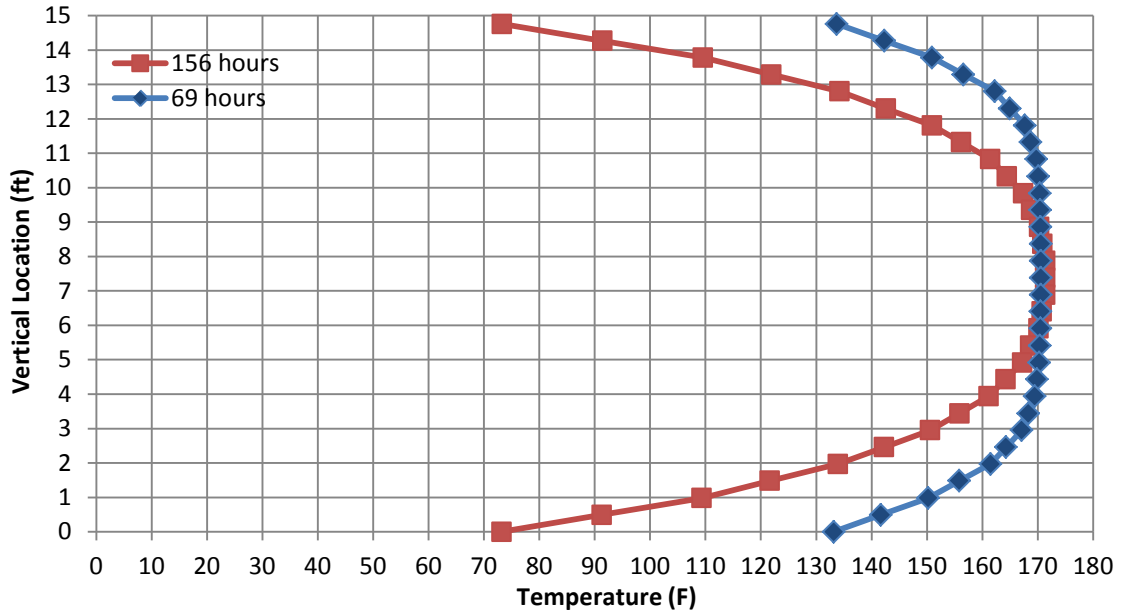


Figure 6-64: Wilmington vertical temperature distribution at 69 and 156 hours

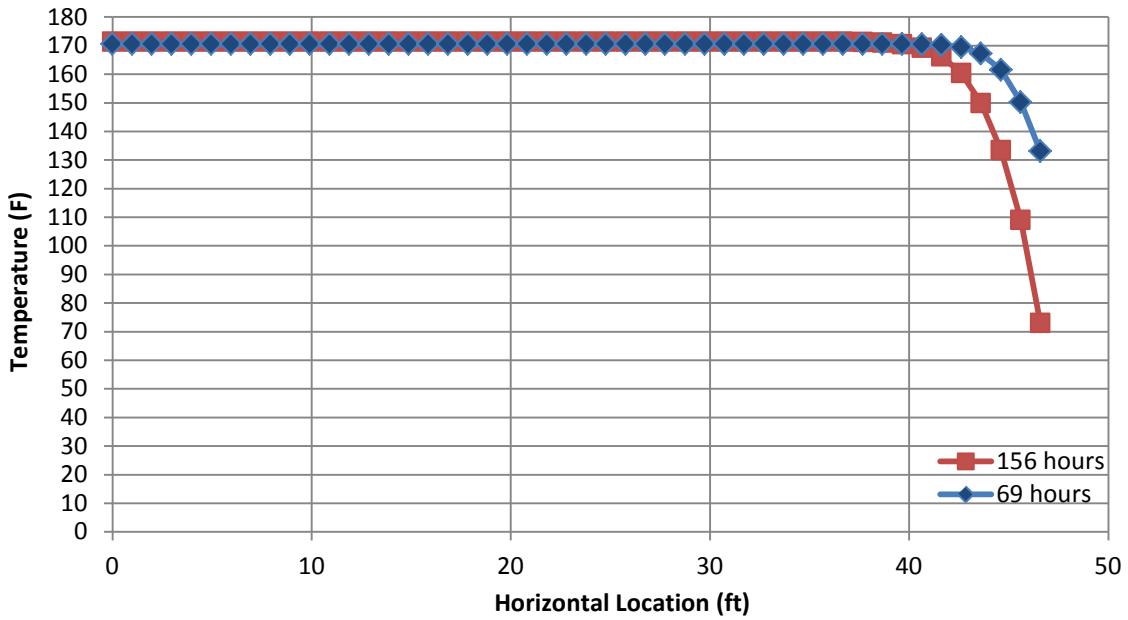


Figure 6-65: Wilmington horizontal temperature distribution at 69 and 156 hours

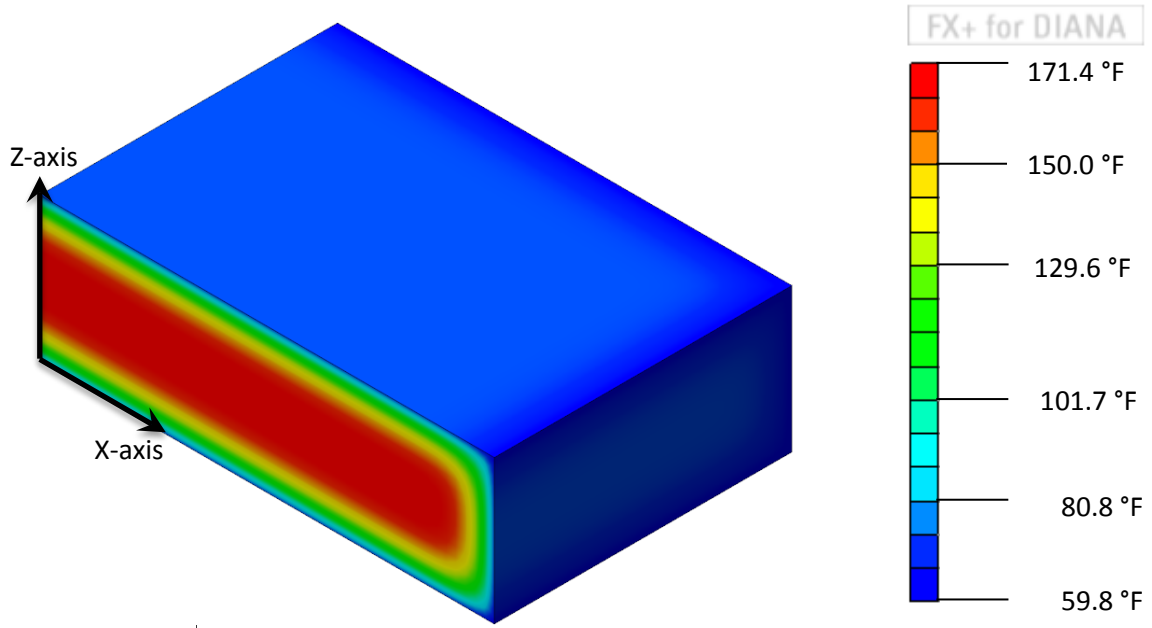


Figure 6-66: Wilmington temperature profile at 156 hours

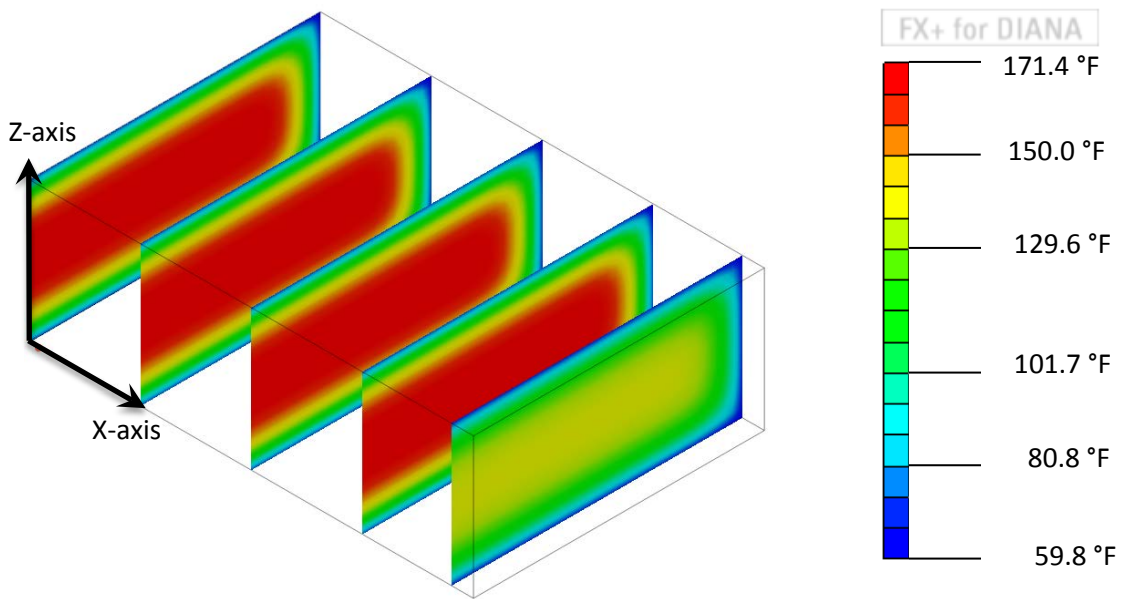


Figure 6-67: Wilmington sliced temperature profile at 156 hours

6.5.2 Structural Analysis Results

Figure 6-68 shows the locations at which the equivalent age, stresses, and tensile strengths were examined. These locations were chosen because they are where some of the biggest compressive and tensile stresses occur due to the footing's boundary conditions.

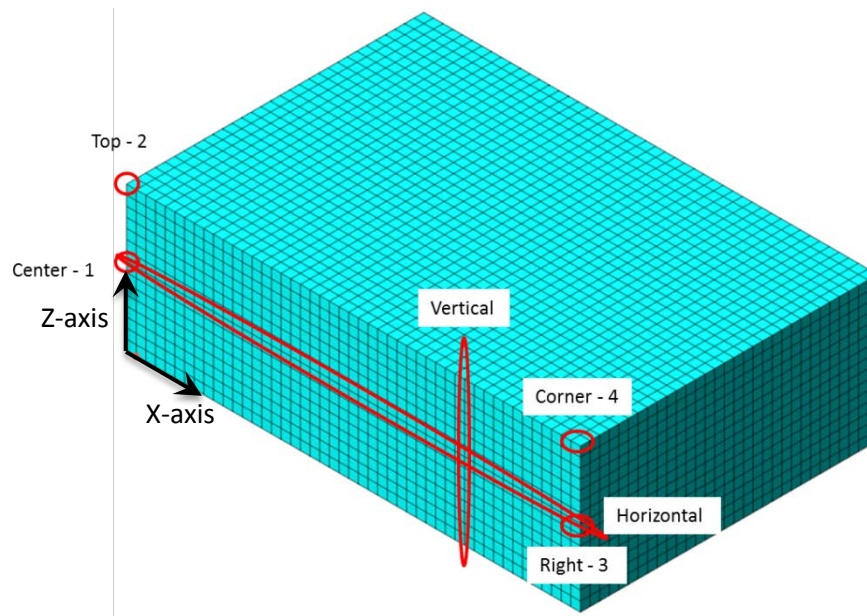


Figure 6-68: Wilmington stress locations

Figure 6-69 and Figure 6-70 show the vertical and horizontal equivalent age profiles, respectively, at the time of form removal, 69 hours, as well as at the time of the maximum temperature differential, 156 hours. As seen in these two figures, the equivalent age increases as the concrete temperature increases. These equivalent ages are used to calculate the tensile strength throughout the concrete which has been plotted against the principal stress in Figures 6-71 and 6-72 at 156 hours. Unlike in previous analyses, these figures show the principal stresses exceeding the tensile strength of the concrete in more than just the most

outer nodes. In Figure 6-71, the stress exceeds the strength up to 1.63 ft below the top concrete surface and up to 0.56 ft below the bottom concrete surface. In Figure 6-72, the stress exceeds the strength up to 1.8 ft below the side concrete surface. These are significantly higher than what was observed in the previous analyses.

Figures 6-73 and 6-74 show the cracking index for the vertical and horizontal profiles, respectively, at 69 and 156 hours. Despite the differences in the strength and induced stresses at these different time periods, the cracking index remains similar in the interior parts of the concrete. Towards the surface of the concrete, however, there are much lower cracking indexes at 156 hours than at 69 hours due to the high stress levels. Through linear interpolation, the cracking index crosses 1 at a distance 1.36 ft below the top surface and at a distance 0.29 ft above the bottom concrete surface in the vertical profile. The cracking index is also found to cross 1 at a distance 1.84 ft from the side surface in the horizontal profile.

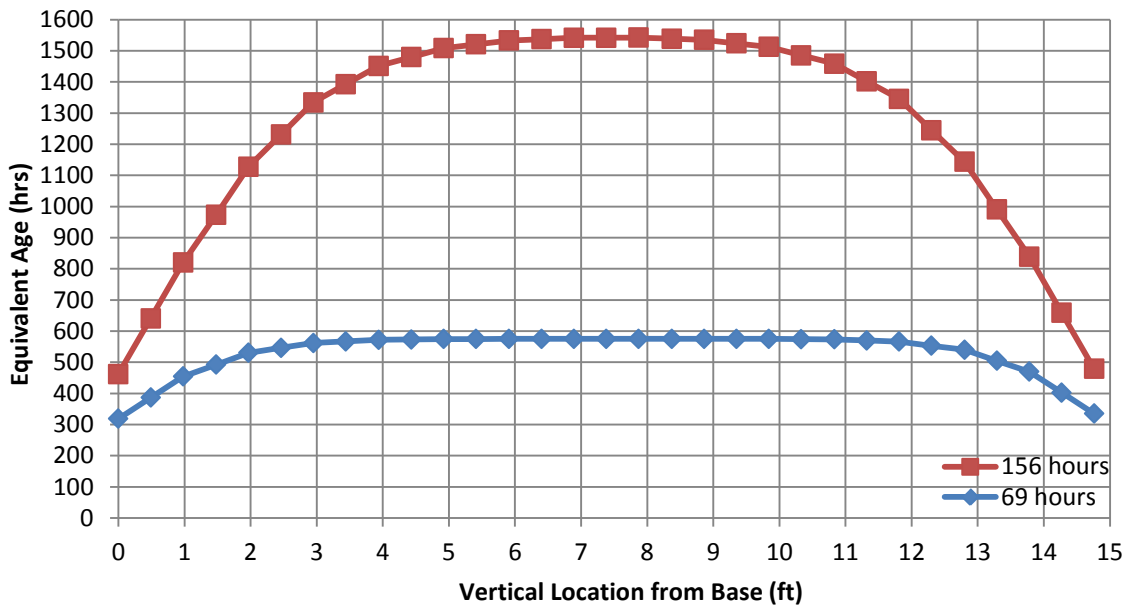


Figure 6-69: Wilmington vertical profile equivalent age at 69 and 156 hours

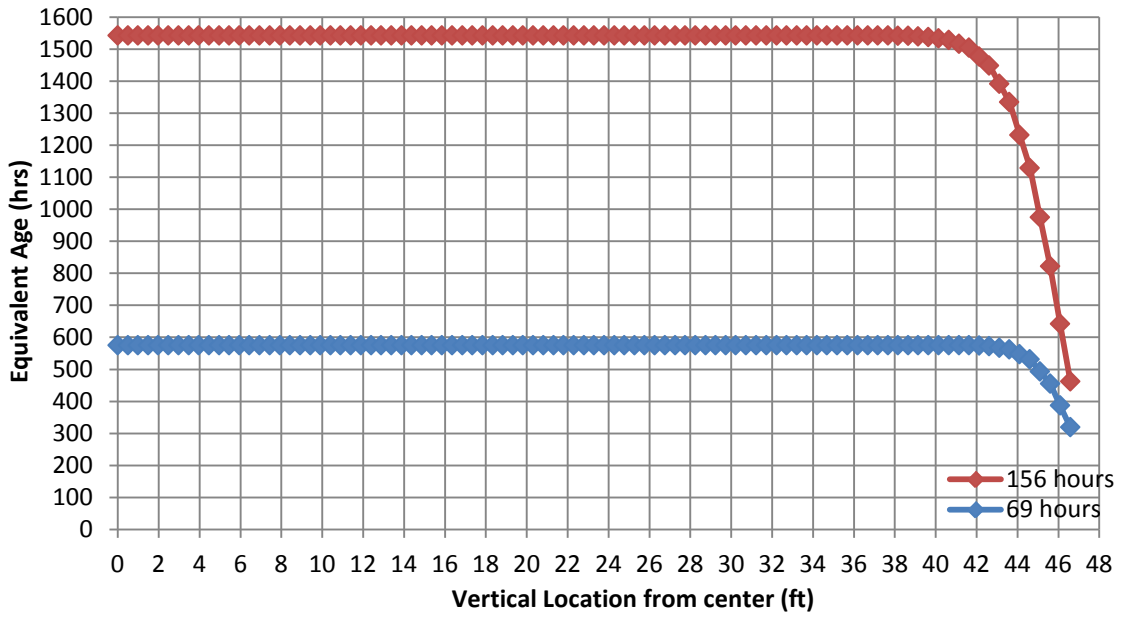


Figure 6-70: Wilmington horizontal profile equivalent age at 69 and 156 hours

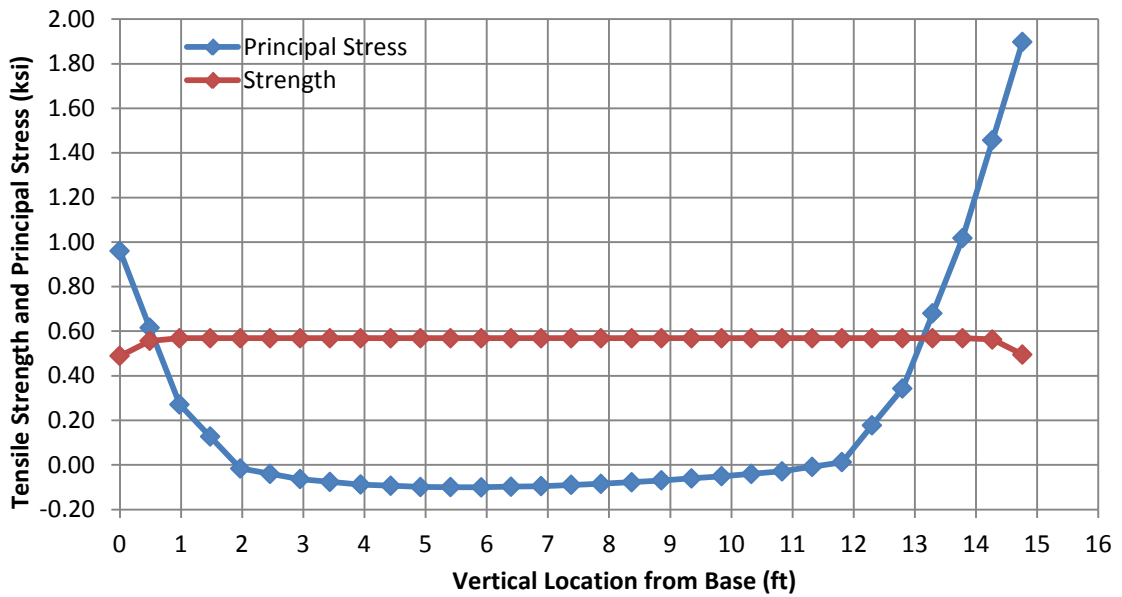


Figure 6-71: Wilmington vertical profile stress and strength vs time at 156 hours

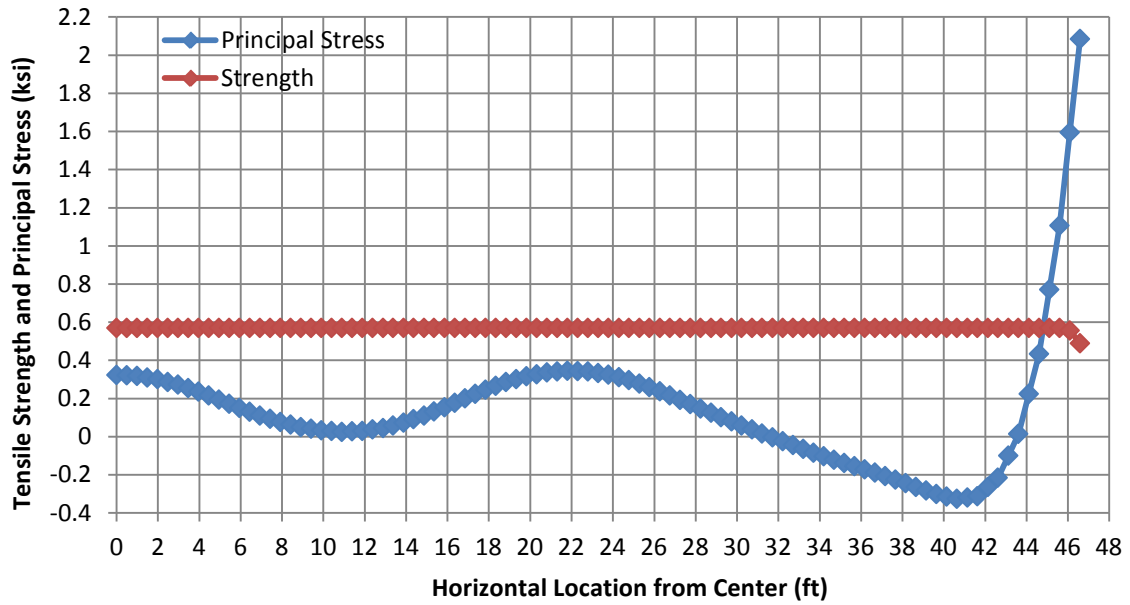


Figure 6-72: Wilmington horizontal profile stress and strength vs time at 156 hours

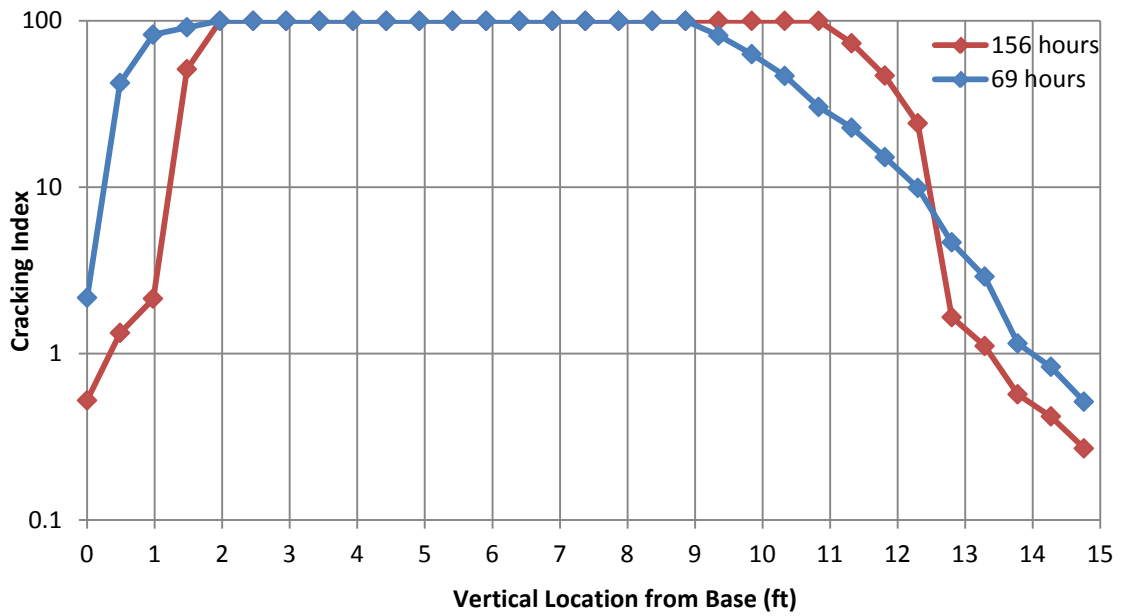


Figure 6-73: Wilmington vertical profile cracking index at 69 and 156 hours

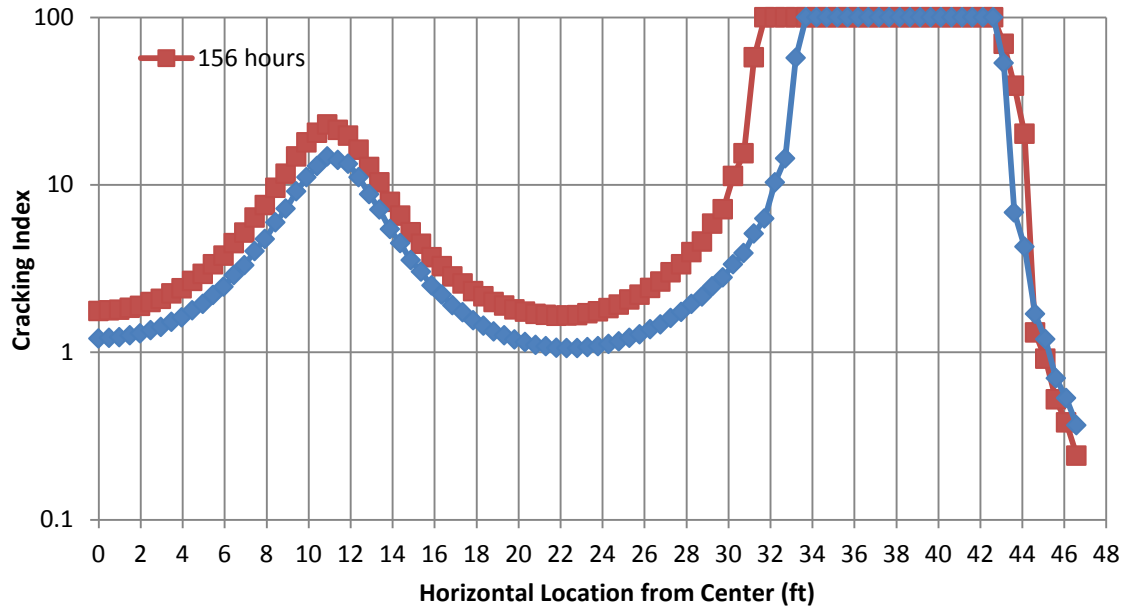


Figure 6-74: Wilmington horizontal profile cracking index at 69 and 156 hours

Figure 6-75 shows the cracking index of the previously chosen key locations over time. Only the side node in this case has a cracking index below 1 for the majority of the analysis. The top and top edge nodes decrease to below 1 after the formwork is removed at 70 hours.

Figure 6-76 shows the 3-D isoparametric view and Figure 6-77 shows the plan view of the cracking index contours below 1 on the concrete block at 156 hours. As was seen in the principal stress graphs and the cracking index graphs, Figures 6-76 and 6-77 shows that the cracking index goes below the index limit of 1 throughout the majority of the concrete block's surface. Unlike previous analyses, the cracking index goes below 1 in not only the outer most nodes, but also in some of the inner nodes as well. In many locations the low cracking index even goes through the second layer of elements. It can also be seen that the cracking index on the surface is much lower than what was seen in previous analyses.

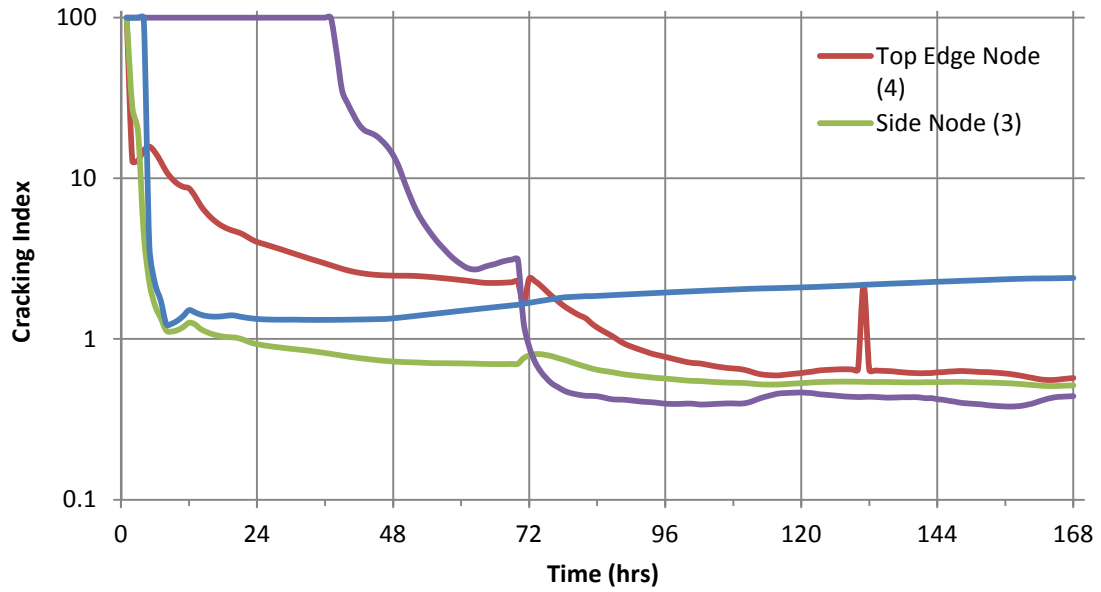


Figure 6-75: Wilmington nodes cracking index vs time

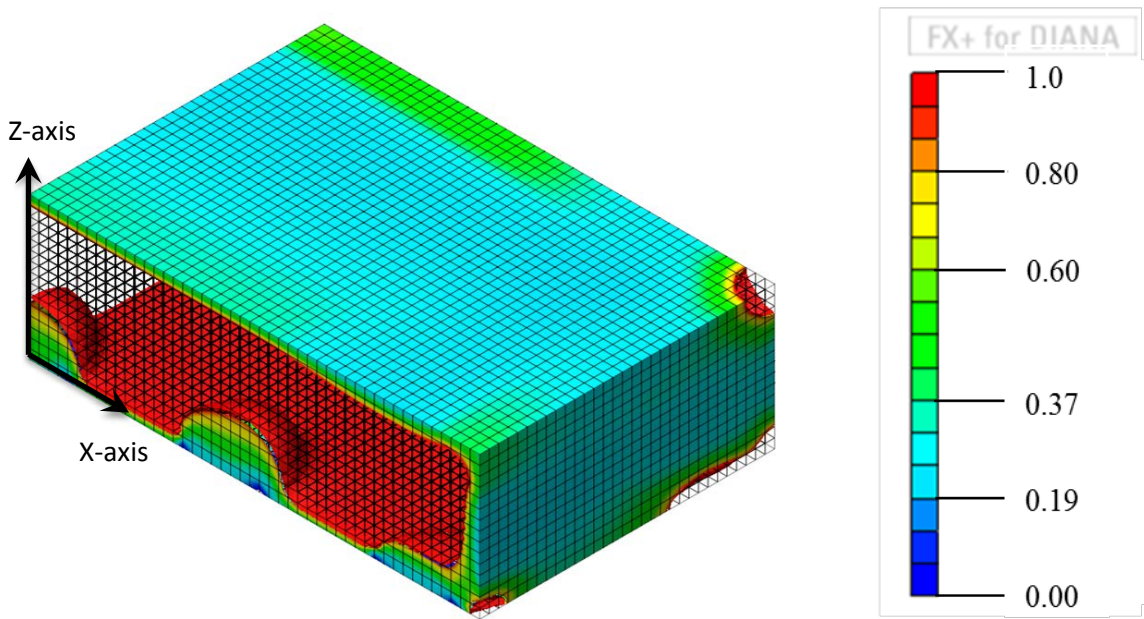


Figure 6-76: Wilmington cracking index contours at 156 hours isoparametric view

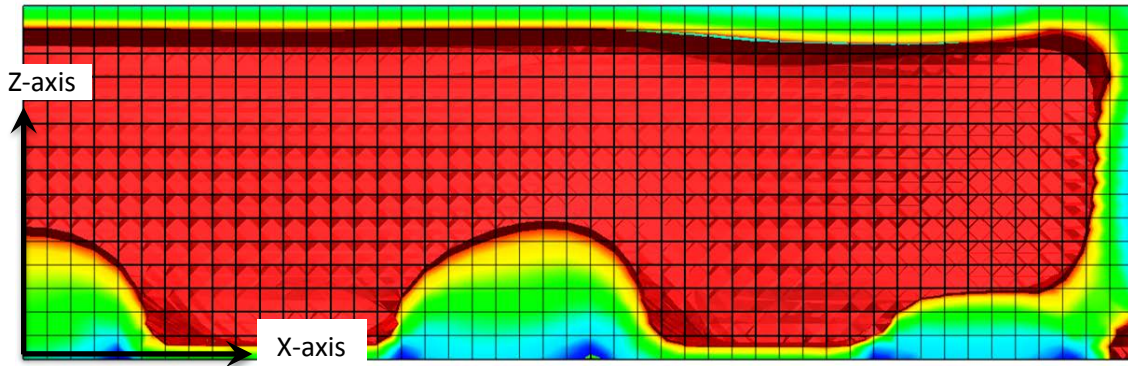


Figure 6-77: Wilmington cracking index contours at 156 hours profile view

6.6 Wilmington Bypass Footing Case Study with Insulation

6.6.1 Thermal Analysis Results

The Wilmington Bypass case study was rerun assuming the formwork and insulation were not taken off prematurely. The model was therefore the same as seen in Figure 6-59 with the exception that the insulation seen was not removed during the analysis. The temperature locations for Figures 6-78 through 6-82 also remained the same as shown in Figure 6-60 from Section 6.4.1.

Figures 6-78 and 6-79 show the vertical and horizontal profile temperature distributions, respectively, over time. As with the Wilmington case study in Section 6.5, the model predicted a maximum temperature of 171.8 °F to occur around 120 hours and that started decreasing around 127 hours. Unlike the case study in Section 6.5, there is not a significant decrease in temperature around the concrete surface due to formwork removal, although there is a slight, gradual decline in the temperature. Also, significant decrease in the internal temperature does not occur until after 168 hours. It is also noted that the center and mid-right nodes have nearly identical temperatures because of the large distances between the center and side of the footing.

Figure 6-80 shows the maximum temperature differentials developed in the DIANA model when the formwork and insulation remains. The model predicted a maximum temperature differential of 52.0 °F to occur at around 160 hours between the center and all surface nodes. This is significantly lower than the 98.4 °F predicted in the model without formwork, but it is still significantly higher than the typical 35 °F limit.

Figures 6-81 and 6-82 show the vertical and horizontal temperature profiles at the same time stamps from the Wilmington case study for comparison. These figures show the higher temperatures at the concrete surface and the smaller temperature differentials overall than are in Figures 6-64 and 6-65. Figure 6-83 show pictorial representation of the temperature distribution throughout the concrete block at 156 hours. This figure shows that the temperatures distribution in this model is very similar to the Wilmington case study, only that the temperatures nearer to the concrete surface are higher.

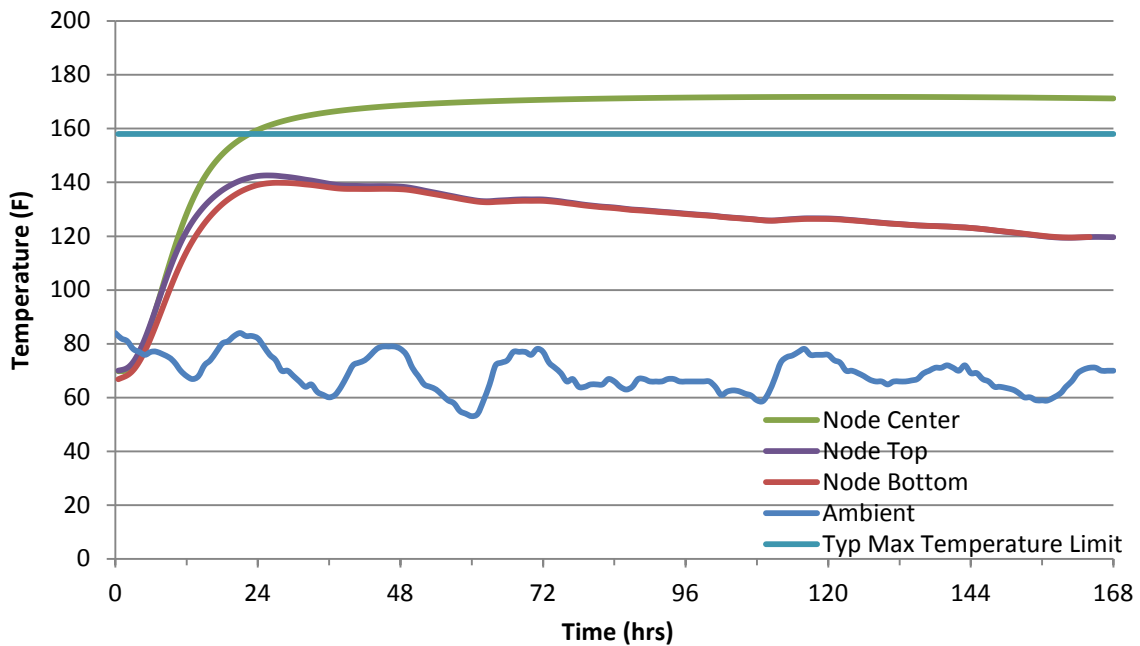


Figure 6-78: Wilmington insulated vertical temperature distribution

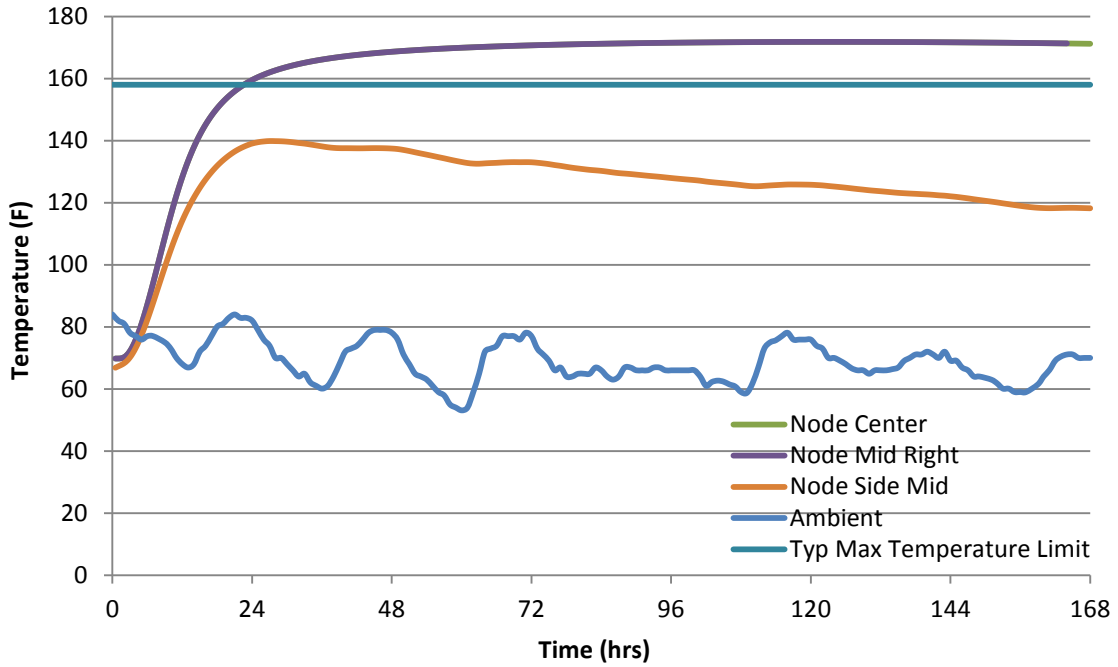


Figure 6-79: Wilmington insulated horizontal temperature distribution

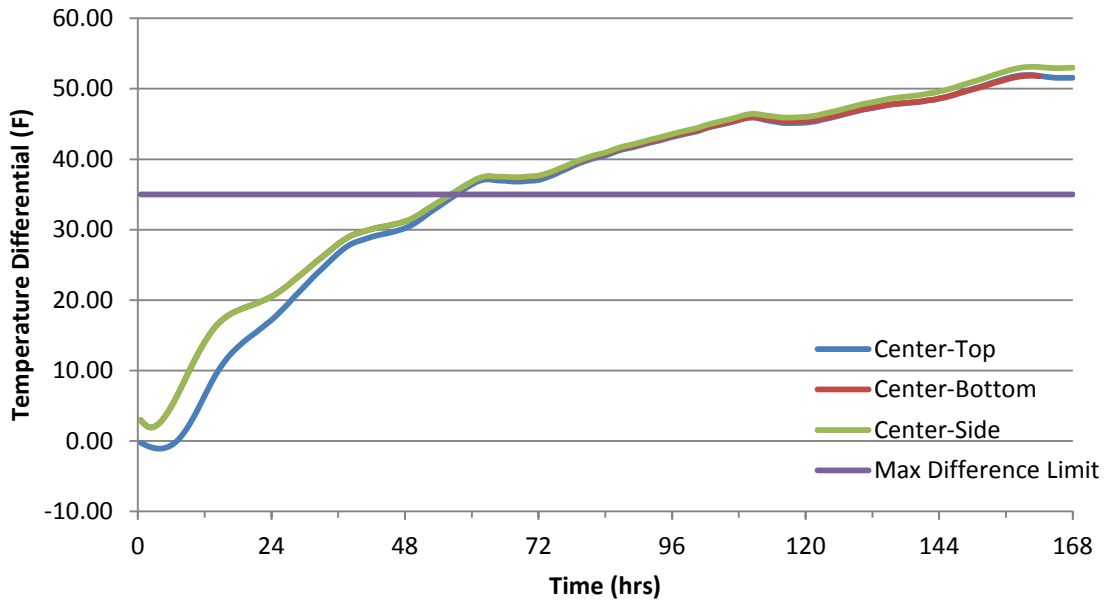


Figure 6-80: Wilmington insulated maximum temperature differentials

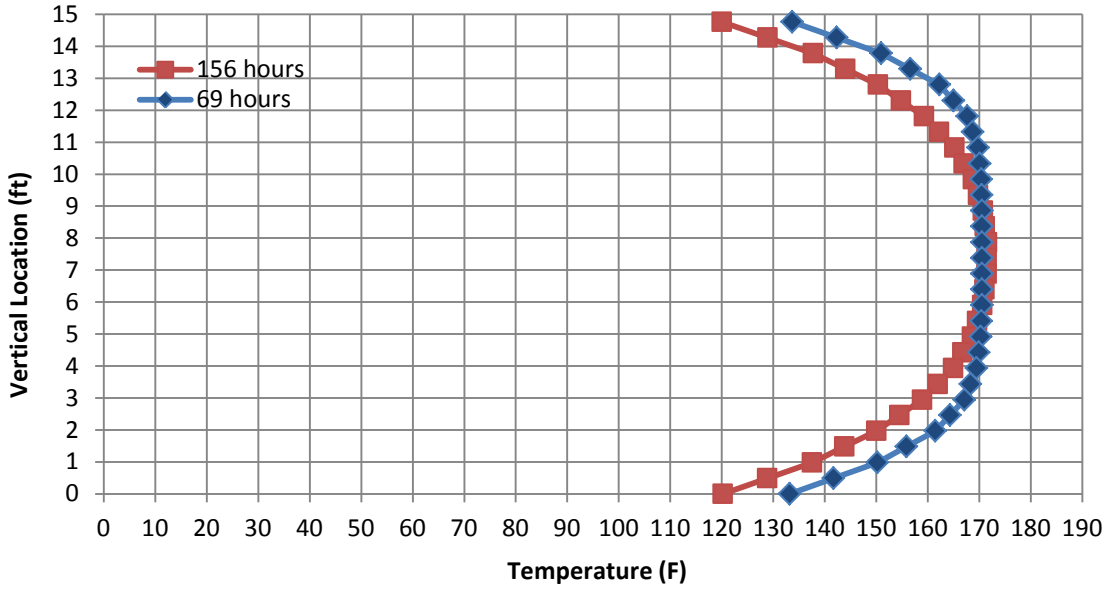


Figure 6-81: Wilmington insulated vertical temperature distribution at 69 and 156 hours

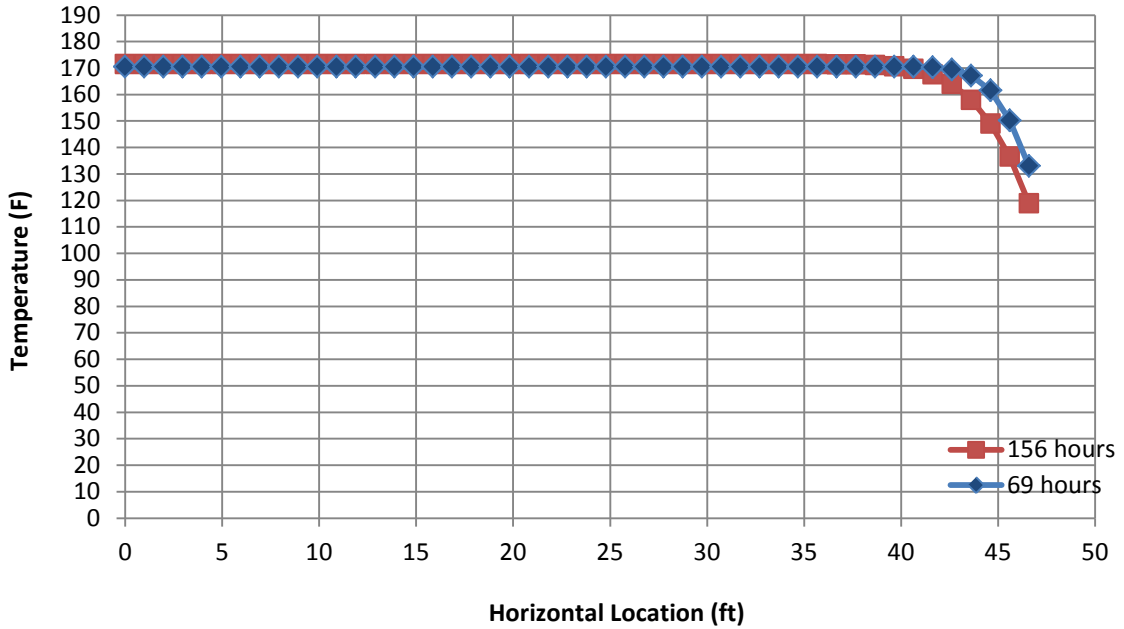


Figure 6-82: Wilmington insulated horizontal temperature distribution at 69 and 156 hours

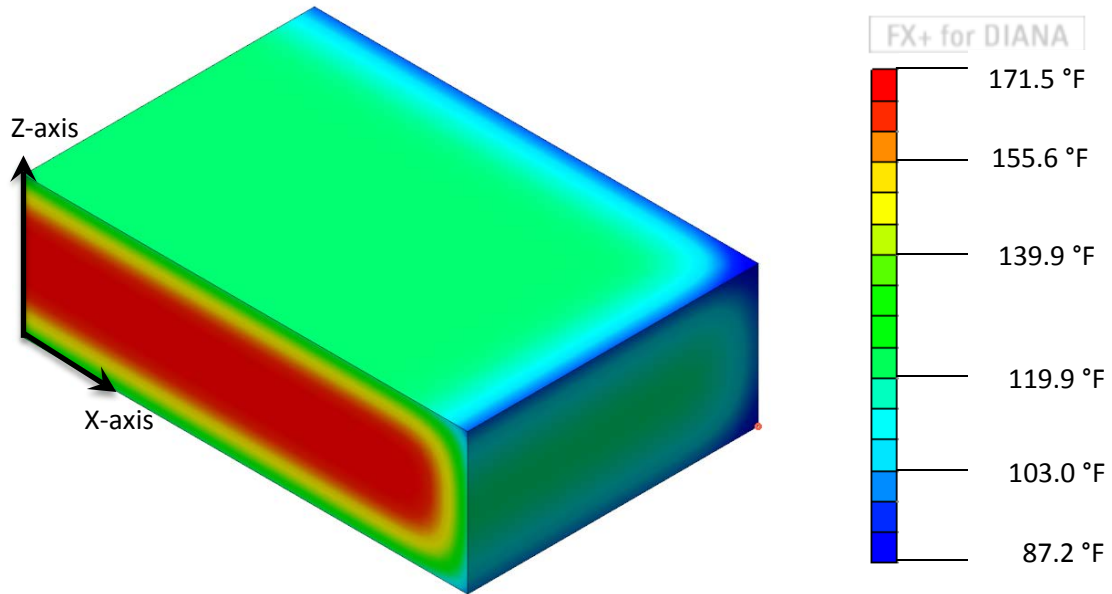


Figure 6-83: Wilmington insulated temperature profile at 156 hours

6.6.2 Structural Analysis Results

The locations at which the equivalent age, stresses, and tensile strengths were assessed were the same as the Wilmington case study in Section 6.4.2. Figure 6-68 shows the locations at which these values were examined.

Figure 6-84 and Figure 6-85 show the vertical and horizontal equivalent age profiles, respectively, at the same time stamps from the Wilmington case study, 69 hours and 156 hours. As seen in the figures, the equivalent age nearer to the concrete surface is greater due to the higher temperatures found closer to the surface than what was found in Section 6.4. These equivalent ages are used to calculate the tensile strength throughout the concrete which has been plotted against the principal stress in Figures 6-86 and 6-87 at 156 hours. Like the Wilmington case study with insulation removal, these figures show the principal stresses still exceed the tensile strength of the concrete in more than just the most outer nodes, but they do

not extend quite as far into the concrete. In Figure 6-86, the stress exceeds the tensile strength up to 0.98 ft below the top concrete surface, but does not exceed the strength at the bottom concrete surface. In Figure 6-87, the stress exceeds the strength up to 1.49 ft below the side concrete surface. These are still significant numbers despite being less than the Wilmington case study with insulation removal.

Figures 6-88 and 6-89 show the cracking index for the vertical and horizontal profiles, respectively, at 69 and 156 hours. Despite the differences in the strength and induced stresses at these different time periods, the cracking index remains similar at both time steps. These figures show that the cracking index is still less than 1.0 for more than one node in each profile even with insulation. Through linear interpolation the cracking index crosses 1.0 at a distance 0.98 ft below the surface in the vertical profile and at a distance 1.39 ft below the surface in the horizontal profile. As with the stress graphs in Figures 6-86

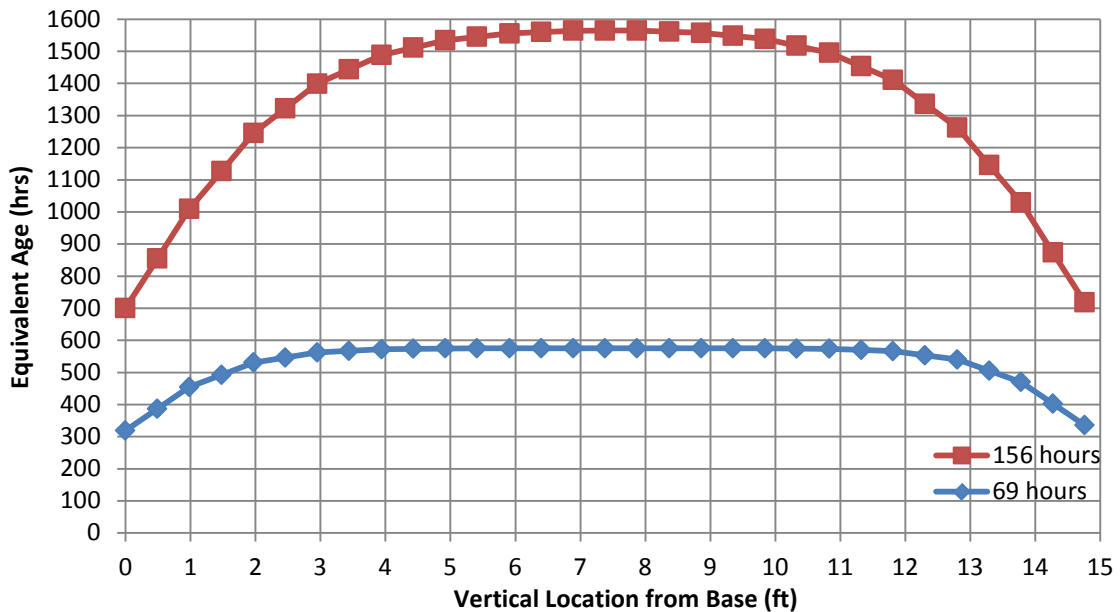


Figure 6-84: Wilmington insulated vertical profile equivalent age at 69 and 156 hours

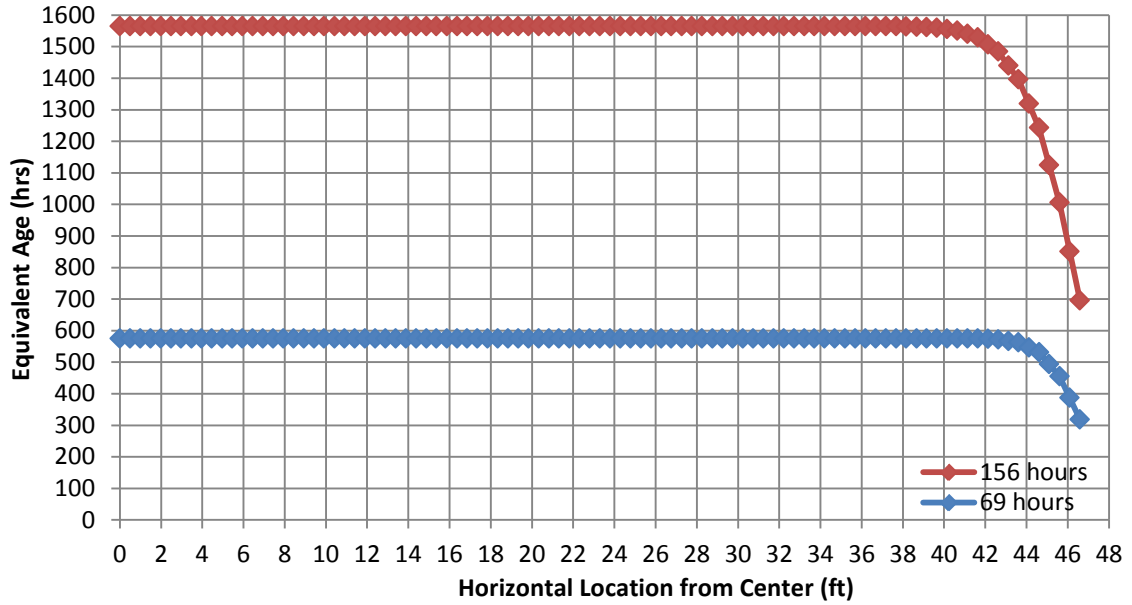


Figure 6-85: Wilmington insulated horizontal profile equivalent age at 69 and 156 hours

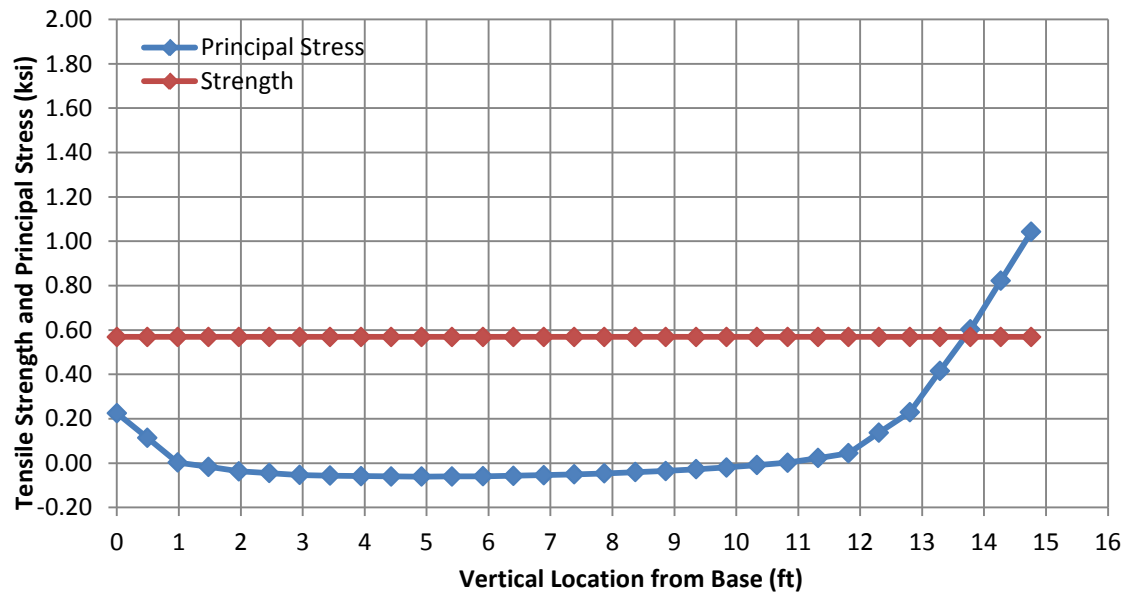


Figure 6-86: Wilmington insulated vertical profile stress and strength vs time at 156 hours

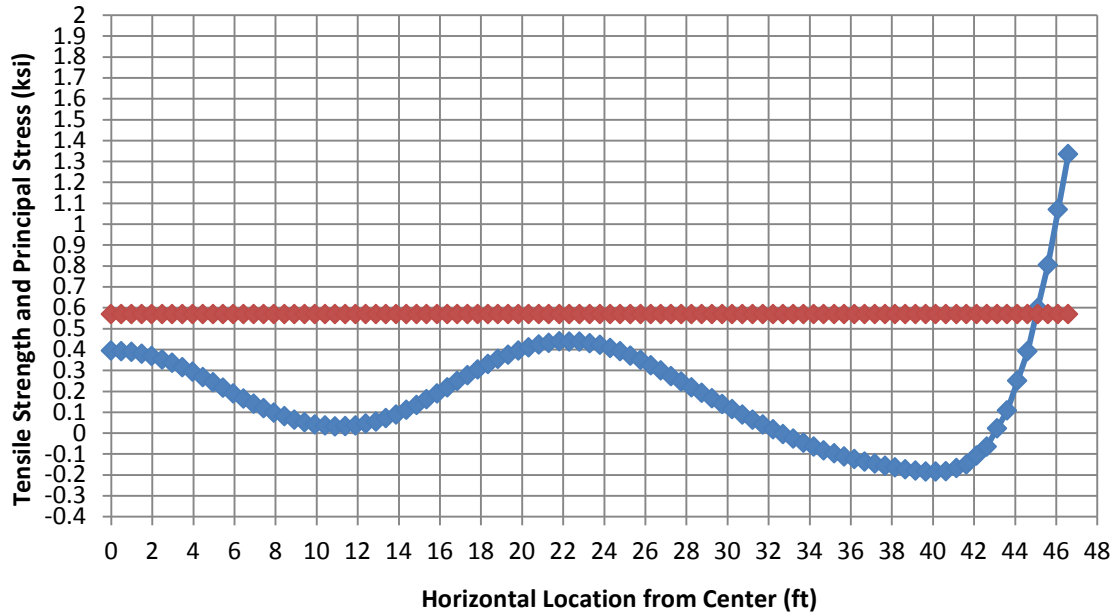


Figure 6-87: Wilmington insulated horizontal profile stress and strength vs time at 156 hours

and 6-87, these numbers are less than the Wilmington case study with insulation removal but still significant. Figure 6-90 shows the cracking index of the previously chosen key locations over time. All of the chosen nodes, with the exception of the side node, never fell below the index limit of 1.0.

Figure 6-91 shows the 3-D isoparametric view and Figure 6-92 shows the plan view of the cracking index contours below 1.0 on the concrete block at 156 hours. These figures show that the extent of the low cracking index has been greatly reduced when the formwork and insulation remained, but is still more severe than Oak Island or Sunset Beach. Only a few locations, in addition to the areas close to the pile supports, does the cracking index go below 1.0 beyond the outermost node. It can also be seen that the cracking index on the surface is lower than what was seen in the Wilmington case study.

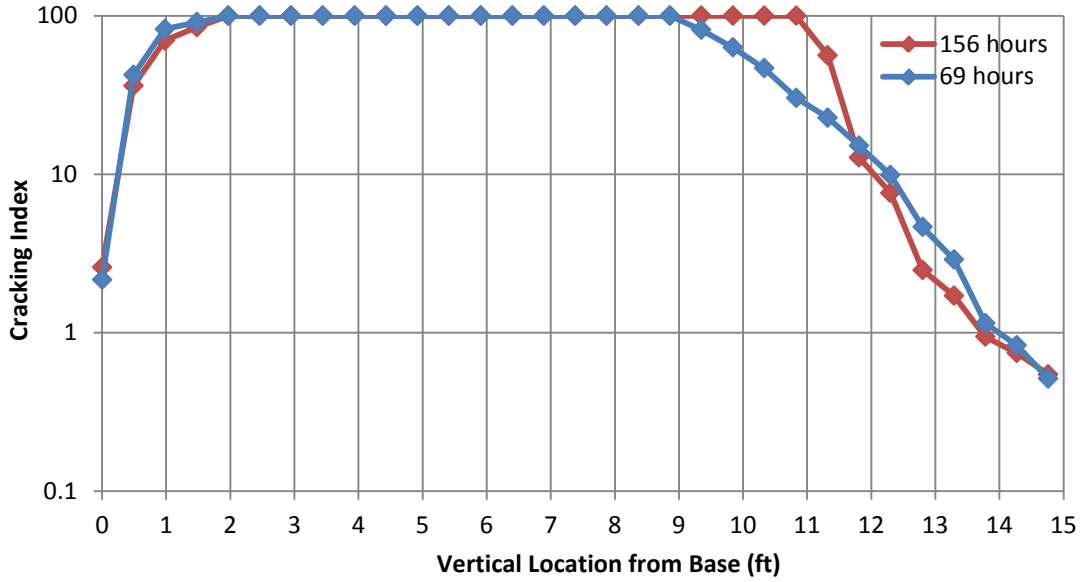


Figure 6-88: Wilmington insulated vertical profile cracking index at 69 and 156 hours

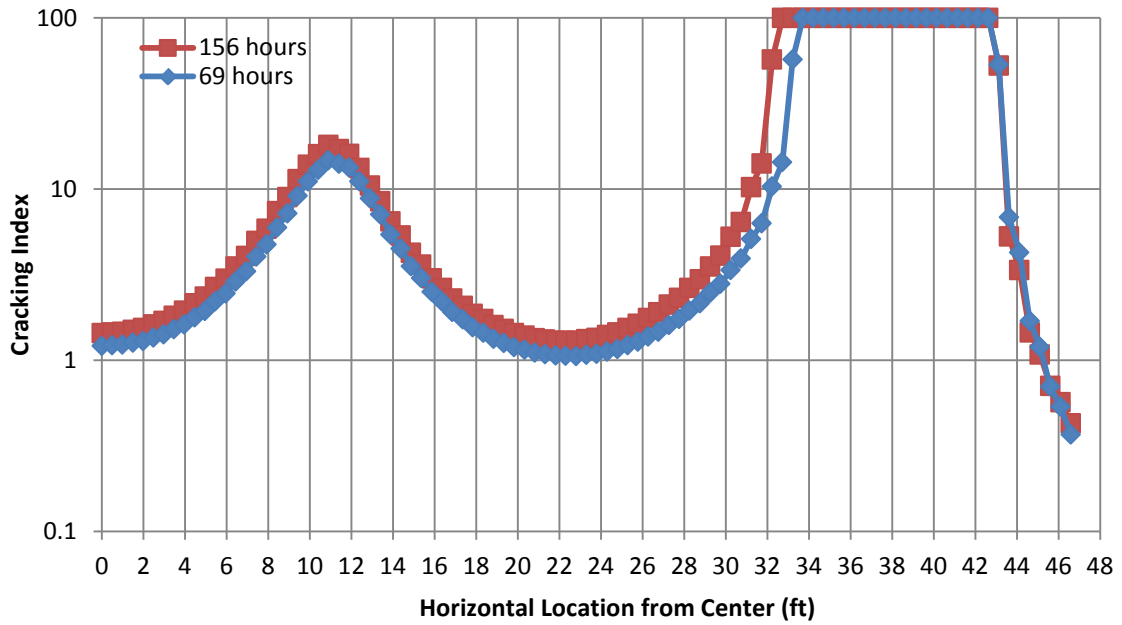


Figure 6-89: Wilmington insulated horizontal profile cracking index at 69 and 156 hours

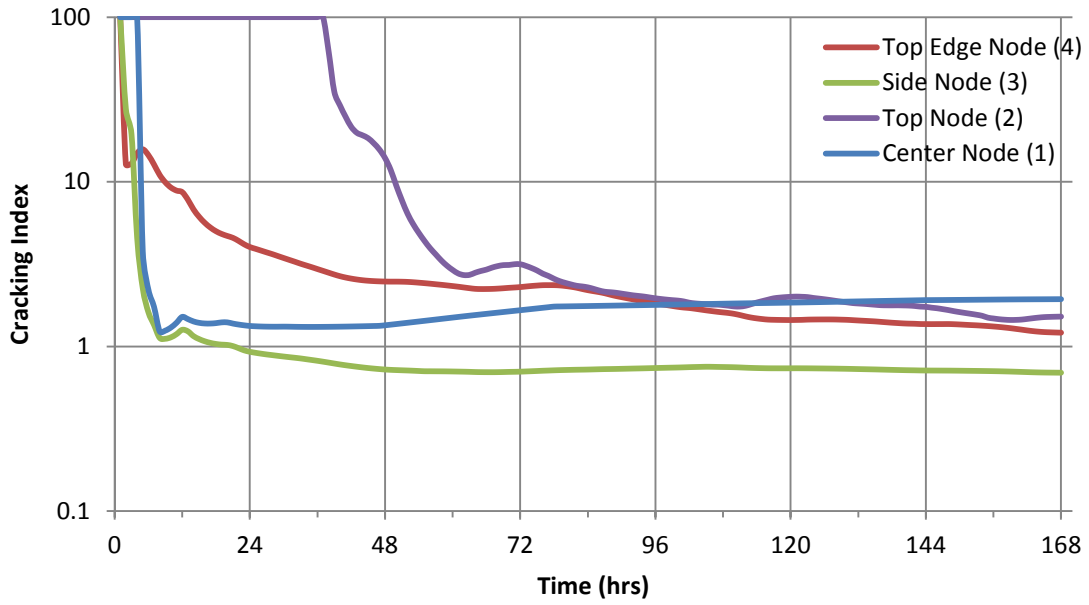


Figure 6-90: Wilmington insulated nodes cracking index vs time

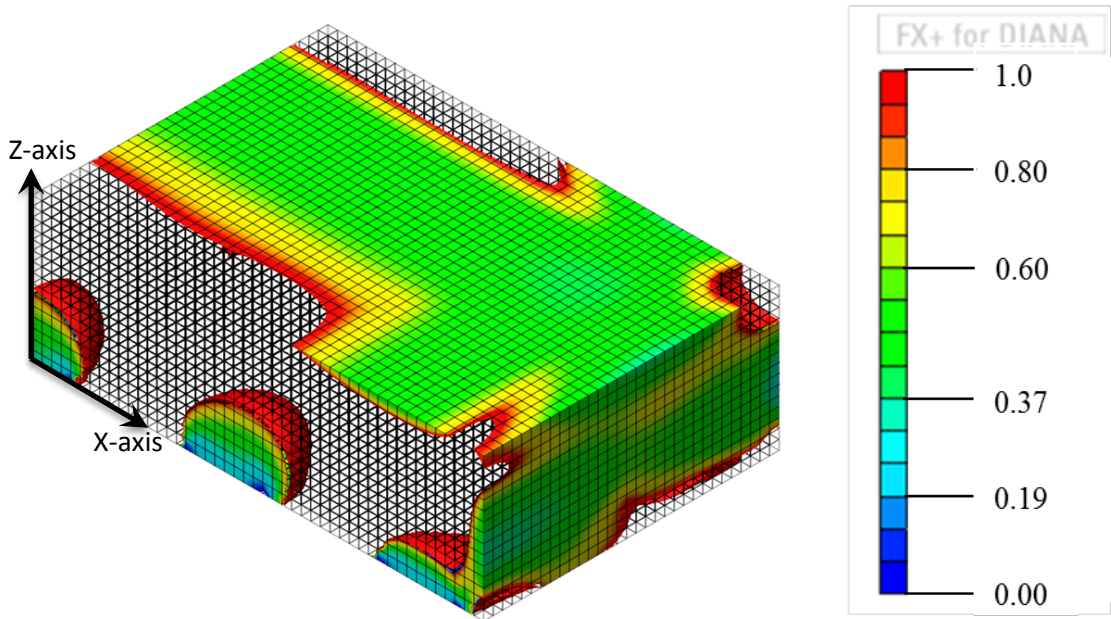


Figure 6-91: Wilmington insulated cracking index contours at 156 hours isoparametric view

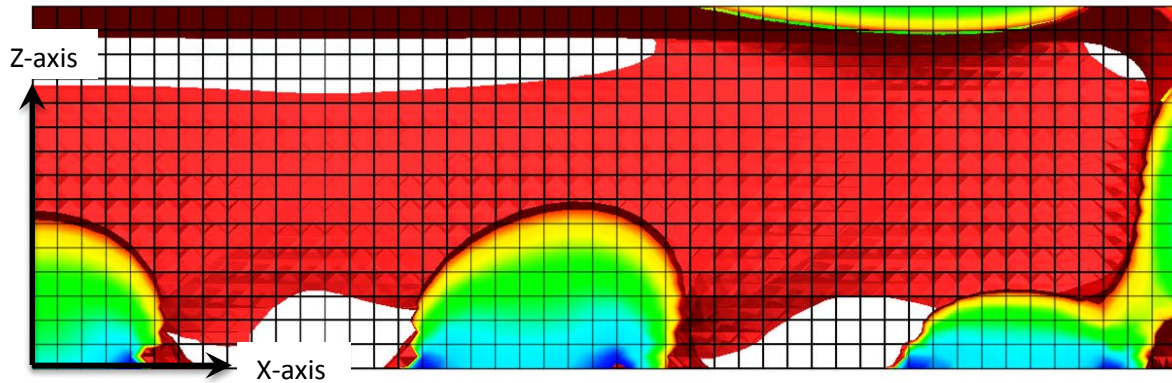


Figure 6-92: Wilmington insulated cracking index contours at 156 hours profile view

6.7 Results Summary

The investigation into the finite element modeling of heat generation, temperature distribution, and the structural response to these temperatures resulted in some key findings:

- The accurate prediction of the temperatures in the laboratory block experiment and the Oak Island footing case study leads to the verification of the thermal model created in DIANA.
- The modeled temperature differentials exceeded the typical limit value of 35 °F at some point in all of the analyses. In Oak Island and Sunset Beach, however, it was the center to side differential not the center to top differential that exceeded the limit.
- An analysis of the induced stresses was performed for all cases, and in each case there were locations where the cracking index was below the limit of 1, indicating the possibility of cracking.
- In the laboratory block experiment, the Oak Island footing, and the Sunset Beach footing, the cracking index was never below 1 except at the most outer nodes near the surface or in highly restrained areas near the pile supports.

- In the Wilmington footing case study, the cracking index was below the limit of 1 for nodes below the surface in both the case of early form removal and the case of no form removal. The potential for cracking was also found to be much worse in the case where the formwork and insulation was removed early at 70 hours.

CHAPTER 7 PARAMETRIC STUDY ANALYSIS RESULTS

7.1 Introduction

An additional parametric dimensional study was conducted to observe the effect of size on mass concrete and understand what may be considered “massive” mass concrete versus “typical” mass concrete. The goal was to assess the possible effect larger footings have on increased cracking potential and to create a better definition of what dimensions should be considered as “massive” mass concrete.

Due to its massive size, the Wilmington Bypass footing was used as the basis for this parametric study. The Wilmington Bypass footing model, where the insulation and formwork remained on for the full analysis, was scaled down using a ratio based on the height chosen for each trial versus the height of the original Wilmington Bypass model. The length, width, height, and pile dimensions, including their locations, were sized down using the appropriate ratio in order to keep the same aspect ratio in each trial. The same number of elements in each direction was also used in each model. Table 7-1 shows the dimensions of each trial footing along with their appropriate ratios, where the ratio is the trial height over the original height.

Table 7-1. Parametric Study Trial Dimensions

	Height (ft)	Length (ft)	Width (ft)	Pile Diam. (ft)	Ratio
Original	14.76	93.18	61.02	8.00	---
Trial 1	12.5	78.89	51.67	6.78	0.85
Trial 2	10	63.11	41.33	5.42	0.68
Trial 3	7.5	47.33	31.0	4.07	0.51
Trial 4	5	31.56	20.67	2.71	0.34

In this chapter, the thermal and stress analysis results of the 4 dimensional trials are presented. The analysis results for the original Wilmington Bypass footing case study with insulation can be found in Section 6.6. The thermal results display the temperature distribution in the concrete block over time as well as the temperature differentials throughout the concrete over time. The stress analysis results display the cracking index of the entire structure as well as key locations for each model. For an explanation of the cracking index refer to Section 6.1.

As with the case studies in Chapter 6, the parametric study trials were modeled using a quarter of the footing, similar to what is seen in Figure 6-1, with the concrete, formwork, and insulation explicitly modeled. Figure 7-1 shows the location of the vertical and horizontal profiles used for the temperature result figures in each trial. Figure 7-2 shows the location of the vertical and horizontal profiles as well as the key nodal locations where the cracking index was examined. The same number of elements in each direction was also used, so the same nodes and elements were examined in each trial.

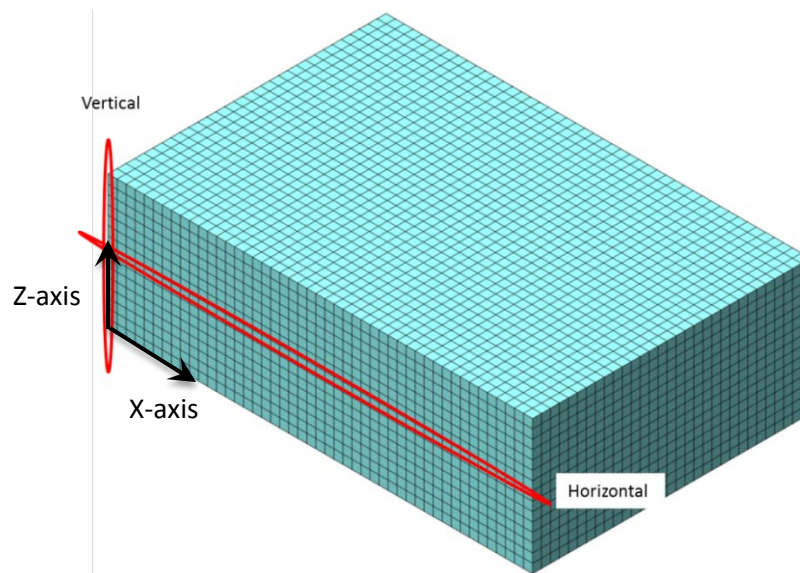


Figure 7-1: Dimensional study temperature locations

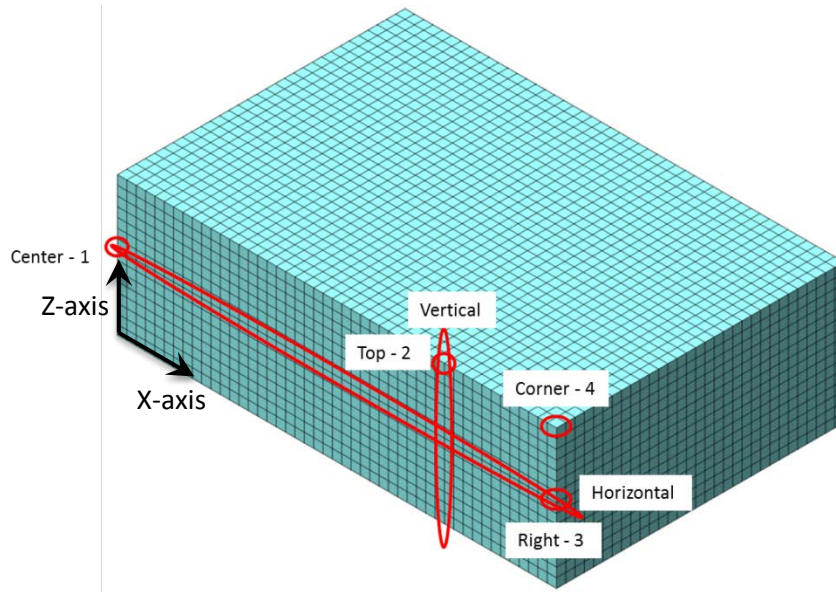


Figure 7-2: Dimensional study cracking index locations

7.2 Dimensional Study Trial 1

7.2.1 Thermal Analysis Results

In the first trial, the Wilmington Bypass footing was scaled down to a height of 12.5 feet. Using the appropriate ratio the model dimensions came out to be 39.44 feet long by 25.83 feet wide by 12.5 feet deep, where a quarter of the footing was modeled. The results from the Trial 1 analysis, seen in Figure 7-3 through Figure 7-12, proved to be very similar to the results seen in the original Wilmington Bypass analysis with insulation found in Section 6.6.

Figures 7-3 and 7-4 show the vertical and horizontal profile temperature distributions, respectively, over time. The model predicted a maximum temperature of 171.2 °F to occur at 99 hours and start decreasing minimally at 104 hours. This is very similar to what was seen in the original Wilmington case study with insulation seen in Section 6.6. It is only slightly lower than the original case's maximum temperature, indicating that the internal heat is not

dissipating much faster in Trial 1. As with the original case study, significant decrease in the internal temperature does not occur until after 168 hours.

Figure 7-5 shows the maximum temperature differentials developed in the DIANA model. The model predicted a maximum temperature differential of 52.6 °F to occur at 160 hours between the center and side surface node. The maximum temperature between the center and top surface node was only slightly lower at 50 °F. This is again very similar to what was seen in the original Wilmington case study with insulation. The only real difference is that the center to top differential is now slightly lower than the center to side differential.

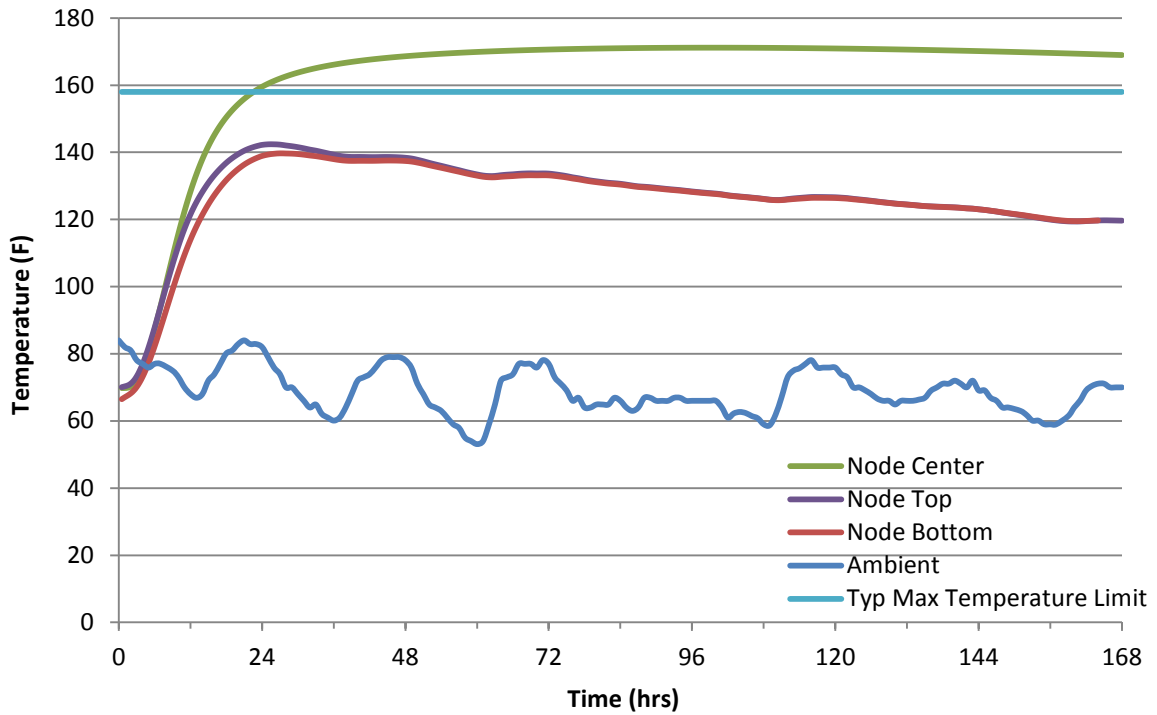


Figure 7-3: Trial 1 vertical temperature distribution

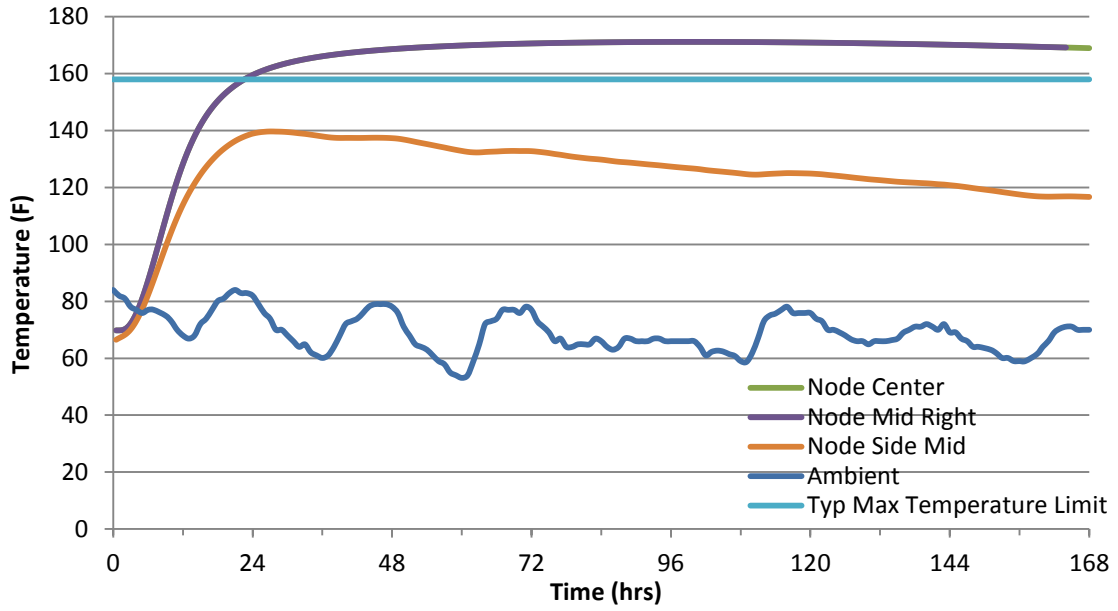


Figure 7-4: Trial 1 horizontal temperature distribution

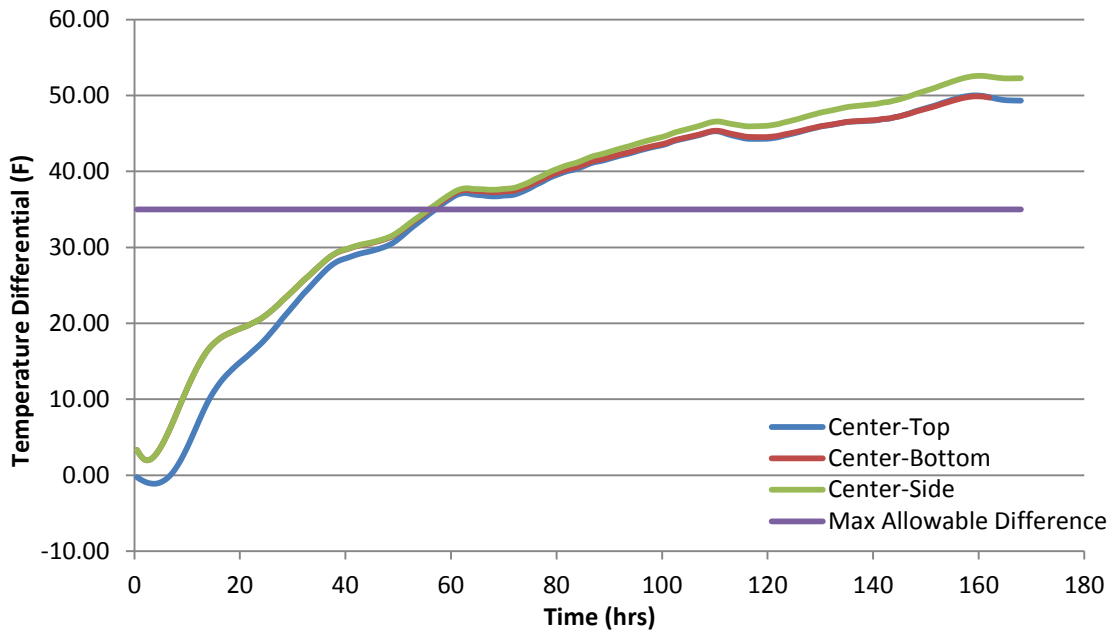


Figure 7-5: Trial 1 maximum temperature differentials

Figure 7-6 and Figure 7-7 show pictorial representations of the temperature distribution throughout the concrete block at the time of the maximum temperature differential, which occurs at 160 hours. These figures show that the temperature distribution in this model is very similar to what was seen in the Wilmington case study with insulation.

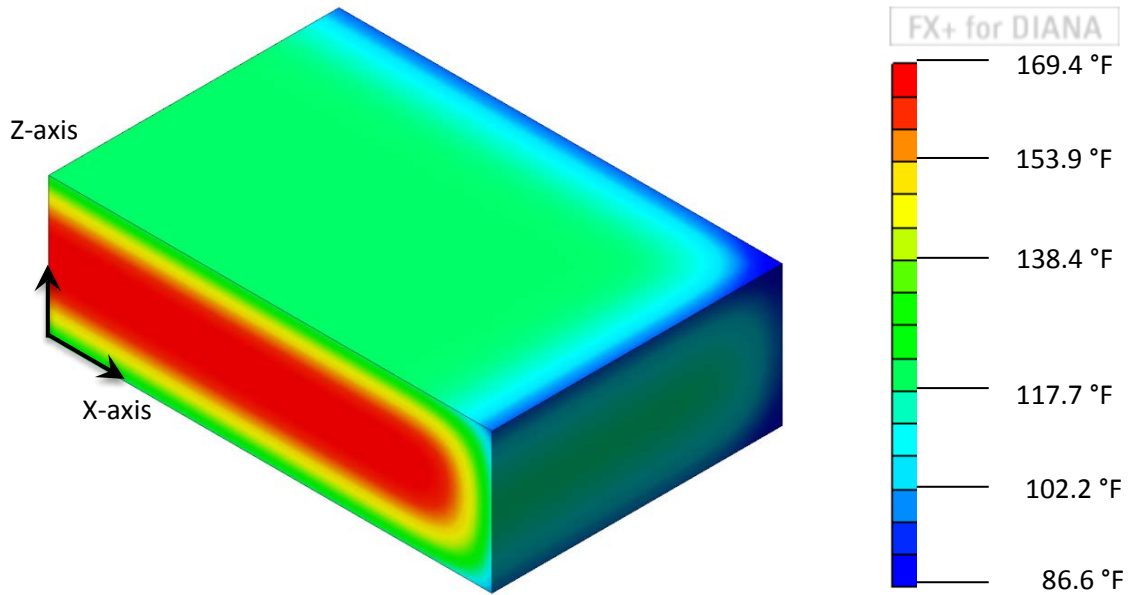


Figure 7-6: Trial 1 temperature profile at 160 hours

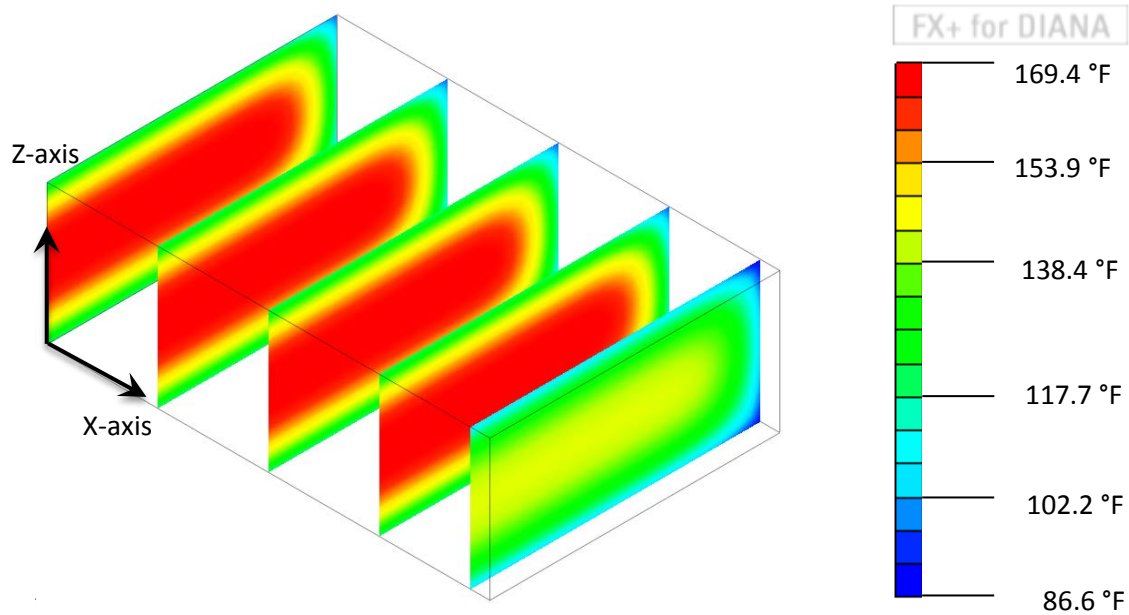


Figure 7-7: Trial 1 sliced temperature profile at 160 hours

7.2.2 Structural Analysis Results

The structural results in Figure 7-8 through 7-12 show the cracking index throughout the concrete footing at specific times as well as over the full 168 hour analysis period. The cracking index was calculated by the comparison of the principal stress versus the tensile strength of the concrete, as seen in the graphs in Chapter 6.

Figures 7-8 and 7-9 show the cracking index for the vertical and horizontal profiles, respectively, at the time of the peak temperature (99 hours) and the time of the maximum temperature differential (160 hours). Despite the differences in the strength and induced stresses at these different time periods, the cracking index remains similar at both time steps. These figures show that the cracking index is similar to that of the Wilmington case study with insulation and is still less than 1 for more than one node in each profile. Through linear interpolation the cracking index crosses 1 at a distance 0.82 ft below the surface in the

vertical profile and at a distance 1.05 ft below the surface in the horizontal profile. These values are slightly lower than what was seen in the original Wilmington case study, but are still very similar. Figure 7-10 shows the cracking index of the previously chosen key locations in Trial 1 over time. The cracking index of the center and top edge nodes never cross the limit of 1, whereas the outer top and side nodes remain below the limit of 1. There is a slight gap in information after 142 hours. This was due to an error in DIANA which caused the loss of some of the stress information during this time period.

Figure 7-11 shows the 3-D isoparametric view and Figure 7-12 shows the plan view of the cracking index contours below 1 on Trial 1 at the time of maximum temperature differential (160 hours). These figures show that the extent of the low cracking index in Trial 1 is very similar to that which was seen in the original Wilmington case study, although it is slightly less extensive.

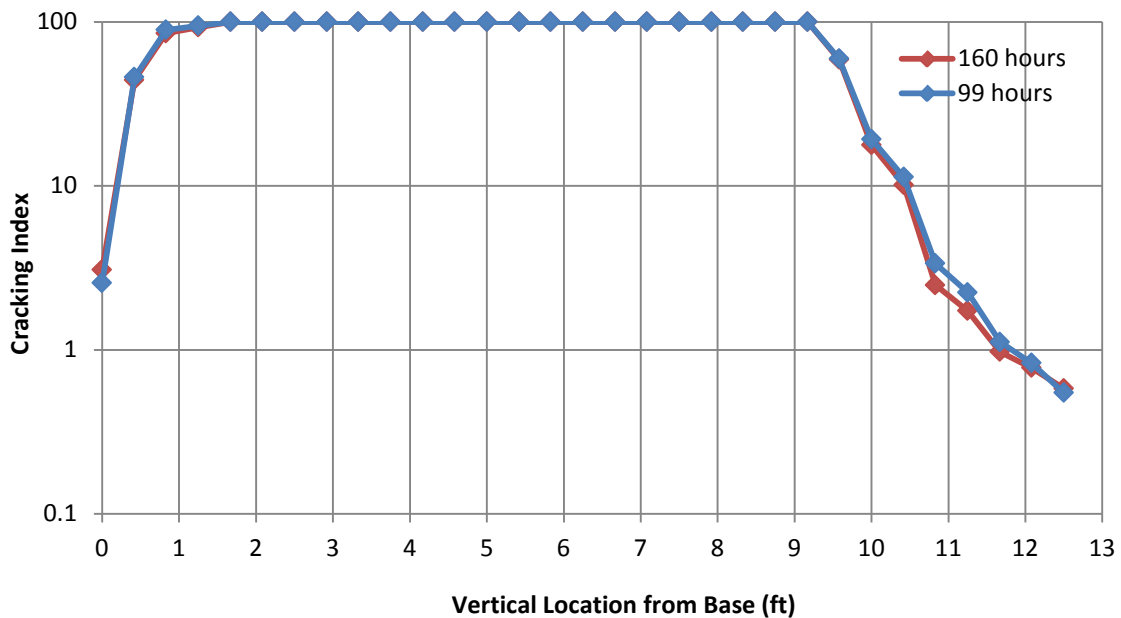


Figure 7-8: Trial 1 vertical profile cracking index at 99 and 160 hours

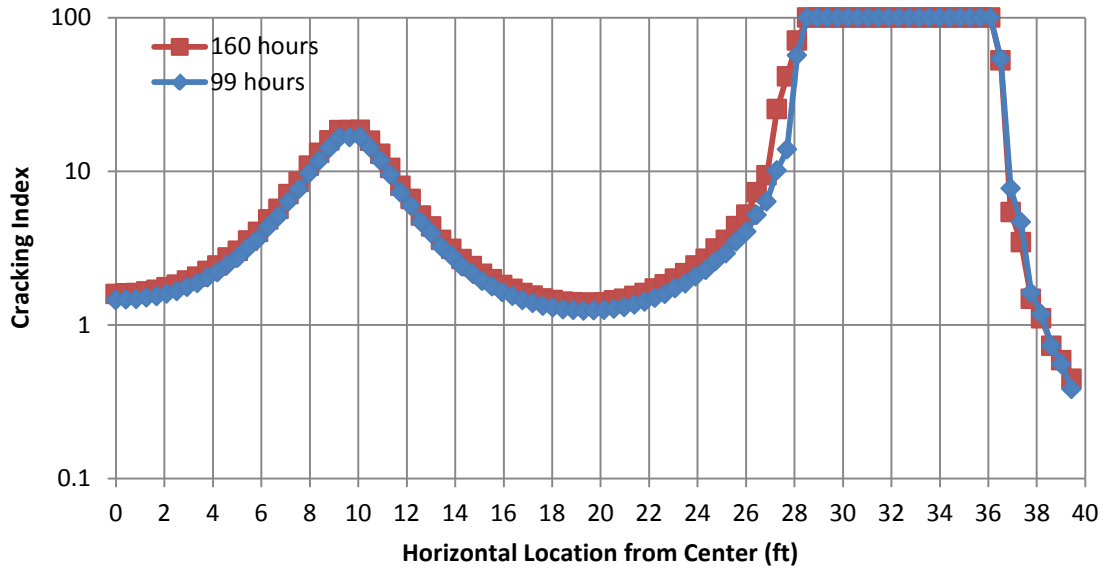


Figure 7-9: Trial 1 horizontal profile cracking index at 99 and 160 hours

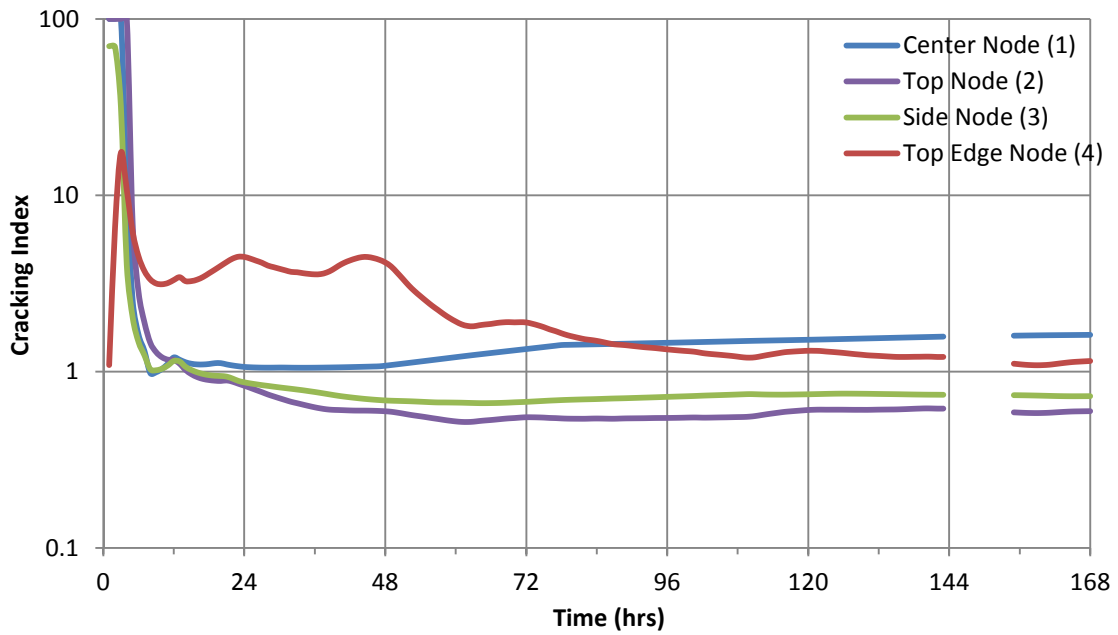


Figure 7-10: Trial 1 nodal cracking index vs time

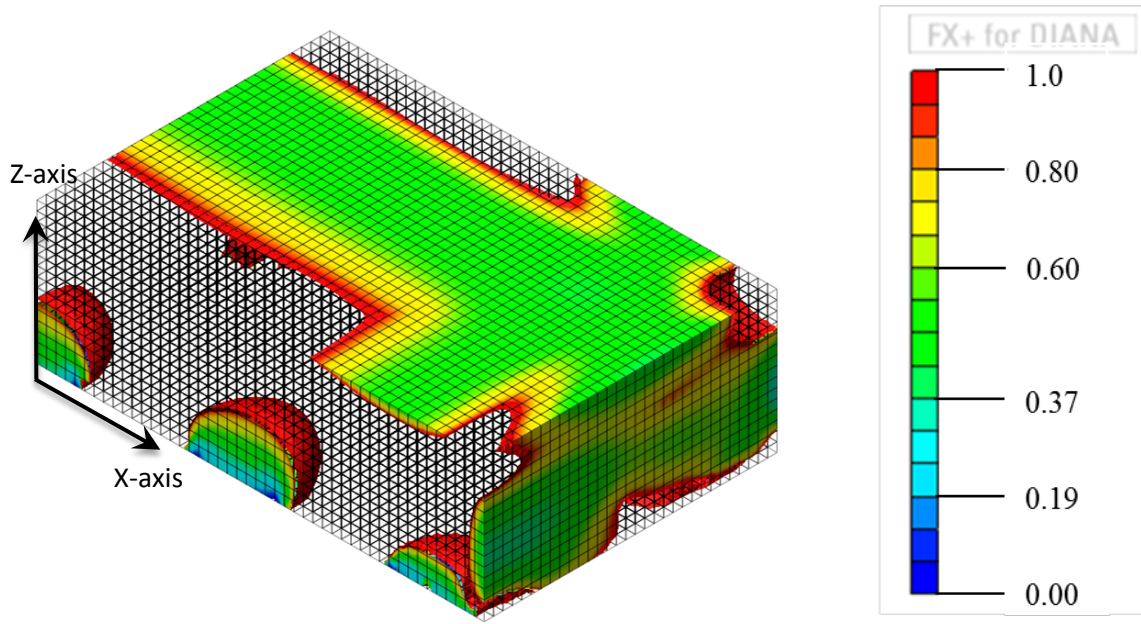


Figure 7-11: Trial 1 cracking index contours at 160 hours isoparametric view

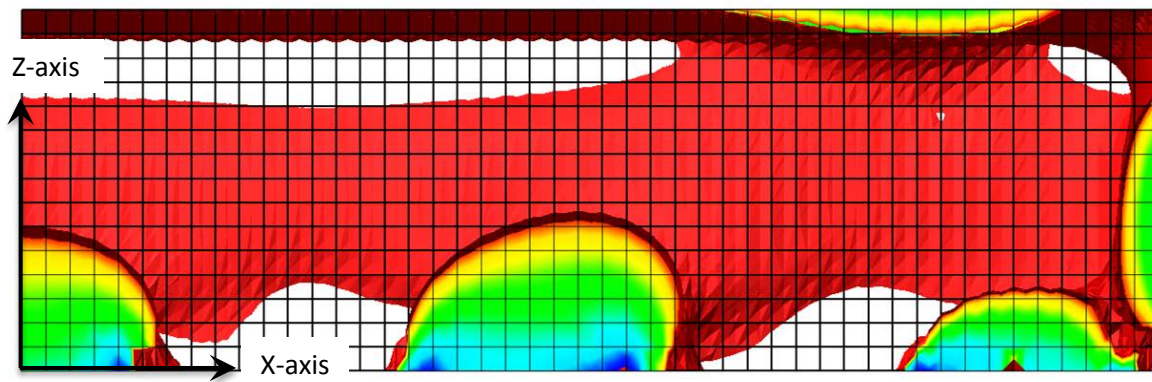


Figure 7-12: Trial 1 cracking index contours at 160 hours profile view

7.3 Dimensional Study Trial 2

7.3.1 Thermal Analysis Results

In the second trial, the Wilmington Bypass footing was scaled down to a height of 10.0 feet. Using the appropriate ratio the model dimensions came out to be 31.56 feet long by 20.67 feet wide by 10.0 feet deep, where a quarter of the footing was modeled. The results from the Trial 2 analysis, seen in Figure 7-13 through Figure 7-22, proved to still be somewhat similar to the results seen in the original Wilmington Bypass case study found in Section 6.6, but also began to show some clear differences.

Figures 7-13 and 7-14 show the vertical and horizontal profile temperature distributions, respectively, over time. The model predicted a maximum temperature of 170.0 °F to occur at 76 hours and start decreasing minimally at 83 hours. This is again similar to what was seen in the original Wilmington case study with insulation, although Trial 2 does have slightly lower temperatures. It is slightly lower than the Trial 1 maximum temperature, indicating that the internal heat is starting to dissipate a little faster in Trial 2. Unlike the previous two case studies, a more noticeable decrease in the internal temperatures starts to take place prior to 168 hours.

Figure 7-15 shows the maximum temperature differentials developed in the DIANA model. The model predicted a maximum temperature differential of 50.7 °F to occur at 160 hours between the center and side surface node. The maximum temperature between the center and top surface node was only slightly lower at 45.2 °F. This difference between the center to top differential and the center to side differential is even bigger than Trial 1, showing that some slight differences are beginning to emerge. The maximum difference is still similar to what was seen in the original Wilmington case study with insulation though.

Figure 7-16 and Figure 7-17 show pictorial representations of the temperature distribution throughout the concrete block at the time of the maximum temperature

differential, which occurs at 160 hours. These figures show that the temperature distribution in this model is very similar to what was seen in the Wilmington case study with insulation.

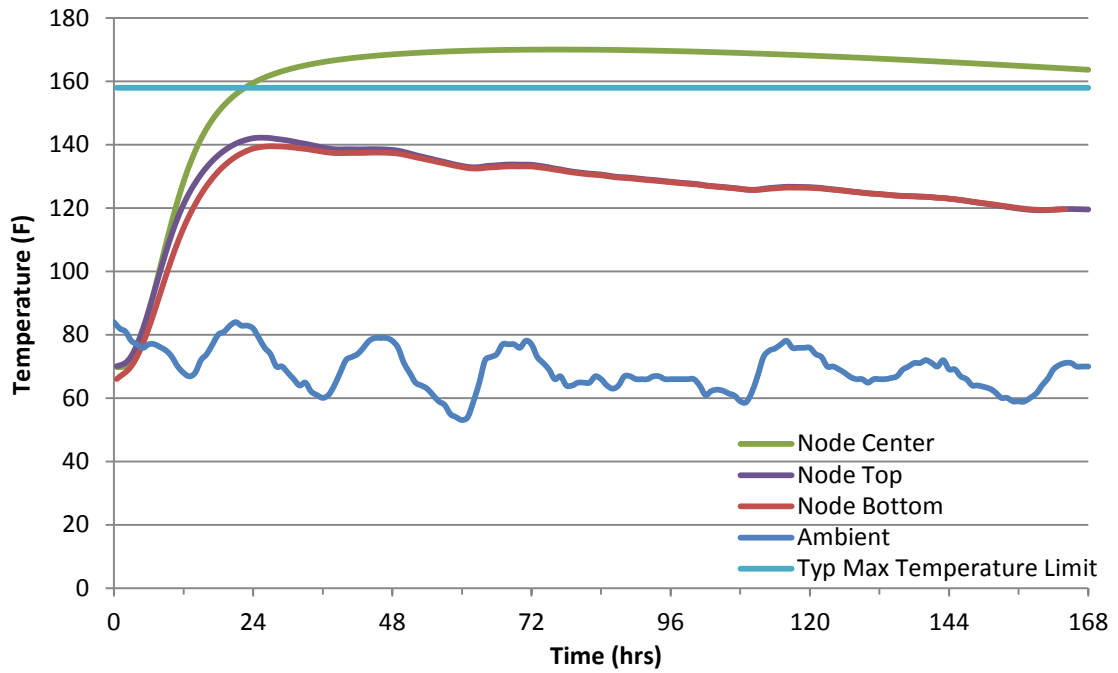


Figure 7-13: Trial 2 vertical temperature distribution

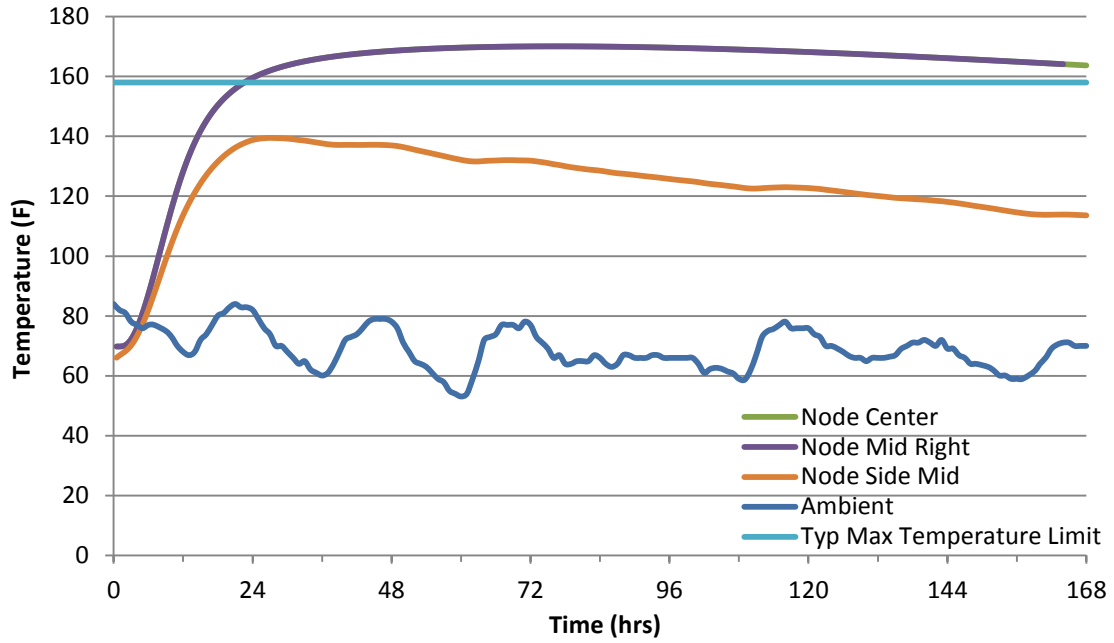


Figure 7-14: Trial 2 horizontal temperature distribution

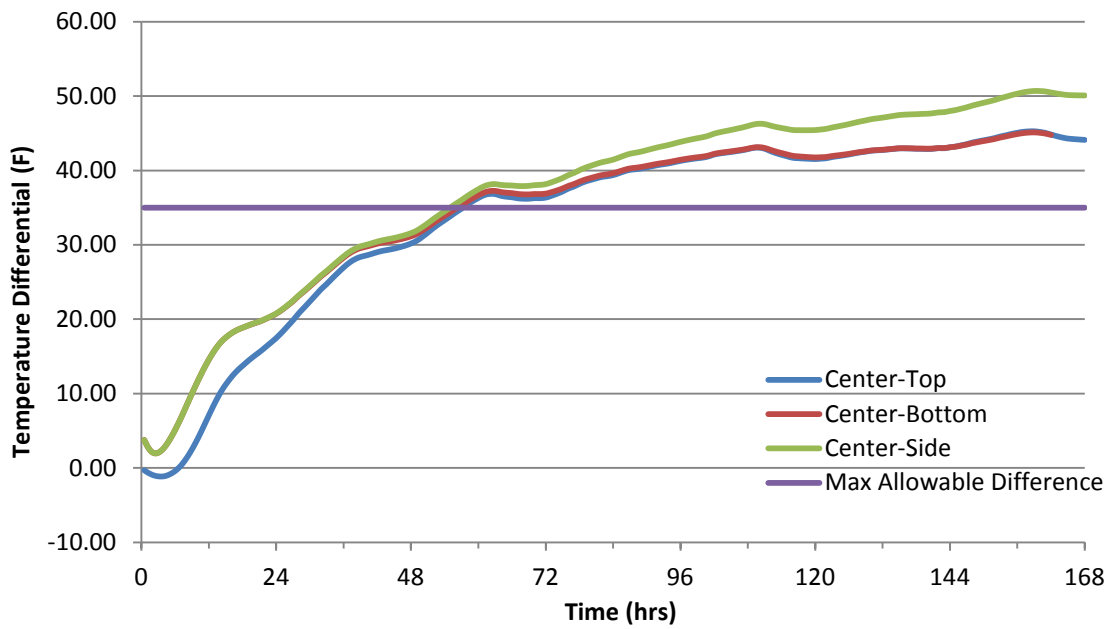


Figure 7-15: Trial 2 maximum temperature differentials

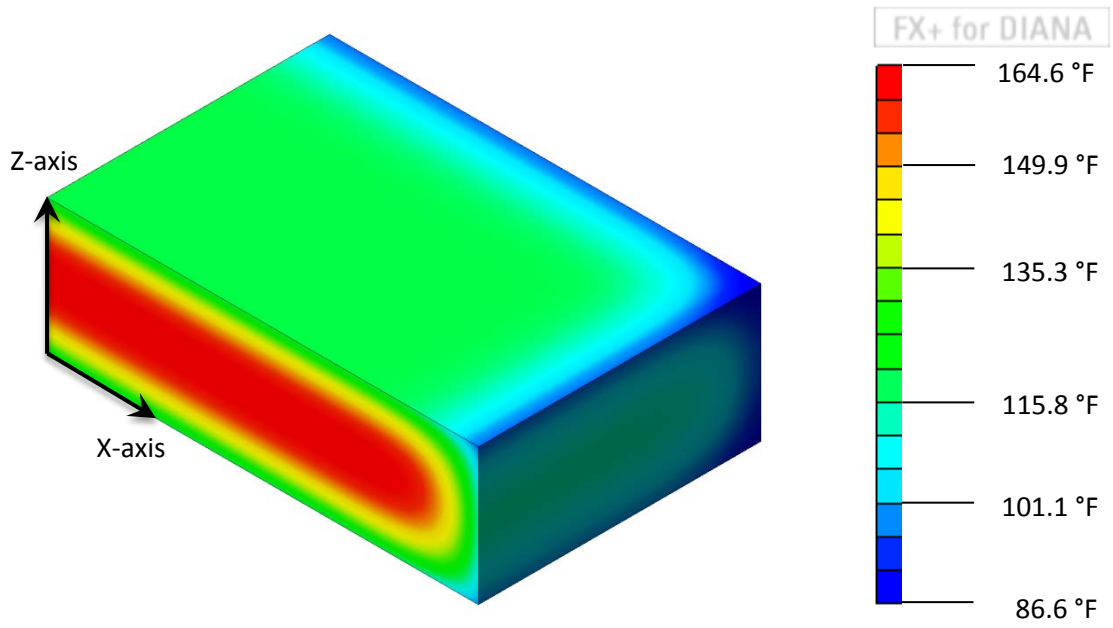


Figure 7-16: Trial 2 temperature profile at 160 hours

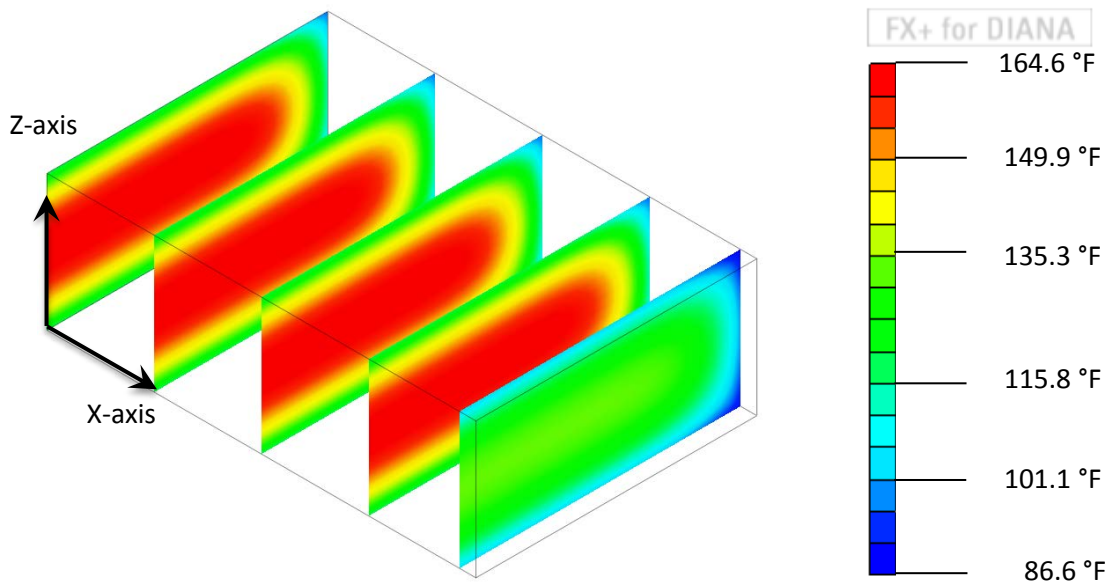


Figure 7-17: Trial 2 sliced temperature profile at 160 hours

7.3.2 Structural Analysis Results

The structural results in Figure 7-18 through 7-22 show the cracking index throughout the concrete footing at specific times as well as over the full 168 hour analysis period. The cracking index was calculated by the comparison of the principal stress versus the tensile strength of the concrete, as seen in the graphs in Chapter 6.

Figures 7-18 and 7-19 show the cracking index for the vertical and horizontal profiles, respectively, at the time of the peak temperature (76 hours) and the time of the maximum temperature differential (160 hours). Despite the differences in the strength and induced stresses at these different time periods, the cracking index remains similar at both time steps. These figures show that the cracking index is similar to Trial 1 with insulation and is still less than 1 for more than one node in each profile, but is starting to look less like the Wilmington case study. Through linear interpolation the cracking index crosses 1 at a distance 0.59 ft below the surface in the vertical profile and at a distance 0.83 ft below the surface in the horizontal profile. These values are noticeably starting to get lower than what was seen in the original Wilmington case study, but are still similar to Trial 1. Figure 7-20 shows the cracking index of the previously chosen key locations in Trial 2 over time. The cracking index of the center and top edge nodes never cross the limit of 1, whereas the outer top and side nodes remain below the limit of 1, similar to Trial 1. The cracking index values in Trial 2, however, are slightly higher than Trial 1, even though they are still below the limit of 1.

Figure 7-21 shows the 3-D isoparametric view and Figure 7-22 shows the plan view of the cracking index contours below 1 on Trial 2 at the time of maximum temperature differential (160 hours). These figures show that the extent of the low cracking index in Trial 2 is still similar to that which was seen in the original Wilmington case study, but is noticeably not as extensive.

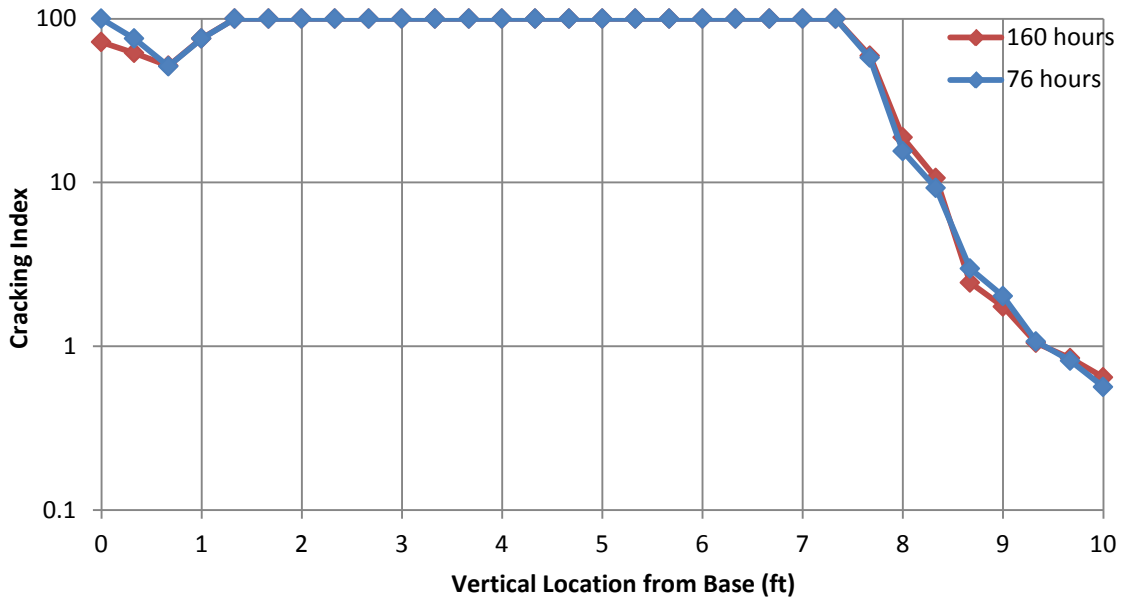


Figure 7-18: Trial 2 vertical profile cracking index at 76 and 160 hours

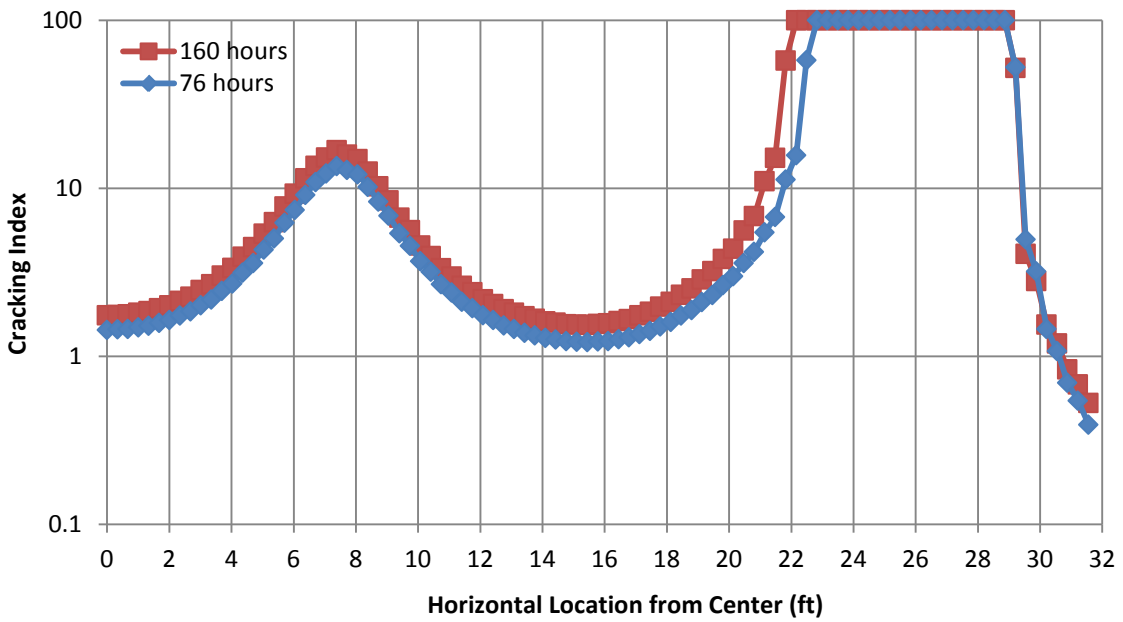


Figure 7-19: Trial 2 horizontal profile cracking index at 76 and 160 hours

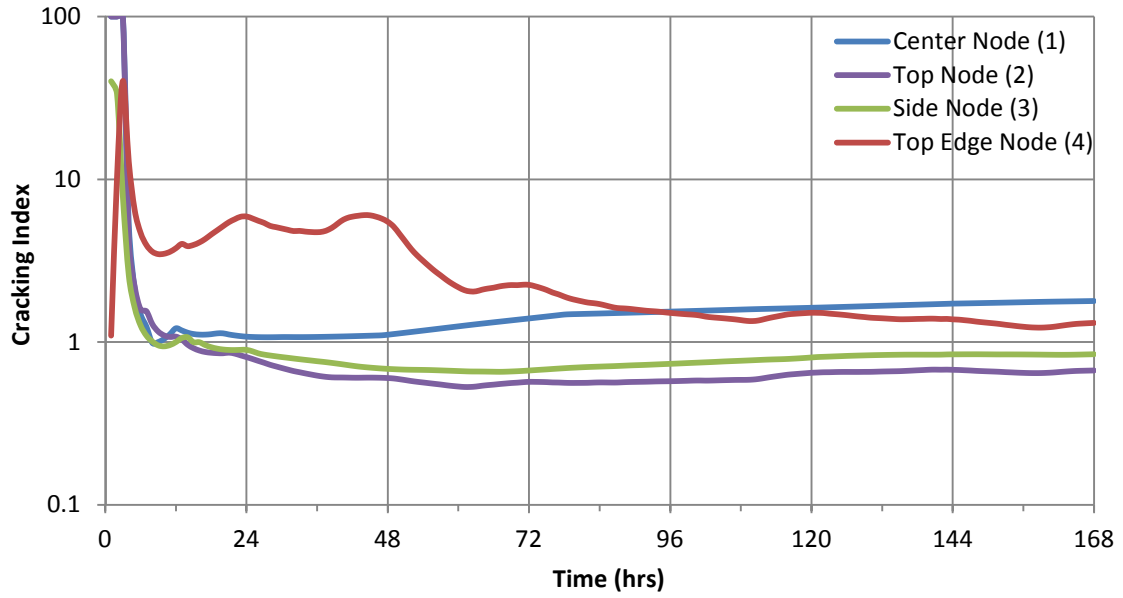


Figure 7-20: Trial 2 nodal cracking index vs time

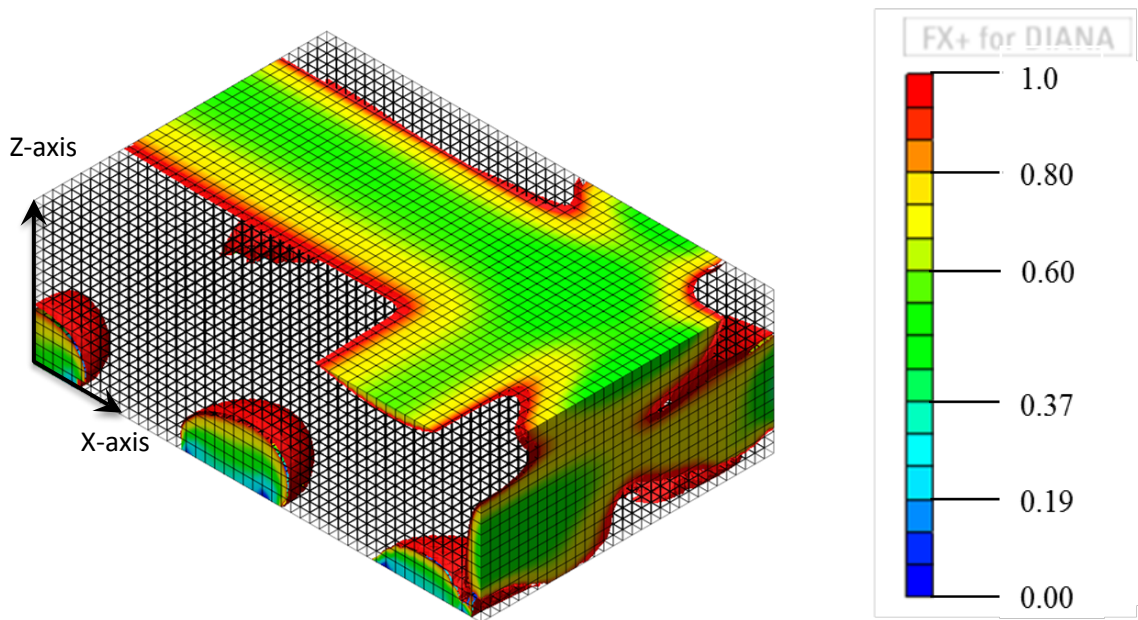


Figure 7-21: Trial 2 cracking index contours at 160 hours isoparametric view

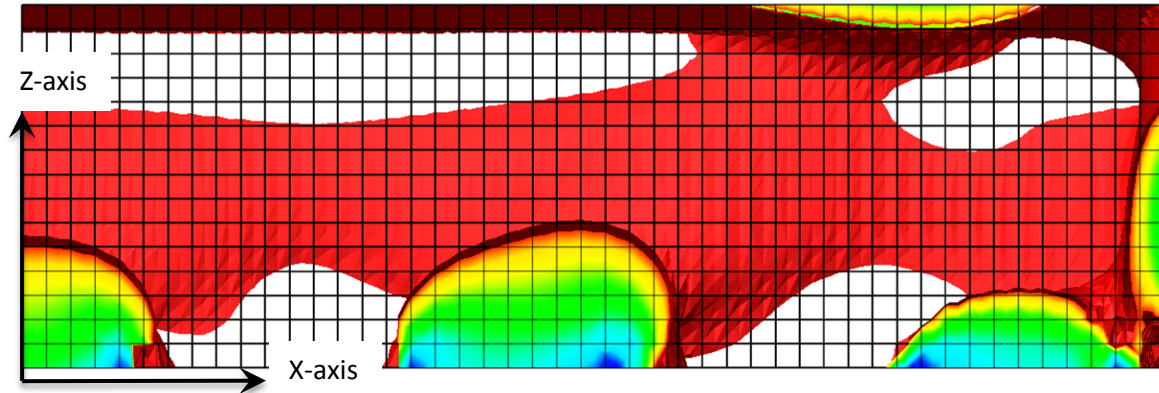


Figure 7-22: Trial 2 cracking index contours at 160 hours profile view

7.4 Dimensional Study Trial 3

7.4.1 Thermal Analysis Results

In the third trial, the Wilmington Bypass footing was scaled down to a height of 7.5 feet. Using the appropriate ratio the model dimensions came out to be 23.67 feet long by 15.5 feet wide by 7.5 feet deep, where a quarter of the footing was modeled. This is very similar to the dimensions of the Sunset Beach footing. The results from the Trial 3 analysis, seen in Figure 7-23 through Figure 7-32, proved to be very different to the results seen in the original Wilmington Bypass case study and the first two Trial case studies.

Figures 7-23 and 7-24 show the vertical and horizontal profile temperature distributions, respectively, over time. The model predicted a maximum temperature of 168.1 °F to occur at 56 hours and start decreasing minimally at 60 hours. This is significantly different than what was seen in the original Wilmington case study with insulation, although the peak temperature is still high due to the mix design used. Also unlike the original case study, and Trials 1 and 2, there is a slightly bigger decrease in the internal temperatures prior to the end of the analysis at 168 hours.

Figure 7-25 shows the maximum temperature differentials developed in the DIANA model. The model predicted a maximum temperature differential of 46.0 °F to occur at 158 hours between the center and side surface node. The maximum temperature difference between the center and top surface node was quite a bit lower at 37.2 °F, which occurred at 109 hours. This difference between the center to top differential and the center to side differential is even bigger than Trial 2, showing this footing is quite a bit different from the other models.

Figure 7-26 and Figure 7-27 show pictorial representations of the temperature distribution throughout the concrete block at the time of the maximum temperature differential, which occurs at 158 hours. These figures show that the temperature distribution in this model is starting to differ from the Trials 1 and 2 and the original footing, as the temperatures in the center are getting lower.

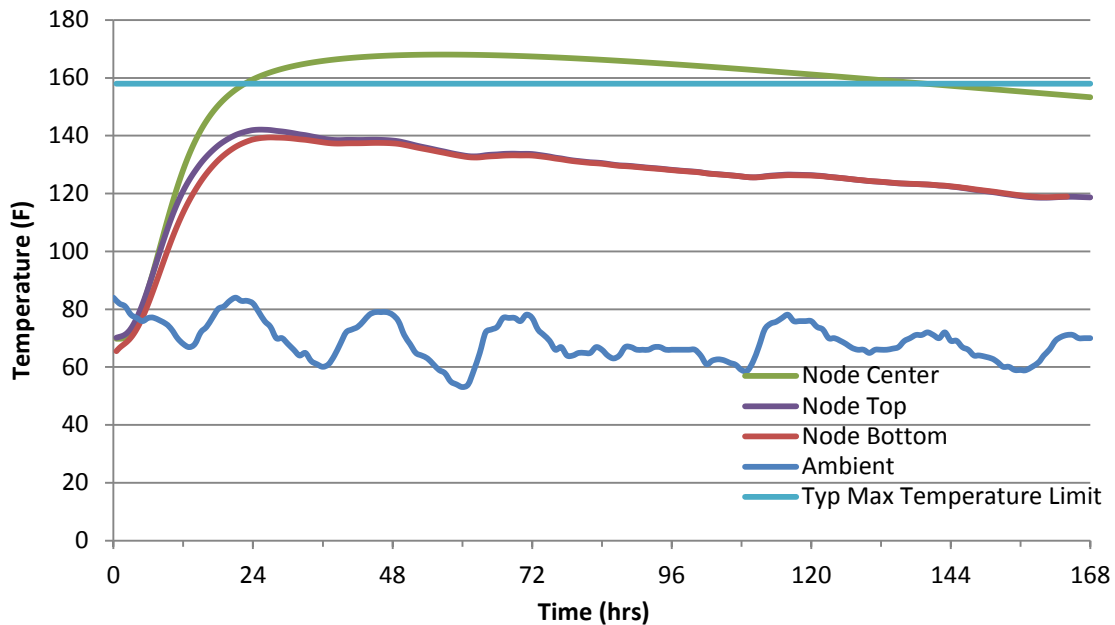


Figure 7-23: Trial 3 vertical temperature distribution

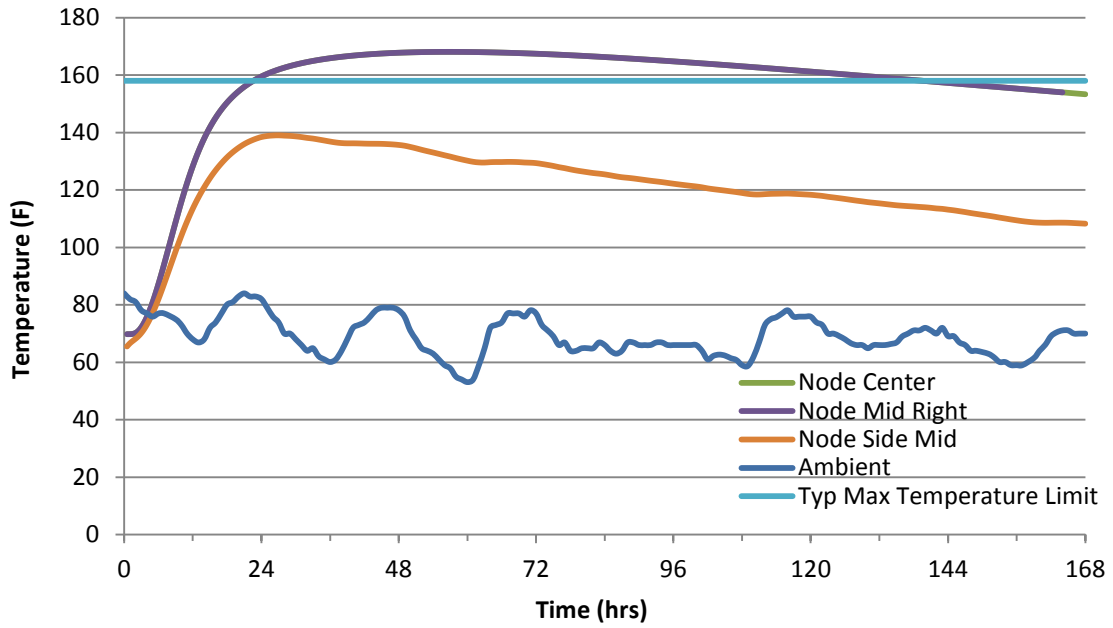


Figure 7-24: Trial 3 horizontal temperature distribution

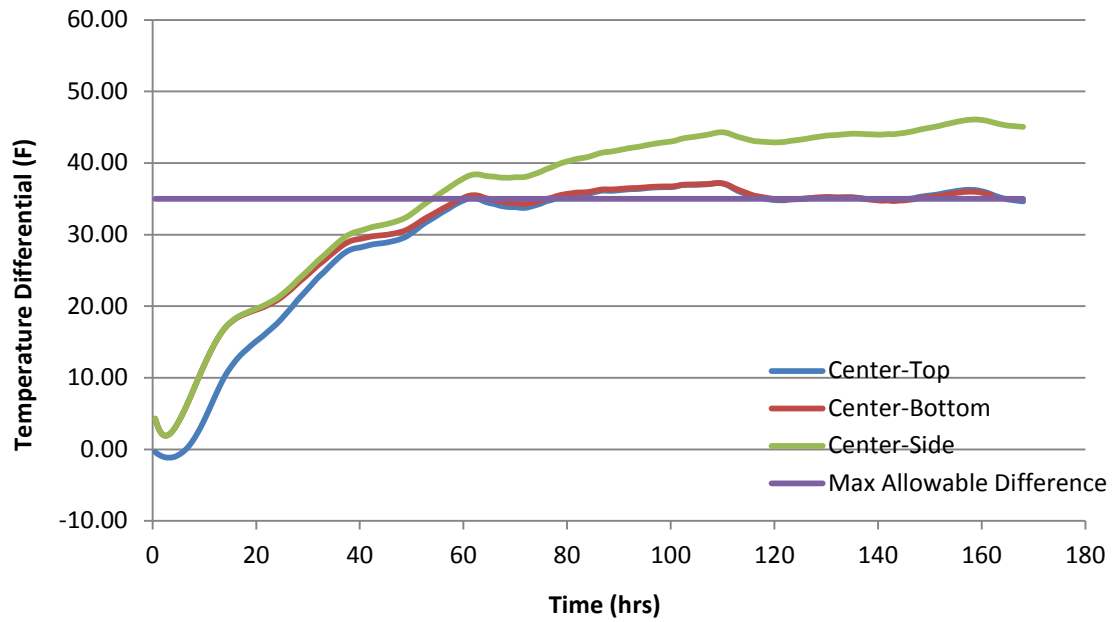


Figure 7-25: Trial 3 maximum temperature differentials

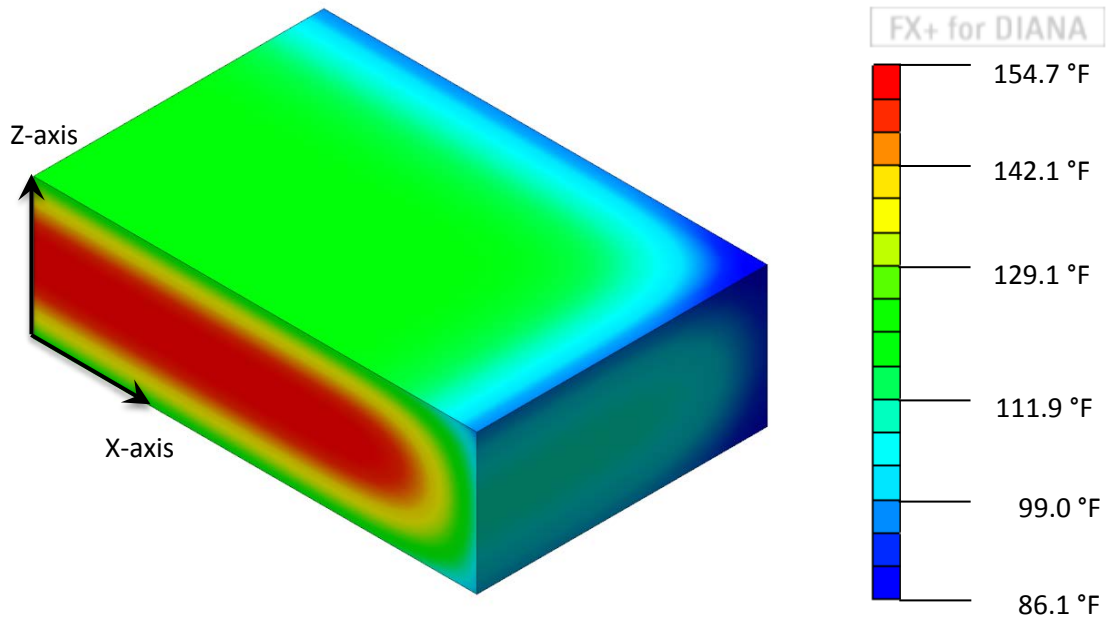


Figure 7-26: Trial 3 temperature profile at 158 hours

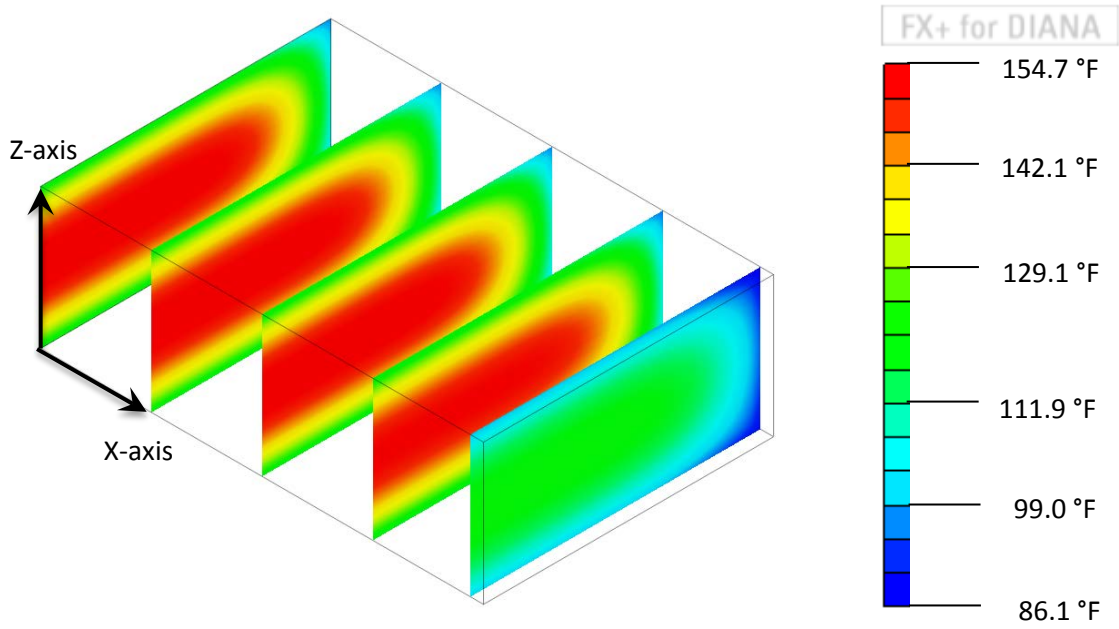


Figure 7-27: Trial 3 sliced temperature profile at 158 hours

7.4.2 Structural Analysis Results

The structural results in Figure 7-28 through 7-32 show the cracking index throughout the concrete footing at specific times as well as over the full 168 hour analysis period. The cracking index was calculated by the comparison of the principal stress versus the tensile strength of the concrete, as seen in the graphs in Chapter 6.

Figures 7-28 and 7-29 show the cracking index for the vertical and horizontal profiles, respectively, at the time of the peak temperature (56 hours) and the time of the maximum temperature differential (158 hours). Unlike the previous trials, the cracking index between these two times is differing a bit, where it is slightly worse at the time of peak temperature (56 hours). These figures show that the cracking index is still less than 1 for more than one node in each profile though. Through linear interpolation it is found that at the time of the maximum temperature difference, the cracking index crosses 1 at a distance 0.25 ft below the surface in the vertical profile and at a distance 0.37 ft below the surface in the horizontal profile. These values are significantly lower than what was seen in the original Wilmington case study and Trial 1. Figure 7-30 shows the cracking index of the previously chosen key locations in Trial 3 over time. The cracking index of the center and top edge nodes never cross the limit of 1, whereas the outer top and side nodes remain below the limit of 1, similar to Trial 1. The cracking index values in Trial 3, however, approach 1 towards the end of the analysis.

Figure 7-31 shows the 3-D isoparametric view and Figure 7-32 shows the plan view of the cracking index contours below 1 on Trial 3 at the time of maximum temperature differential (158 hours). These figures show that the extent of the low cracking index in Trial 3 is noticeably different to what was seen in the original Wilmington case study, as it is significantly less extensive. It is very similar to what was observed in Oak Island and Sunset Beach, which seems to indicate a lower probability of significant cracking.

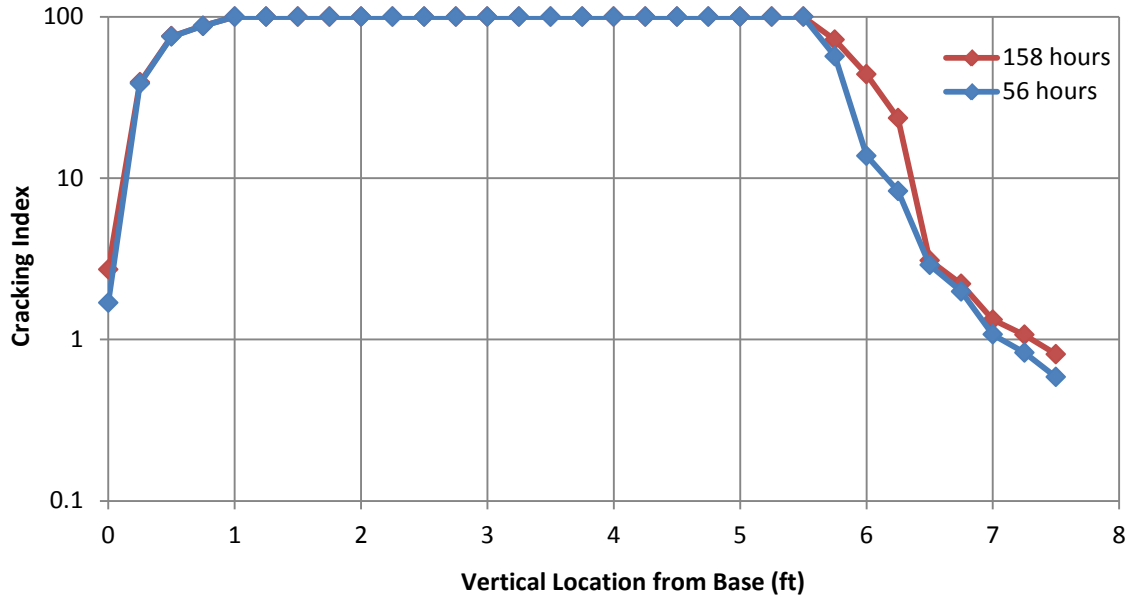


Figure 7-28: Trial 3 vertical profile cracking index at 56 and 158 hours

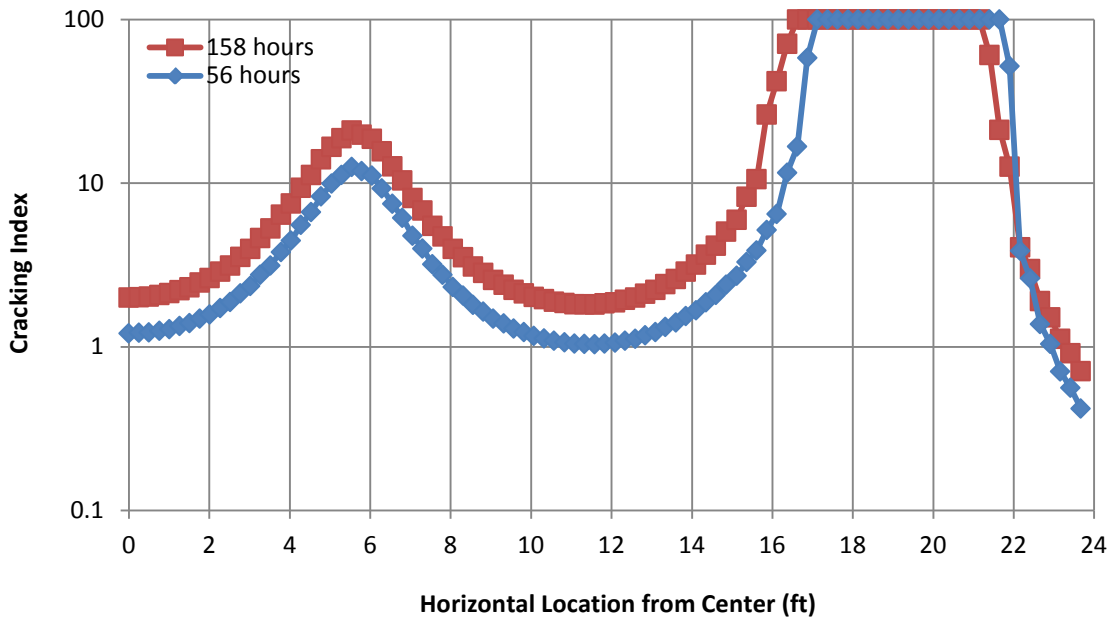


Figure 7-29: Trial 3 horizontal profile cracking index at 56 and 158 hours

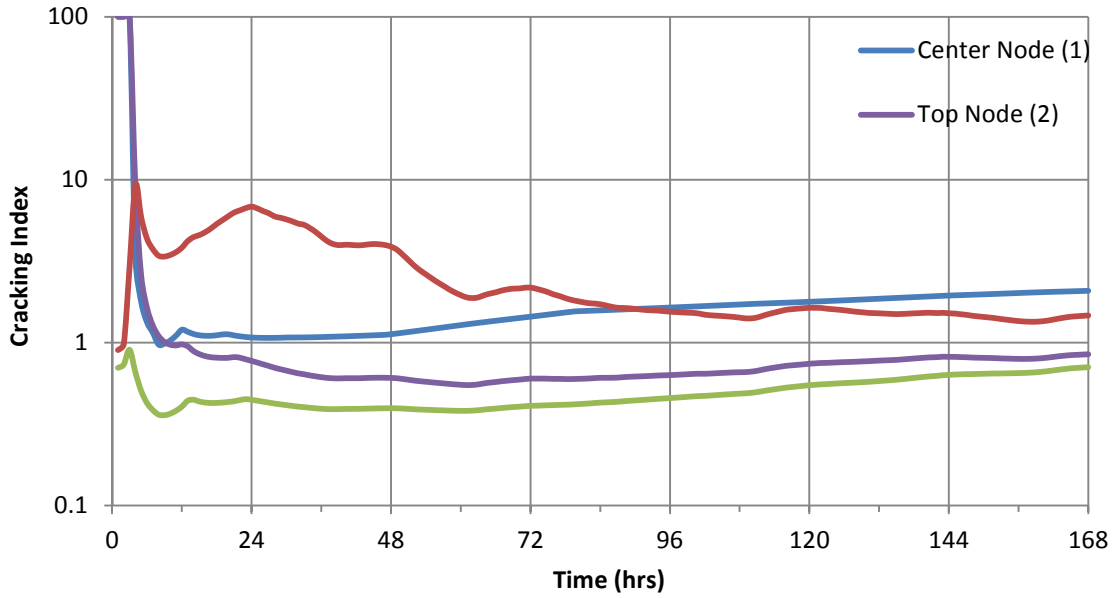


Figure 7-30: Trial 3 nodal cracking index vs time

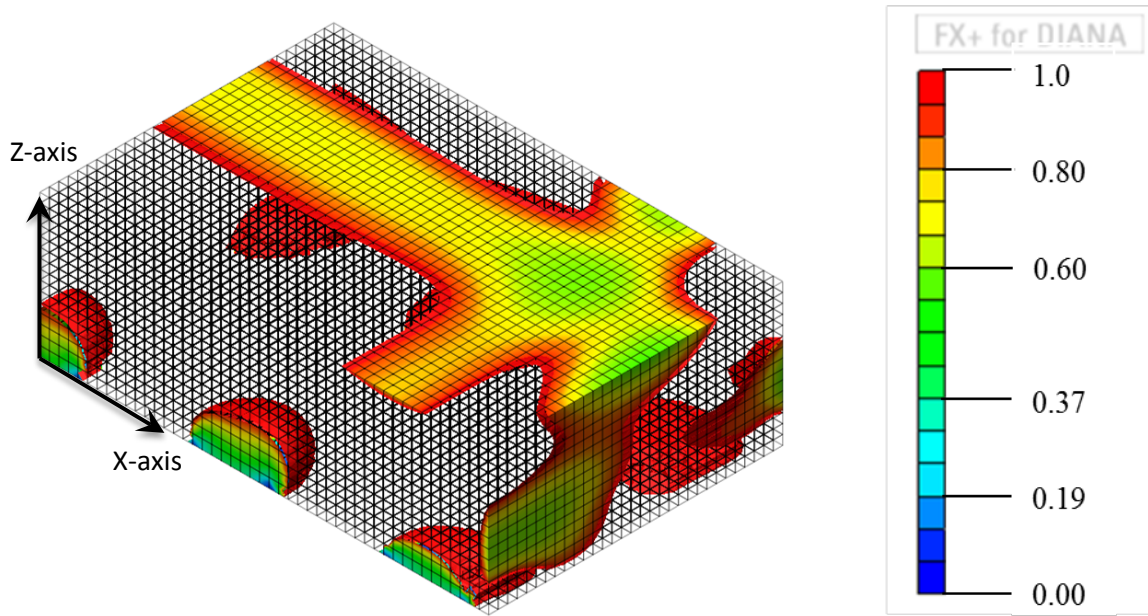


Figure 7-31: Trial 3 cracking index contours at 158 hours isoparametric view

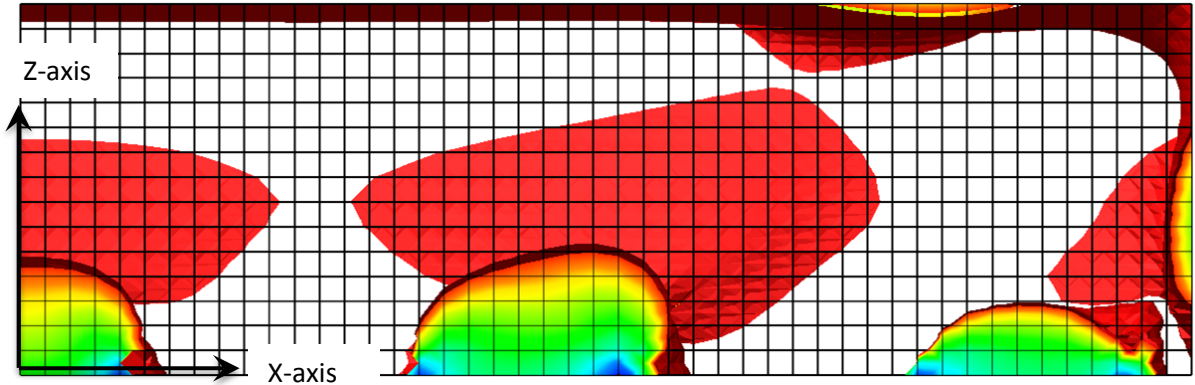


Figure 7-32: Trial 3 cracking index contours at 158 hours profile view

7.5 Dimensional Study Trial 4

7.5.1 Thermal Analysis Results

In the final trial, the Wilmington Bypass footing was scaled down to a height of 5.0 feet, which is within the range of the minimum dimension most specifications use to consider an element mass concrete. Using the appropriate ratio the model dimensions came out to be 15.78 feet long by 10.33 feet wide by 5.0 feet deep, where a quarter of the footing was modeled. This is smaller than any of the previous case studies except for the laboratory block experiment. The results from the Trial 4 analysis, seen in Figure 7-33 through Figure 7-42, proved to be very different to the results seen in the original Wilmington Bypass case study as well as the other trials.

Figures 7-33 and 7-34 show the vertical and horizontal profile temperature distributions, respectively, over time. The model predicted a maximum temperature of 163.9 °F to occur at 42 hours and start decreasing at 46 hours. This is much lower than what was seen in the original Wilmington case study with insulation, although the peak temperature is still higher than the typical maximum allowable temperature due to the mix design used.

Also unlike the original case study, and Trials 1 and 2, there is a significant decrease in the internal temperatures prior to the end of the analysis at 168 hours.

Figure 7-35 shows the maximum temperature differentials developed in the DIANA model. The model predicted a maximum temperature differential of 38.3 °F to occur at 109 hours between the center and side surface node. The maximum temperature difference between the center and top surface node was quite a bit lower at 28.9 °F, which occurred at 61 hours. This difference between the center to top differential and the center to side differential is similar to that of Trial 3. As is expected, this model has the lowest temperature differentials, where the maximum differential is very close to the typical maximum allowable differential of 35 °F.

Figure 7-36 and Figure 7-37 show pictorial representations of the temperature distribution throughout the concrete block at the time of the maximum temperature differential, which occurs at 109 hours. These figures show that the temperature distribution in this model is very different from the original Wilmington case study, as the interior concrete is at a much lower temperature due to the increased rate of heat dissipation.

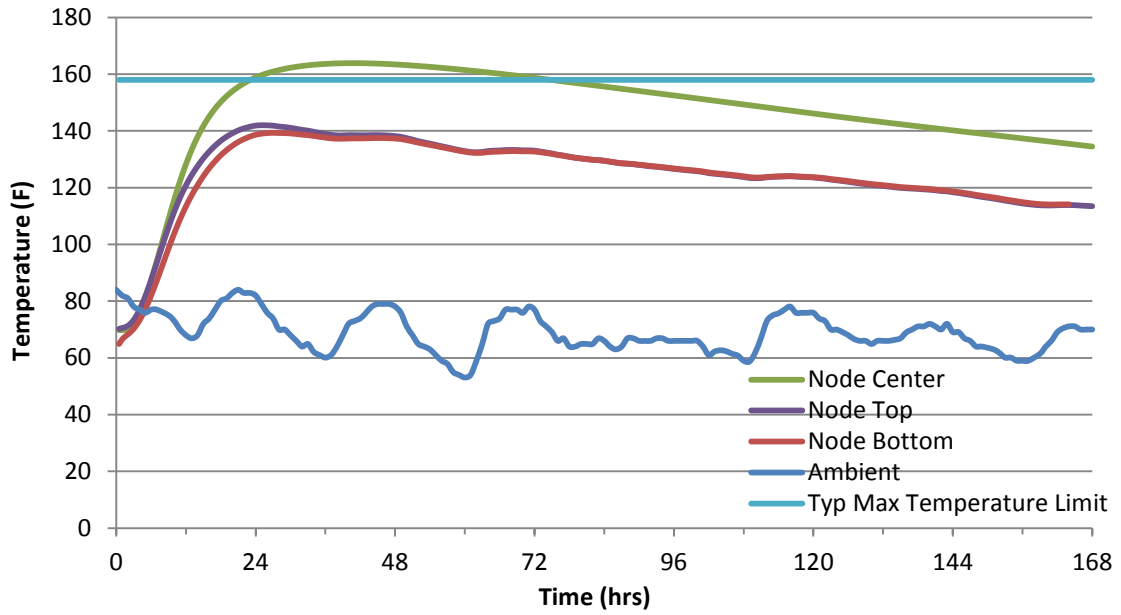


Figure 7-33: Trial 4 vertical temperature distribution

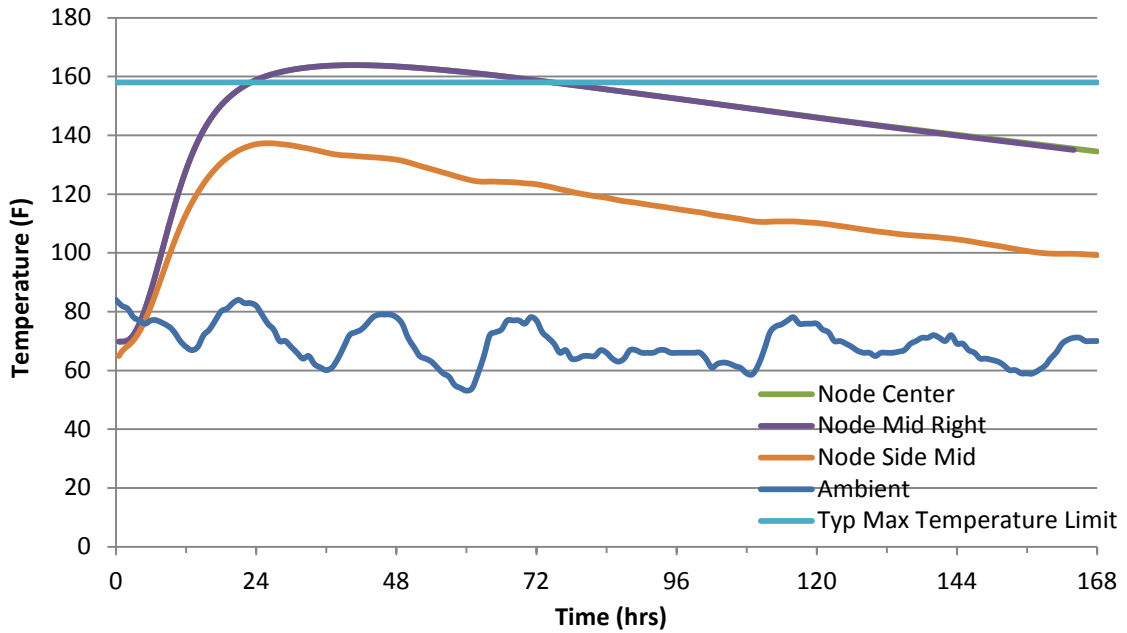


Figure 7-34: Trial 4 horizontal temperature distribution

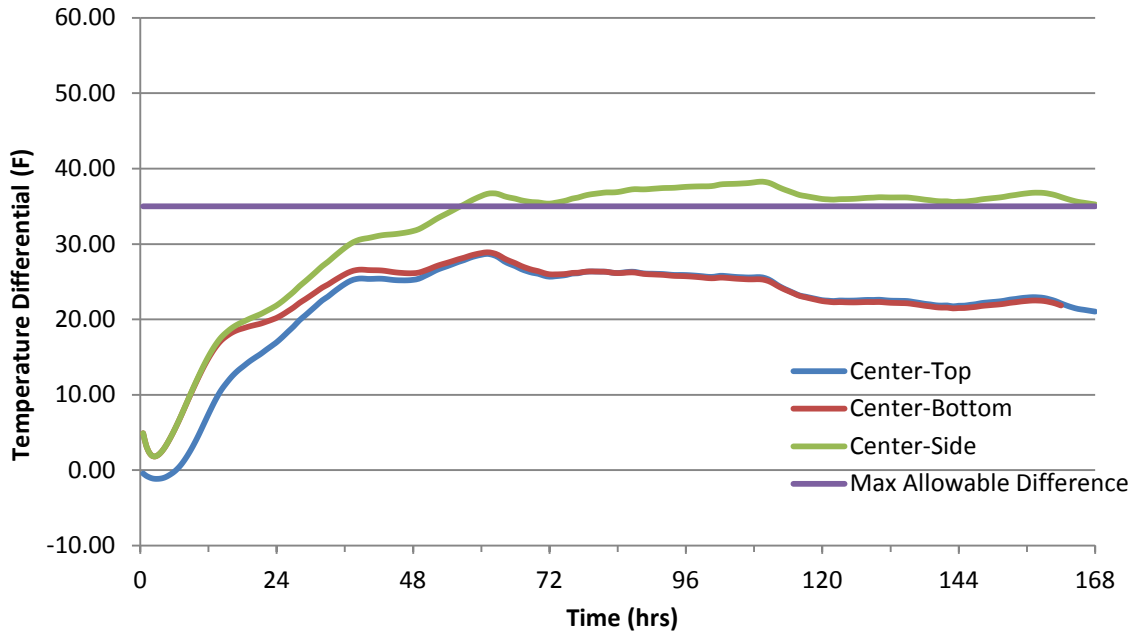


Figure 7-35: Trial 4 maximum temperature differentials

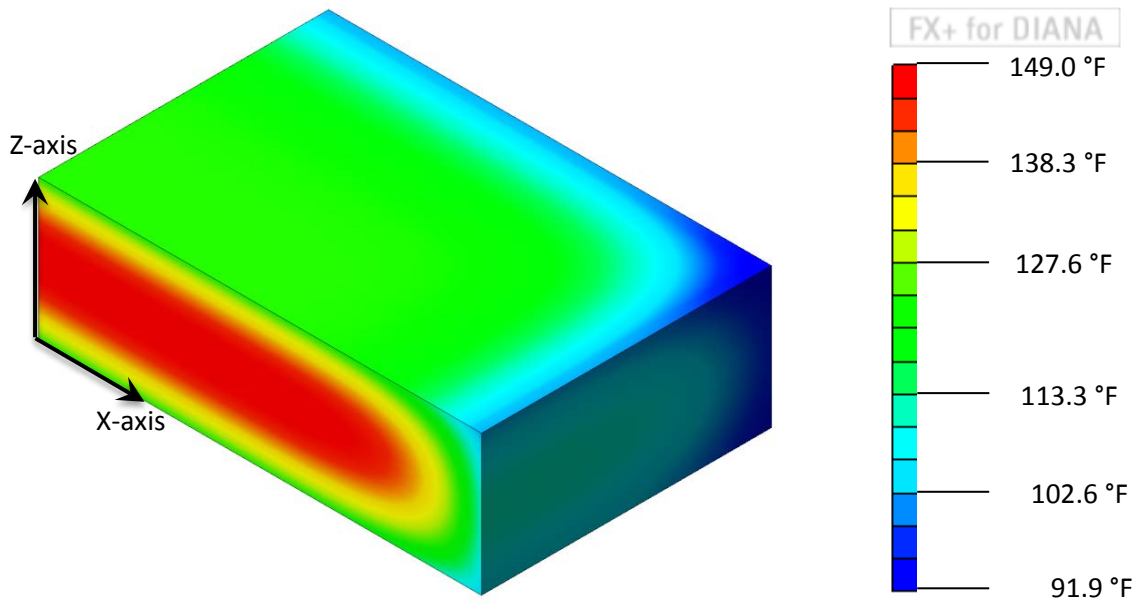


Figure 7-36: Trial 4 temperature profile at 109 hours

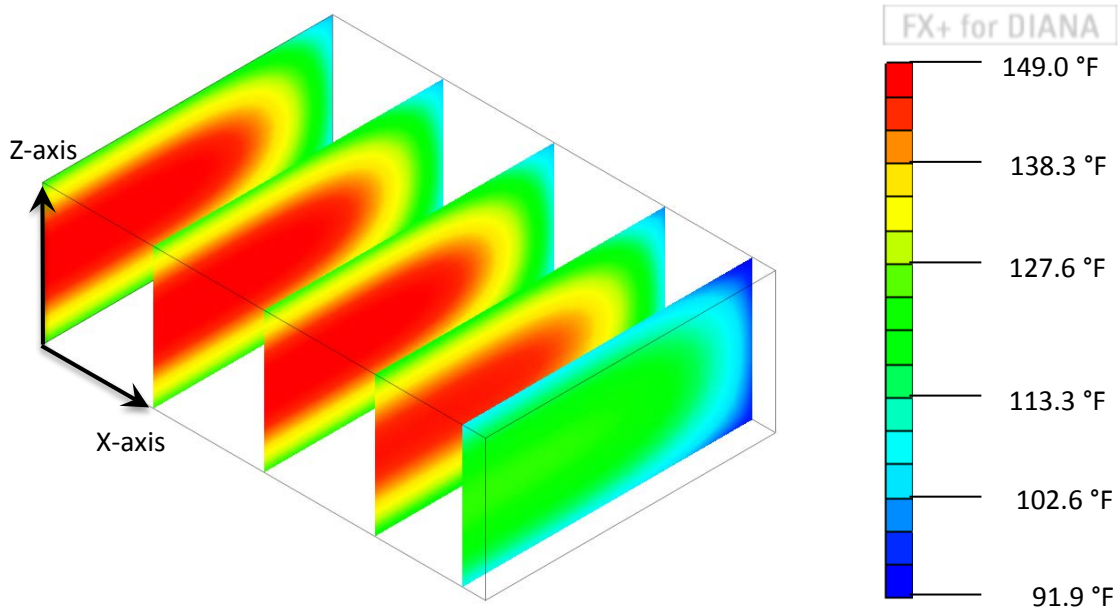


Figure 7-37: Trial 4 sliced temperature profile at 109 hours

7.5.2 Structural Analysis Results

The structural results in Figure 7-38 through 7-42 show the cracking index throughout the concrete footing at specific times as well as over the full 168 hour analysis period. The cracking index was calculated by the comparison of the principal stress versus the tensile strength of the concrete, as seen in the graphs in Chapter 6.

Figures 7-38 and 7-39 show the cracking index for the vertical and horizontal profiles, respectively, at the time of the peak temperature (42 hours) and the time of the maximum temperature differential (109 hours). Like Trial 3, the cracking index between these two slightly differs, where it is slightly worse at the time of peak temperature (56 hours). These figures show that the cracking index is still less than 1 for more than one node in each profile but only at the time of the peak temperature. Through linear interpolation it is found that at the time of the maximum temperature difference, the cracking index crosses 1 right at the node on the top surface in the vertical profile and at a distance only 0.17 ft below

the surface in the horizontal profile. This value is significantly lower than what was seen in the original Wilmington case study and Trial 1 and 2.

Figure 7-40 shows the cracking index of the previously chosen key locations in Trial 4 over time. Unlike the previous trials, the cracking index at these points in Trial 4 re-crosses the limit of 1 prior to the end of the analysis at 168 hours. The top edge remains above a cracking index of 1 throughout the entire analysis.

Figure 7-41 shows the 3-D isoparametric view and Figure 7-42 shows the plan view of the cracking index contours below 1 on Trial 4 at the time of maximum temperature differential (109 hours). These figures show that the extent of the low cracking index in Trial 4 is significantly less extensive than any of the other 3 trials. This indicates a very low probability of cracking at this footing size.

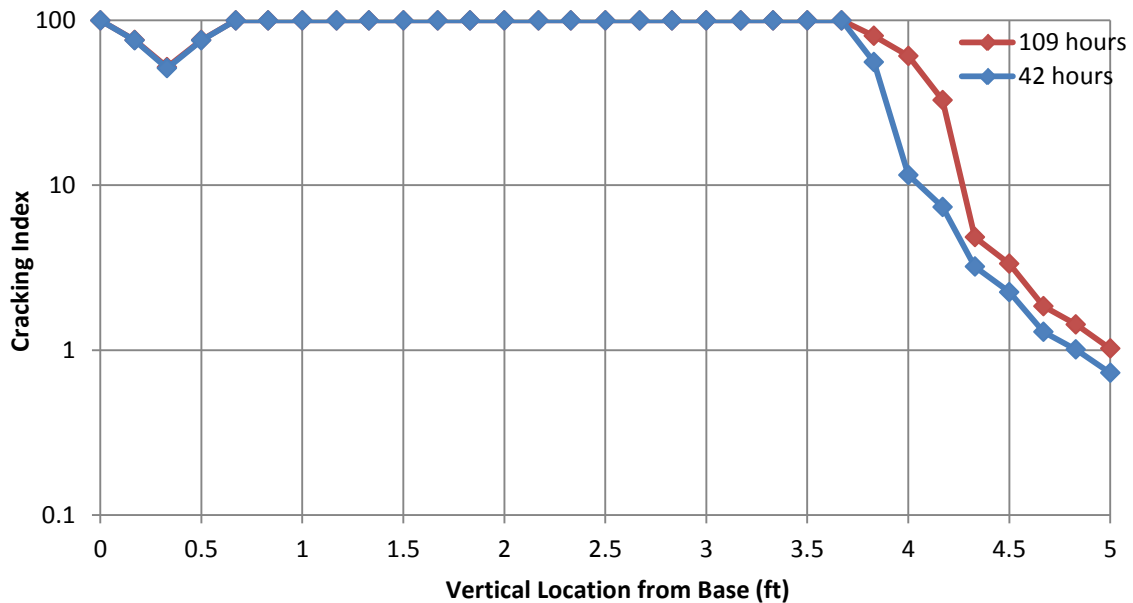


Figure 7-38: Trial 4 vertical profile cracking index at 42 and 109 hours

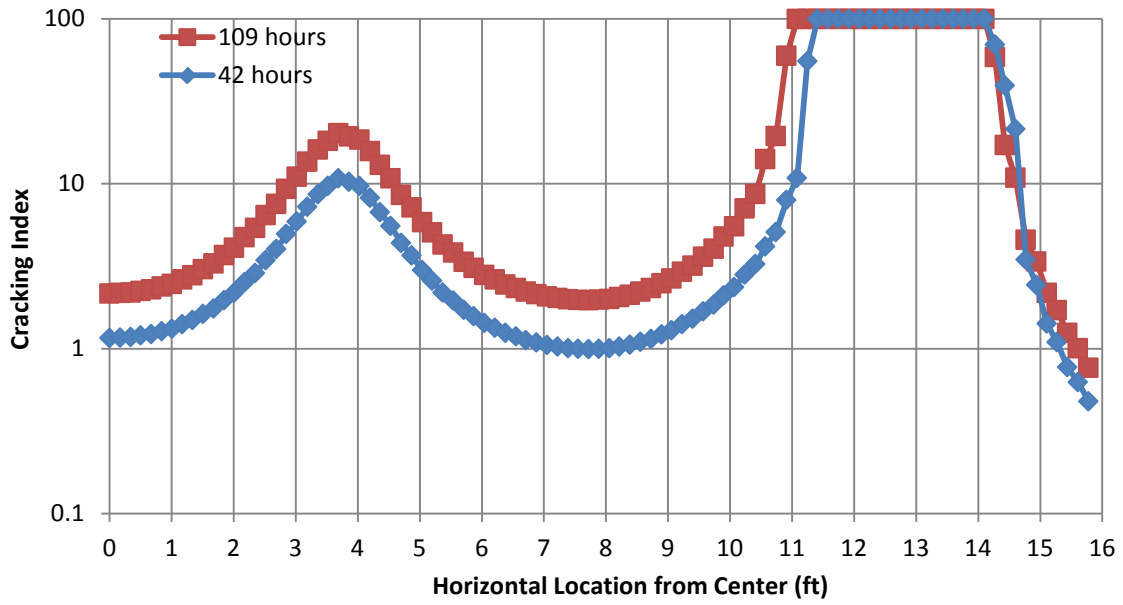


Figure 7-39: Trial 4 horizontal profile cracking index at 42 and 109 hours

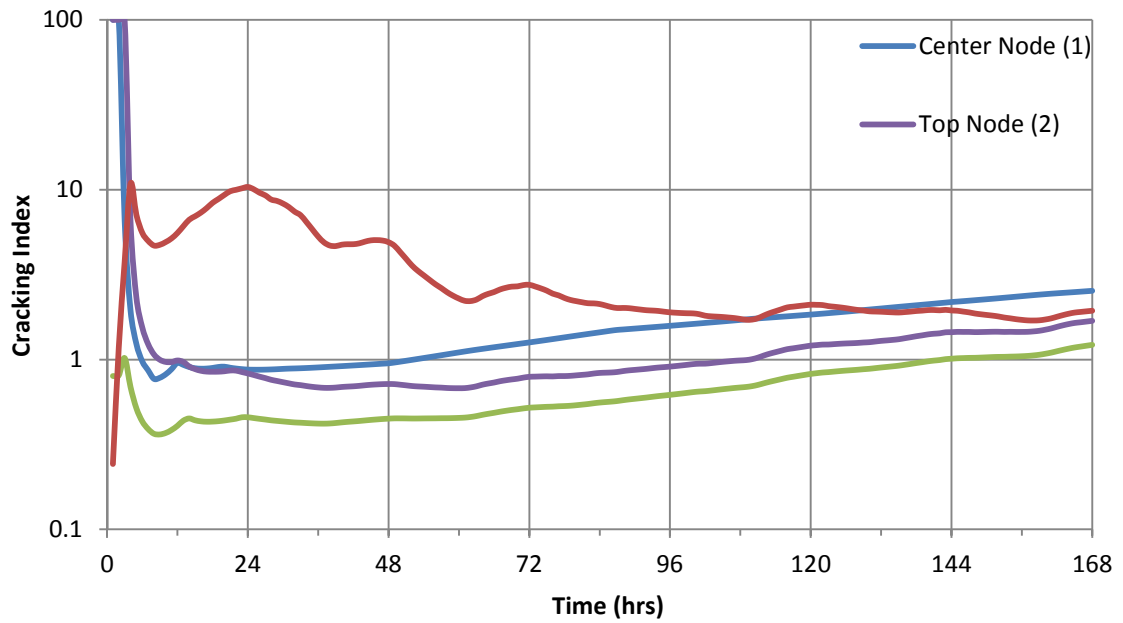


Figure 7-40: Trial 4 nodal cracking index vs time

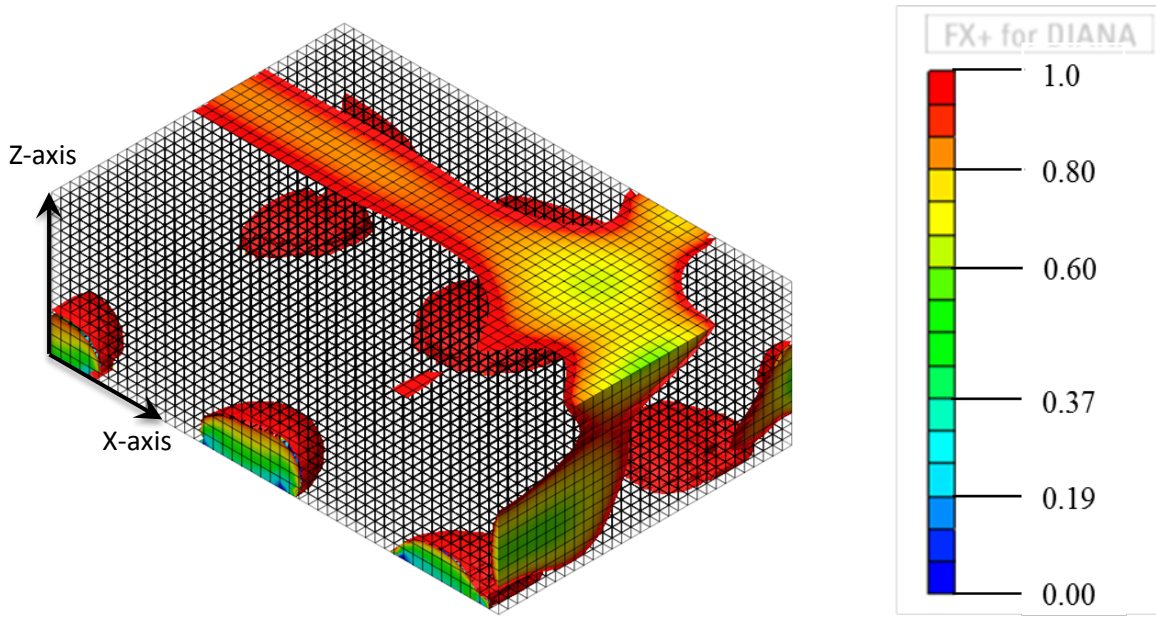


Figure 7-41: Trial 4 cracking index contours at 109 hours isoparametric view

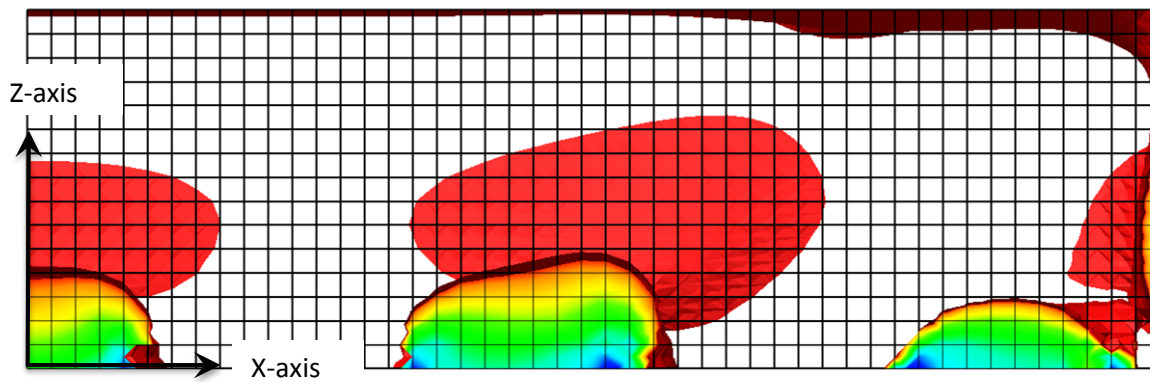


Figure 7-42: Trial 4 cracking index contours at 109 hours profile view

CHAPTER 8

DISCUSSION OF RESULTS

8.1 Introduction

In this chapter, the analysis results presented in Chapter 6 and the experimental results and site visit observations presented in Chapter 3 are discussed. Specifically, the results of the experimental concrete block as well as the results from the Oak Island, Sunset Island, and Wilmington Bypass Bridges will be discussed and also related to the actual site observations found in Chapter 3 and the experimental observations of the laboratory experiment from Chapter 5. Figures of the site observations can also be found in Appendix B for reference. The model validation, the cracking potential of the case studies and the lab experiment, and the idea of mass concrete versus “massive” mass concrete will be discussed using the results of the parametric study from Chapter 7.

8.2 Model Validation

The laboratory block experiment was performed to verify the finite element model created in DIANA. Based on the results from the thermal model, it can be concluded that the model created in DIANA accurately predicted the heat production and thermal distribution created from hydrating cement. The good performance of the overall model also validates the use of the heat of hydration empirical model (Eqs. 4-1 through 4-7) as it correctly modeled the rate of heat production as well as the concrete’s maximum temperature. The model was able to accurately capture all of the temperatures within the concrete, except for the surface temperature rise due to the exposure to direct sunlight. The addition of a boundary condition to model the effect of direct sunlight would lead to increased accuracy in the modeling of the concrete temperatures.

The Oak Island and Sunset Beach Bridge footings are very similar in size: Oak Island was a little bit longer whereas Sunset Beach was a bit wider. Both also had the same depth. This resulted in very similar temperature distributions, maximum temperatures, and

maximum temperature differentials. Only Oak Island, however, had temperature data that could be used to validate the thermal model, although the exact locations of the temperature sensors were unknown. The results from the Oak Island case study closely matched the measured temperatures from the field data, although they were not as accurate as in the experimental block study. Better, more accurate information and records about the footing construction and the concrete used would result in more accurate predictions of the temperature distribution over time in the footings. In addition, separating the footing into lifts in the model at the time of the pour would help model the time it took to pour the concrete instead of assuming it to be cast at a single time period. This would also help to create a more accurate model.

8.3 Cracking Potential

The block experiment was also observed for its cracking potential. The temperature results, both the experimental and the model, indicate that the temperature differential in the concrete exceeded the typical limit of 35 °F. This was mainly found to occur between the center and the top surface, and is caused by the lack of insulation on the top concrete surface. Along with these temperature results, the structural analysis results show locations along the block where the cracking index is below the limit of 1. This is mostly restricted to the outermost nodes though. In spite of the temperature differentials and the cracking index, there was no significant cracking found in the concrete block at the laboratory. This lead to the conclusion that the low cracking index found only at the surface indicates a low potential for cracking, and will only result in small surface cracks, if any.

Both the Oak Island and the Sunset Beach case study results showed the maximum temperature differential surpassing the typical limit of 35 °F as well, although this was mainly limited to the center to side differential. Oak Island was found to have slightly larger temperature differentials than Sunset Beach though. In addition, as with the block experiment, the structural results for both case studies show locations along the footings where the cracking index is below the limit of 1, but these were mostly limited to the

outermost nodes. Higher concentrations of cracking potential were found at the top edges near the middle edge of the concrete footing, as well. As these results are similar to that found in the block experiment, it would indicate that there is a low potential for thermal cracking to occur. Any cracking that might occur would likely only be minor superficial surface cracks.

No cracking potential calculated in the finite element model was found to correlate with the two large cracks extending across the middle of the Oak Island footing as there were no low cracking index values in that area. It is much more likely that these cracks are the results of other structural actions. Further analysis would be required. It was also found that there was no significant cracking potential in the areas where many vertical cracks were observed along the front face of the footing. It is much more likely that those cracks are a result of the corrugated sheet piling embedded close to the front face. It is likely that the close proximity of the steel to the surface amplified the effect of local stress concentrations causing a greater potential for cracking. The Sunset Beach footing was also observed to have some cracking along the footing's top surface. These cracks were actually measured to be larger than many of the cracks observed on the Oak Island footing. There is no indication from the models, however, that Sunset Beach would have more severe cracking than Oak Island. It is possible that minor surface cracks over time, after being left untreated, resulted in wider cracks.

The Wilmington case studies were found to have a much higher cracking potential than the other case studies, even without early formwork and insulation removal. In both cases, the maximum temperature differential significantly surpassed the typical maximum limit of 35 °F, where the case study with early form and insulation removal led to a maximum differential of almost 100 °F on all faces of the footing. Similar to the previous case studies, the structural results from both case studies show locations along the footings where the cracking index is below the limit of 1. In the Wilmington case studies, however, the cracking index is below 1 well beyond the outermost nodes, especially in the case with

early formwork removal. The case with early form removal has very low cracking indices, which extend along all faces of the footing. This correlates well with the cracking observed in the field, as extensive map cracking was observed on the top face of the footing. There were also a significant number of vertical cracks along all of the side faces of the footing. The bottom face of the footing could not be observed for cracks. When observing the results of the study when the formwork and insulation remained on, it can be observed that the cracking extent and potential is greatly reduced. This then leads to the conclusion that much of the cracking found on the Wilmington footing is a result of not following the construction guidelines by prematurely removing the formwork and insulation.

8.4 Schmidt Method vs Finite Element Model

A sample model of the predicted early age temperature rise within the concrete completed by the contractor was available for the Wilmington Bypass footing. This prediction was completed using Schmidt's Model with 4 layers of insulation, an effective cement weight of 362 kg/m^3 , a diffusivity of $0.113 \text{ M}^2/\text{day}$ and a time interval of 0.5 days. An assumed ambient temperature of $88 \text{ }^\circ\text{F}$ was used for the summer model. The predicted results are presented in Figure 8-1 and Figure 8-2. A comparison of the Schmidt model results versus the FE model results is presented in Figure 8-3 and Figure 8-4. As was found by Riding et al. (2006), the temperatures modeled in Schmidt's model underestimated the maximum temperature and overestimated the time to maximum temperature compared to what was found in the finite element model presented in Section 6.5.1. The maximum temperature found in Schmidt's model was $157.1 \text{ }^\circ\text{F}$ whereas the maximum temperature found in the finite element model was $171.8 \text{ }^\circ\text{F}$, an underestimation of 9%. The time to maximum temperature found in Schmidt's model was 14 days (336 hours) whereas the time to maximum temperature found in the finite element model was around 120 hours, and overestimation of 180%. In addition, Figure 8-4 shows that the finite element predicted maximum temperature differential is much greater than the typical limit of $35 \text{ }^\circ\text{F}$, whereas the maximum temperature differential predicted by the Schmidt model does not even reach

this limit. This could be partially due to the use of more insulation, but Schmidt's model is far from matching the finite element predictions. The errors found in the Schmidt models can be significant though, and care should be taken whenever these are being used as the temperature predictions for a mass concrete element.

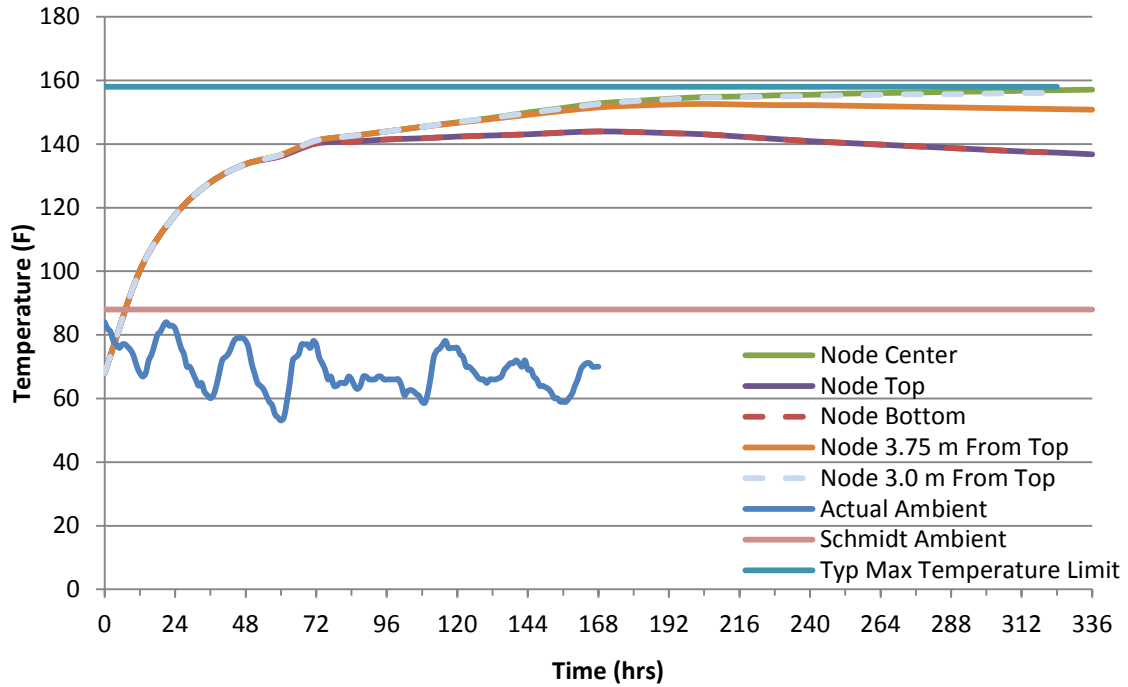


Figure 8-1: Wilmington Schmidt model temperature results

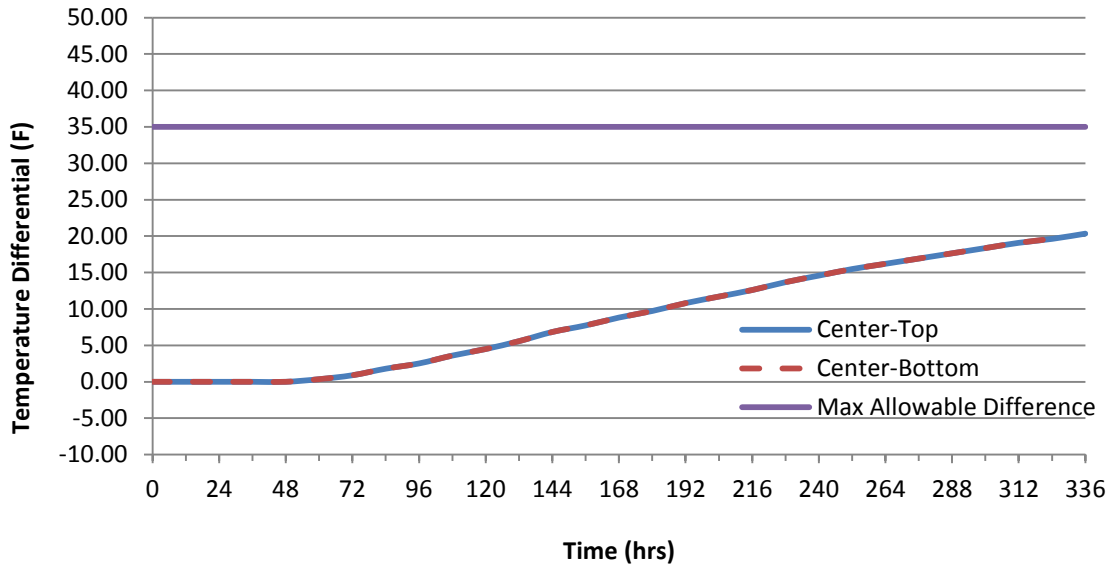


Figure 8-2: Wilmington Schmidt model temperature differentials

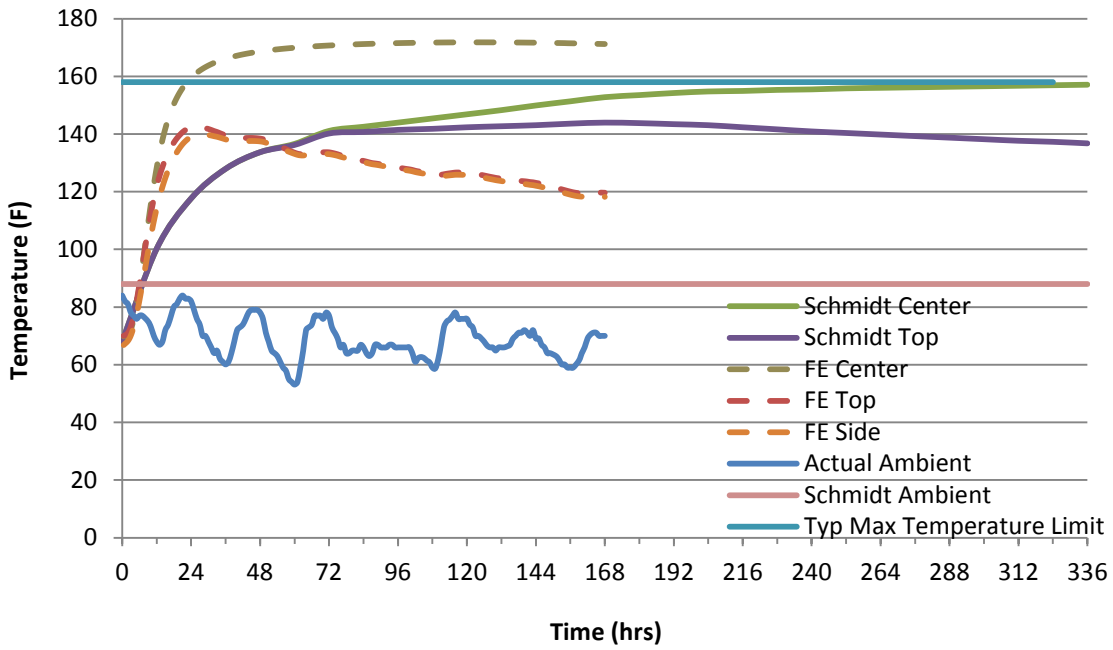


Figure 8-3: Wilmington Schmidt model vs FE Model temperature comparison

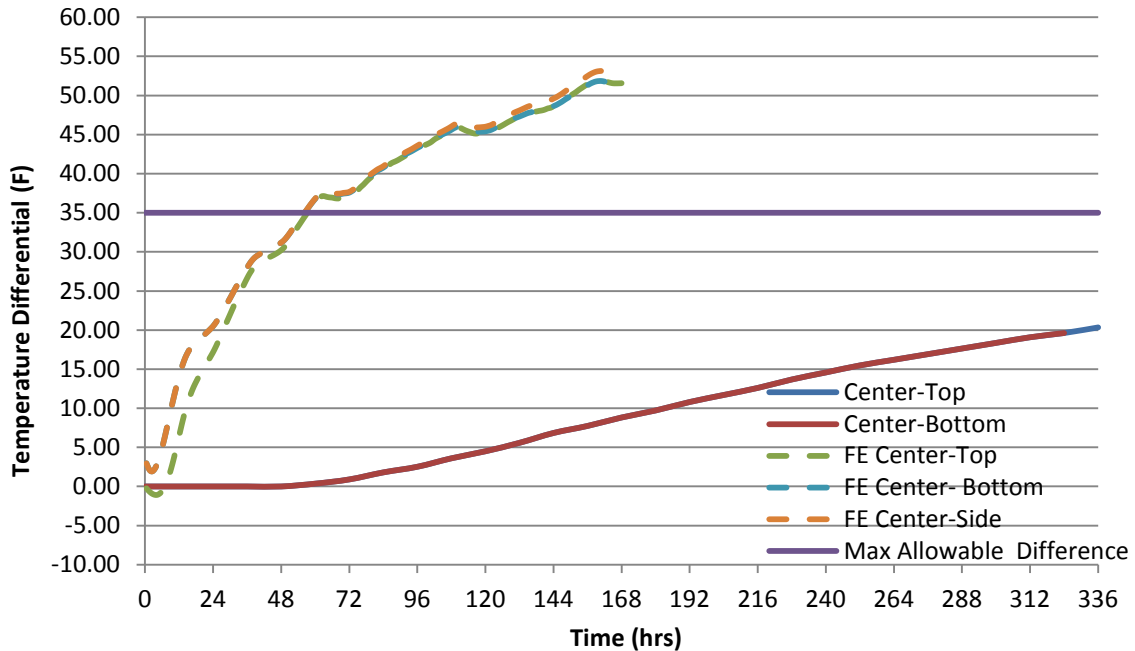


Figure 8-4: Wilmington Schmidt model vs FE Model differential comparison

8.5 Mass Concrete vs Massive Mass Concrete

The Wilmington Bypass footing was significantly larger than the other case studies this project evaluated. This resulted in higher maximum temperatures as well as higher temperature differentials. Even the Wilmington Bypass footing case study without the formwork and insulation removal reached a maximum temperature differential value of 52 °F, significantly larger than the 35 °F limit. In addition to this, the cracking index of this footing with no formwork or insulation removal was more extensive than what was seen in the Oak Island and Sunset Beach case studies.

As a result of these observations a dimensional parametric study was conducted. A summary of the results is found in Figures 8-5 through 8-8. Figure 8-5 shows the maximum temperature versus the minimum dimension for the parametric study as well as for Oak Island and Sunset Beach. It should be noted that the maximum temperature in the parametric

study is never as low as the Oak Island and Sunset Beach case studies, or below the typical maximum temperature limit, due to the mix design that was used. Wilmington and the parametric study used a different concrete mix design than Oak Island and Sunset Beach. Figure 8-6 shows the maximum temperature differential versus the minimum dimension. It should be noted that the graph shows the center to side maximum as well as the center to top maximum. Figures 8-7 and 8-8 show the cracking index below one at the times of maximum temperature differential and peak temperature, respectively.

In the first trial with a minimum dimension of 12.5 feet, the results were very similar to the original Wilmington Bypass analysis. As seen in Figures 8-5 and 8-6, the maximum temperature differential and the peak temperature of Trial 1 is very close to the original analysis. The extent of low cracking indexes, and thus the extent of high tensile stresses, was also found to be close to identical. In the second trial with a minimum dimension of 10 feet, the results were also somewhat similar to the Wilmington analysis, however noticeable differences were present. In the thermal results the maximum temperature differential and the peak temperature of Trial 2 were still similar to the original and Trial 1, only a little lower. It should also be noted that in this trial the difference between the center-top and center-side differentials was much bigger. The extent of low cracking indexes in Trial 2 was not as severe as Trial 1, but it was still determined to have a higher potential for thermal cracking. In the third trial with a minimum dimension of 7.5 feet, there was a distinct difference in the results compared to Trial 1, Trial 2, and the original Wilmington Bypass analysis. The maximum temperature differential and the peak temperature decrease a noticeable amount with this dimension. The maximum differential was still above the typical limit of 35 °F, however the difference between the center and top was very near this limit. It is possible that with a more current mix design this differential would have been much closer to the typical differential limit. The extent of low cracking indexes in Trial 3's structural results was also unlike the previous trial results. Instead, it resembled the structural results from the Oak Island case study, which was found to have a low potential for thermal cracking. In the final trial, Trial 4, with a minimum dimension of 5 feet, the results did not resemble the

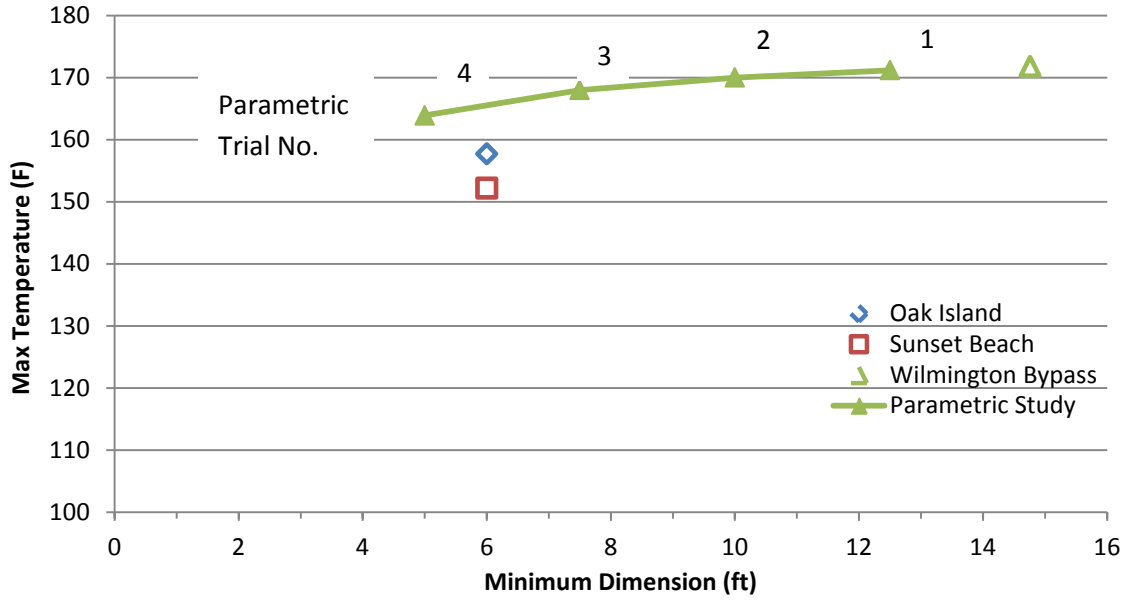


Figure 8-5: Maximum temperature comparison for parametric study

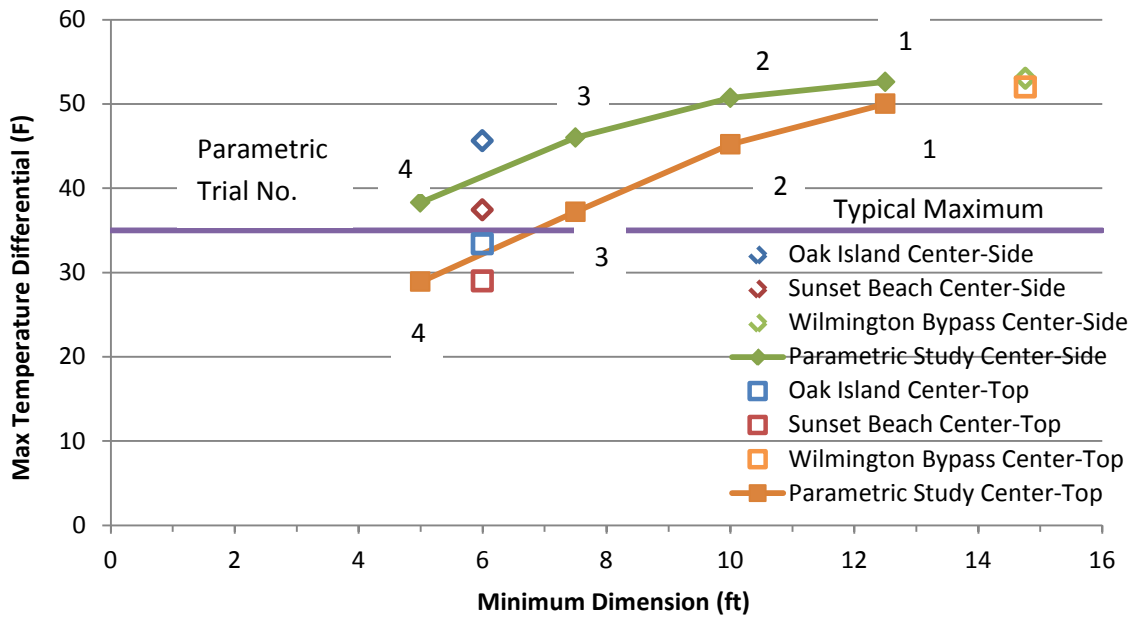


Figure 8-6: Maximum temperature comparison for parametric study

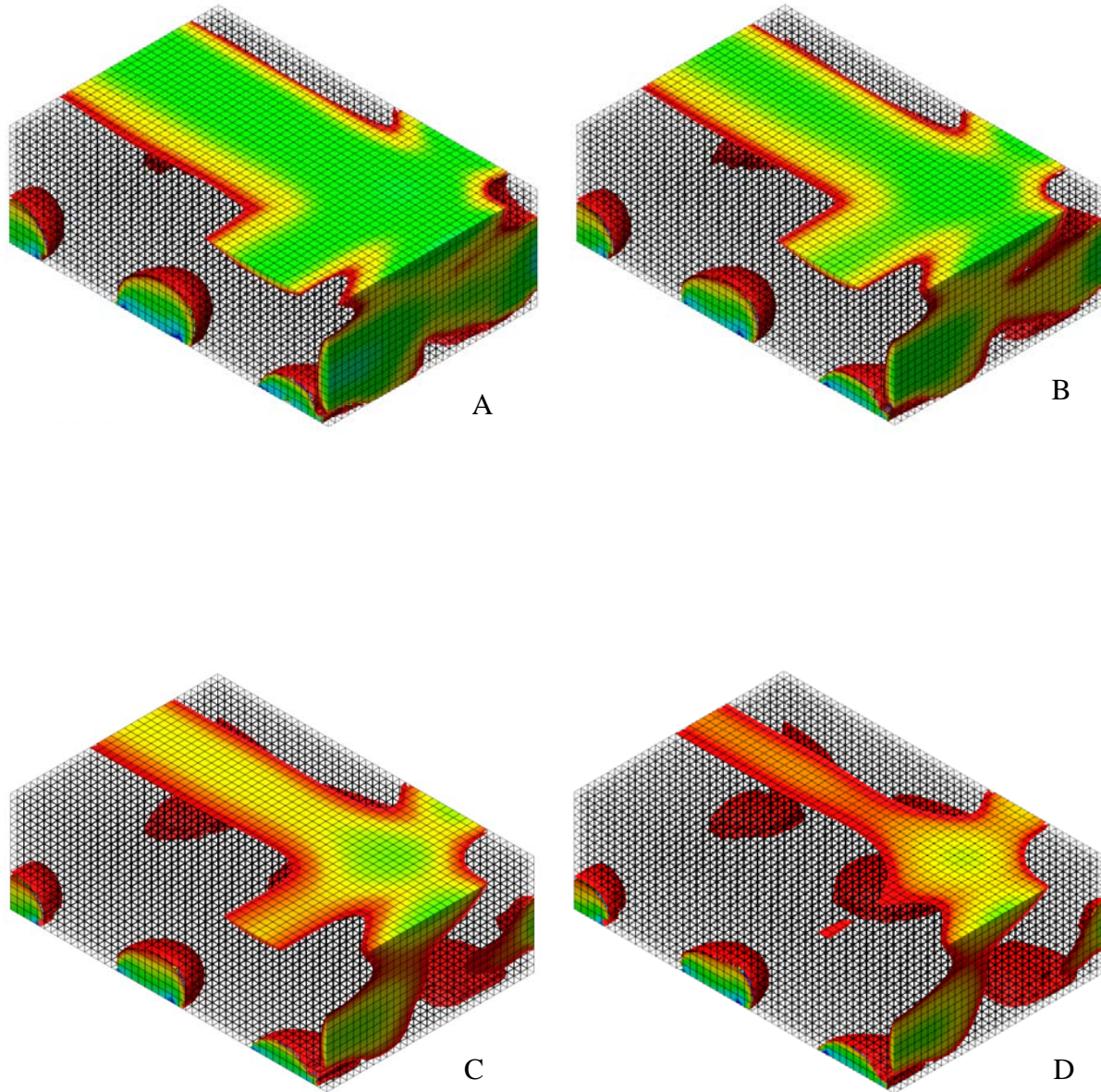


Figure 8-7: Cracking index of Trials 1-4 at time of maximum difference

- A) Trial 1 – Min dimension of 12.5 feet at 160 hours
- B) Trial 2 – Min dimension of 10.0 feet at 160 hours
- C) Trial 3 – Min dimension of 7.5 feet at 158 hours
- D) Trial 4 – Min dimension of 5.0 feet at 109 hours

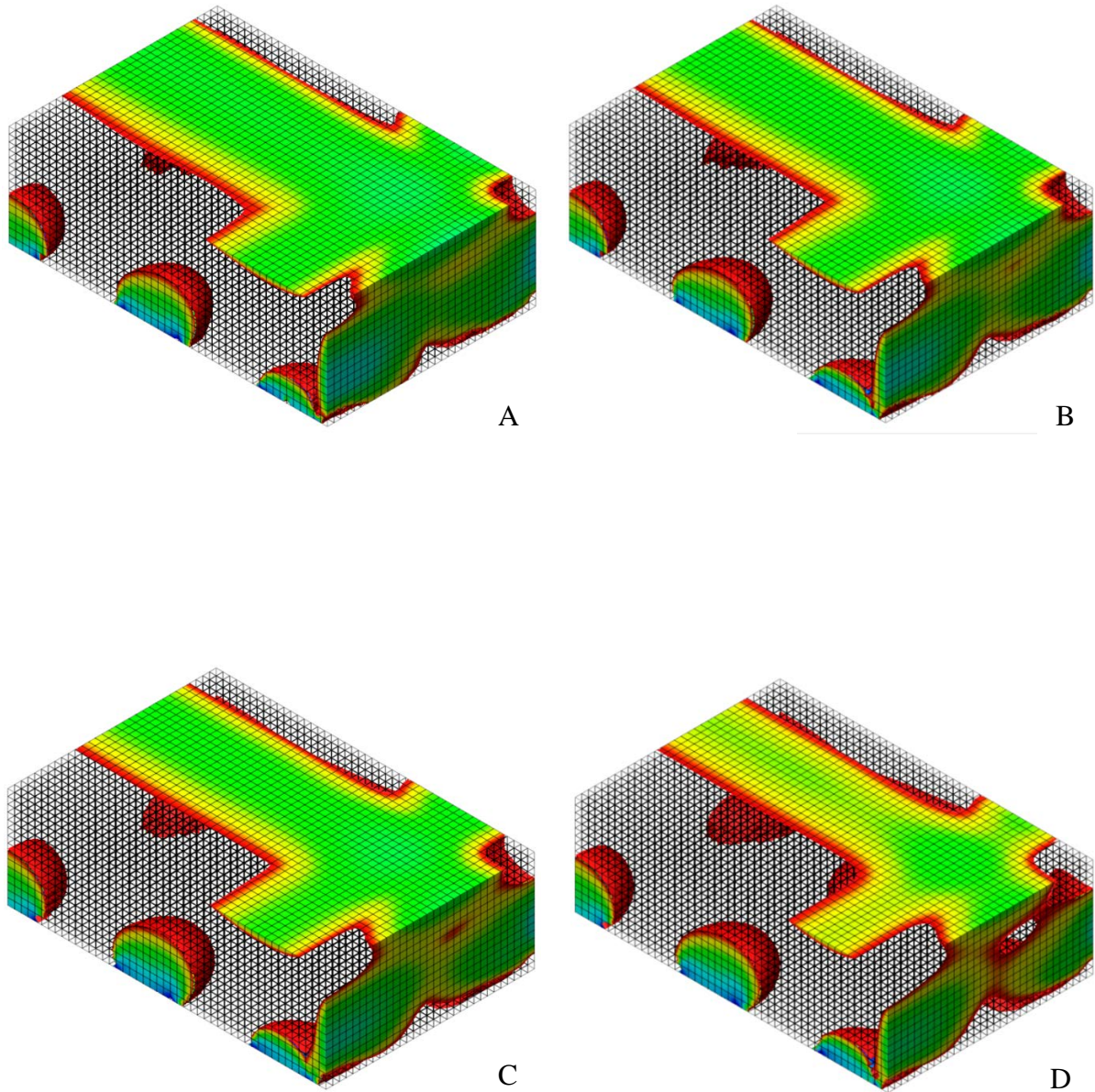


Figure 8-8: Cracking index of Trials 1-4 at time of peak temperature

A) Trial 1 – Min dimension of 12.5 feet at 99 hours

B) Trial 2 – Min dimension of 10.0 feet at 76 hours

C) Trial 3 – Min dimension of 7.5 feet at 56 hours

D) Trial 4 – Min dimension of 5.0 feet at 42 hours

Wilmington results. The maximum peak temperature was much lower, almost to the typical allowable limit of 158 °F, and the maximum differential was right at the typical allowable limit, although the center to top differential was below the limit. The extent of low cracking indexes in Trial 4 was also significantly less and almost non-existent. It had a very low potential for cracking.

These results show that when the more reasonably sized mass concrete elements of Oak Island, Sunset Beach, Trial 3 and Trial 4 follow the thermal plans set up in most specifications, the footings were found to have a low potential for significant thermal cracking. When very large mass concrete elements, such as the Wilmington Bypass footing and Trial 1, follow the thermal plans set up in most specifications, the footings were found to still have a higher potential for significant cracking. From the observations of this parametric study, it may be concluded that a minimum dimension limit of 10 feet should be considered as “massive” mass concrete beyond which further assessment and measures are required to control the high likelihood of thermal cracking. Although the trial with a minimum dimension of 10 feet was not as severe as Trial 1 or the original Wilmington Bypass footing, the choice of this dimension results in a conservative limit for the parameters considered in this study which are representative of NCDOT practices.

CHAPTER 9 CONCLUSIONS AND RECOMMENDATIONS

9.1 Key Findings

A finite element model was developed using the TNO DIANA commercial software to model the heat generation and temperature distribution created during concrete early age hydration. The predicted temperatures from the block experiment and the Oak Island case study models were compared to actual measured temperatures to validate the accuracy of the developed model. Analysis of the results from these models and their comparisons to the measured data resulted in the following findings:

- ConcreteWorks was determined to be unsuitable for this research due to its inability to perform 3D stress analysis, the lack of access to stress information, the inability to choose boundary conditions, and various errors that occurred during the use of the program.
- The finite element model created in TNO DIANA accurately predicts the heat production and subsequent temperature changes during early age concrete hydration.
- The empirical model originally developed by Schindler and Folliard (2005), and later improved by Poole (2007) and Riding (2012), is a good replacement for modeling the early age heat of hydration development when isothermal calorimetry tests are not readily available.
- The addition of a boundary condition to model the effect of direct sunlight would lead to increased accuracy in the modeling of concrete temperatures along the surface.
- Better records should be kept concerning the footing construction and the properties of the concrete used in order to achieve more accurate predictions of the temperature distribution over time in the footings.

The thermal and structural analysis models were implemented on the experimental concrete block as well as the Oak Island, Sunset Island, and Wilmington Bypass case studies

to assess them for their thermal cracking potential. The results were then related to the field observations. The outcomes of these studies resulted in the following findings:

- The biggest temperature differentials were found to occur between the center and the farthest side, even though typically temperatures are measured at the center and closest surface.
- Reasonably sized mass concrete structures, such as the Oak Island and the Sunset Beach footings, that follow the typical control plans do not have a high likelihood of significant thermal cracking. Small surface cracks are possible, however, especially near the top side edge of the concrete where high concentrations of stresses were found.
- The two large cracks found on the top surface of the Oak Island footing likely were not caused by mass concrete thermal effects, as is shown in the thermal analysis results. Instead, they are likely the result of another structural action. Further analysis would be required.
- “Massive” mass concrete footings, such as the Wilmington Bypass footing, have a much higher risk of significant thermal cracking even when the typical NCDOT control plans are followed. More care should be taken in controlling the temperatures in such “massive” mass concrete structures.
- When temperature control plans are not followed extreme thermal gradients will form, creating a very high cracking potential and increasing the likelihood of significant thermal cracking.

A dimensional parametric study was also conducted based on the Wilmington Bypass footing to study the effect of size on mass concrete and understand what may be considered “massive” mass concrete versus typical mass concrete. The outcomes of this study resulted in the following findings:

- The trials with minimum dimensions of 7.5 feet and 5 feet behaved similarly to what was seen in the Oak Island and Sunset Beach, or “typical mass concrete”, case studies.
- The trials with minimum dimensions of 12.5 feet and 10 feet behaved similarly to what was seen in the Wilmington Bypass, or “massive” mass concrete, case study.
- It is recommended that an element with a minimum dimension of 10 feet should be considered “massive” mass concrete within the parameters and conditions considered in the parametric study. Special assessment and measures are required in the design and construction of such elements.

The typical NCDOT mass concrete standards were compared to similar standards and specifications from other States and government organizations. The following findings were found based on the review of these specifications:

- A maximum temperature differential of 35 °F is used in all specifications and standards, including North Carolina’s.
- Typical minimum dimensions for all specifications and standards range from 3 ft to 6 ft. Based on the results from this research, a minimum dimension of 6 ft is reasonable, although specifying 5 ft would reduce the likelihood of thermal cracking further.
- The use of silica fume may not be necessary.
- The North Carolina specifications do not define a maximum allowable temperature limit after placement.
- North Carolina does not require a minimum curing period before formwork removal, unlike Texas, Virginia, and ACI 301-10.
- North Carolina requires no immediate remedial actions if the temperature differential limit is exceeded unlike Virginia, Florida, and South Carolina. Only the revision of the temperature control plan for any remaining placements is required.

- Virginia was found to have the most complete mass concrete specifications, with guidelines covering materials used, contractor submittals, concrete placement, concrete curing and protection, as well as remedial measures.
- As discussed by Riding et al. (2006), the typical standard of using Schmidt's Method to predict the temperatures during early age hydration of mass concrete was found to give a poor prediction of the maximum temperature of the concrete when ACI's generic adiabatic temperature charts, found in Chapter 4 of ACI 207.2R-07, were used.

9.2 Recommendations for Implementation

Based on the findings of this research, the following additions and revisions to current NCDOT mass concrete specifications are recommended. The recommendations have been divided into two categories: typical mass concrete and special cases. The typical mass concrete recommendations are recommendations that should be implemented for all mass concrete elements. Special case recommendations are recommendations that require more in-depth calculations, analysis, and/or monitoring and should be considered for more extreme cases of mass concrete, specifically when mass concrete elements are significantly larger than the mass concrete size limit. This "massive" mass concrete should be defined as a structure with a minimum dimension of 10 feet or greater, based on this research, until future research provides a better definition. The recommendations are as follows:

1) Typical Mass Concrete Recommendations

- i. A maximum allowable temperature after placement of 158 °F should be specified, as given by ACI 301-10.
- ii. Concrete should remain covered and monitored until the difference between the internal concrete temperature and the average daily ambient temperature, not just the concrete surface, is below 35 °F, but in no case should the concrete be cured and protected for less than 7 days after placement.

- iii. The forms may be stripped early when the concrete strength is high enough (as determined by the maturity curves or match-cast cylinders) to withstand the anticipated thermal gradient between the core temperature and the 48-hour average air temperature, or as directed by the Engineer. The contractor should use match-cured cylinders based on the temperature of the coolest surface thermocouple or a maturity curve based on the equivalent age method from ASTM C 1074. In no event will form stripping be allowed before the surface concrete reaches at least 80% of its design strength. After form stripping, concrete shall be protected from freezing temperatures for 48 hours by the use of insulating blankets or other methods approved by the Engineer.
- iv. Consider material specifications allowing the use of granulated slag replacement of cement by 50 – 70% and/or a ternary mix of granulated slag, class f fly ash, and Portland cement, where there is at least 20% fly ash by weight and 40% portland cement by weight. The use of class f fly ash replacement of cement by 30% is also allowed.
- v. Require temperature sensors at the surface nearest to the center of mass of the concrete as well as at the farthest surface from the center and at the center of mass.
- vi. As part of the contractor's submittal of the concrete protection plan, the Contractor shall provide an analysis of the anticipated range of peak temperatures, maximum temperature gradients, time to peak temperature, as well as the time it takes to cool to the allowable temperature differential in the mass concrete elements using his proposed mix design, casting procedures, and materials. The following methods can be used:
 - c) Schmidt method with the measured adiabatic temperature curves from a semi-adiabatic calorimetry test.
 - d) An equivalent method as approved by the Engineer.

If Schmidt's method is used with ACI's generic adiabatic temperature curves care should be taken by the Engineer in recognition of the errors that this method produces.

- vii. Require immediate remedial actions from the contractor if the temperature differentials are exceeded:
 - a) Immediate action to control the differential on the concrete element being cast.
 - b) Revise the thermal plan to ensure future mass concrete pours meet the temperature limits.
 - c) Require crack sealing by way of epoxy injection for crack widths greater than 0.006 in, as found in the Virginia DOT specifications.
 - d) The Engineer may, at his sole discretion, direct that all or a portion of the damaged or unacceptable concrete be removed and replaced based on extent of damage.

At no point shall the contract proceed until a revised thermal plan is approved by the Engineer.

- viii. Require construction processes and materials used in the field to be documented and preserve these records. This would help with any future modeling if necessary.
- 2) Special Case ("massive" mass concrete) Recommendations
- i. As part of the contractor's submittal of the concrete protection plan (as under section vi in typical mass concrete), require the Contractor to submit temperature predictions using more precise methods. Specifically, the use of the Schmidt method with the generic ACI adiabatic temperature curves may not be used. Finite element methods are the preferred analysis technique, but Schmidt's method using the measured adiabatic temperature curves may also be used.

- ii. Require the cementitious constituent material properties (chemical makeup) and concrete thermal properties, including the coefficient of thermal expansion, thermal diffusivity, and heat capacity, to be submitted along with the concrete mix design.

9.3 Future Research

The following topics are recommended for future research:

- Analyze the North Carolina footings, especially the Oak Island footing, for possible structural causes for the observed cracking.
- Assess the feasibility of using precast stay-in-place forms (see Figure 8-1) to ease construction and to help mitigate the likelihood of thermal cracking. Cracking mitigation would come from the insulating effect of the precast concrete controlling temperature differentials as well its ability to keep cracking from occurring on the concrete footing's exposed surfaces. This construction method would also be consistent with accelerated bridge construction (ABC) practices by increasing the rate at which the mass concrete footings could be placed.

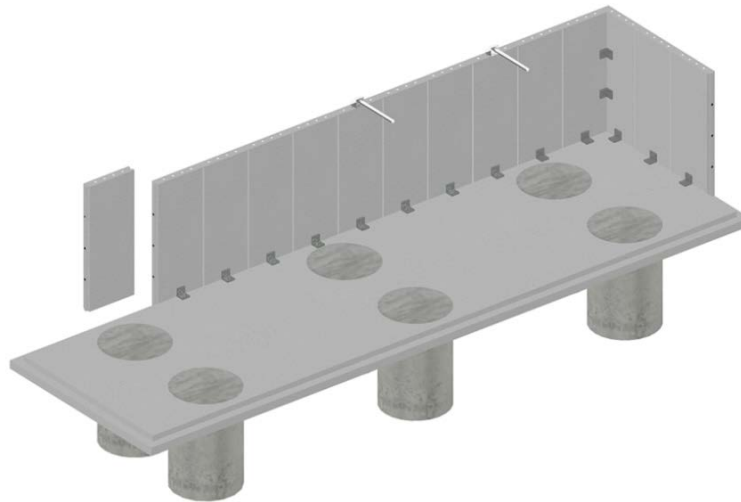


Figure 9-1: Sample model of precast stay-in-place forms

- Assess the feasibility of using Riding et al.'s (2012) empirical model to model the adiabatic temperature rise in Schmidt's model. A generalized excel spreadsheet could then be created for general use among NCDOT projects.
- Analyze the effect of thermal shock from steel reinforcement and other embedded steel at the time of casting, such as sheet piling, on the probability of cracking.
- Investigate the potential benefits of using less retarder between lifts during mass concrete construction in an attempt to reduce the maximum core temperature, and consequently the temperature differential.

LIST OF REFERENCES

- ACI Committee 207. (2005). *Guide to Mass Concrete (ACI 207.1R-05)*. Farmington Hill, MI: American Concrete Institute.
- ACI Committee 207. (2007). *Report on Thermal and volume Change Effects on Cracking of Mass Concrete (ACI 207.2R-07)*. Farmington Hill, MI: American Concrete Institute.
- ACI Committee 207. (2005). *Cooling and Insulating Systems for Mass Concrete (ACI 207.4R-05)*. Farmington Hill, MI: American Concrete Institute.
- ACI Committee 301. (2010). *Specifications for Structural Concrete (ACI 301-10)*. Farmington Hill, MI: American Concrete Institute.
- ASTM C 39, (2011). *Standard Test Method for Compressive Strength of Cylinder Concrete Specimens*. West Conshoocken, PA: ASTM International.
- ASTM C 192, (2007). *Standard Practice for Making and Curing Concrete Test Specimens in the Laboratory*. West Conshoocken, PA: ASTM International.
- ASTM C 469, (2010). *Standard Test Method for Static Modulus of Elasticity and Poisson's Ratio of Concrete in Compression*. West Conshoocken, PA: ASTM International.
- ASTM C 490, (2011). *Standard Practice for Use of Apparatus for the Determination of Length Change of Hardened Cement Paste, Mortar, and Concrete*. West Conshoocken, PA: ASTM International.
- ASTM C 496, (2011). *Standard Test Method for Splitting Tensile Strength of Cylindrical Concrete Specimens*. West Conshoocken, PA: ASTM International.
- ASTM C 511, (2009). *Standard Specification for Mixing Rooms, Moist Cabinets, Moist Rooms and Water Storage Tanks Used in the Testing of Hydraulic Cements and Concretes*. West Conshoocken, PA: ASTM International.
- ASTM C 1074, (2011). *Standard Practice for Estimating Concrete Strength by the Maturity Method*. West Conshoocken, PA: ASTM International.
- Bentz, D., Peltz, M., Duran-Herrera, A., Valdez, P., and Juarez, C. (2011). "Thermal properties of high-volume fly ash mortars and concretes". *Journal of Building Physics*, Vol. 34, No. 3, 263–275.

- CESAR (2011). “CESAR-LCPCv5: Concrete at Early Ages Analysis”. Montreuil, France: itech. 15 January, 2012. <<http://www.itech-soft.com/cesar/>>
- ConcreteWorks (2005). “ConcreteWorks Version 2.0: User’s Manual”. Austin, Texas: Concrete Durability Center. 12 October, 2011. <<http://www.texasconcreteworks.com/>>
- Emanuel, J. H., and Hulsey, J. L. (1977). “Prediction of the Thermal Coefficient of Expansion of Concrete”. *ACI Journal*, Vol. 74, No. 4, 149–155.
- FEMMASSE (2013). “HEAT-MLS version 8.5: Computer program for the analysis of the thermal and mechanical behavior of hardening concrete USER MANUAL”. Sittard, the Netherlands: Femmasse. 16 January, 2012. <<http://www.femmasse.com/>>
- Ge, Z. (2005). *Predicting Temperature and Strength Development of the Field Concrete*. Dissertation. Iowa State University, Ames, Iowa.
- Gajda, J., and Vangeem, M. (2002). “Controlling Temperatures in Mass Concrete”. *Concrete International*, Vol. 24, No. 1, 58–62.
- Kim, Soo Geun. (2010). *Effect of heat generation from cement hydration on mass concrete placement*. MS Thesis. Iowa State University, Ames, Iowa. ProQuest Dissertations and Theses. Web. 30, May 2012.
- Lu, H. R., Swaddiwudhipong, S., and Wee, T. H. (2000). “Evaluation of Internal Restrained Strain in Concrete Members at Early Age”. *ACI Materials Journal*, Vol. 97, No. 5, 612–618.
- Mehta, P.K., and Monteiro, P.J.M. (2006). *Concrete – Microstructure, Properties and Materials*. 3rd Edition. New York, NY: The McGraw-Hill Companies, Inc.
- Mindess, Sidney, Young, J. Francis, and Darwin, David. (2003). *Concrete*. 2nd Edition. Upper Saddle River, NJ: Prentice Hall.
- Palyvos, J. A. (2008). “A survey of wind convection coefficient correlations for building envelope energy systems’ modeling”. *Applied Thermal Engineering*, Vol. 28, No. 8-9, 801–808.
- Poole, Jonathan. (2007). *Modeling Temperature Sensitivity and Heat Evolution of Concrete*. Dissertation. University of Texas, Austin, Texas. ProQuest Dissertations and Theses. Web. 30, May 2012

- Riding, Kyle Austin. (2007). *Early Age Concrete Thermal Stress Measurement and Modeling*. Dissertation. University of Texas, Austin, Texas. ProQuest Dissertations and Theses. Web. 13, October 2011.
- Riding, K. A., Poole, J. L., Schindler, A. K., Juenger, M. C. G., and Folliard, K. J. (2006). "Evaluation of Temperature Prediction Methods for Mass Concrete Members". *ACI Materials Journal*, Vol. 103, No. 5, 357–365.
- Riding, K. A., Poole, J. L., Folliard, K. J., Juenger, M. C. G., and Schindler, A. K. (2011). "New Model for Estimating Apparent Activation Energy of Cementitious Systems". *ACI Materials Journal*, Vol. 108, No. 5, 550–557.
- Riding, K. A., Poole, J. L., Folliard, K. J., Juenger, M. C. G., and Schindler, A. K. (2012). "Modeling Hydration of Cementitious Systems". *ACI Materials Journal*, Vol. 109 No. 2, 225–234.
- Schindler, A. K., and Folliard, K. J. (2005). "Heat of Hydration Models for Cementitious Materials". *ACI Materials Journal*, Vol. 102, No. 1, 24–33.
- Tia, M., Ferraro, C., Lawrence, A., Smith, S., and Ochiai, E. (2010). "Development of Design Parameters for Mass Concrete Using Finite Element Analysis". Gainesville, Florida: University of Florida.
- Townsend, C.L. (1981). *Control of Cracking in Mass Concrete Structures*. United States Department of the Interior, Bureau of Reclamation. Engineering Monograph No. 34. Denver: United States Government Printing Office.
- Ulm, F., & Coussy, O. (2001). "What Is a "Massive" Concrete Structure at Early Ages? Some Dimensional Arguments". *Journal of Engineering Mechanics*, Vol. 127, No. 5, 512–522.
- Unified Facilities Guide Specifications (UFGS). Washington, DC: National Institute of Building Sciences. (2012).

APPENDICES

APPENDIX A
Mass Concrete State Specifications Survey and Research Results

A1. Summary of State DOT's Responses to Questions on Early-Age Thermal Cracking of Mass Concrete

1. How do you define a mass concrete member? Do you consider a member with its minimum dimension at least 3 feet or more as a mass concrete member?

Alabama: We don't have a specified definition of a mass concrete member, generally speaking a mass concrete member to us is a large seal footing used for deep-water foundations.

Louisiana: Mass concrete is defined as a structural concrete placement having a least dimension of 48 inches or greater, or if designated on the plans or in the project specifications as being mass concrete. Drilled shafts are exempt from mass concrete requirements.

South Carolina: Mass concrete is defined as a pour that has dimensions of 5 feet or greater in 3 different directions. In the case of a circular cross-section, a mass concrete placement is defined as a pour that has a diameter of 6 feet or greater and a length of 5 feet or greater. Mass concrete requirements do not apply to Drilled Shafts (Class 4000DS) and Foundation Seals (Class 4000S).

Texas: Mass placements are defined as placements with a least dimension greater than or equal to 5 ft., or designated on the plans.

Virginia: Mass concrete is selected by the engineer based on past experience, which is usually guided by temperature differential (maximum 35 °F) and the maximum temperature (160 °F for fly ash and 170 °F for slag concrete) during the placement. The geometry, the size of the element (usually minimum dimension at least 3 ft) and the concrete strength level (which is affected by the w/cm and the cementitious content) also play a significant role in the initial selection.

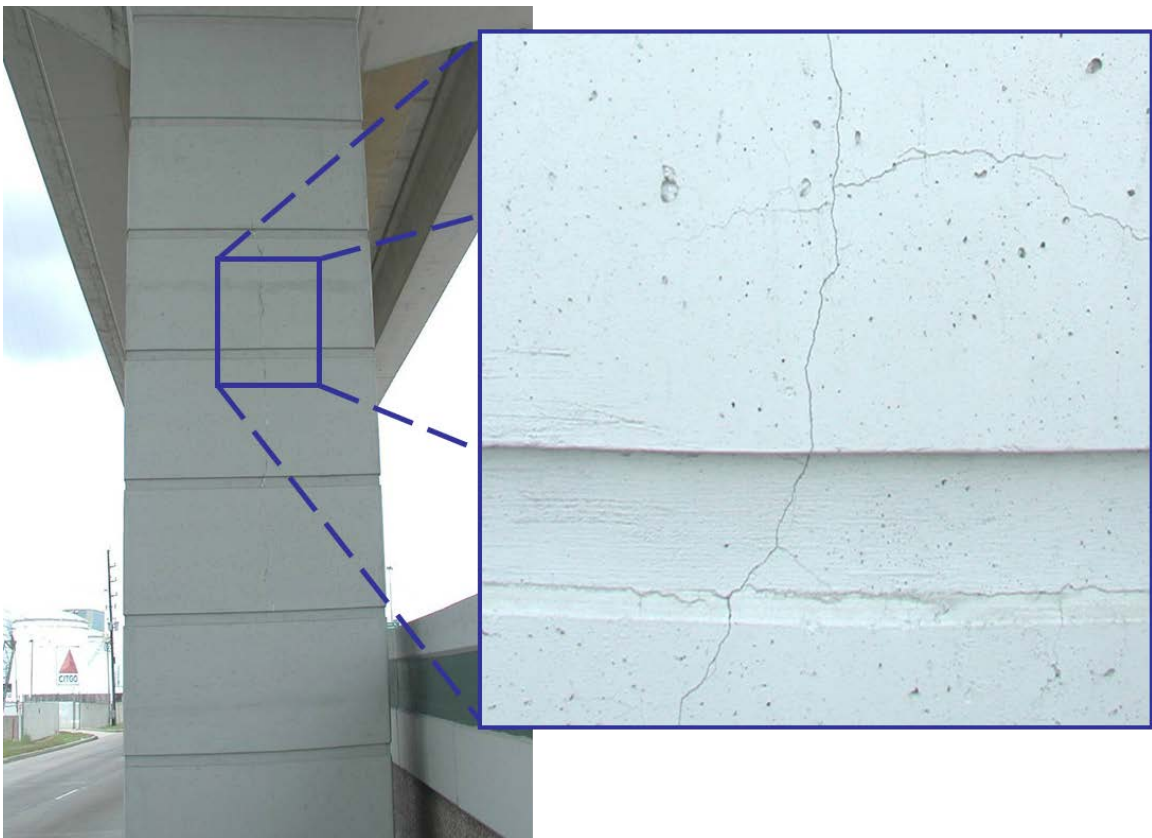
2. **Have you encountered early-age thermal cracking problem with mass concrete members such as large footings, pile caps, bridge columns and piers, bent caps, and abutments, etc. If so, please describe a few typical examples.**

Alabama: We have experienced thermal cracking due to heat of hydration in large underwater seal footings. We have countered the effects by reinforcing the perimeter of the footings.

Louisiana: We did experience cracking on a large hammerhead cap but this was due to using an accelerator in this large pour.

South Carolina: I am not aware of any, but our construction office would be a better source of information.

Texas: On structures built prior to the current version of TxDOT's Standard Specifications (2004), we believe we have longitudinal cracking on many of the large single column piers related to thermal issues of the concrete during hydration.



Virginia: In a large bridge footing at Blacksburg at Smart Road wide thermal cracks were observed. It was attributed to the high temperatures, which also had high differentials. The width of the cracks was reduced with further cooling of the element.

On a large spread footing near Richmond, VA large thermal cracks were observed. The concrete mix was redesigned using a 75% ground-granulated blast furnace slag replacement of the hydraulic cement, which mitigated the problem.

3. Do you use general specifications or specific project specifications for the construction of mass concrete members?

Alabama: We use our general specs for mass concrete.

Louisiana: Use special provisions for now. It will be included in general specifications soon.

South Carolina: Typically, we use general specifications.

Texas: Standard Specifications (2004) – Item 420, “Concrete Structures”

Virginia: We have project specifications generally using the same limiting values. Now, a general specification is being developed for mass concrete.

4. Can excerpts of the specifications be obtained from your official website? If so, please provide a link to the site.

Alabama: See <http://www.dot.state.al.us/conweb/specifications.htm>

Louisiana: See the 2006 Louisiana Standard Specifications for Roads and Bridges as amended 09/11, Subsection 901.13.

South Carolina:

http://www.scdot.org/doing/StandardSpecifications/pdfs/2007_full_specbook.pdf

Section 702.4.2.5

Texas: ftp://ftp.dot.state.tx.us/pub/txdot-info/des/specs/specbook.pdf, Item 420.

Virginia: No.

5. If the specifications are not available on your website, would you please provide a copy of the excerpts that cover the construction of mass concrete members?

Alabama: See above.

Louisiana: See above.

South Carolina: See above.

Texas: See web (Item 420, "Concrete Structures", Sections 420.4.A.2, 420.4.G.1, 420.4.G.14)

Virginia: See Virginia Department of Transportation Special Provision for Hydraulic Cement Concrete Operations for Massive Construction, July 30, 2009

6. Have you had any prior experience in using precast concrete stay-in-place forms for casting mass concrete members? If so, please give a few specific examples.

Alabama: We have not used precast members for large footing pours. We have had contractors use precast culvert segments for forms for some smaller footings for grade separations.

Louisiana: Yes. It has been used for several projects to cast low water footings.

South Carolina: I believe we may have allowed precast concrete stay-in-place forms in the past, but I am not sure if they were ever used.

Texas: No.

Virginia: No prior experience..

7. Based on your experience, what is your opinion (pros and cons) regarding the use of precast concrete stay-in-place forms for casting mass concrete members?

Alabama: No experience with mass concrete.

Louisiana: The contractor proposed to use the precast concrete stay-in-place form for economical reasons. Need to make sure that the anchorage for the stay-in-place form is properly designed. The connections between the stay-in-place form and footing will not be subject to corrosion problem. The stay-in-place form could potentially deteriorate and fall. Make sure the bridge locations are suitable for this condition. The projects where we used this type of form are in the water therefore it was not a concern.

South Carolina: Due to our seismic design requirements, I would have a concern about the additional mass that would be added to the structure.

Texas: Do not use.

Virginia: No prior experience to judge.

A2. Compilation of Mass Concrete Specifications for Recent NCDOT Projects and other State DOTs

Oak Island Bridge

MASS CONCRETE (SPECIAL)

This special provision applies to all interior bent footings on this project with a thickness of six feet or greater.

The Contractor shall provide an analysis of the anticipated thermal developments in the mass concrete elements using his proposed mix design, casting procedures, and materials. Additionally, the Contractor shall describe the measures and procedures he intends to use to limit the temperature differential to 35°F or less between the interior and exterior of the designated mass concrete elements during curing. The proposed plan to control the temperature differential shall be submitted to the Department for review and comments at the time approval is requested for the mass concrete mix design.

Maintenance of the specified thermal differential may be accomplished through a combination of the following:

- A. Selection of concrete ingredients to minimize the heat generated by hydration of the cement.
- B. Cooling component materials to reduce the temperature of the concrete while in its plastic state.
- C. Controlling the rate of placing the concrete.
- D. Insulating the surface of the concrete to prevent heat loss.
- E. Providing supplemental heat at the surface of the concrete to prevent heat loss.
- F. Other acceptable methods which may be developed by the Contractor.

Mass concrete shall be Class AA, vibrated, air-entrained, and shall contain an approved set-retarding, water-reducing admixture, and 30% flyash and 5% microsilica by weight of the total cementitious material. The total cementitious material shall not exceed 690 lbs. per cubic yard of concrete. The maximum water-cementitious material ratio shall be 0.366 for rounded aggregate and 0.410 for angular aggregate. The slump of the concrete shall not exceed three inches. The Contractor shall submit compressive strength results, the average of at least three cylinders made in the laboratory, of his proposed mix design. These cylinders shall show a minimum strength of 5000 psi at 28 days.

Minimum compressive strength at 28 days of field placed concrete shall be 4500 psi.

The Contractor shall meet the temperature monitoring requirements listed below for all footings on the plans which are six feet thick or greater. At the discretion of the Engineer, all temperature monitoring requirements may be waived provided the Contractor has proven to the satisfaction of the Engineer that he can limit the temperature differential to 35° or less between the interior and exterior of the footing.

The Contractor shall provide and install a **minimum of six temperature sensing devices in each mass concrete pour** to monitor temperature differentials between the interior and exterior of the pour unless otherwise directed by the Engineer. These devices shall be accurate within $\pm 2^{\circ}\text{F}$ within the temperature range of 40°F to 180°F. One temperature sensing probe shall be placed near the center of mass of the pour, and another temperature sensing probe shall be placed at approximately two inches clear from the surface of the concrete furthest from the center of mass.

The Engineer shall approve the locations of the other temperature sensing probes.

The monitoring devices shall be read and readings recorded at one-hour intervals, beginning when casting is complete and continuing until the maximum temperature is reached and two consecutive readings indicate a temperature differential decrease between the interior and exterior of the element. At the option of the Contractor, an approved strip-chart recorder furnished by the Contractor may record the temperature. If monitoring indicates the 35°F differential has been exceeded, the Contractor shall make the necessary revisions to the approved plan to reduce the differential on any remaining placements to 35°F or less. The Department must approve any revisions to the plan prior to implementation.

Flyash and microsilica used in the mass concrete mix shall meet the requirements of Articles 1024-5 and 1024-7 of the Standard Specifications. Portland Cement shall meet the requirements of AASHTO M85 for Portland Cement Type II. The temperature of mass concrete at the time of **placement shall not be less than 40°F nor more than 75°F.**

The placement of the mass concrete shall be continuous until the work is completed and the resulting structures shall be monolithic and homogeneous.

The entire cost of this work shall be included in the unit contract price bid for Class AA Concrete.

Sunset Beach Bridge

MASS CONCRETE (SPECIAL)

This special provision applies to all interior bent footings on this project with **a thickness of six feet or greater.**

The Contractor shall provide an analysis of the anticipated thermal developments in the mass concrete elements using his proposed mix design, casting procedures, and materials. Additionally, the Contractor shall describe the measures and procedures he intends to use to limit the temperature differential to 35°F or less between the interior and exterior of the designated mass concrete elements during curing. The proposed plan to control the temperature differential shall be submitted to the Department for review and comments at the time approval is requested for the mass concrete mix design.

Maintenance of the specified thermal differential may be accomplished through a combination of the following:

- A. Selection of concrete ingredients to minimize the heat generated by hydration of the cement.
- B. Cooling component materials to reduce the temperature of the concrete while in its plastic state.
- C. Controlling the rate of placing the concrete.
- D. Insulating the surface of the concrete to prevent heat loss.
- E. Providing supplemental heat at the surface of the concrete to prevent heat loss.
- F. Other acceptable methods which may be developed by the Contractor.

Mass concrete shall be Class AA, vibrated, air-entrained, and shall contain an approved set-retarding, water-reducing admixture, and 30% flyash and 5% microsilica by weight of the total cementitious material. The total cementitious material shall not exceed 690 lbs. per cubic yard of concrete. The maximum water-cementitious material ratio shall be 0.366 for rounded aggregate and 0.410 for angular aggregate. The slump of the concrete shall not exceed three inches. The Contractor shall submit compressive strength results, the average of at least three cylinders made in the laboratory, of his proposed mix design. These cylinders shall show a minimum strength of 5000 psi at 28 days.

Minimum compressive strength at 28 days of field placed concrete shall be 4500 psi.

The Contractor shall meet the temperature monitoring requirements listed below for all footings on the plans which are six feet thick or greater. At the discretion of the Engineer, all temperature monitoring requirements may be waived provided the Contractor has proven to the satisfaction of the Engineer that he can limit the temperature differential to 35° For less between the interior and exterior of the footing.

The Contractor shall provide and install a minimum of six temperature sensing devices in each mass concrete pour to monitor temperature differentials between the interior and exterior of the pour unless otherwise directed by the Engineer. These devices shall be accurate within $\pm 2^{\circ}\text{F}$ within the temperature range of 40°F to 180°F . One temperature sensing probe shall be placed near the center of mass of the pour, and another temperature sensing probe shall be placed at approximately two inches clear from the surface of the concrete furthest from the center of mass.

The Engineer shall approve the locations of the other temperature sensing probes.

The monitoring devices shall be read and readings recorded at one-hour intervals, beginning when casting is complete and continuing until the maximum temperature is reached and two consecutive readings indicate a temperature differential decrease between the interior and exterior of the element. At the option of the Contractor, an approved strip-chart recorder furnished by the Contractor may record the temperature. If monitoring indicates the 35°F differential has been exceeded, the Contractor shall make the necessary revisions to the approved plan to reduce the differential on any remaining placements to 35°F or less. The Department must approve any revisions to the plan prior to implementation.

Flyash and microsilica used in the mass concrete mix shall meet the requirements of Articles 1024-5 and 1024-7 of the Standard Specifications. Portland Cement shall meet the requirements of AASHTO M85 for Portland Cement Type II. The temperature of mass concrete at the time of placement shall not be less than 40°F nor more than 75°F .

The placement of the mass concrete shall be continuous until the work is completed and the resulting structures shall be monolithic and homogeneous.

The entire cost of this work shall be included in the unit contract price bid for Class AA Concrete.

US17 Wilmington Bypass Bridge

MASS CONCRETE (SPECIAL)

Mass Concrete elements are those designated in the contract plans.

The Contractor shall provide an analysis of the anticipated thermal developments in the mass concrete elements using his proposed mix design, casting procedures, and materials. Additionally, the Contractor shall describe the measures and procedures he intends to use to limit the temperature differential to 20°C or less between the interior and exterior of the designated mass concrete elements during curing. The proposed plan to control the temperature differential shall be submitted to the Department for review and comments at the time approval is requested for the mass concrete mix design.

Maintenance of the specified thermal differential may be accomplished through a combination of the following:

- A. Selection of concrete ingredients to minimize the heat generated by hydration of the cement.
- B. Cooling component materials to reduce the temperature of the concrete while in its plastic state.
- C. Controlling the rate of placing the concrete.
- D. Insulating the surface of the concrete to prevent heat loss.
- E. Providing supplemental heat at the surface of the concrete to prevent heat loss.
- F. Other acceptable methods which may be developed by the Contractor.

Mass concrete shall be Class AA, vibrated, air-entrained, and shall contain an approved set-retarding, water-reducing admixture, and flyash or ground granulated blast furnace slag in the amount of 25-30% by weight of the total cementitious material (portland cement plus flyash). The total cementitious material shall not exceed 410 kg per cubic meter of concrete. The maximum water-cementitious material ratio shall be 0.366 for rounded aggregate and 0.410 for angular aggregate. The slump of the concrete shall not exceed 75 mm. The Contractor shall submit compressive strength results, the average of at least three cylinders made in the laboratory, of his proposed mix design. These cylinders shall show a minimum strength of 34.475 MPa at 28 days.

Minimum compressive strength at 28 days of field placed concrete shall be 31 MPa.

The Contractor shall meet the temperature monitoring requirements listed below for all caps and footings designated as mass concrete elements on the plans which are 1.8 meters thick or greater. The contractor shall also meet the temperature monitoring requirements for all other caps and footings designated as mass concrete until he has proven to the satisfaction of the Engineer that he can limit the temperature differential to 20° C or less between the interior and exterior of the footing. All temperature monitoring requirements may be waived at the discretion of the Engineer.

The Contractor shall provide and install a minimum of six temperature sensing devices in each mass concrete pour to monitor temperature differentials between the interior and exterior of the pour unless otherwise directed by the Engineer. These devices shall be accurate within $\pm 1^{\circ}\text{F}$ within the temperature range of 4°C to 82°C. One temperature sensing probe shall be placed near the center of mass of the pour, and another temperature sensing probe shall be placed at approximately 50 mm clear from the surface of the concrete furthest from the center of mass.

The locations of the other temperature sensing probes shall be approved by the Engineer.

The monitoring devices shall be read and readings recorded at one-hour intervals, beginning when casting is complete and continuing until the maximum temperature is reached and two consecutive readings indicate a temperature differential decrease between the interior and exterior of the element. At the option of the Contractor, the temperature may be recorded by an approved strip-chart recorder furnished by the Contractor. If monitoring indicates the 20°C differential has been exceeded, the Contractor shall make the necessary revisions to the approved plan to reduce the differential on any remaining placements to 20°F or less. Revisions to the approved plan must be approved by the Department prior to implementation.

Flyash and ground granulated blast furnace slag used in the mass concrete mix shall meet the requirements of Articles 1024-5 and 1024-6 of the Standard Specifications. Cement shall be Type II meeting the requirements of Subarticle 1024-1(B) of the Standard Specifications.

The temperature of mass concrete at the time of placement shall not be less than 4°C nor more than 24°C.

Florida (Portland Cement Concrete Standards)

346-2.2 Types of Cement: Unless a specific type of cement is designated elsewhere, use Type I, Type P, Type IS, Type II, Type II (MH) or Type III cement in all classes of concrete. Use Type II (MH) for all mass concrete elements.

346-2.3 Pozzolans and Slag: Use fly ash or slag materials as a cement replacement, on an equal weight replacement basis, in all classes of concrete with the following limitations:

(1) Mass Concrete:

- a. Fly Ash - Ensure that the quantity of cement replaced with fly ash is 18% to 50% by weight, except where the core temperature is expected to rise above 165°F. In that case, ensure that the percentage of fly ash is 35% to 50% by weight.
- b. Slag - Ensure that the quantity of cement replaced with slag is 50% to 70% by weight. Ensure that slag is 50% to 55% of total cementitious content by weight when used in combination with silica fume, ultrafine fly ash and/or metakaolin.
- c. Fly Ash and Slag - Ensure that there is at least 20% fly ash by weight and 40% portland cement by weight for mixes containing portland cement, fly ash and slag.

346-3.3 Mass Concrete: When mass concrete is designated in the Contract Documents, provide an analysis of the anticipated thermal developments in the mass concrete elements for all expected project temperature ranges using the selected mix design, casting procedures, and materials.

Use a Specialty Engineer competent in the design and temperature control of concrete in mass elements. The Specialty Engineer shall follow the procedure outlined in Section 207 of the ACI Manual of Concrete Practice to formulate, implement, administer and monitor a temperature control plan, making adjustments as necessary to ensure compliance with the

Contract Documents. The Specialty Engineer shall select the concrete design mix proportions that will generate the lowest maximum temperatures possible to ensure that a 35°F differential temperature between the concrete core and the exterior surface is not exceeded. The mass concrete maximum allowable temperature is 180°F. If either the differential temperature or the maximum allowable temperature is exceeded, the Specialty Engineer shall be available for immediate consultation.

Describe the measures and procedures intended for use to maintain a temperature differential of 35°F or less between the interior core center and exterior surface(s) of the designated mass concrete elements during curing. Submit both the mass concrete mix design and the proposed mass concrete plan to monitor and control the temperature differential to the Engineer for acceptance. Provide temperature monitoring devices to record temperature development between the interior core center and exterior surface(s) of the elements in accordance with the accepted mass concrete plan.

The Specialty Engineer, or a qualified technician employed by the Specialty Engineer, must personally inspect and approve the installation of monitoring devices and verify that the process for recording temperature readings is effective for the first placement of each size and type mass component. Submit to the Engineer for approval the qualification of all technicians employed to inspect or monitor mass concrete placements. For placements other than the first, designate an employee(s) approved by the Specialty Engineer, as qualified to inspect monitoring device installation, to record temperature readings, to be in contact at all times with the Specialty Engineer if adjustments must be made as a result of the temperature differential or the maximum allowable temperature being exceeded, and to immediately implement adjustments to temperature control measures as directed by the Specialty Engineer. Read the monitoring devices and record the readings at intervals no greater than 6 hours. The readings will begin when the mass concrete placement is complete and continue until the maximum temperature differential and the temperature is reached and a decreasing temperature differential is confirmed as defined in the temperature control plan. Do not remove the temperature control mechanisms until the core temperature is within 50°F of the ambient temperature. Furnish a copy of all temperature readings to the Engineer as they are recorded, the determined temperature differentials and a final report within three days of completion of monitoring of each element.

If the 35°F differential or the 180°F maximum allowable temperature has been exceeded, take immediate action as directed by the Specialty Engineer to retard further growth of the temperature differential. Describe methods of preventing thermal shock in the temperature control plan. Use a Specialty Engineer to revise the previously accepted plan to ensure compliance on future placements. Do not place any mass concrete until the Engineer has accepted the mass concrete plan(s). When mass concrete temperature differentials or maximum allowable temperature has been exceeded, provide all analyses and test results deemed necessary by the Engineer for determining the structural integrity and durability of the mass concrete element, to the satisfaction of the Engineer. The Department will make no compensation, either monetary or time, for the analyses or tests or any impacts upon the project.

Texas-DOT Standard Specifications (2004)

420.4

A.2 Removal of Forms and Falsework

Keep in place weight-supporting forms and falsework for bridge components and culvert slabs until the concrete has attained a compressive strength of 2,500 psi in accordance with Section 420.4.K, "Removal of Forms and Falsework." Keep all forms for mass placements defined in Section 420.4.G.14, "Mass Placements," in place for 4 days following concrete placement

G.1 Place Temperature:

Place concrete according to the following temperature limits for the classes of concrete defined in Section 421.4.A, "Classification and Mix Design":

- Place mass concrete, defined by Section 420.4.G.14, "Mass Placements," only when its temperature at the time of placement is between 50 and 75°F.

G.14. Mass Placements. Mass placements are defined as placements with a **least dimension greater than or equal to 5 ft.**, or designated on the plans. For monolithic mass placements, develop and obtain approval for a plan to ensure the following during the heat dissipation period:

- the temperature differential between the central core of the placement and the exposed concrete surface **does not exceed 35°F** and
- the temperature at the central core of the placement **does not exceed 160°F.**

Base this plan on the equations given in the Portland Cement Association's *Design and Control of Concrete Mixtures*. Cease all mass placement operations and revise the plan as necessary if either of the above limitations is exceeded.

Include a combination of the following elements in this plan:

- selection of concrete ingredients including aggregates, gradation, and cement types, to minimize heat of hydration;
- use of ice or other concrete cooling ingredients;
- use of liquid nitrogen dosing systems;
- controlling rate or time of concrete placement;
- use of insulation or supplemental external heat to control heat loss;
- use of supplementary cementing materials; or
- use of a cooling system to control the core temperature.

Furnish and install 2 sets of temperature recording devices, maturity meters, or other approved equivalent devices at designated locations. Use these devices to simultaneously measure the temperature of the concrete at the core and the surface. Maintain temperature control methods for 4 days unless otherwise approved. Maturity meters may not be used to predict strength of mass concrete.

South Carolina-SCDOT 2007 Standard Specifications For Highway Construction

702.4.2.5 Mass Concrete Placement

1 Use procedures for mass concrete placement for a pour that has dimensions of 5 feet or greater in 3 different directions. In the case of a circular cross-section, a mass concrete placement is defined as a pour that has a diameter of 6 feet or greater and a length of 5 feet or greater. Mass concrete requirements do not apply to Drilled Shafts (Class 4000DS) and Foundation Seals (Class 4000S).

2 For all mass concrete pours, do not allow the mix temperature to exceed 80°F measured at discharge into the forms. Maintain a temperature differential of 35°F or less between the interior and exterior of all mass pour elements during curing.

3 Before placing mass concrete, submit to the BCE for review and acceptance a Mass Concrete Placement Plan containing, but not limited to, the following:

- Analysis of the anticipated thermal developments within mass pour placements using the proposed materials and casting methods,
- Temperature Control Plan outlining specific measures to control the temperature differential within the limits noted above, and
- Details of the proposed monitoring system.

4 Submit for review by the OMR all special concrete mix designs, which are part of the Temperature Control Plan.

5 Provide temperature monitoring devices to record temperature development between the interior and exterior of the element at points accepted by the BCE and closely monitor the mass pour temperature differential. Generally, use one monitoring point in the center of the largest mass of concrete and a second point approximately 2 inches inside the face nearest to the first monitoring point. Continue monitoring temperature until the interior temperature is within 35°F of the lowest ambient temperature or a maximum of two weeks. Provide the RCE with a copy of each set of readings as they are taken and a temperature chart for each mass pour element showing temperature readings vs. time.

6 If the monitoring indicates that the proposed measures are not controlling the concrete temperature differential within the 35°F specified, make the necessary revisions to the Temperature Control Plan and submit the revised plan for review.

7 The Contractor assumes all risks connected with placing a mass pour of concrete. RCE review of the Contractor's Mass Concrete Placement Plan will in no way relieve the Contractor of the responsibility for obtaining satisfactory results. Should any mass concrete

placed under this specification prove unsatisfactory, make the necessary repairs or remove and replace the material at no expense to the Department.

8 Provide the control of temperatures in mass concrete pours in addition to any other requirements found on the Plans and/or in the Special Provisions that apply to the work in question. Include all costs associated with temperature controls for mass concrete placement in the unit cost of the concrete.

Virginia-SCDOT 2007 Standard Specifications For Highway Construction

HYDRAULIC CEMENT CONCRETE OPERATIONS FOR MASSIVE CONSTRUCTION

I. DESCRIPTION

This work shall consist of furnishing and placing hydraulic cement concrete for the massive cast-in-situ concrete bridge components, including the 12 ft diameter drilled shafts and the 8 ft wide struts at the top of the 12 ft diameter drilled shafts in accordance with this Special Provision and in conformity with the dimensions, lines, and grades shown on the Contract Drawings or as established by the Engineer.

This Special Provision supplements and modifies Sections 217 and 404 of the Specifications.

II. MATERIALS

- (a) Class F fly ash or granulated iron blast-furnace slag shall be used in all concrete designated mass concrete.
- (b) High-early-strength (Type III) cement, calcium chloride, and accelerating type admixtures shall not be used.
- (c) A retarding admixture, pretested with job materials under job conditions, shall be used, if acceptable to the Engineer, whenever necessary to prevent cold joints due to the quantity of concrete placed, to permit revibration of the concrete, to offset the effects of high concrete temperature, or to reduce the maximum temperature and rate of temperature rise.
- (d) Fly ash, Class F, shall replace 25% to 40% by mass of the design cement content.
- (e) Granulated iron blast-furnace slag shall replace from 50% to 75% by mass of the design cement content.
- (f) Cementitious material content shall be the minimum required to meet the target strength.

III. PROCEDURES

- (a) This Special Provision applies to all reinforced concrete elements whose **minimum dimension exceeds 5 feet**, or where indicated on the plans.
- (b) This work shall be performed with reference to the following American Concrete Institute's (ACI) publications, as superseded by this Special Provision:
 - 1. "Mass Concrete", ACI 207.1R-95.
 - 2. "Effect of Restraint, Volume Change, and Reinforcement on Cracking of Massive Concrete", ACI 207.2R-95.
 - 3. "Control of Cracking Concrete Structures", ACI 224R-01.
 - 4. "Specifications of Structural Concrete for Buildings", Chapter 14, ACI 301-89.

- (c) Submittals: The Contractor shall submit the following to the Engineer for review:
1. Working Drawings: Describe the intended concrete placing sequence in the massive concrete bridge components.
 2. Shop Drawings: Reinforcing steel to be placed in the elements if different size, spacing, or depth of reinforcing bars to be used than those shown on the Contract Drawings.
 3. Documentation: For each proposed concrete mix design, the following information shall be submitted:
 - a. Describe the methods to be used to construct the massive concrete bridge components within the criteria set forth in this Special Provision. Illustrate dimensions of proposed mass concrete pours. Mass concrete pours shall be laid out to minimize surface area for a given volume. Pours that combine elements considered mass concrete and non-mass concrete shall not be permitted.
 - b. Design calculations prepared to document that the methods chosen to install the massive concrete bridge components are in accordance with the referenced ACI publications as superseded by this Special Provision. Calculations shall include:
 1. A table of calculated peak temperatures for the range of expected air and concrete temperatures at time of placement.
 2. A calculation of maximum temperature gradients within the element during the curing period.
 3. A calculation of time to peak temperature.
 4. A calculated curve of maximum allowable temperature difference vs. concrete strength for each element under consideration, for the allowable crack widths indicated on the plans, or in Table 4.1 of ACI 224 where no allowable crack widths are shown on the plans.
 5. Insulation requirements for the forms and exposed portions of the concrete to keep the thermal gradients within allowable limits.
 6. A calculation of the time to reach the peak temperature difference, as well as the estimated time to cool to the allowable differential temperature specified in III.(e).3 below.
 - c. Mix design showing proportions and sources for all components, and results of strength tests of sample cylinders. Mix designs shall also include the heat of hydration of the cementitious materials in the mix, as well as the thermal expansion coefficient of the concrete per USACE CRD-C39-81 if the allowable temperature difference curve will be used..
 - d. Catalogue information on any admixtures proposed to be added to the concrete mix.
 - e. Proposed methods to reduce concrete temperatures and temperature differentials, such as precooling of concrete or insulation. Internal cooling pipes shall not be permitted.
 4. All submittals must be signed and sealed by a Professional Engineer registered in the Commonwealth of Virginia.
- (d) Placing:
1. The maximum temperature of the concrete for massive components when deposited shall be 95 F, or lower if required by the ACI 207 analysis to prevent exceeding the maximum allowable temperature.

(e) Curing and protection:

1. The minimum curing period shall be 1 week. Curing methods shall be in accordance with section 404 of the Specifications, and shall not result in excessive temperature differentials. With the Engineer's approval, the forms may be stripped prior to the end of the curing period.
2. The maximum allowable temperature in any portion of the mass concrete shall be 170 F for slag and cement mixes and 160 F for fly ash and cement mixes in the prescribed proportions. The Engineer may, at its sole discretion, direct that concrete that has exceeded these temperatures be removed, or otherwise mitigated, at no cost to the Department.
3. The maximum allowable thermal gradient between the core and skin temperatures of a pour is limited to 35 F, unless the analysis submitted under section C.3.b.(d) demonstrates that the element is sufficiently reinforced to prevent crack widths in excess of those listed on the plans or in Table 4.1 of ACI 224.
4. Thermocouples shall be placed in each pour of all mass concrete elements. One pair of thermocouples shall be placed at the centroid of the pour, or wherever the point of expected maximum temperature is anticipated. If there is any doubt as to the location of the predicted maximum temperature, then additional thermocouples shall be placed as required or as directed by the Engineer.
5. For elements such as footings, slabs, or pier caps cast on the ground or in a horizontal position, in addition to the pair of thermocouples located at the point of maximum temperature, one pair each of thermocouples shall be cast at the elevation of the bottom mat and top mat of reinforcing steel vertically in line with the thermocouples cast in paragraph (4) above. The thermocouples located at the elevation of the top and bottom mats shall have the same concrete cover as the reinforcing mats.
6. For elements such as columns and walls cast in a vertical position, in addition to the thermocouples located at the point of maximum temperature, one pair each of thermocouples shall be cast on the north face and one on the south face in line with the thermocouples cast at the centroid. These thermocouples shall be located in the same vertical plane as the reinforcing steel mats and shall have the same concrete cover as the reinforcing mats.
7. The Engineer may direct that additional thermocouples be placed if the area of maximum thermal gradient cannot be readily determined.
8. Both thermocouples from each pair shall be connected to a datalogger or other recording device. The datalogger shall record the temperatures at each thermocouple at least once every hour from the time the thermocouple is covered with concrete until 3 days after the peak temperature is reached, or as directed by the Engineer. The datalogger shall have a printed tape or electronic data storage capability. The Engineer may, at his sole discretion, discontinue monitoring of mass concrete elements deemed to be similar to previously monitored elements and placed under similar temperature conditions.
9. To determine concrete strength for stripping and allowable thermal gradients, the Contractor may elect to use either match-cured cylinders or a maturity curve. A separate analysis shall be required for each approved mass concrete design mix.
10. Match-cured cylinders shall be cured in ovens, water baths, or under the form insulation blankets to simulate the temperature of the coolest surface thermocouple in

the pour. Sufficient number of cylinders shall be cast to allow an accurate plot of the strength development of the concrete. At a minimum, 18 pairs of cylinders shall be cast, with two cylinders each broken at the end of 1, 2, 3, 4, 5, 6, 7, 10, and 14 days. Additional cylinders may be required if it is anticipated that the concrete will not reach peak temperature until after 10 days from the pour.

11. Maturity curves shall be developed using the ASTM C1074 procedures for the “equivalent age” method.
12. The forms may be stripped when the concrete strength is high enough (as determined by the maturity curves or match-cast cylinders) to withstand the anticipated thermal gradient between the core temperature and the 48-hour average air temperature, or as directed by the Engineer. In no event will form stripping be allowed before the surface concrete reaches at least 80% of its design strength. After form stripping, concrete shall be protected from freezing temperatures for 48 hours by the use of insulating blankets or other methods approved by the Engineer.

(f) Remedial Measures

If temperature differentials are exceeded and cracking occurs, or if other damage is evident, the Contractor shall core or otherwise test the concrete elements as directed by the Engineer to determine the extent of the damage.

The Contractor shall submit a proposed remediation plan for the approval of the Engineer. The Engineer may, at its sole discretion, direct that all or a portion of the damaged or unacceptable concrete be removed and replaced without additional compensation.

At a minimum, the following remedial measures are required for crack widths exceeding 0.012 inches:

1. All cracks over .006” shall be epoxy injected. Epoxy bonding compounds shall be clear and the type shall be in accordance with Section 243 of the Specifications. All ports and mastic compound shall be removed from portions of the structure that can be viewed by the public.

All remedial work, including coring and crack sealing required shall be incidental to the bid unit cost for concrete.

Louisiana- Portland Cement Concrete

901.08 COMPOSITION OF CONCRETE:

(a) Cement:

For concrete placements having a least dimension of 48 inches (1200 mm) or greater or if designated on the plans or the project specifications as being mass concrete, the allowable cement type shall be Type II portland cement, Type IP portland-pozzolan cement, or Type IS portland blast-furnace slag cement. The cement, or combination of cement and fly ash or ground granulated blast furnace slag, shall be certified to generate a heat of hydration of not more than 70 calories/gram (290 kJ/kg) at 7 days.

(b) Chemical Admixtures:

A water-reducing admixture will be required for mass concrete

901.11 TEMPERATURE LIMITATIONS:

(b) Hot Weather Limitations:

(1) Bridge Decks, Approach Slabs, and Mass Concrete: Hot weather concreting practices will be required when the job site temperature in the shade and away from artificial heat is 80°F (27°C) and rising. When internal temperature of plastic concrete reaches 85°F (30°C), the contractor shall prevent the temperature of succeeding batches from going beyond 90°F (32°C) by approved methods. If necessary, forms shall be pre-cooled by approved methods immediately prior to concrete placement.

Maryland- Structure Performance Specifications (ICC)

3.5.3: Materials-Concrete

H) Mass Concrete is defined as a structural concrete placement with the least dimension of the placed element of 72 inches or greater as defined in the Special Provisions included in the documents.

Massachusetts- Supplemental Specifications

901.64 Protection from Adverse Weather (Cold Weather Requirements)

Where it may be expected that considerable heat will be generated by the hydration of the concrete, and in some cases where heat is not rapidly dissipated, suitable coverings shall be used to protect concrete. Heavy footings in which the concrete is placed at a concrete temperature of 20°C (70°F) where protection is provided by the surrounding earth, except on top, shall be protected by a tarpaulin placed over the top with an air space between the concrete and the tarpaulin and sufficient added artificial heat shall be provided to maintain the minimum required concrete surface temperature. Mass concrete, when concrete as such is so specified on the plans or so defined by the Engineer, placed at a concrete temperature of 20°C (70°F), shall be protected by enclosure with tight wooden forms at least 16 millimeters (5/8 inch) in thickness except at corners and edges and sufficient added artificial heat shall be provided to maintain the minimum required concrete surface temperature. Double sheathing, insulation board or tarpaulins with a dead air space between the covering and the forms shall be placed to equally protect such corners and edges. Supplemental enclosures and added artificial heat will be utilized when required to maintain the minimum concrete surface temperature

Mass Concrete 50 ± 13 mm
slump

Arkansas- Division 800 Structures

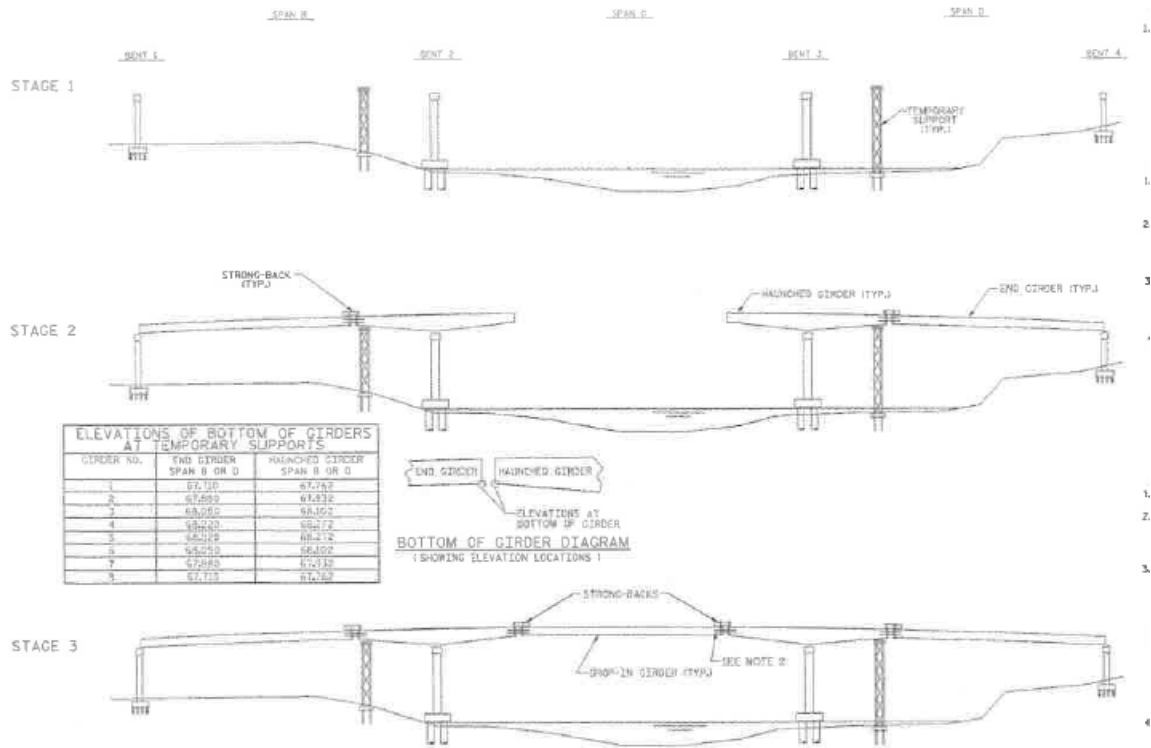
Class B concrete shall be used in mass concrete.

Federal Lands Highways- Std. Specs

- ACI 211.1 Standard Practice for Selecting Proportions for Normal, Heavy Weight and Mass Concrete

APPENDIX B
Mass Concrete Site Visit Field Report Drawings

Figure B-1: Oak Island Field Report 9/12/2011



NOTES

- THIS BRIDGE IS DESIGNED FOR THE ERECTION SEQUENCE SHOWN. THE CONTRACTOR HAS THE OPTION TO DEVIATE FROM THE PROPOSED ERECTION SEQUENCE. IF THE CONTRACTOR CHOOSES TO DEVIATE FROM THE PROPOSED ERECTION SEQUENCE, HE WILL BE RESPONSIBLE FOR ANALYZING THE EFFECTS OF THE PROPOSED CHANGES TO THE PERMANENT STRUCTURE DURING THE CONSTRUCTION PHASE AND IN THE FINAL CONDITION. CALCULATIONS SHOWING BRIDGE EFFECTS MUST BE SUBMITTED FOR APPROVAL. ANY APPROVED CHANGES WILL BE REFLECTED IN REVISED CONTRACT PLANS FURNISHED BY THE CONTRACTOR. ALL ENGINEERING WORK FOR THE REVISIONS MUST BE PERFORMED BY A PROFESSIONAL ENGINEER REGISTERED IN NORTH CAROLINA. ANY WORK REQUESTED BY THE CONTRACTOR TO COMPLETE THE DEVIATION FROM THE PROPOSED ERECTION SEQUENCE SHALL BE PERFORMED AT NO ADDITIONAL COST TO THE DEPARTMENT.
- THE CONTRACTOR IS RESPONSIBLE FOR DESIGNING THE TEMPORARY SUPPORTS, STRONG-BACKS AND A CONNECTION THAT WILL PREVENT RELATIVE ROTATION BETWEEN THE DROP-IN GIRDERS AND HAUNCHED GIRDERS. THE DESIGNER SHALL FOLLOW THE AASHTO BRIDGE DESIGN SPECIFICATIONS FOR BRIDGE TEMPORARY WORKS. THIS AND SHALL BE COMPLETED BY A PROFESSIONAL ENGINEER REGISTERED IN NORTH CAROLINA. THE CONTRACTOR SHALL SUBMIT SIGNED AND SEALED WORKING DRAWINGS AND CALCULATIONS FOR APPROVAL BY THE ENGINEER.
- THE CONTRACTOR SHALL ENSURE THAT BEARINGS ARE PROPERLY SEATED AND FUNCTIONING AFTER POST-TENSIONING IS COMPLETED.
- BEAMS SHALL NOT BE MORE THAN 1/4" OUT OF VERTICAL OR TRANSVERSE ALIGNMENT.
- FOR DETAILS OF POST-TENSIONING OPERATIONS, SEE SHEET TITLED "POST-TENSION".
- THE COST OF THE MATERIALS, LABOR AND ANY INCIDENTAL ITEMS RELATED TO THE INSTALLATION AND REMOVAL OF TEMPORARY SUPPORTS AND STRONG-BACKS SHALL BE INCLUDED IN MAINTENANCE AND REMOVAL OF TEMPORARY ACCESS.

DESIGN BY: R. S. MARTIN DATE: 4/20/2010
 CHECKED BY: R. S. MARTIN DATE: 4/20/2010

Bridge Inspection Field Sketch

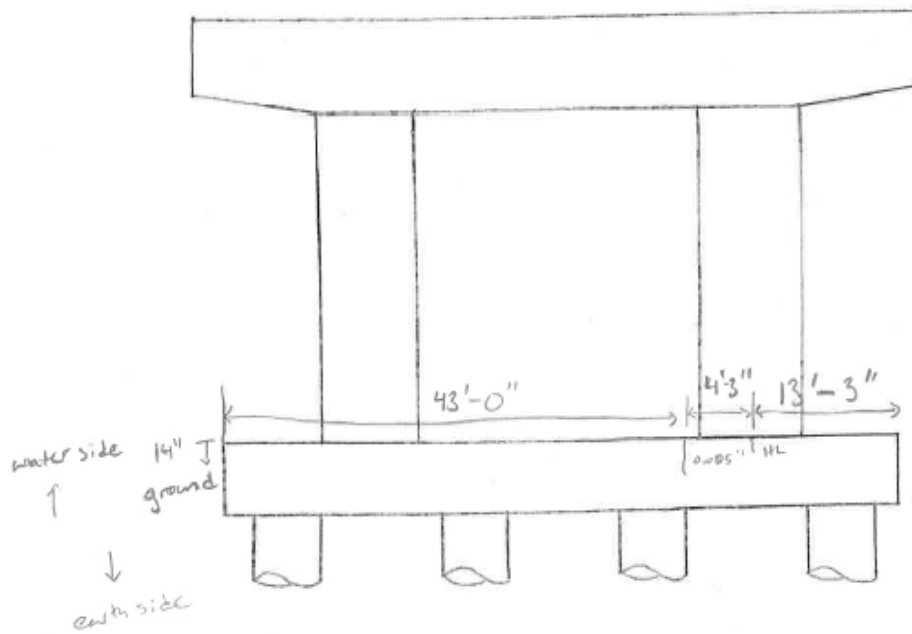
Structure Name: Bent 2

Drawn By: Andrew Edwards

Date: 9/12/2011

Notes: _____

bent 2



Elevation

Bridge Inspection Field Sketch

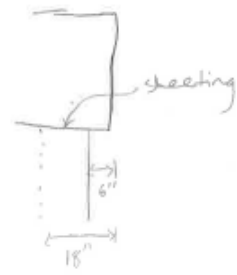
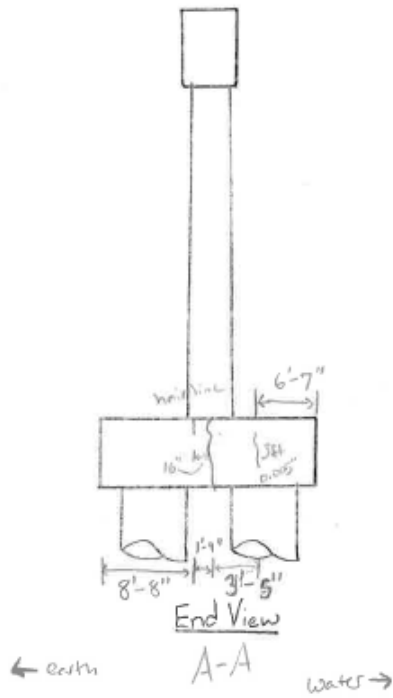
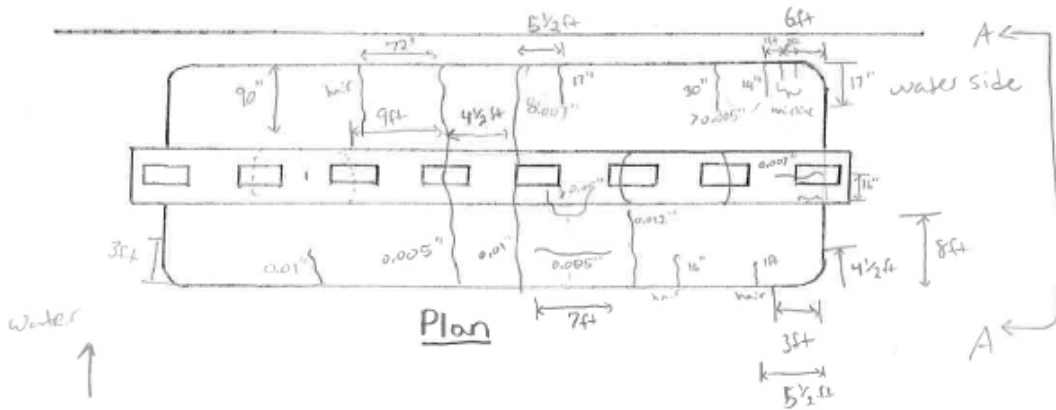
Structure Name: Bert 2

Drawn By Andrew

Date: 9/12/2011

Notes: Facing water ↑

Dimensions: 20'-0" x 60'-6"



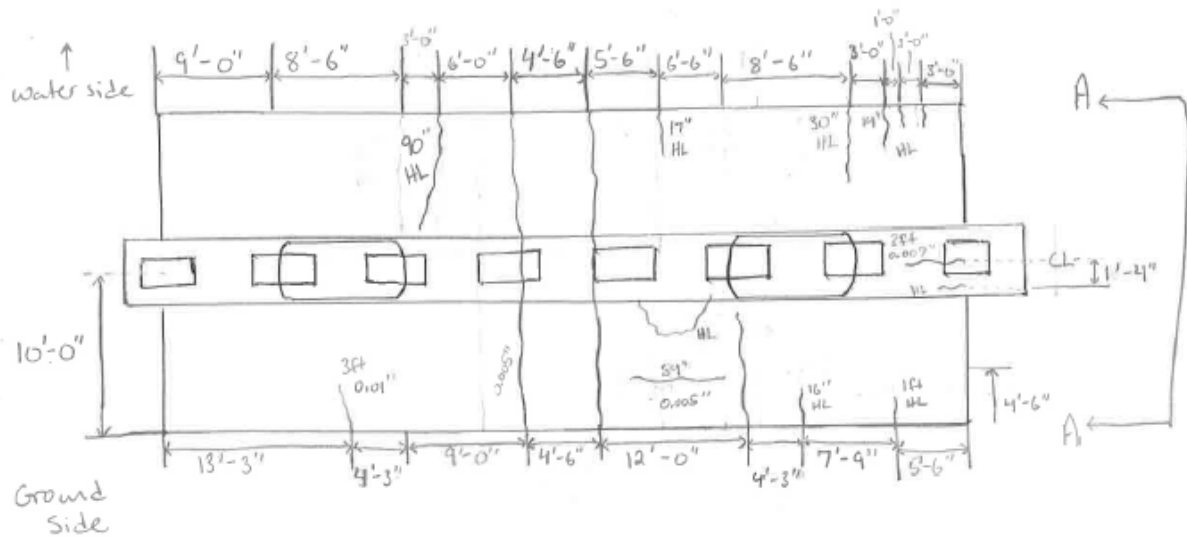
Bridge Inspection Field Sketch

Structure Name: Bent 2 (resketch)

Drawn By: Andrew

Date: 9/16/2011

Notes: Facing water ↑



Bridge Inspection Field Sketch

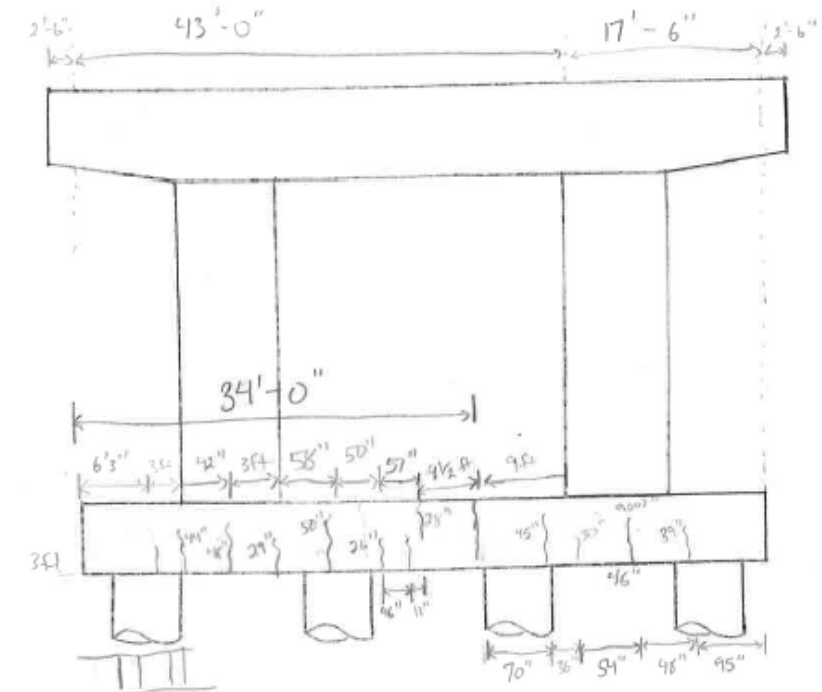
Structure Name: Bent 2

Drawn By: Andrew

Date: 9/12/2011

Notes: Facing Land

cracks at sheeting



Elevation

cracks at sheeting (every 3ft)
 hairline

Bridge Inspection Field Sketch

Structure Name: Bert 3

Drawn By: Andrew

Date: 9/12/2011

Notes: Facing water

* guessing from distance

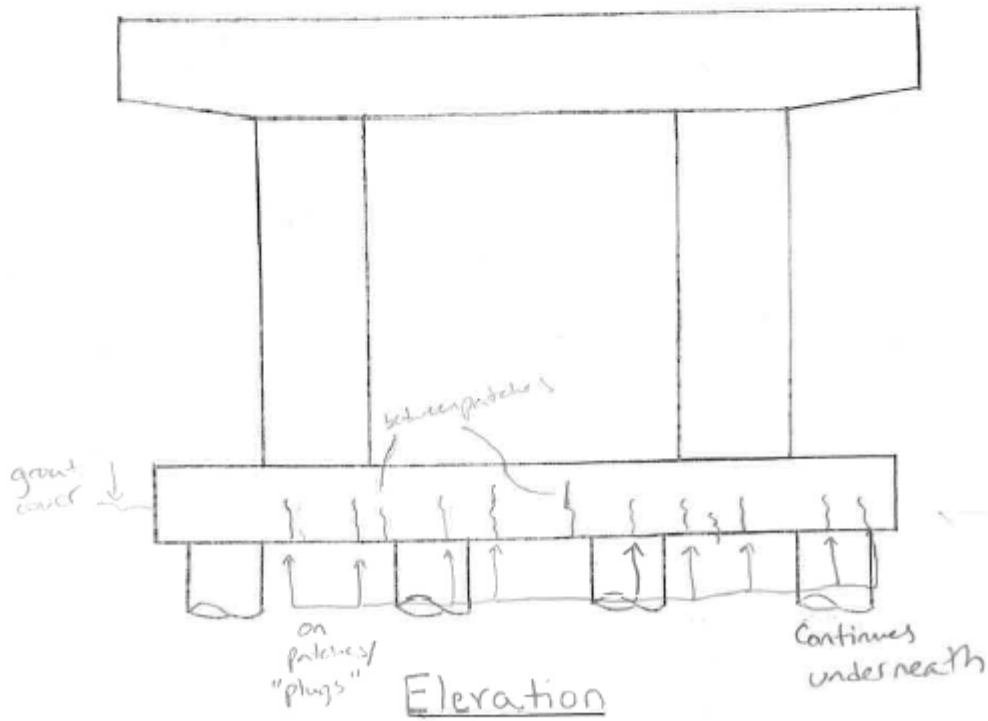
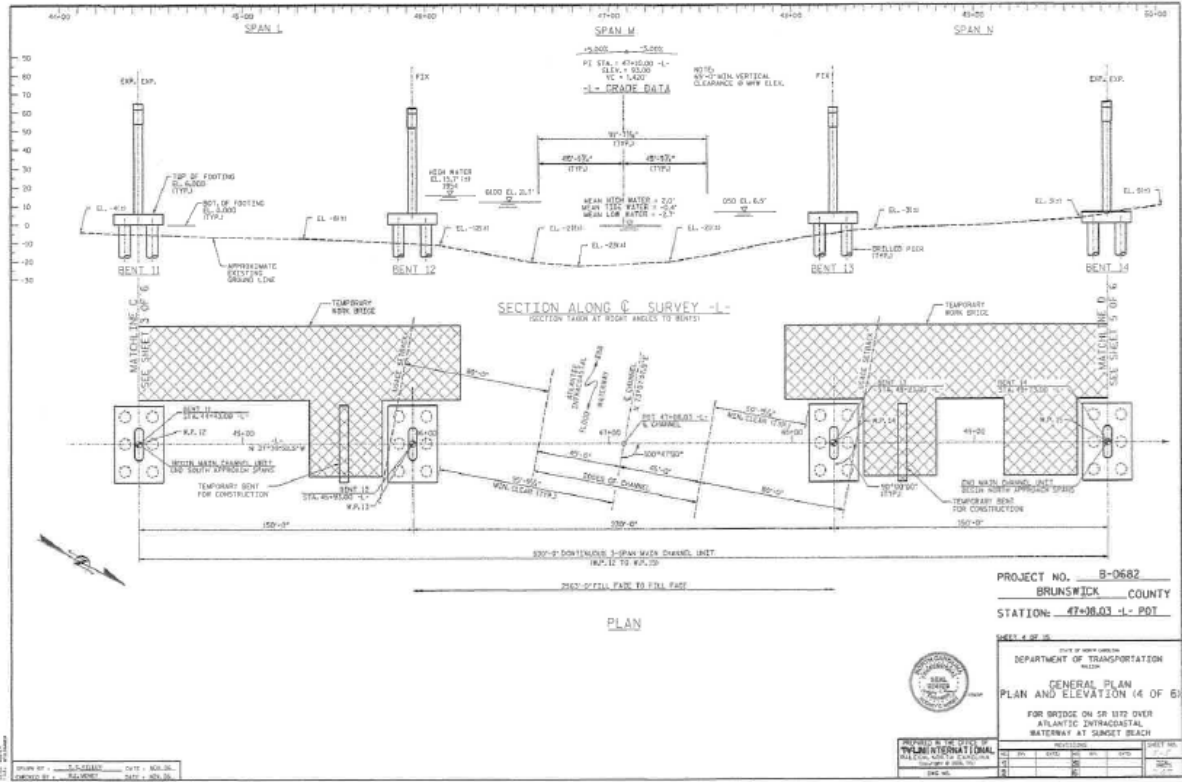


Figure B-2: Sunset Beach Field Report 9/12/2011



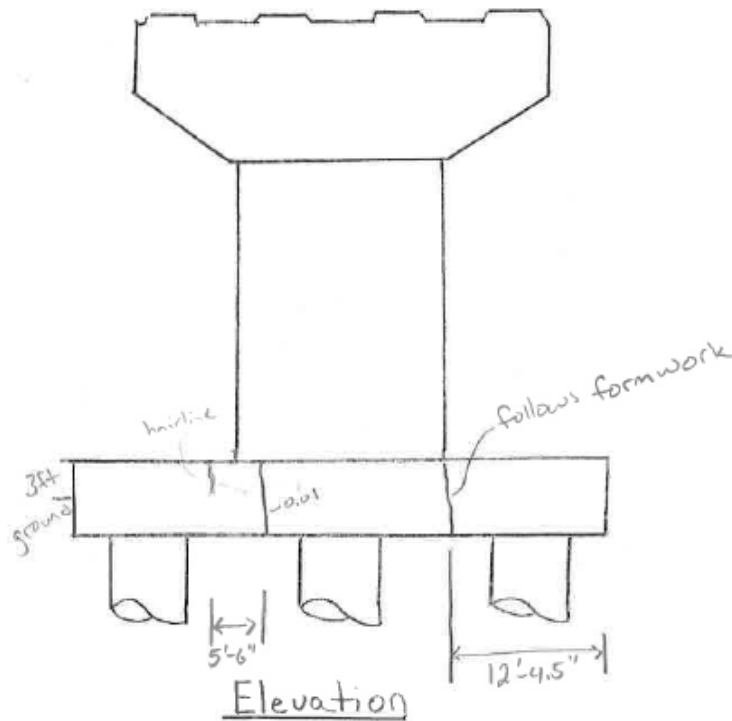
Bridge Inspection Field Sketch

Structure Name: _____

Drawn By: Andrew

Date: 9/12/2011

Notes: _____



Bridge Inspection Field Sketch

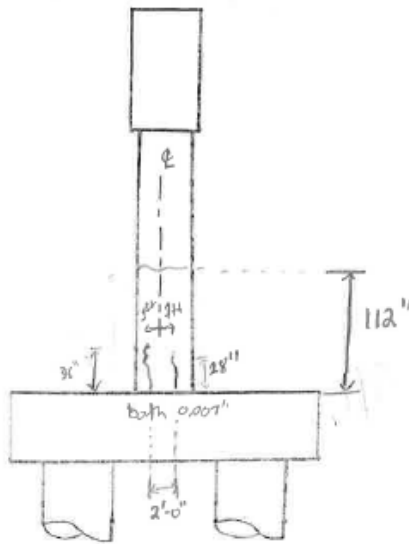
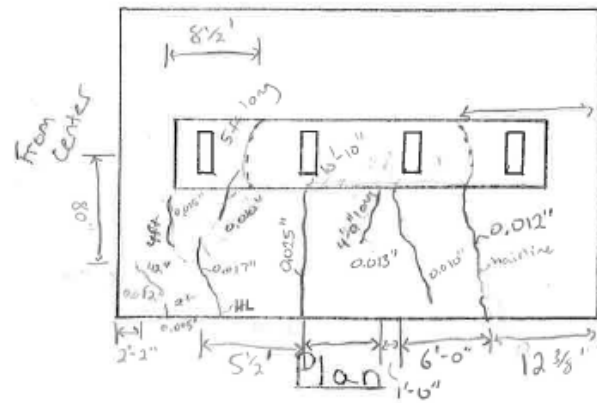
Structure Name: _____

Drawn By: Andrew

Date: 9/12/2011

Notes: _____

Form lines go every 6 feet from right to left
with 6' on the left end



Bridge Inspection Field Sketch

Structure Name: _____ (resketch)

Drawn By: Andrew

Date: _____

Notes: Form lines go every 6 feet from right to left
with 6ft on the left end

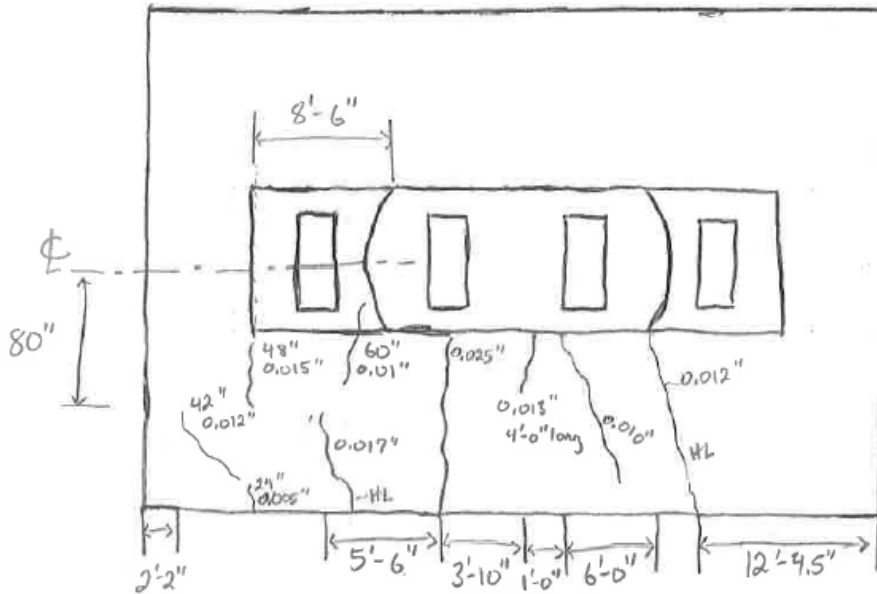
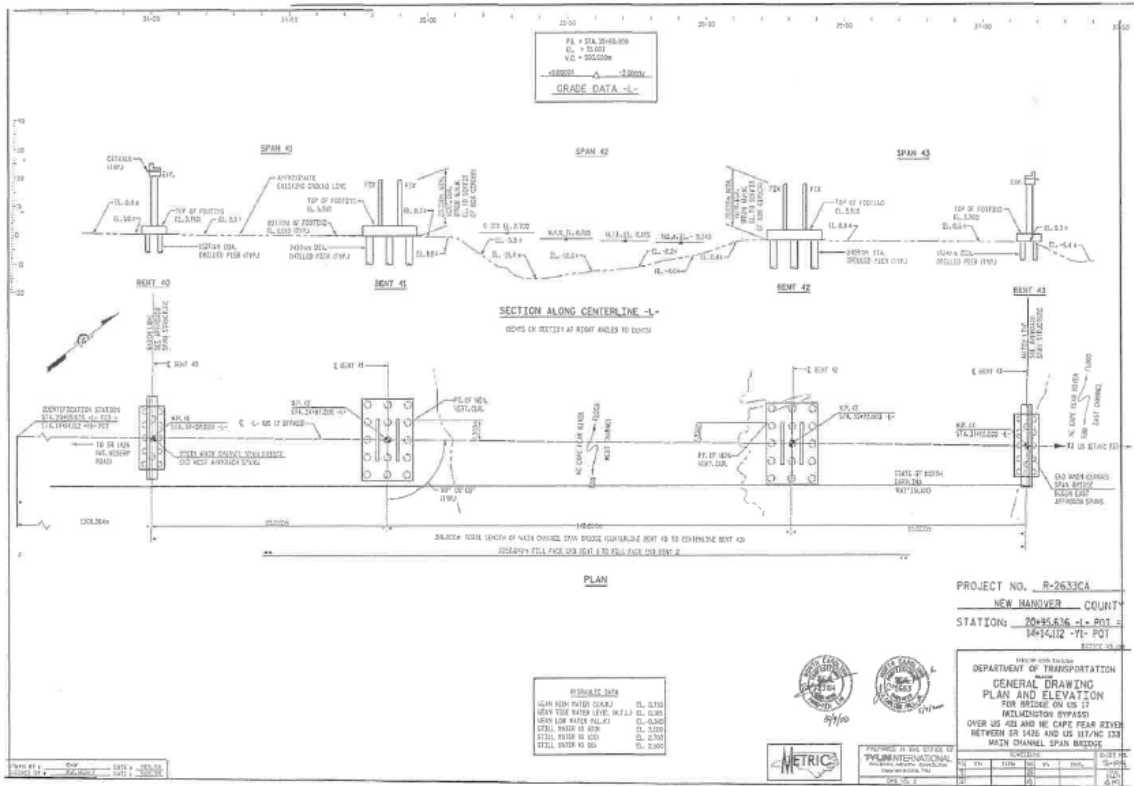


Figure B-3: US17 Wilmington Bypass Field Report 9/12/2011



Bridge Inspection Field Sketch

Structure Name: Bert 41/42

Drawn By: Andrew Edwards

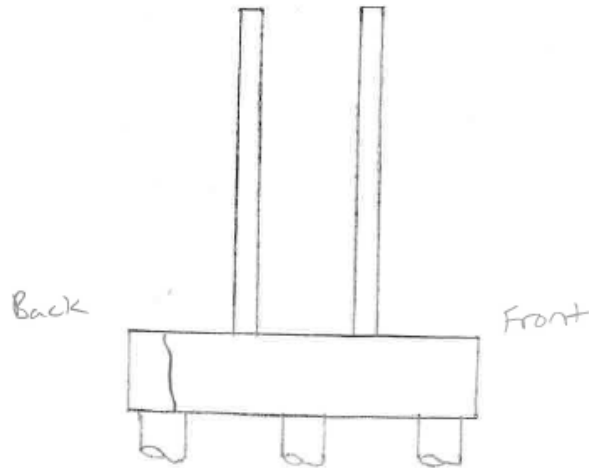
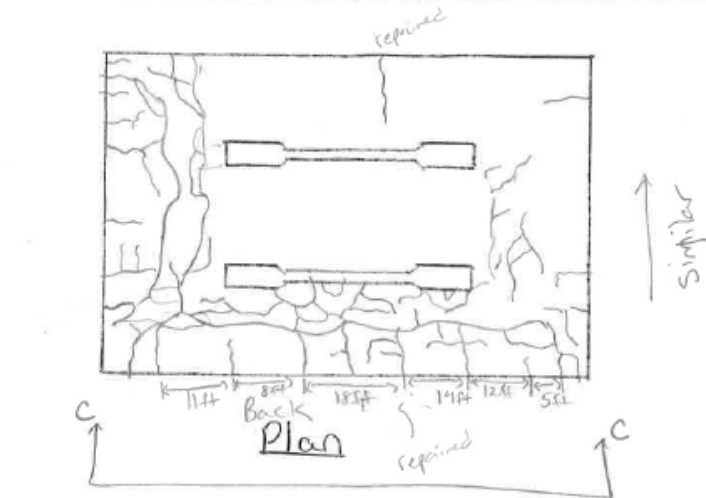
Date: 9/13/2011

Notes: _____

* 3-4 foot blocks of map cracking

Right side

* 28.4m x 18.6m



End View

Bridge Inspection Field Sketch

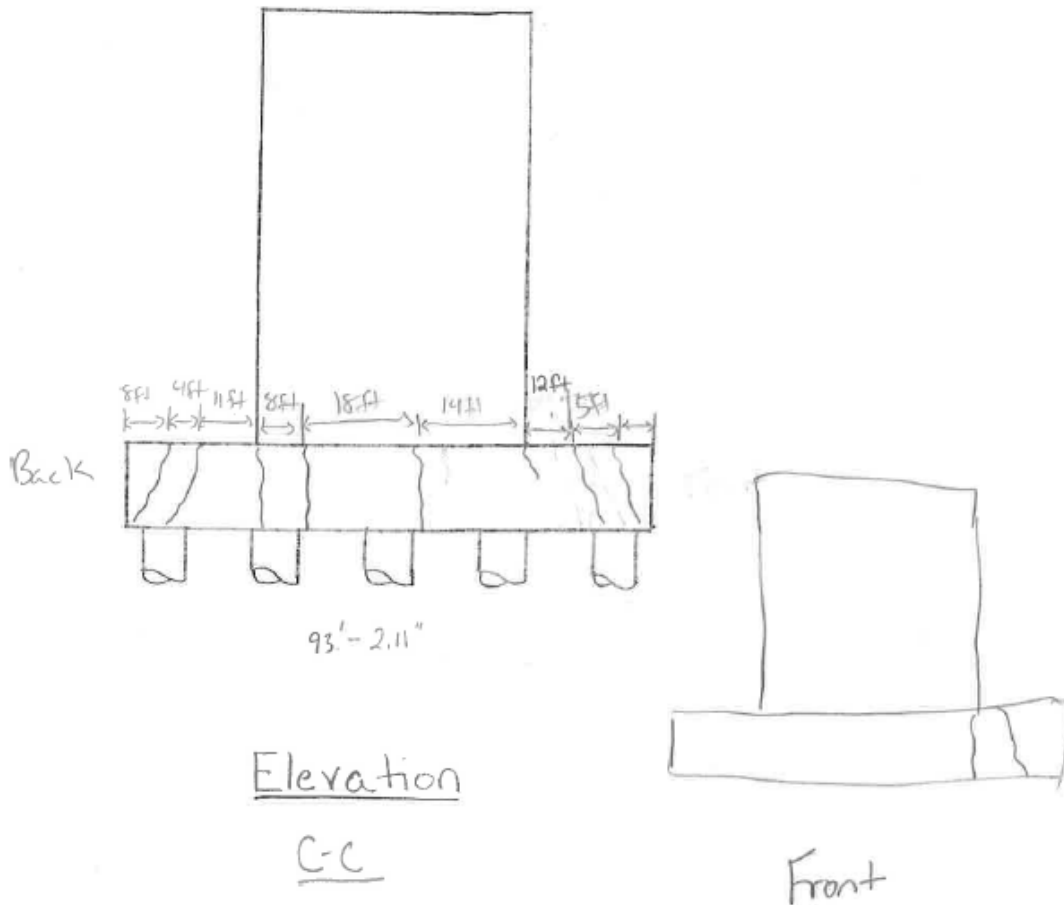
Structure Name: Best 41/42

Drawn By: Andrew Edwards

Date: 9/13/2011

Notes: _____

Back side



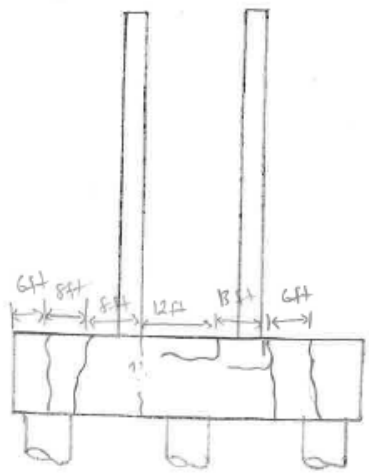
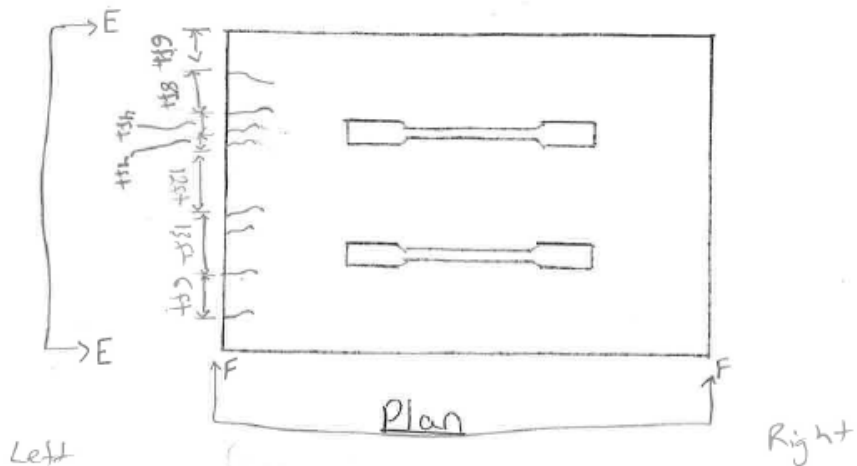
Bridge Inspection Field Sketch

Structure Name: Bent 41/42 (2)

Drawn By: Andrew

Date: 9/13/2011

Notes: _____



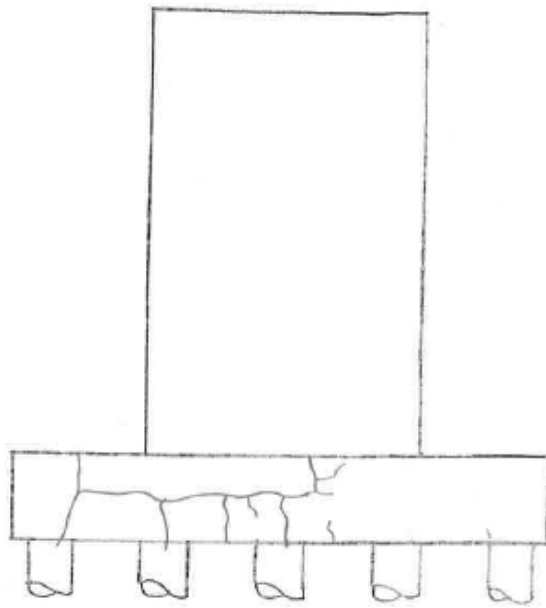
Bridge Inspection Field Sketch

Structure Name: Bent 41/42 (2)

Drawn By: Andrew

Date: 9/13/2011

Notes: Back Side



Elevation

F-F

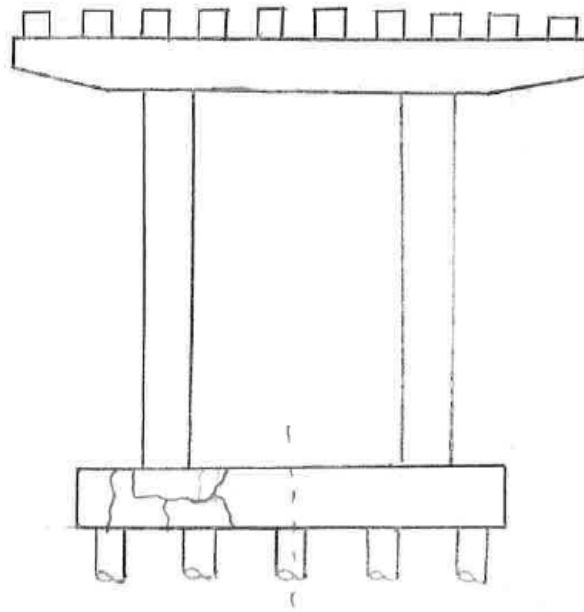
Bridge Inspection Field Sketch

Structure Name: Bent 40/43

Drawn By: _____

Date: _____

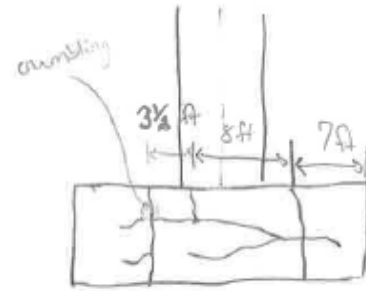
Notes: _____



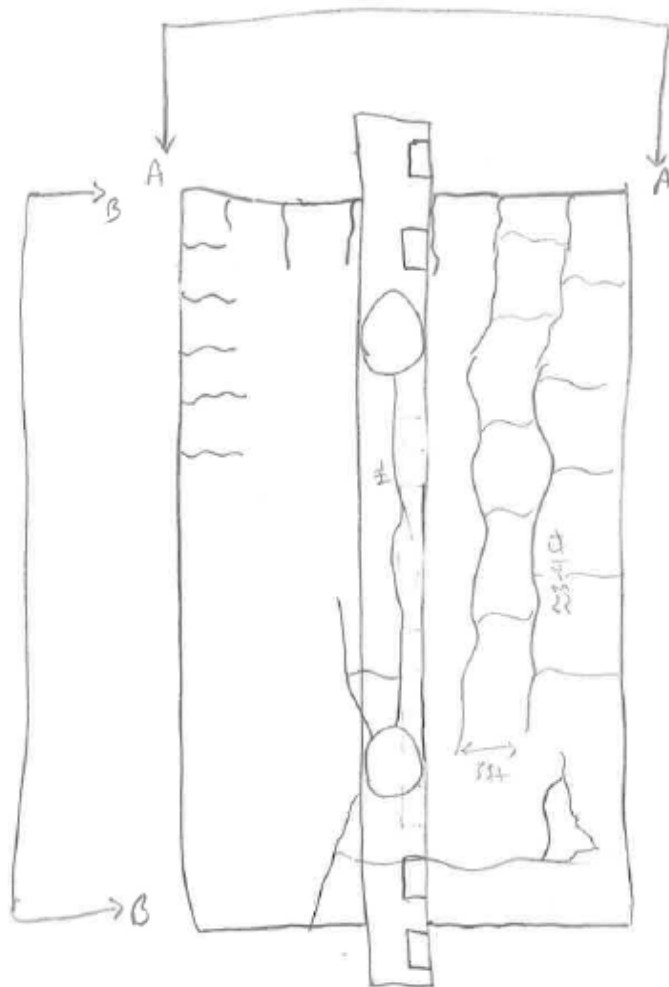
Elevation

B-B

Bent 40/43



A-A



Bridge Inspection Field Sketch

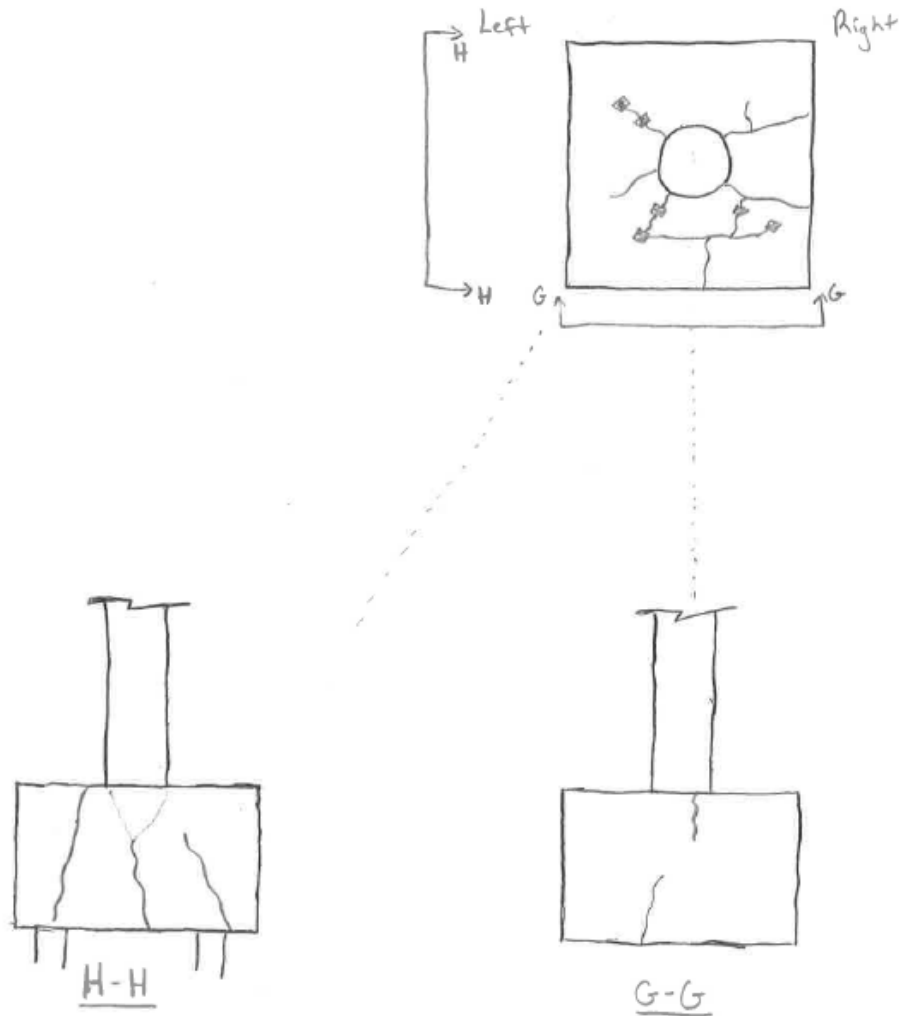
Structure Name: Best 44/39 ??

Drawn By: Andrew Edwards

Date: 9/13/2011

Notes: ■ = anchor patch

* Only showing one footing, where as there are actually
2 identical footings next to each other



APPENDIX C
Sample Input Commands for DIANA Model: Sunset Beach

C1. Batch File Input Commands

Translated from FX+ for DIANA neutral file (version 1.2.0).

'DIRECTIONS'

```
1 1.00000E+000 0.00000E+000 0.00000E+000
2 0.00000E+000 1.00000E+000 0.00000E+000
3 0.00000E+000 0.00000E+000 1.00000E+000
4 0.00000E+000 0.00000E+000 -1.00000E+000
```

'COORDINATES'

```
1 0.00000E+000 4.11480E+000 0.00000E+000
2 0.00000E+000 4.11480E+000 3.04800E-001
3 0.00000E+000 4.11480E+000 6.09600E-001
4 0.00000E+000 4.11480E+000 9.14400E-001
5 0.00000E+000 4.11480E+000 1.21920E+000
6 0.00000E+000 4.11480E+000 1.52400E+000
7 0.00000E+000 4.11480E+000 1.82880E+000
8 0.00000E+000 3.82089E+000 0.00000E+000
9 0.00000E+000 3.82089E+000 3.04800E-001
10 0.00000E+000 3.82089E+000 6.09600E-001
11 0.00000E+000 3.82089E+000 9.14400E-001
12 0.00000E+000 3.82089E+000 1.21920E+000
13 0.00000E+000 3.82089E+000 1.52400E+000
14 0.00000E+000 3.82089E+000 1.82880E+000
15 0.00000E+000 3.52697E+000 0.00000E+000
```

Lines Skipped

```
10412 5.94360E+000 1.17566E+000 1.21920E+000
10413 5.94360E+000 8.81743E-001 1.21920E+000
10414 5.94360E+000 1.17566E+000 9.14400E-001
10415 5.94360E+000 8.81743E-001 9.14400E-001
10416 5.94360E+000 1.17566E+000 6.09600E-001
10417 5.94360E+000 8.81743E-001 6.09600E-001
10418 5.94360E+000 1.46957E+000 1.21920E+000
10419 5.94360E+000 5.87829E-001 1.21920E+000
10420 5.94360E+000 5.87829E-001 9.14400E-001
10421 5.94360E+000 5.87829E-001 6.09600E-001
```

'MATERI'

```
1 NAME CONCRETE
```

THERMX 9.65412E-006
 CONDUCT 7.92000E+003
 CONREA 0.00000E+000 7.92000E+003 1.00000E+000 7.92000E+003
 CAPACI 2.48640E+006
 REACTI 0.00000E+000 1.00000E-001 2.00000E-001 2.40000E-001
 2.90000E-001 3.40000E-001 4.00000E-001 4.70000E-001
 5.60000E-001 6.50000E-001 7.39000E-001 8.28000E-001
 9.17000E-001 1.00000E+000
 CAPART 2.48640E+006 2.48640E+006 2.48640E+006 2.48640E+006
 2.48640E+006 2.48640E+006 2.48640E+006 2.48640E+006
 2.48640E+006 2.48640E+006 2.48640E+006 2.48640E+006
 2.48640E+006 2.48640E+006
 USRHTP OURMAT
 ARRHEN 3.87193E+003
 EQUAGE ARRTYP
 TEMREF 2.00000E+001
 MAXPRD 1.88544E+008
 YOUNG 2.53790E+004
 POISON 2.00000E-001
 DENSIT 1.80478E-004
 FTMATU 0.00000E+000 2.64150E+001 7.45930E+001 1.70593E+002
 3.38593E+002 6.74593E+002
 FTVALU 0.00000E+000 2.01300E+000 2.68900E+000 2.88900E+000
 3.05400E+000 3.92300E+000
 SHRINF 0.00000E+000 -2.33500E-005 -3.03500E-005 -2.33500E-005
 -3.03500E-005 -3.73500E-005 -5.83300E-005 -6.76600E-005
 -7.00000E-005 -7.70000E-005 -9.10000E-005 -9.33400E-005
 -1.00300E-004 -9.80100E-005 -1.05000E-004 -1.19000E-004
 -1.26000E-004 -1.26000E-004
 SHTIME 0.00000E+000 2.40000E+001 4.80000E+001 1.44000E+002
 1.68000E+002 1.95000E+002 2.88000E+002 3.12000E+002
 3.60000E+002 4.83500E+002 6.48000E+002 6.97500E+002
 8.17000E+002 8.64000E+002 1.00800E+003 1.15200E+003
 1.32000E+003 1.48800E+003
 MAXWEL 1
 ,1 MATYOU 0.00000E+000 1.70310E+004 2.64150E+001 1.70310E+004
 7.45930E+001 2.17240E+004 1.70593E+002 2.37900E+004
 3.38593E+002 2.50790E+004 6.74593E+002 2.53790E+004
 8.00000E+002 2.53790E+004 1.20000E+003 2.53790E+004
 1.50000E+003 2.53790E+004
 2 NAME BASE_FORM
 CONDUCT 1.87200E+005

CONREA 0.00000E+000 1.87200E+005 1.00000E+000 1.87200E+005
 CAPACI 3.81510E+006
 3 NAME SIDE_FORM
 CONDUCT 1.87200E+005
 CONREA 0.00000E+000 1.87200E+005 1.00000E+000 1.87200E+005
 CAPACI 3.81510E+006
 4 NAME TOP_INSULATION
 CONDUCT 2.24850E+002
 CONREA 0.00000E+000 2.24850E+002 1.00000E+000 2.24850E+002
 CAPACI 2.08240E+004
 5 NAME SIDE_INSULATION
 CONDUCT 2.24850E+002
 CONREA 0.00000E+000 2.24850E+002 1.00000E+000 2.24850E+002
 CAPACI 2.08240E+004
 6 NAME BASE_INSULATION
 CONDUCT 2.24850E+002
 CONREA 0.00000E+000 2.24850E+002 1.00000E+000 2.24850E+002
 CAPACI 2.08240E+004
 7 NAME TOP_CONVEC
 CONVEC 6.28200E+004
 CONVTT 1.45757E+005 1.38524E+005 7.46960E+004 7.46700E+004
 9.04810E+004 6.04500E+004 4.29120E+004 4.19000E+003
 4.57560E+004 5.80800E+004 5.09700E+004 8.11440E+004
 1.36451E+005 1.27714E+005
 TIME 1.20000E+001 2.40000E+001 3.60000E+001 4.80000E+001
 6.00000E+001 7.20000E+001 8.40000E+001 9.60000E+001
 1.08000E+002 1.20000E+002 1.32000E+002 1.44000E+002
 1.56000E+002 1.68000E+002
 8 NAME SIDE_CONVEC
 CONVEC 6.28200E+004
 CONVTT 1.45757E+005 1.38524E+005 7.46960E+004 7.46700E+004
 9.04810E+004 6.04500E+004 4.29120E+004 4.19000E+003
 4.57560E+004 5.80800E+004 5.09700E+004 8.11440E+004
 1.36451E+005 1.27714E+005
 TIME 1.20000E+001 2.40000E+001 3.60000E+001 4.80000E+001
 6.00000E+001 7.20000E+001 8.40000E+001 9.60000E+001
 1.08000E+002 1.20000E+002 1.32000E+002 1.44000E+002
 1.56000E+002 1.68000E+002
 9 NAME BASE_CONVEC
 CONVEC 6.28200E+004
 CONVTT 1.45757E+005 1.38524E+005 7.46960E+004 7.46700E+004
 9.04810E+004 6.04500E+004 4.29120E+004 4.19000E+003

```

4.57560E+004 5.80800E+004 5.09700E+004 8.11440E+004
1.36451E+005 1.27714E+005
TIME 1.20000E+001 2.40000E+001 3.60000E+001 4.80000E+001
6.00000E+001 7.20000E+001 8.40000E+001 9.60000E+001
1.08000E+002 1.20000E+002 1.32000E+002 1.44000E+002
1.56000E+002 1.68000E+002
'GEOMET'
1 NAME TOP_CONVEC
2 NAME SIDE_CONVEC
3 NAME BASE_CONVEC
4 NAME CONCRETE
5 NAME BASE
6 NAME SIDE_FORM
7 NAME TOP_INSULATION
8 NAME BASE_INSULATION
9 NAME SIDE_INSULATION
'DATA'
1 NAME CONCRETE
2 NAME BASE
3 NAME SIDE_FORM
5 NAME SIDE_INSULATION
6 NAME BASE_INSULATION
7 NAME TOP_CONVEC
8 NAME SIDE_CONVEC
9 NAME BASE_CONVEC
'ELEMENTS'
CONNECT
3313 BQ4HT 2945 2946 2968 2967
3314 BQ4HT 2946 2947 2969 2968
3315 BQ4HT 2947 2948 2970 2969
3316 BQ4HT 2948 2949 2971 2970
3317 BQ4HT 2949 2950 2972 2971
3318 BQ4HT 2950 2951 2973 2972
3319 BQ4HT 2951 2952 2974 2973
3320 BQ4HT 2952 2953 2975 2974
3321 BQ4HT 2953 2954 2976 2975
3322 BQ4HT 2954 2955 2977 2976

Lines Skipped

4399 BQ4HT 3824 3785 4030 4033
1 CHX60 1 4081 2 4082 9 4083 8 4084 4089 4090 4091 4092 106 4085 107 4086

```

114 4087 113 4088
2 CHX60 2 4093 3 4094 10 4095 9 4082 4090 4099 4100 4091 107 4096 108 4097
115 4098 114 4086
3 CHX60 3 4101 4 4102 11 4103 10 4094 4099 4107 4108 4100 108 4104 109 4105
116 4106 115 4097
4 CHX60 4 4109 5 4110 12 4111 11 4102 4107 4115 4116 4108 109 4112 110 4113
117 4114 116 4105
5 CHX60 5 4117 6 4118 13 4119 12 4110 4115 4123 4124 4116 110 4120 111 4121
118 4122 117 4113
6 CHX60 6 4125 7 4126 14 4127 13 4118 4123 4131 4132 4124 111 4128 112 4129
119 4130 118 4121
7 CHX60 8 4083 9 4133 16 4134 15 4135 4092 4091 4139 4140 113 4087 114 4136
121 4137 120 4138
8 CHX60 9 4095 10 4141 17 4142 16 4133 4091 4100 4145 4139 114 4098 115 4143
122 4144 121 4136
9 CHX60 10 4103 11 4146 18 4147 17 4141 4100 4108 4150 4145 115 4106 116
4148 123 4149 122 4143
10 CHX60 11 4111 12 4151 19 4152 18 4146 4108 4116 4155 4150 116 4114 117
4153 124 4154 123 4148

Lines Skipped

1764 CHX60 2197 7951 2198 7979 2205 7980 2204 7976 8331 8334 8354 8351 2302
8333 2303 8352 2310 8353 2309 8349
1765 HX8HT 1 106 113 8 2311 2312 2334 2333
1766 HX8HT 106 211 218 113 2312 2313 2335 2334
1767 HX8HT 211 316 323 218 2313 2314 2336 2335
1768 HX8HT 316 421 428 323 2314 2315 2337 2336
1769 HX8HT 421 526 533 428 2315 2316 2338 2337
1770 HX8HT 526 631 638 533 2316 2317 2339 2338
1771 HX8HT 631 736 743 638 2317 2318 2340 2339
1772 HX8HT 736 841 848 743 2318 2319 2341 2340
1773 HX8HT 841 946 953 848 2319 2320 2342 2341
1774 HX8HT 946 1051 1058 953 2320 2321 2343 2342

Lines Skipped

3310 HX8HT 2747 3977 3978 2746 3291 4079 4080 3290
3311 HX8HT 3822 4041 3312 2939 3643 4044 3275 2745
3312 HX8HT 3311 3312 2939 2767 4059 4043 4023 3957
MATERI
/ 1-1764 / 1

/ 1765-2058 2269-2304 / 2
/ 2059-2268 2305-2310 / 3
/ 2311-2640 / 4
/ 2935-3018 3055-3312 / 5
/ 2641-2934 3019-3054 / 6
/ 3313-3680 / 7
/ 3681-4031 / 8
/ 4032-4399 / 9

DATA

/ 1-1764 / 1
/ 1765-2058 2269-2304 / 2
/ 2059-2268 2305-2640 / 3
/ 2935-3018 3055-3312 / 5
/ 2641-2934 3019-3054 / 6
/ 3313-3680 / 7
/ 3681-4031 / 8
/ 4032-4399 / 9

GEOMET

/ 3313-3680 / 1
/ 3681-4031 / 2
/ 4032-4399 / 3
/ 1-1764 / 4
/ 1765-2058 2269-2304 / 5
/ 2059-2268 2305-2310 / 6
/ 2311-2640 / 7
/ 2641-2934 3019-3054 / 8
/ 2935-3018 3055-3312 / 9

'LOADS'

CASE 1

WEIGHT

3 -1.27100E+002

'TIMELO'

LOAD 1

TIMES 0.00000E+000 1.68000E+002 /
FACTOR 1.00000E+000 1.00000E+000 /

'GROUPS'

ELEMEN

434 "Concrete" / 1-1764 /
435 "Base" / 1765-2058 2269-2304 /
436 "Side Form" / 2059-2268 2305-2310 /
437 "Top Insulation" / 2311-2640 /
438 "Base Insulation" / 2641-2934 3019-3054 /

439 "Side Insulation" / 2935-3018 3055-3312 /
440 "Top Convec" / 3313-3680 /
441 "Side Convec" / 3681-4031 /
442 "Base Convec" / 4032-4399 /
'SUPPOR'
/ 99-105 204-210 309-315 414-420 519-525 624-630 729-735 834-840 939-945
1044-1050 1149-1155 1254-1260 1359-1365 1464-1470 1569-1575 1674-1680 1779-1785
1884-1890 1989-1995 2094-2100 2199-2205 2304-2310 7621 7620 7618 7617 7081 7080
7078 7077 7074 7072 6541 6540 6538 6537 6534 6532 6529 5998 5997 5994 5992 5989
5987 5984 5454 5452 5449 5447 5444 5442 4909 4907 4904 4902 4899 4898 4896 6001

Lines Skipped

7347 7167 7357-6637(-180) 7007 6819-6779(-10) 6619 6999 7519 6989-6959(-10)
7139-7179(10) 7359-7339(-10) 7319 7329 / TR 2
/ 1-105 4366-4364(-1) 4360 4359 4355 4354 4095-4093(-1) 4084-4081(-1) 4383 4382
4378 4377 4373 4372 4111-4109(-1) 4103-4101(-1) 4399-4397(-1) 4393 4392 4388
4387 4127-4125(-1) 4119-4117(-1) 4415 4411 4410 4406 4405 4142 4141
4135-4133(-1) 4431 4430 4426 4425 4421 4420 4416 4157 4156 4152 4151 4147 4146
4444 4443 4439 4438 4432 4175 4174 4168-4166(-1) 4162 4161 4463 4459 4458 4454

Lines Skipped

6627-6987(180) 7347 7167 7357-6637(-180) 7007 6819-6779(-10) 6619 6999 7519
6989-6959(-10) 7139-7179(10) 7359-7339(-10) 7319 7329 / TR 1
/ 43-64(7) 148-358(105) 36-22(-7) 239 267 162 155 260 246 141 134 4819 4809 4204
4627 4829 4659 4657 4369 4637 4647 4201 4366 4629 4237 4639 4649 4336 4338 4303
4270 4305 4333 4300 4272 4239 4267 4234 4206 4619 1618-1639(7) 1723-1933(105)
1513-1303(-105) 1611-1597(-7) 1422 1842 1814 1394 1527 1415 1737 1835 1821 1709
1499 1401 1520 1506 1716 1730 6629 6609 6777 7137 7327 7509 7529 6827 7187 6957
6967-6607(-180) 7147 7157 7337 6977-6617(-180) 6627-6987(180) 7347 7167
7357-6637(-180) 7007 6819-6779(-10) 6619 6999 7519 6989-6959(-10) 7139-7179(10)
7359-7339(-10) 7319 7329 / TR 3
/ 43-64(7) 148-358(105) 36-22(-7) 239 267 162 155 260 246 141 134 4819 4809 4204
4627 4829 4659 4657 4369 4637 4647 4201 4366 4629 4237 4639 4649 4336 4338 4303
4270 4305 4333 4300 4272 4239 4267 4234 4206 4619 1618-1639(7) 1723-1933(105)
1513-1303(-105) 1611-1597(-7) 1422 1842 1814 1394 1527 1415 1737 1835 1821 1709
1499 1401 1520 1506 1716 1730 6629 6609 6777 7137 7327 7509 7529 6827 7187 6957
6967-6607(-180) 7147 7157 7337 6977-6617(-180) 6627-6987(180) 7347 7167
7357-6637(-180) 7007 6819-6779(-10) 6619 6999 7519 6989-6959(-10) 7139-7179(10)
7359-7339(-10) 7319 7329 / RO 1
/ 43-64(7) 148-358(105) 36-22(-7) 239 267 162 155 260 246 141 134 4819 4809 4204

4627 4829 4659 4657 4369 4637 4647 4201 4366 4629 4237 4639 4649 4336 4338 4303
4270 4305 4333 4300 4272 4239 4267 4234 4206 4619 1618-1639(7) 1723-1933(105)
1513-1303(-105) 1611-1597(-7) 1422 1842 1814 1394 1527 1415 1737 1835 1821 1709
1499 1401 1520 1506 1716 1730 6629 6609 6777 7137 7327 7509 7529 6827 7187 6957
6967-6607(-180) 7147 7157 7337 6977-6617(-180) 6627-6987(180) 7347 7167
7357-6637(-180) 7007 6819-6779(-10) 6619 6999 7519 6989-6959(-10) 7139-7179(10)
7359-7339(-10) 7319 7329 / RO 2
/ 43-64(7) 148-358(105) 36-22(-7) 239 267 162 155 260 246 141 134 4819 4809 4204
4627 4829 4659 4657 4369 4637 4647 4201 4366 4629 4237 4639 4649 4336 4338 4303
4270 4305 4333 4300 4272 4239 4267 4234 4206 4619 1618-1639(7) 1723-1933(105)
1513-1303(-105) 1611-1597(-7) 1422 1842 1814 1394 1527 1415 1737 1835 1821 1709
1499 1401 1520 1506 1716 1730 6629 6609 6777 7137 7327 7509 7529 6827 7187 6957
6967-6607(-180) 7147 7157 7337 6977-6617(-180) 6627-6987(180) 7347 7167
7357-6637(-180) 7007 6819-6779(-10) 6619 6999 7519 6989-6959(-10) 7139-7179(10)
7359-7339(-10) 7319 7329 / RO 3

'BOUNDA'

CASE 4

ELEMEN

3313 EXTEMP 1.00000E+000
3314 EXTEMP 1.00000E+000
3315 EXTEMP 1.00000E+000
3316 EXTEMP 1.00000E+000
3317 EXTEMP 1.00000E+000
3318 EXTEMP 1.00000E+000
3319 EXTEMP 1.00000E+000
3320 EXTEMP 1.00000E+000
3321 EXTEMP 1.00000E+000
3322 EXTEMP 1.00000E+000

Lines Skipped

4398 EXTEMP 1.00000E+000

4399 EXTEMP 1.00000E+000

'TIMEBO'

BOUNDA 4

TIMES 0.00000E+000 2.00000E+000 4.00000E+000 6.00000E+000 8.00000E+000
1.00000E+001 1.20000E+001 1.60000E+001 2.40000E+001 2.60000E+001
2.80000E+001 3.20000E+001 3.40000E+001 3.60000E+001 3.80000E+001
4.00000E+001 4.20000E+001 4.40000E+001 4.60000E+001 4.80000E+001
5.00000E+001 5.20000E+001 5.60000E+001 5.80000E+001 6.00000E+001
6.20000E+001 6.40000E+001 6.60000E+001 6.80000E+001 7.00000E+001
7.20000E+001 7.40000E+001 7.60000E+001 7.80000E+001 8.20000E+001
8.40000E+001 8.60000E+001 8.80000E+001 9.00000E+001 9.20000E+001
9.40000E+001 9.60000E+001 9.80000E+001 1.02000E+002 1.04000E+002

1.06000E+002 1.08000E+002 1.10000E+002 1.12000E+002 1.14000E+002
 1.16000E+002 1.18000E+002 1.20000E+002 1.22000E+002 1.24000E+002
 1.26000E+002 1.28000E+002 1.30000E+002 1.32000E+002 1.34000E+002
 1.36000E+002 1.38000E+002 1.40000E+002 1.42000E+002 1.44000E+002
 1.48000E+002 1.50000E+002 1.52000E+002 1.56000E+002 1.58000E+002
 1.60000E+002 1.62000E+002 1.64000E+002 1.66000E+002 1.68000E+002 /
 FACTOR 1.32000E+001 1.30000E+001 1.41000E+001 1.58000E+001 1.63000E+001
 1.31000E+001 7.60000E+000 5.20000E+000 -2.00000E-001 9.00000E-001
 2.60000E+000 7.40000E+000 5.80000E+000 5.80000E+000 6.40000E+000
 7.40000E+000 9.00000E+000 1.01000E+001 7.80000E+000 1.07000E+001
 1.37000E+001 1.46000E+001 1.45000E+001 1.47000E+001 1.37000E+001
 1.39000E+001 1.27000E+001 1.30000E+001 1.24000E+001 1.22000E+001
 1.11000E+001 1.04000E+001 1.28000E+001 1.18000E+001 1.27000E+001
 1.30000E+001 1.31000E+001 1.28000E+001 1.28000E+001 1.32000E+001
 1.29000E+001 1.33000E+001 1.36000E+001 1.43000E+001 1.49000E+001
 1.44000E+001 1.48000E+001 1.50000E+001 1.39000E+001 1.39000E+001
 1.45000E+001 1.49000E+001 1.43000E+001 1.43000E+001 1.43000E+001
 1.39000E+001 1.57000E+001 1.52000E+001 1.60000E+001 1.53000E+001
 1.61000E+001 1.62000E+001 1.53000E+001 1.62000E+001 1.61000E+001
 1.67000E+001 1.66000E+001 1.57000E+001 1.52000E+001 1.56000E+001
 1.53000E+001 1.69000E+001 1.70000E+001 1.71000E+001 1.80000E+001 /

'INIVAR'

TEMPER 2

/ 1-2310 10351-10336(-1) 10079-10064(-1) 9807-9792(-1) 9535-9520(-1)
 9263-9248(-1) 8991-8976(-1) 8719-8704(-1) 8447-8432(-1) 8175-8160(-1)
 7903-7888(-1) 7631-7616(-1) 7359-7344(-1) 7087-7072(-1) 6815-6800(-1)
 6543-6528(-1) 6271-6256(-1) 5999-5984(-1) 5727-5712(-1) 5455-5440(-1)
 5183-5168(-1) 4911-4896(-1) 4639-4624(-1) 4367-4352(-1) 4095-4081(-1)

Lines Skipped

6255-6240(-1) 5983-5968(-1) 5711-5696(-1) 5439-5424(-1) 5167-5152(-1)
 4895-4880(-1) 4623-4608(-1) 4351-4336(-1) / 1.720000e+01

TEMPER 3

/ 3327-3313(-1) 3336 3335 3337-3343 3334-3328(-1) 3344-3355 3358 3357 3359 3356
 3360-3377 3380 3379 3381-3391 3378 3392-3399 3402 3401 3403-3407 3400 3408-3421
 3423 3422 3424-3443 3446 3445 3447-3455 3444 3456-3465 3468 3467 3469-3471 3466
 3472-3487 3490 3489 3491-3503 3488 3504-3509 3512 3511 3513-3519 3510 3520-3531
 3534 3533 3535 3532 3536-3553 3556 3555 3557-3567 3554 3568-3575 3578 3577

Lines Skipped

1891-1896 1996-2001 2101-2106 8-99(7) 113-204(7) 218-309(7) 323-414(7)
428-519(7) 533-624(7) 638-729(7) 743-834(7) 848-939(7) 953-1044(7) 1058-1149(7)
1163-1254(7) 1268-1359(7) 1373-1464(7) 1478-1569(7) 1583-1674(7) 1688-1779(7)
1793-1884(7) 1898-1989(7) 2003-2094(7) 2108-2199(7) / 1.560000e+01
'UNITS'
FORCE N
LENGTH M
TEMPER CELSIU
TIME HOUR
MASS 1.29600E+007
'END'

C2. Staggered Analysis Command File

```
*FILOS
INITIA
*INPUT
*FORTRAN
USE "USRHTP.dll"
*HEATTR
BEGIN INITIA
  BEGIN NONLIN
    EQUAGE EQAINI=0.000000001
    HYDRAT DGRINI 0.01
  END NONLIN
  TEMPER INPUT FIELD=2 Factor=1.0
END INITIA
BEGIN EXECUT
  NONLIN ITERAT MAXITE 30
  SIZES 0.5(48) 1(144)
END EXECUT
BEGIN OUTPUT
  FXPLUS
  FILE "Flow1"
  EQUAGE
  REACTI
  TEMPER
END OUTPUT
*NONLIN
BEGIN TYPE
  BEGIN PHYSIC
    TEMPER
    VISCOE
    MATURI
    SHRINK
  END PHYSIC
END TYPE
BEGIN EXECUT
  TIME STEPS EXPLIC SIZES 0.5(48) 1(144)
  LOAD LOADNR 4
  BEGIN ITERAT
    BEGIN CONVER
      SIMULT
      FORCE TOLCON=1.0E-6
```

```
DISPLA TOLCON=1.0E-6
END CONVER
END ITERAT
END EXECUT
BEGIN OUTPUT FXPLUS FILE="Struc1"
DISPLA TOTAL TRANSL GLOBAL
STRAIN TOTAL GREEN GLOBAL
STRAIN SHRINK GREEN
STRESS CRACK CAUCHY INTPNT
STRESS TOTAL CAUCHY GLOBAL
STRESS TOTAL CAUCHY CRKIND
STATUS CRACK
TEMPER
END OUTPUT
*END
```

C3. Phased Analysis Command File: Wilmington Bypass

```
*FILOS
INITIA
*INPUT
*FORTRAN
USE "USRHTP.dll"
*PHASE
BEGIN ACTIVE
  ELEMEN "Concrete" "Base" "Side Form" "Top Insulation" "Base Insulation" \
  "Side Insulation" "Top Convec" "Bottom Convec" "Side Convec" /
  REINFO
END ACTIVE
*HEATTR
BEGIN INITIA
  BEGIN NONLIN
  EQUAGE EQAINI=0.000000001
  HYDRAT DGRINI 0.01
  END NONLIN
  TEMPER INPUT FIELD=1 Factor=1.0
END INITIA
BEGIN EXECUT
  NONLIN ITERAT MAXITE 30
  SIZES 0.5(48) 1(46)
END EXECUT
BEGIN OUTPUT
  FXPLUS
  FILE "Flow-70"
  EQUAGE
  REACTI
  TEMPER
END OUTPUT
*NONLIN
BEGIN TYPE
  BEGIN PHYSIC
  TEMPER
  VISCOE
  MATURI
  SHRINK
  END PHYSIC
END TYPE
BEGIN EXECUT
```

```

TIME STEPS EXPLIC SIZES 1.0(70)
BEGIN ITERAT
  MAXITE=30
  BEGIN CONVER
  FORCE TOLCON=1.0E-6
  DISPLA TOLCON=1.0E-6
  END CONVER
END ITERAT
END EXECUT
BEGIN OUTPUT FXPLUS FILE="Struc-70"
  DISPLA TOTAL TRANSL GLOBAL
  STRAIN TOTAL GREEN GLOBAL
  STRAIN SHRINK GREEN
  STRESS TOTAL CAUCHY GLOBAL
  STRESS TOTAL CAUCHY CRKIND
  STATUS CRACK
  TEMPER
END OUTPUT

*PHASE
BEGIN ACTIVE
  ELEMEN "Concrete" "Top Convec 2" "Bottom Convec 2" "Side Convec 2" /
  REINFO
END ACTIVE
*HEATTR
BEGIN INITIA
  BEGIN NONLIN
  EQUAGE EQAINI=0.000000001
  HYDRAT DGRINI 0.01
  END NONLIN
  TIME=70
  TEMPER INPUT
END INITIA
BEGIN EXECUT
  NONLIN ITERAT MAXITE 30
  SIZES 1(98)
END EXECUT
BEGIN OUTPUT
  FXPLUS
  FILE "Flow-168"
  EQUAGE
  REACTI

```

```

    TEMPER
  END OUTPUT
*NONLIN
BEGIN TYPE
  BEGIN PHYSIC
    TEMPER
    VISCOE
    MATURI
    SHRINK
  END PHYSIC
END TYPE
BEGIN EXECUT
  BEGIN START
    TIME=70
    INITIA STRESS PHASE
    STEPS
  END START
  BEGIN ITERAT
    BEGIN CONVER
      SIMULT
      FORCE TOLCON=1.0E-6
      DISPLA TOLCON=1.0E-6
    END CONVER
  END ITERAT
END EXECUT
BEGIN EXECUT
  TIME STEPS EXPLIC SIZES 1(98)
  BEGIN ITERAT
    BEGIN CONVER
      SIMULT
      FORCE TOLCON=1.0E-6
      DISPLA TOLCON=1.0E-6
    END CONVER
  END ITERAT
END EXECUT
BEGIN OUTPUT FXPLUS FILE="Struc-168"
  DISPLA TOTAL TRANSL GLOBAL
  STRAIN TOTAL GREEN GLOBAL
  STRAIN SHRINK GREEN
  STRESS TOTAL CAUCHY GLOBAL
  STRESS TOTAL CAUCHY CRKIND
  STATUS CRACK

```

TEMPER
END OUTPUT

C4. Heat of Hydration User Supplied Subroutine

```
SUBROUTINE USRHTP(USRKEY, TE, RE, EQAG, TIME, MAXPRD, ARRHEN,
HTP)
```

```
CDEC$ ATTRIBUTES DLLEXPORT::USRHTP
```

```
C
```

```
Character*6 USRKEY
```

```
DOUBLE PRECISION TE, RE, EQAG, TIME, MAXPRD, ARRHEN, HTP
```

```
DOUBLE PRECISION A, B, C, D, ALPHA, BETA
```

```
INTENT(IN) TE, RE, EQAG, TIME, MAXPRD, ARRHEN
```

```
INTENT(OUT) HTP
```

```
C
```

```
If (USRKEY.EQ.'OURMAT') Then
```

```
  A= MAXPRD*((14.82669838/(EQAG))**0.928058973)
```

```
  B= ((0.928058973)/(EQAG))
```

```
  ALPHA= 0.777789302
```

```
  BETA=(exp(-(14.82669838/(EQAG))**0.928058973))
```

```
  C=ALPHA*BETA
```

```
  D= (exp((ARRHEN)*((1.0/(273.0+20.0))-(1.0/(273.0+TE))))))
```

```
  HTP= (A*B*C*D)
```

```
C
```

```
  print *, "HTP=", HTP
```

```
  print *, "ARRHEN=", ARRHEN
```

```
  print *, "MAXPRD=", MAXPRD
```

```
  print *, "EQAG=", EQAG
```

```
  print *, "TE=", TE
```

```
  print *, "USRKEY=", USRKEY
```

```
  print *, "TIME=", TIME
```

```
  print *, "RE=", RE
```

```
Else
```

```
  print *, "Invalid Input"
```

```
End If
```

```
C
```

```
END SUBROUTINE USRHTP
```